

# INTERNATIONAL SOCIETY FOR SOIL MECHANICS AND GEOTECHNICAL ENGINEERING



*This paper was downloaded from the Online Library of the International Society for Soil Mechanics and Geotechnical Engineering (ISSMGE). The library is available here:*

<https://www.issmge.org/publications/online-library>

*This is an open-access database that archives thousands of papers published under the Auspices of the ISSMGE and maintained by the Innovation and Development Committee of ISSMGE.*

# Foundations and retaining structures – Research and practice

## Fondations et structures de soutènement – la recherche et la pratique

H.G.Poulos – *Coffey Geosciences Pty and The University of Sydney, Australia*

J.P.Carter – *The University of Sydney, Australia*

J.C.Small – *The University of Sydney, Australia*

**ABSTRACT:** This paper presents a broad review of shallow and deep foundations and retaining structures and the most significant methods developed to predict their behaviour. Static and some cyclic loading effects are considered, but dynamic behaviour has been excluded. Emphasis has been placed on methods that have been validated or found to be reliable for use in engineering practice. These include some well-tried and tested methods and others that have been suggested and validated in recent times by geotechnical researchers. Recommendations are made about preferred methods of analysis as well as those whose use should be discontinued. In addition, some observations are made about the future directions that the design of foundations and retaining walls may take, as there are still many areas where uncertainty exists. Some of the latter have been identified.

**RÉSUMÉ:** Ce papier a pour objet donner une vue générale des types de fondations profondes et peu profondes et des structures de soutènement ainsi que des méthodes les plus significatives développées pour prédire leur comportement. Les effets de charges statiques et cycliques sont considérés mais le comportement dynamique a été exclu. L'accent a été mis sur les méthodes qui ont été validées ou reconnues fiables dans la pratique de l'ingénierie. Ce qui inclus tant quelques méthodes qui ont fait leurs preuves que des méthodes qui ont été suggérées et testées récemment par des chercheurs en géotechnique. Des préconisations sont formulées sur les méthodes d'analyse à privilégier et sur celles qui devraient être abandonnées. De plus, quelques pistes quant aux futures directions que devrait prendre le design des fondations et des structures de soutènement sont proposées, car dans de nombreux domaines des incertitudes subsistent. Parmi ces dernières, certaines sont identifiées.

### 1 INTRODUCTION

The design of foundations and retaining structures constitutes one of the most enduring and frequent series of problems encountered in geotechnical engineering. Rational design methods based on soil mechanics principles were established over 50 years ago, and the classic book by Terzaghi and Peck (1948) crystallized the broad design techniques of the time, providing practitioners with an invaluable source of knowledge and experience to apply to their problems. Since the publication of that book, an enormous amount of research has been carried out to improve and refine methods of design, and to gain a better understanding of foundation behaviour and the factors which govern this behaviour. Despite this vast volume of research, many practitioners still rely on the traditional methods of design, and are not aware of some of the research developments which have occurred. In some cases, these developments have verified the traditional design methods, but in other cases, some of those methods have been found to be inaccurate or inappropriate. Examples of the latter category of cases are Terzaghi's bearing capacity theory, which tends to over-estimate the capacity of shallow foundations, and the method of settlement analysis of piles suggested by Terzaghi (1943) which focuses, inappropriately, on consolidation rather than shear deformation.

The reluctance to adopt new research into practice is not surprising, as the concerns of the practitioner tend to be rather different to those of the researcher. The concerns of the practitioner include finding answers to the following questions:

- How can I characterize the site most economically?
- How can I carry out the most convenient design?
- How can I estimate the required design parameters?
- How can I optimize the cost versus performance of the foundation or retaining structure?
- How can I ensure that the design can be constructed effectively?

In contrast, questions, which the researcher tries to address, include:

- What are the main features of the behaviour of the particular foundation or retaining structure?
- What are the key parameters affecting this behaviour?
- How can I refine the analysis and design method to incorporate these parameters?
- How can I describe the behaviour most accurately?

While there is of course some overlap in some of these questions, there is often an over-riding emphasis on cost and speed of design by the practitioner, which appears to be excessively commercial to the researcher. Conversely, the researcher often tends to focus on detail, which appears to be unimportant to the practitioner. In addition, the practitioner all too rarely can afford the luxury of delving into the voluminous literature that abounds in today's geotechnical world. As a consequence, there appears to be an ever-increasing "gap" between the researcher and the practitioner.

This paper attempts to decrease the gap between research and practice, and has two main objectives:

- To summarize some of the findings of research in foundation and retaining structure engineering over the past 30 years or so;
- To evaluate the applicability of some of the commonly used design approaches in the light of this research.

Because of the broad scope of the subject, some limitation of scope is essential. Thus, attention will be concentrated on design of foundations and retaining structures under static loading conditions. The important issue of design for dynamic loading will not be considered herein, nor will issues related to construction be addressed in detail. The following subjects will be dealt with:

- Design philosophy and design criteria;
- Bearing capacity of shallow foundations;
- Settlement of shallow foundations;
- Pile foundations;

- Raft and piled raft foundations;
- Retaining structures, with an emphasis on the assessment of earth pressures and the design of flexible structures;
- Assessment of geotechnical parameters.

At the dawn of a new millennium, it seems appropriate to attempt to make an assessment of those traditional design methods that should be discarded, those that should be modified, and those that should be retained. The conclusions will therefore summarize some methods in these three categories. In addition, the conclusions will propose a number of topics that deserve further research, and conversely, some which may be considered to be too mature for further extensive investigation. Clearly, such suggestions represent the subjective opinions of the authors and may be subject to challenge by others.

## 2 DESIGN APPROACHES AND DESIGN CRITERIA

### 2.1 Design philosophy for design against failure

When designing against failure, geotechnical engineers generally adopt one of the following procedures:

1. The overall factor of safety approach
2. The load and resistance factor design approach (LRFD)
3. The partial safety factor approach
4. A probabilistic approach.

Each of these procedures is discussed briefly below.

#### 2.1.1 Overall factor of safety approach

It was customary for most of the 20<sup>th</sup> century for designers to adopt an overall factor of safety approach when designing against failure. The design criterion when using this approach can be described as follows:

$$R_u / F \geq \sum P_i \quad (2.1)$$

where  $P_i$  = applied loading;  $R_u$  = ultimate load capacity or strength;  $F$  = overall factor of safety.

Factors of safety were usually based on experience and precedent, although some attempts were made in the latter part of the century to relate safety factors to statistical parameters of the ground and the foundation type. Typical values of  $F$  for shallow foundations range between 2.5 and 4, while for pile foundations, values between 2 and 3.5 have been used. Figure 2.1 shows typical values for a variety of geotechnical situations (Meyerhof, 1995a).

#### 2.1.2 LRFD approach

In recent years, there has been a move towards a limit state design approach. Such an approach is not new, having been proposed by Brinch Hansen (1961) and Simpson *et al.* (1981), among others. Pressure from structural engineers has hastened the application of limit state design to geotechnical problems.

One approach within the limit state design category is the LRFD approach, which can be represented by the following design criterion:

$$\Phi R_u \geq \sum a_i P_i \quad (2.2)$$

where  $\Phi$  = strength reduction factor;  $R_u$  = ultimate load capacity or strength;  $P_i$  = applied loading component  $i$  (e.g., dead load, live load, wind load, etc.);  $a_i$  = load factor applied to the load component  $P_i$ .

Values of  $a_i$  are usually specified in codes or standards, while values of  $\Phi$  are also often specified in such documents. The LRFD approach is sometimes referred to as the "American Approach" to limit state design, because of its increasing popularity in North America.

#### 2.1.3 Partial factor of safety approach

In this approach, the design criterion for stability is:

$$R' \geq \sum a_i P_i \quad (2.3)$$

where  $R'$  = design resistance, calculated using the design strength parameters obtained by reducing the characteristic strength values of the soil with partial factors of safety;  $a_i$ ,  $P_i$  are as defined above.

The partial factor of safety approach is sometimes referred to as the "European Approach" because of the considerable extent of its application in parts of that continent.

#### 2.1.4 Probabilistic approach

In this approach, the design criterion can be stated simply as:

$$\text{Probability of failure} \leq \text{Acceptable probability} \quad (2.4)$$

Typical values of the acceptable probability of failure are shown in Figure 2.2 for various classes of engineering projects (Whitman, 1984).

Much has been written about the application of probability theory to geotechnical engineering, but despite enthusiastic support for this approach from some quarters, it does not appear to have been embraced quantitatively by most design engineers. Exceptions are within geotechnical earthquake engineering, environmental geotechnics and in some facets of offshore geotechnics, but it is rarely applied in the design of foundations or retaining structures. An excellent discussion of the use of probabilistic methodologies is given by Whitman (2000).

#### 2.1.5 Discussion of approaches

While a considerable proportion of design practice is still carried out using the overall factor of safety approach, there is an increasing trend towards the application of limit state design methods. Becker (1996) has explored fully the issues involved in the alternative approaches, and provides a useful comparison of the LRFD and partial safety factor approaches which is shown in Figure 2.3.

Considerable debate has taken place recently in relation to the partial factor (European) approach, and a number of reservations have been expressed about it (Gudehus, 1998). Particular problems can be encountered when it is applied to problems involving soil-structure interaction, and the results of analyses in which reduced strengths do not always lead to the worst cases for design. For example, in the design of a piled raft, if the pile capacity is reduced (as is customary), the negative bending moment within the raft may be underestimated when the pile is not located under a column. Thus, in many cases, it is preferable to adopt the LRFD approach, and compute the design values using the best-estimate geotechnical parameters, after which an appropriate factor can be applied to the computed results.

## 2.2 Design loadings and combinations

Conventional foundation design is usually focussed on static vertical loading, and most of the existing design criteria address foundation response to vertical loads. It is however important to recognize that consideration may need to be given to lateral and moment loadings, and that in some cases, cyclic (repeated) loadings and dynamic loadings may be important. In this paper, the primary focus will be placed on static vertical loads, but some cases involving horizontal static loading and cyclic loading will also be addressed.

Load combinations which need to be considered in design are usually specified in structural loading codes. Typical load combinations are shown in Table 2.1 for both ultimate and serviceability load conditions (Standards Australia, 1993). Other combinations are also specified, including liquid and earth pressure loadings.

Table 2.1. Typical load factors for load combinations (Standards Australia, AS 1170-1993).

Case	Combinations for ultimate limit state	Combinations for serviceability limit state	
		Short Term	Long Term
Dead + live	1.25G + 1.5Q 0.8G + 1.5Q	G + 0.7Q	G + 0.4Q
Dead + live + wind	1.25G + Wu + 0.4Q 0.8G + Wu	G + Ws G + 0.7Q + Ws	-
Dead + live + earthquake	1.25G + 1.6E + 0.4Q 0.8G + 1.6E	-	-

Note: G = dead load; Q = live load; Wu = ultimate wind load; Ws = serviceability wind load; E = earthquake load.

### 2.3 Design criteria

Criteria for foundation design typically rely on past experience and field data with respect to both ultimate limit state (stability) design and serviceability design. Some of these criteria are summarized in this section.

#### 2.3.1 Ultimate limit state design

Typical values of overall factor of safety for various types of failure are summarized in Table 2.2 (Meyerhof, 1995a). Meyerhof has also gathered data on the factor of safety in the context of the probability of stability failure and of the coefficients of variation of the loads and soil resistance, and these data are shown in Figure 2.1.

Values of partial factors of safety for soil strength parameters for a range of circumstances are summarized in Table 2.3. As indicated above, the use of factored soil strength data can sometimes lead to designs, which are different from those using conventional design criteria, and must be used with caution.

Table 2.4 summarizes typical geotechnical reduction factors ( $\Phi_g$ ) for foundations. These values are applied in the LRFD design approach to the computed ultimate load capacity, to obtain

Table 2.2 Typical overall factors of safety (Meyerhof, 1995a)

Failure type	Item	Factor of safety
Shearing	Earthworks	1.3 – 1.5
	Earth retaining structures, excavations, offshore foundations	1.5 – 2
	Foundations on land	2 – 3
Seepage	Uplift, heave	1.5 – 2
	Exit gradient, piping	2 – 3
Ultimate pile loads	Load tests	1.5 – 2
	Dynamic formulae	3

Table 2.3. Typical values of partial factors of safety for soil strength parameters (after Meyerhof, 1995a).

Item	Brinch Hansen		Denmark DS165	Euro-code 7	Canada CFEM	Canada NBCC	USA ANSI A58
	1953	1956	1965	1993	1992	1995	1980
Friction ( $\tan \phi$ )	1.25	1.2	1.25	1.25	1.25	See Note 1	See Note 2
Cohesion c (slopes, earth pressures)	1.5	1.5	1.5	1.4-1.6	1.5	"	"
Cohesion c (Spread foundations)	-	1.7	1.75	1.4-1.6	2.0	"	"
Cohesion c (Piles)	-	2.0	2.0	1.4-1.6	2.0	"	"

Note 1: Resistance factor of 1.25-2.0 on ultimate resistance using unfactored strengths.

Note 2: Resistance factor of 1.2-1.5 on ultimate resistance using unfactored strengths.

Table 2.4. Typical values of geotechnical reduction factor  $\Phi_g$ .

Item	Brinch Hansen (1965)	Denmark DS415 (1965)	Euro-code 7 (1993)	Canada CFEM (1992)	Canada NBCC (1995)	Australian Piling Code (1995)
Ultimate Pile Resistance – load tests	0.62	0.62	0.42 - 0.59	0.5 0.62	0.62	0.5 0.9*
Ultimate Pile Resistance – dynamic formulae	0.5	0.5	-	0.5	0.5	0.45 0.65*
Ultimate pile-resistance – penetration tests	-	-	-	0.33- 0.5	0.4	0.40 0.65*

\*Value depends on assessment of circumstances, including level of knowledge of ground conditions, level of construction control, method of calculation, and method of test interpretation (for dynamic load tests).

the design load capacity (strength) of the foundation, as per Equation (2.2). The assessment of an appropriate value for design requires the application of engineering judgement, including the level of confidence in the ground information, the soil data and the method of calculation or load test interpretation employed.

#### 2.3.2 Serviceability design

The general criteria for serviceability design are:

$$\text{Deformation} \leq \text{Allowable deformation} \quad (2.5a)$$

$$\text{Differential deformation} \leq \text{Allowable differential deformation} \quad (2.5b)$$

These criteria are usually applied to settlements and differential settlements, but are also applicable to lateral movements and rotations. The following discussion will however relate primarily to vertical settlements.

The following aspects of settlement and differential settlement need to be considered, as illustrated in Figure 2.4:

- Overall settlement;
- Tilt, both local and overall;
- Angular distortion (or relative rotation) between two points, which is the ratio of the difference in settlement divided by the distance between the two points;
- Relative deflection (for walls and panels).

Data on allowable values of the above quantities have been collected by a number of sources, including Meyerhof (1947), Skempton and MacDonald (1955), Polshin and Tokar (1957), Bjerrum (1963), Grant *et al.* (1974), Burland and Wroth (1974), Burland *et al.* (1977), Wahls (1994), Boscardin and Cording (1989), Barker *et al.* (1991) and Boone (1996). Some of the recommendations distilled from this information are summarized in Table 2.5. Information on criteria for bridges is also included in this table as the assessment of such aspects as ride quality and function requires estimates to be made of the deformations and settlements.

Boone (1996) has pointed out that the use of a single criterion, such as angular distortion, to assess building damage excludes many important factors. A more rational approach requires consideration of the following factors:

- Flexural and shear stiffness of building sections
- Nature of the ground movement profile
- Location of the structure within the settlement profile
- Degree of slip between the foundation and the ground
- Building configuration.



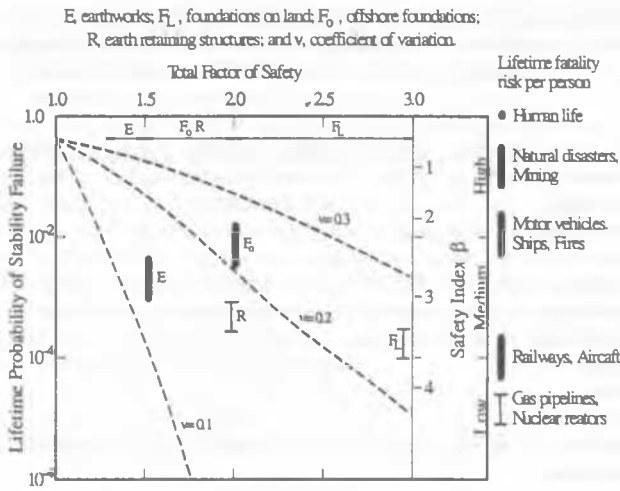


Figure 2.1. Lifetime probability of failures for overall factor of safety approach (Meyerhof, 1995)

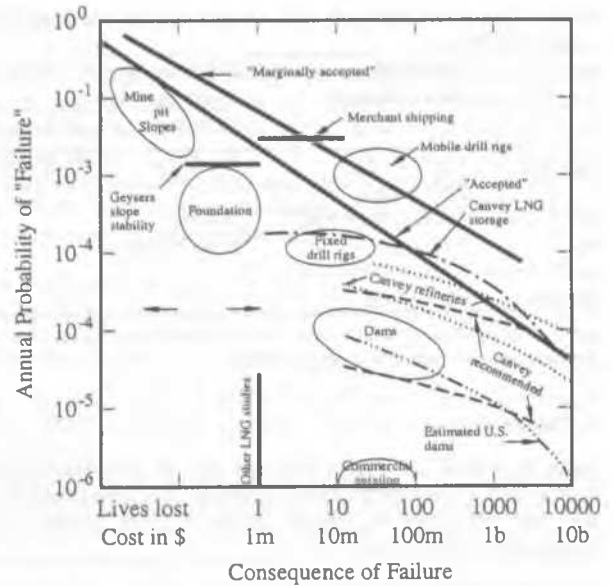
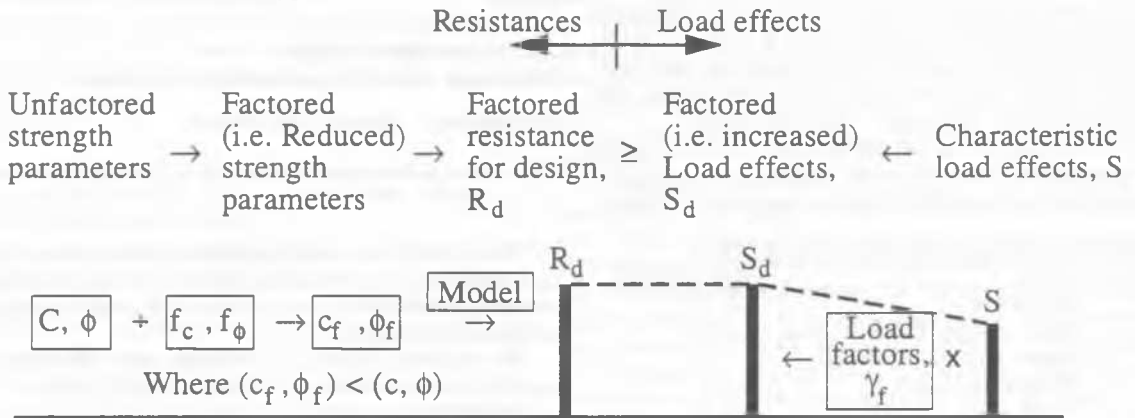


Figure 2.2. Risks for engineering projects (Whitman, 1984).

European approach:  
(factored strength approach)



North American approach:  
(factored resistance approach)

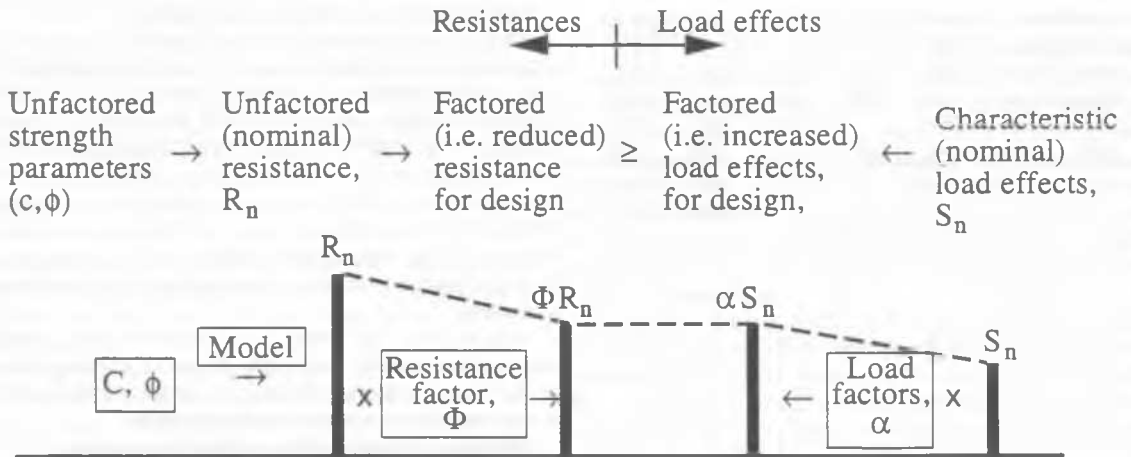


Figure 2.3. LRFD (North American) approach vs partial factor (European) approach (Becker, 1996).

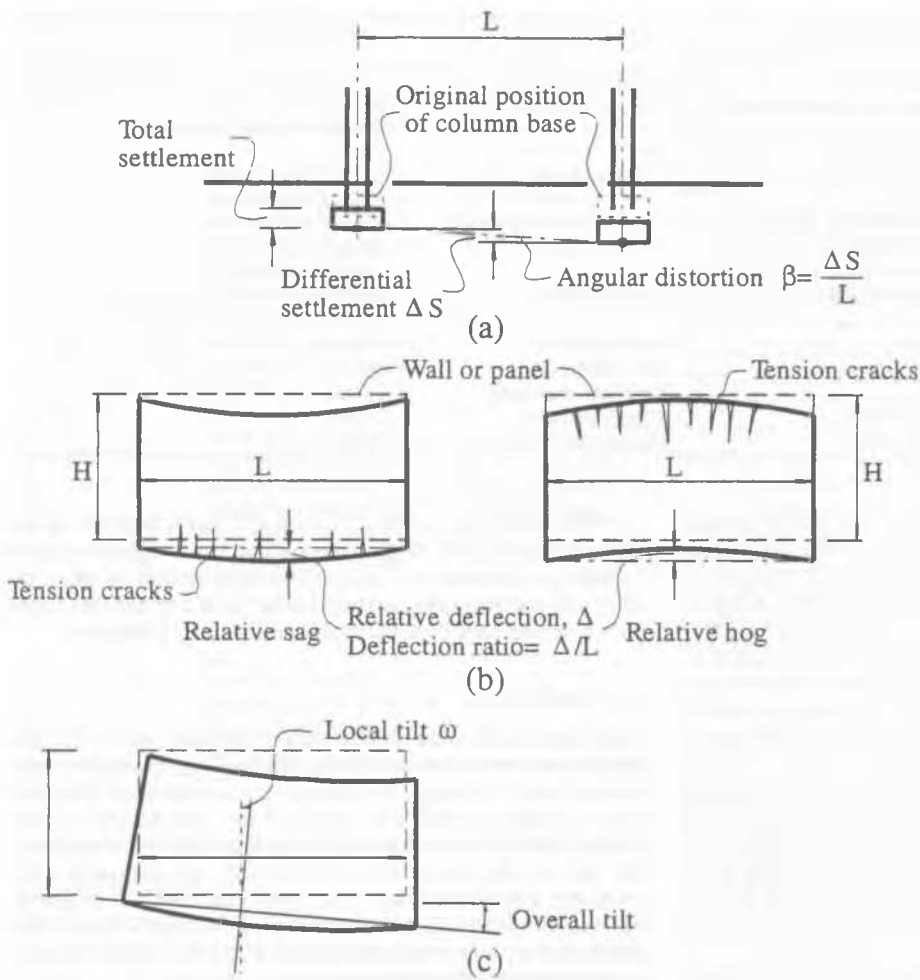


Figure 2.4. Definitions of differential settlement and distortion for framed and load-bearing wall structures (after Burland and Wroth, 1974).

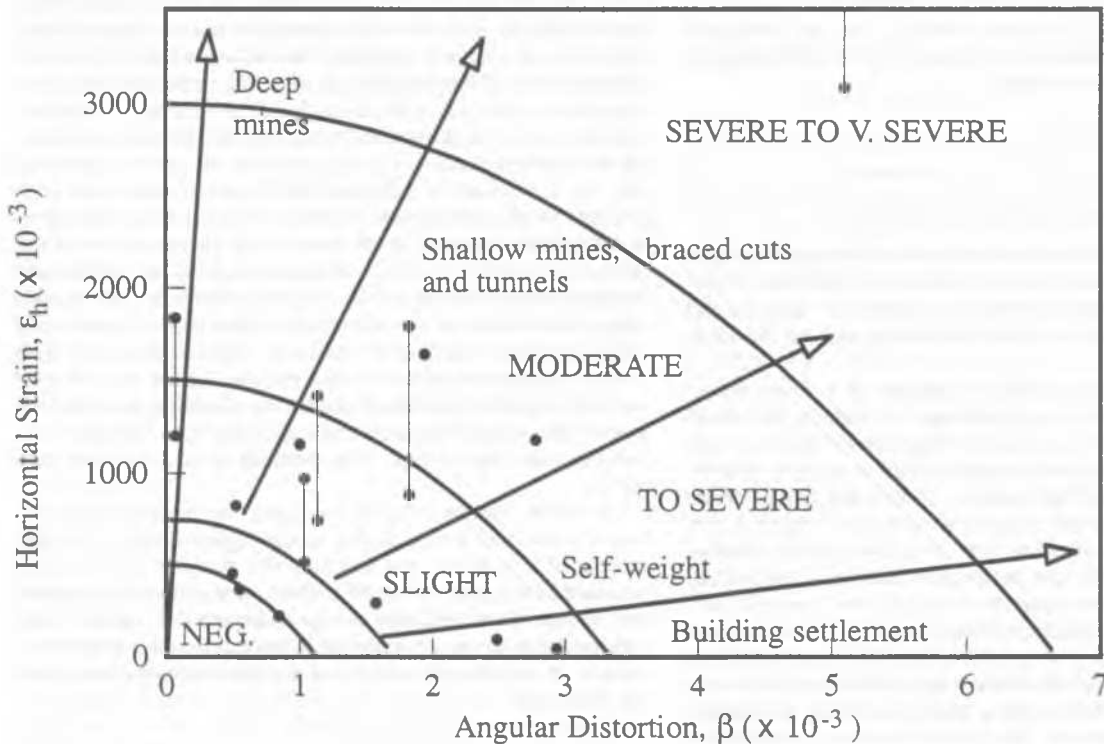


Figure 2.5. Relationship of damage to angular distortion and horizontal extension strain (after Boscardin and Cording, 1989).

Table 2.5. Summary of criteria for settlement and differential settlement of structures.

Type of structure	Type of damage/concern	Criterion	Limiting value(s)	
Framed buildings and reinforced load bearing walls	Structural damage	Angular distortion	1/150 – 1/250	
		Cracking in walls and partitions	Angular distortion (1/1000-1/1400) for end bays	
	Visual appearance	Tilt	1/300	
		Connection to services	Total settlement	50 – 75 mm (sands) 75 – 135 mm (clays)
Tall buildings Structures with unreinforced load bearing walls	Operation of lifts & elevators	Tilt after lift installation	1/1200 – 1/2000	
		Cracking by sagging	Deflection ratio	1/2500 ( $L/H = 1$ ) 1/1250 ( $L/H = 5$ )
	Cracking by hogging	Deflection ratio		1/5000 ( $L/H = 1$ ) 1/2500 ( $L/H = 5$ )
Bridges – general	Ride quality	Total settlement	100 mm	
	Structural distress	Total settlement	63 mm	
	Function	Horizontal movement	38 mm	
Bridges – multiple span	Structural damage	Angular distortion	1/250	
Bridges – single span	Structural damage	Angular distortion	1/200	

The importance of the horizontal strain in initiating damage was pointed out by Boscardin and Cording (1989), and Figure 2.5 shows the relationship they derived relating the degree of damage to both angular distortion and horizontal strain. Clearly, the larger the horizontal strain, the less is the tolerable angular distortion before some form of damage occurs. Such considerations may be of particular importance when assessing potential damage arising from tunnelling operations. For bridges, Barker *et al.* (1991) also note that settlements were more damaging when accompanied by horizontal movements.

It must also be emphasized that, when applying the criteria in Table 2.5, consideration be given to the settlements which may have already taken place prior to the construction or installation of the affected item. For example, if the concern is related to architectural finishes, then assessment is required only of the settlements and differential settlements which are likely to occur after the finishes are in place.

More detailed information on the severity of cracking damage for buildings is given by Day (2000), who has collected data from a number of sources, including Burland *et al.* (1977), and Boone (1996). Day has also collected data on the relationship between the absolute value of differential settlement  $\Delta_{max}$  and the angular distortion ( $\Delta s/L$ ) to cause cracking, and has concluded that the following relationship, first suggested by Skempton and MacDonald (1956), is reasonable:

$$\Delta_{max} \approx 8900(\Delta s / L)(mm) \quad (2.5c)$$

#### 2.4 Categories of analysis and design methods

In assessing the relative merits of analysis and design methods, it is useful to categorize the methods in some way. It has been proposed previously (Poulos, 1989) that methods of analysis and design can be classified into three broad categories, as shown in Table 2.6.

Category 1 procedures probably account for a large proportion of the foundation design performed throughout the world. Category 2 procedures have a proper theoretical basis, but they generally involve significant simplifications, especially with respect to soil behaviour. The majority of available design charts fall into one or other of the Category 2 methods. Category 3 procedures generally involve the use of a site-specific analysis based on relatively advanced numerical or analytical techniques, and require the use of a computer. Many of the Category 2 design charts have been developed from Category 3 analyses, and are then condensed into a simplified form. The most advanced Category 3 methods (3C) have been used relatively sparsely, but increasing research effort is being made to develop such methods, in conjunction with the development of more sophisticated models of soil behaviour.

From a practical viewpoint, Category 1 and 2 methods are the most commonly used. In the following sections, attention will be focussed on evaluating such methods with respect to more refined and encompassing methods, many of which fall into Category 3, or else have been derived from Category 3 analyses.

#### 2.5 Analysis tools

Hand calculations and design charts probably still form the backbone of much standard design practice in geotechnical engineering today. However, the designer has available a formidable array of computational tools. Many of the calculations in Categories 1 and 2, which previously required laborious evaluation, can now be carried out effectively, rapidly and accurately with computer spreadsheets and also with mathematical programs such as MATHCAD, MATLAB and MATHEMATICA. The ability of these tools to provide instant graphical output of results is an invaluable aid to the designer.

The development of powerful numerical analyses such as finite element and finite difference analyses now provide the means for carrying out more detailed Category 3 analyses, and of using more realistic models of soil behaviour. In principle, there is virtually no problem that cannot be handled numerically, given adequate time, budget and information on loadings, *in situ* conditions and soil characteristics. Yet, the same limitations that engineers of previous generations faced, still remain. Time is always an enemy in geotechnical engineering practice, and money all too often is limited. Loadings are almost always uncertain, and the difficulties of adequate site characterization are ever-present. Despite substantial research into soil behaviour, mysteries persist in relation to the stress-strain characteristics of soil response to general loading conditions, and the quantitative description of this behaviour. The two-phase behaviour of saturated soils (not to mention the three-phase behaviour of unsaturated soils), also pose a formidable challenge to those who seek to rely solely on high-level numerical analyses for their designs. It must also be recognized that the potential for obtaining irrelevant answers when using complex numerical methods is very great, especially when the user of such methods is relatively inexperienced.

For these reasons, while recognizing the immense contribution of numerical geomechanics to our understanding of the behaviour of foundations and retaining structures, attention will be focussed in this paper on more conventional methods of analysis and design. Such methods are an indispensable part of engineering practice, and are essential in providing a check on the results of more complex numerical analyses whenever the latter are employed.

Table 2.6. Categories of analysis and design.

Category	Sub-division	Characteristics	Method of parameter estimation
1	-	Empirical – not based on soil mechanics principles	Simple in-situ or laboratory tests, with correlations
2	2A	Based on simplified theory or charts – uses soil mechanics principles – amenable to hand calculation; simple linear elastic or rigid plastic soil models	Routine relevant in-situ or laboratory tests – may require some correlations
	2B	As for 2A, but theory is non-linear (deformation) or elasto-plastic (stability)	
3	3A	Based on theory using site-specific analysis, uses soil mechanics principles. Theory is linear elastic (deformation) or rigid plastic (stability)	Careful laboratory and/or in-situ tests which follow the appropriate stress paths
	3B	As for 3A, but non-linearity is allowed for in a relatively simple manner	
	3C	As for 3A, but non-linearity is allowed for via proper constitutive soil models	

### 3 BEARING CAPACITY OF SHALLOW FOUNDATIONS

#### 3.1 Design issues

In relation to shallow foundations, the key design issues include:

- Estimation of the ultimate bearing capacity of the foundation with, where relevant, appropriate allowance for the combined effects of vertical, horizontal and moment loading;
- Estimation of the total and differential settlements under vertical and combined loading, including any time-dependence of these foundation movements;
- Estimation of foundation movements due to moisture changes in the underlying soil, where these changes are induced by factors other than the loading applied directly to the foundation;
- Structural design of the foundation elements.

In this section, the first two of these design issues will be addressed, while section 4 deals with settlement issues.

Conventionally, the issues of ultimate capacity and settlement are treated separately in design analyses. For most hand calculation methods this separation is necessary, because to do otherwise would render the analysis intractable. However, in some design applications it may be important to conduct more sophisticated analysis in order to understand fully the characteristic foundation behaviour. Very often these sophisticated analyses will employ numerical techniques requiring computer solution. In this section hand methods of analysis are discussed, and some useful solutions derived from more sophisticated analysis are also identified.

#### 3.2 Ultimate load capacity

Prediction of the ultimate bearing capacity of a foundation is one of the most significant problems in foundation engineering, and consequently there is an extensive literature detailing both theoretical and experimental studies of this topic. A list of the principal contributions to the study of this subject may be found, for example, in Vesic (1973), Chen and McCarron (1991) and Tani and Craig (1995).

Bearing capacity failure occurs as the soil supporting the foundation fails in shear. This may involve either a general fail-

ure mechanism or punching shear failure. General shear failure usually develops in soils that exhibit brittle stress-strain behaviour and in this case the failure of the foundation may be sudden and catastrophic. Punching shear failure normally develops in soils that exhibit compressible, plastic stress-strain behaviour. In this case, failure is characterised by progressive, downward movement or "punching" of the foundation into the underlying soil. This failure mode is also the mechanism normally associated with deep foundations such as piles and drilled shafts.

Different methods of analysis are used for the different failure modes. For the general shear mode, a rational approach based on the limiting states of equilibrium is employed. The approach is based on the theory of plasticity and its use has been validated, at least in principle, by laboratory and field testing. For the punching shear mode, a variety of approaches have been suggested, none of which is strictly correct from the point of view of rigorous applied mechanics, although most methods predict ultimate capacities which are at least comparable to field test results.

In the discussion that follows, particular emphasis is given to:

- Estimating the ultimate capacity of foundations subjected to combined loading, i.e., combinations of vertical and horizontal forces and moments,
- Estimating the ultimate capacity for cases of eccentrically applied forces, and
- Estimating the ultimate capacity of foundations on non-homogeneous soils including layered deposits.

##### 3.2.1 Conventional bearing capacity theory

A rational approach for predicting the bearing capacity of a foundation suggested by Vesic (1975) has now gained quite widespread acceptance in foundation engineering practice. This method takes some account of the stress-deformation characteristics of the soil and is applicable over a wide range of soil behaviour. This approach is loosely based on the solutions obtained from the theory of plasticity, but empiricism has been included in significant measure, to deal with the many complicating factors that make a rigorous solution for the capacity intractable.

For a rectangular foundation the general bearing capacity equation, which is an extension of the expression first proposed by Terzaghi (1943) for the case of a central vertical load applied to a long strip footing, is usually written in the form:

$$q_u = \frac{Q_u}{BL} = c N_c \zeta_{cr} \zeta_{cs} \zeta_{ci} \zeta_{cg} \zeta_{cd} + \frac{1}{2} B \gamma N_\gamma \zeta_{\gamma r} \zeta_{\gamma s} \zeta_{\gamma i} \zeta_{\gamma g} \zeta_{\gamma d} + q N_q \zeta_{qr} \zeta_{qs} \zeta_{qi} \zeta_{qg} \zeta_{qd} \quad (3.1)$$

where  $q_u$  is the ultimate bearing pressure that the soil can sustain,  $Q_u$  is the corresponding ultimate load that the foundation can support,  $B$  is the least plan dimension of the footing,  $L$  is the length of the footing,  $c$  is the cohesion of the soil,  $q$  is the overburden pressure, and  $\gamma$  is the unit weight of the soil. It is assumed that the strength of the soil can be characterised by a cohesion  $c$  and an angle of friction  $\phi$ . The parameters  $N_c$ ,  $N_\gamma$  and  $N_q$  are known as the general bearing capacity factors which determine the capacity of a long strip footing acting on the surface of soil represented as a homogeneous half-space. The factors  $\zeta$  allow for the influence of other complicating features. Each of these factors has double subscripts to indicate the term to which it applies ( $c$ ,  $\gamma$  or  $q$ ) and which phenomenon it describes ( $r$  for rigidity of the soil,  $s$  for the shape of the foundation,  $i$  for inclination of the load,  $t$  for tilt of the foundation base,  $g$  for the ground surface inclination and  $d$  for the depth of the foundation). Most of these factors depend on the friction angle of the soil,  $\phi$ , as indicated in Table 3.1. Details of the sources and derivations for them may be found in Vesic (1975), Caquot and Kerisel (1948, 1953), Davis and Booker (1971) and Kulhawey *et al.* (1984). The unusual case of foundations subjected to a combination of a concentric vertical load and a torsional moment has also been studied by Perau (1997).

Table 3.1. Bearing capacity factors.

Parameter	Cohesion	Self-weight	Surcharge
Bearing Capacity	$N_c = (N_q - 1)\zeta_{\alpha} \phi$ $N_c = 2 + \pi$ if $\phi = 0$	$N_\gamma = 0.0663e^{9.3\phi}$ Smooth $N_\gamma = 0.1054e^{9.6\phi}$ Rough $\phi > 0$ in radians $N_\gamma = 0$ if $\phi = 0$	$N_q = e^{\pi \tan \phi} \tan^2 \left( 45^\circ + \frac{\phi}{2} \right)$
Rigidity <sup>1,2</sup>	$\zeta_{\alpha} = \zeta_{qr} - \left( \frac{1 - \zeta_{qr}}{N_c \tan \phi} \right)$ or for $\phi = 0$ $\zeta_{\alpha} = 0.32 + 0.12 \left( \frac{B}{L} \right) + 0.60 \log_{10} I_r$	$\zeta_{\gamma r} = \zeta_{qr}$	$\zeta_{qr} = \exp \left[ \left( \frac{-4.4 + 0.6 \frac{B}{L}}{L} \right) \tan \phi + \left[ \frac{3.07 \sin \phi \log_{10} 2I_r}{(1 + \sin \phi)} \right] \right]$
Shape	$\zeta_{\alpha} = 1 + \left( \frac{B}{L} \right) \left( \frac{N_q}{N_c} \right)$	$\zeta_{\gamma r} = 1 - 0.4 \left( \frac{B}{L} \right)$	$\zeta_{qr} = 1 + \left( \frac{B}{L} \right) \tan \phi$
Inclination <sup>3</sup>	$\zeta_{\alpha} = \zeta_{qi} - \left( \frac{1 - \zeta_{qi}}{N_c \tan \phi} \right)$ or for $\phi = 0$ $\zeta_{\alpha} = 1 - \left( \frac{nT}{cN_c B' L'} \right)$ $\zeta_{\alpha} = \zeta_{qr} - \left( \frac{1 - \zeta_{qr}}{N_c \tan \phi} \right)$	$\zeta_{\gamma r} = \left[ 1 - \frac{T}{N + B' L' c \cot \phi} \right]^{n+1}$	$\zeta_{qi} = \left[ 1 - \frac{T}{N + B' L' c \cot \phi} \right]^n$
Foundation tilt <sup>4</sup>	or for $\phi = 0$ $\zeta_{\alpha} = 1 - \left( \frac{2\alpha}{\pi + 2} \right)$	$\zeta_{\gamma r} = (1 - \alpha \tan \phi)^2$	$\zeta_{qr} = \zeta_{\gamma r}$
Surface inclination <sup>5</sup>	$\zeta_{\alpha} = \zeta_{qs} - \left( \frac{1 - \zeta_{qs}}{N_c \tan \phi} \right)$ or for $\phi = 0$ $\zeta_{\alpha} = 1 - \left( \frac{2\omega}{\pi + 2} \right)$	$\zeta_{\gamma s} = \zeta_{qs}$ or for $\phi = 0$ $\zeta_{\gamma s} = 1$	$\zeta_{qs} = (1 - \tan \omega)^2$ or for $\phi = 0$ $\zeta_{qs} = 1$
Depth <sup>6</sup>	or for $\phi = 0$ $\zeta_{\alpha} = 1 + 0.33 \tan^{-1} \left( \frac{D}{B} \right)$	$\zeta_{\gamma d} = 1$	$\zeta_{qd} = 1 + 2 \tan \phi (1 - \sin \phi)^2 \tan^{-1} \left( \frac{D}{B} \right)$

1. The rigidity index is defined as  $I_r = G / (c + q \tan \phi)$  in which  $G$  is the elastic shear modulus of the soil and the vertical overburden pressure,  $q$ , is evaluated at a depth of  $B/2$  below the foundation level. The critical rigidity index is defined as:

$$I_{rc} = \frac{1}{2} \exp \left[ (3.30 - 0.45B/L) \cot \left( 45^\circ - \frac{\phi}{2} \right) \right]$$

2. When  $I_r > I_{rc}$ , the soil behaves, for all practical purposes, as a rigid plastic material and the modifying factors  $\zeta_r$  all take the value 1. When  $I_r < I_{rc}$ , punching shear is likely to occur and the factors  $\zeta_r$  may be computed from the expressions in the table.

3. For inclined loading in the  $B$  direction ( $\theta = 90^\circ$ ),  $n$  is given by:  $n = n_B = (2 + B/L) / (1 + B/L)$ . For inclined loading in the  $L$  direction ( $\theta = 0^\circ$ ),  $n$  is given by:

$$n = n_L = (2 + L/B) / (1 + L/B)$$

For other loading directions,  $n$  is given by:  $n = n\theta = nL \cos^2 \theta + nB \sin^2 \theta$ .  $\theta$  is the plan angle between the longer axis of the footing and the ray from its centre to the point of application of the loading.  $B'$  and  $L'$  are the effective dimensions of the rectangular foundation, allowing for eccentricity of the loading, and  $T$  and  $N$  are the horizontal and vertical components of the foundation load.

4.  $\alpha$  is the inclination from the horizontal of the underside of the footing.

5. For the sloping ground case where  $\phi = 0$ , a non-zero value of the term  $N_\gamma$  must be used. For this case is  $N_\gamma$  negative and is given by:

$$N_\gamma = -2 \sin \omega$$

$\omega$  is the inclination below horizontal of the ground surface away from the edge of the footing.

6.  $D$  is the depth from the soil surface to the underside of the footing.

In Table 3.1 closed-form expressions have been presented for the bearing capacity factors. As noted above, some are only approximations. In particular, there have been several different solutions proposed in the literature for the bearing capacity factors  $N_\gamma$  and  $N_q$ . Solutions by Prandtl (1921) and Reissner (1924) are generally adopted for  $N_c$  and  $N_q$ , although Davis and Booker (1971) produced rigorous plasticity solutions which indicate that the commonly adopted expression for  $N_q$  (Table 3.1) is slightly non-conservative, although it is generally accurate enough for most practical applications. However, significant discrepancies have been noted in the values proposed for  $N_\gamma$ . It has not been possible to obtain a rigorous closed form expression for  $N_\gamma$ , but several authors have proposed approximations. For example, Terzaghi (1943) proposed a set of approximate values and Vesic (1975) suggested the approximation,  $N_\gamma \approx 2(N_q + 1)\tan\phi$ , which has been widely used in geotechnical practice, but is now known to be non-conservative with respect to more rigorous solutions obtained using the theory of plasticity for a rigid plastic body (Davis and Booker, 1971). An indication of the degree of non-conservatism that applies to these approximate solutions is given in Figure 3.1, where the rigorous solutions of Davis and Booker are compared with the traditional values suggested by Terzaghi. It can be seen that for values of friction angle in the typical range from  $30^\circ$  to  $40^\circ$ , Terzaghi's solutions can oversitmate this component of the bearing capacity by factors as large as 3.

Analytical approximations to the Davis and Booker solutions for  $N_\gamma$  for both smooth and rough footings are presented in Table 3.1. These expressions are accurate for values of  $\phi$  greater than about  $10^\circ$ , a range of considerable practical interest. It is recommended that the expressions derived by Davis and Booker, or their analytical approximations presented in Table 3.1, should be used in practice and the continued use of other inaccurate and non-conservative solutions should be discontinued.

Although for engineering purposes satisfactory estimates of load capacity can usually be achieved using Equation (3.1) and the factors provided in Table 3.1, this quasi-empirical expression can be considered at best only an approximation. For example, it assumes that the effects of soil cohesion, surcharge pressure and self-weight are directly superposable, whereas soil behaviour is highly non-linear and thus superposition does not necessarily hold, certainly as the limiting condition of foundation failure is approached.

Recent research into bearing capacity problems has advanced our understanding of the limitations of Equation (3.1). In particular, problems involving non-homogeneous and layered soils, and cases where the foundation is subjected to combined forms of loading have been investigated in recent years, and more rigorous solutions for these cases are now available. Some of these developments are discussed in the following sections.

### 3.2.2 Bearing capacity under combined loading

The bearing capacity Equation (3.1) was derived using approximate empirical methods, with the effect of load inclination incorporated by the addition of (approximate) inclination factors. The problem of the bearing capacity of a foundation under combined loading is essentially three-dimensional in nature, and recent research (e.g., Murff, 1994; Martin, 1994; Bransby and Randolph, 1998; Taiebat and Carter, 2000a, 2000b) has suggested that for any foundation, there is a surface in load space, independent of load path, containing all combinations of loads, i.e., vertical force ( $V$ ), horizontal force ( $H$ ) and moment ( $M$ ), that cause failure of the foundation. This surface defines a failure envelope for the foundation. A summary of recent developments in defining this failure envelope is presented in this section.

Most research conducted to date into determining the shape of the failure envelope has concentrated on undrained failure within the soil (i.e.,  $\phi = 0$  and  $c = s_u$  = the undrained shear strength) and the results are therefore relevant to cases of relatively rapid loading of fine-grained soils, including clays. For these cases several different failure envelopes have been suggested and in all cases they can be written in the following form:

$$f\left(\frac{V}{As_u}, \frac{H}{As_u}, \frac{M}{ABs_u}\right) = 0 \quad (3.2)$$

where  $A$  is the plan area of the foundation,  $B$  is its width or diameter, and  $s_u$  is the undrained shear strength of the soil below the base of the foundation.

Bolton (1979) presented a theoretical expression for the vertical capacity of a strip footing subjected to inclined load. Bolton's expression, modified by the inclusion of a shape factor of  $\zeta_s$ , provides the following expression for the ultimate capacity:

$$f = \left(\frac{V}{A}\right) - \zeta_s s_u \left[ \frac{1 + \pi - \text{Arcsin}\left(\frac{H}{As_u}\right) + \sqrt{1 - \left(\frac{H}{As_u}\right)^2}}{\sqrt{1 - \left(\frac{H}{As_u}\right)^2}} \right] = 0 \quad (3.3)$$

For square and circular foundations it is reasonable to adopt a value of  $\zeta_s = 1.2$ .

Based on the results of experimental studies of circular foundations performed by Osborne *et al.* (1991), Murff (1994) suggested a general form of three-dimensional failure locus as:

$$f = \sqrt{\left(\frac{M}{D}\right)^2 + \alpha_1 H^2} + \alpha_2 \left(\frac{V^2}{V_c} - V\left(1 + \frac{V_t}{V_c}\right) + V_t\right) = 0 \quad (3.4)$$

where  $\alpha_1$  and  $\alpha_2$  are constants,  $M$  is the moment applied to the foundation,  $V_c$  and  $V_t$  are respectively the compression and tension capacities under pure vertical load. A finite value of  $V_t$  could be mobilised in the short term due to the tendency to develop suction pore pressures in the soil under the footing. A simple form of Equation (3.4), suitable for undrained conditions, assuming  $V_t = -V_c = -V_u$ , is as follows:

$$f = \sqrt{\left(\frac{M}{\alpha_3 V_u D}\right)^2 + \left(\frac{H}{\alpha_4 V_u}\right)^2} + \left(\frac{V}{V_u}\right)^2 - 1 = 0 \quad (3.5)$$

It may be seen that  $\alpha_3 V_u D$  and  $\alpha_4 V_u$  represents the capacity of the foundation under pure moment,  $M_u$ , and pure horizontal load,  $H_u$ , respectively. Therefore Equation (3.5) can also be expressed as:

$$f = \sqrt{\left(\frac{M}{M_u}\right)^2 + \left(\frac{H}{H_u}\right)^2} + \left(\frac{V}{V_u}\right)^2 - 1 = 0 \quad (3.6)$$

A finite element study to determine the failure locus for long strip foundations on non-homogeneous clays under combined loading was presented by Bransby and Randolph (1998). The results of the finite element analyses were supported by upper bound plasticity analyses, and the following failure locus was suggested for rapid (undrained) loading conditions:

$$f = \left(\frac{V}{V_u}\right)^2 + \alpha_3 \sqrt{\left(\frac{M^*}{M_u}\right)^{\alpha_1} + \left(\frac{H}{H_u}\right)^{\alpha_2}} - 1 = 0 \quad (3.7)$$

in which

$$\frac{M^*}{ABs_{uo}} = \frac{M}{ABs_{uo}} - \left(\frac{Z}{B}\right)\left(\frac{H}{As_{uo}}\right) \quad (3.8)$$

where  $M^*$  is the moment calculated about a reference point above the base of the footing at a height  $Z$ ,  $B$  is the breadth of the strip footing,  $\alpha_1$ ,  $\alpha_2$  and  $\alpha_3$  are factors depending on the degree

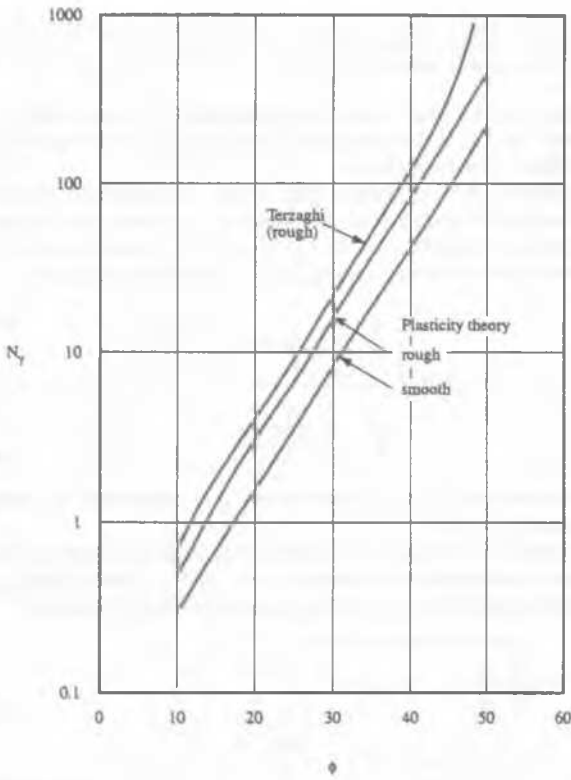


Figure 3.1. Bearing capacity factor  $N_q$  (after Davis and Booker, 1971).

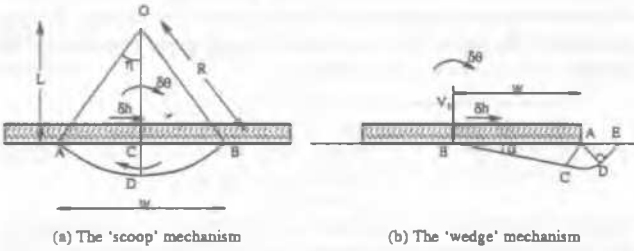


Figure 3.2. 'Scoop' and 'wedge' mechanisms proposed by Bransby and Randolph (1997).

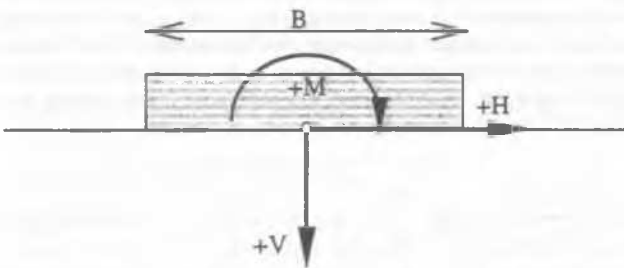


Figure 3.3. Conventions for loads and moment applied to foundations.

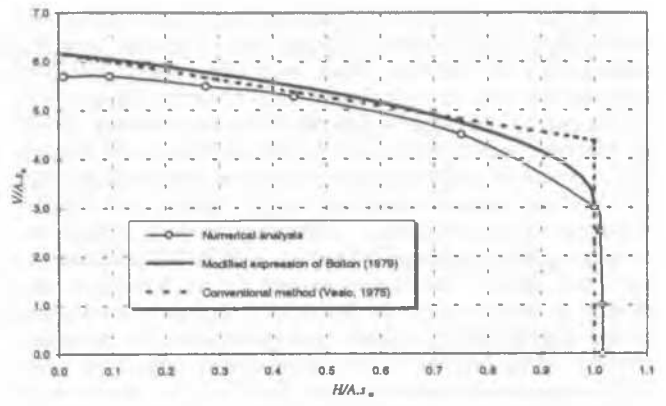


Figure 3.4. Failure loci for foundations under inclined loading ( $M = 0$ ).

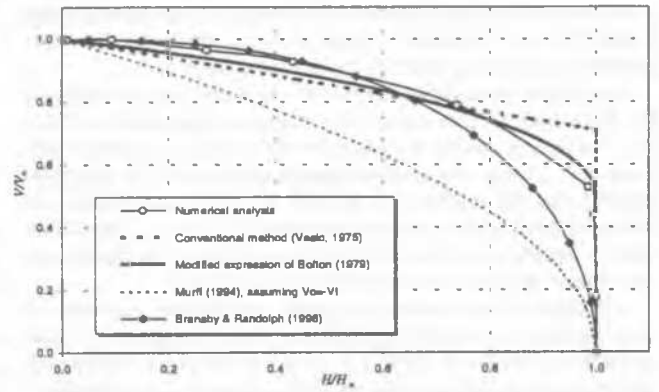


Figure 3.5. Non-dimensional failure loci in the  $V-H$  plane ( $M=0$ ).

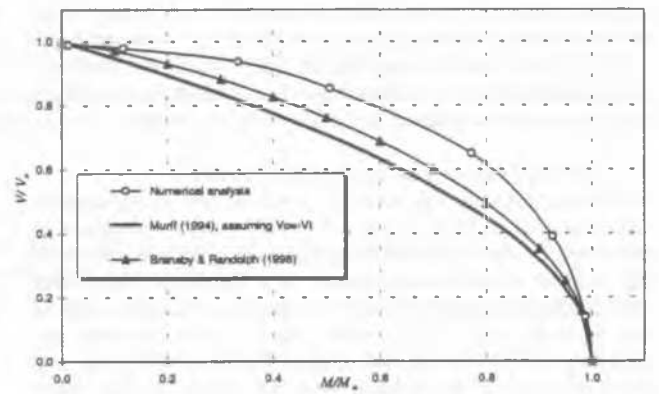


Figure 3.6. Non-dimensional failure loci in the  $V-M$  plane ( $H=0$ ).

of non-homogeneity, and  $s_{uo}$  is the undrained shear strength of the soil at the level of the foundation base. Bransby and Randolph (1998) proposed that the collapse mechanism for a footing under combined loading is based on two different component mechanisms: the 'scoop' mechanism and the 'wedge' mechanism, as illustrated in Figure 3.2.

Three-dimensional analyses of circular foundations subjected to combined loading under undrained conditions has been described by Taiebat and Carter (2000a). They compared predictions of a number of the failure criteria described previously with their three-dimensional finite element predictions of the failure surface. The sign conventions for loads and moment used in this study are based on the right-handed axes and clockwise positive conventions, ( $V, M, H$ ), as described by Butterfield *et al.* (1997) and shown in Figure 3.3.

#### Vertical-Horizontal (V-H) Loading

Taiebat and Carter's finite element prediction of the failure envelope in the  $V-H$  plane is presented in Figure 3.4, together with the conventional solution of Vesic (1975), Equation (3.1), and the modified expression of Bolton (1979), Equation (3.4) with a shape factor  $\zeta_s = 1.2$ . Comparison of the curves in Figure 3.4 shows that the numerical analyses generally give a more conservative bearing capacity for foundations subjected to inclined load. The results of the numerical analyses are very close to the results of the modified theoretical expression of Bolton (1979).

All three methods indicate that there is a critical angle of inclination, measured from the vertical direction, beyond which the ultimate horizontal resistance of the foundation dictates the failure of the foundation. Where the inclination angle is more than the critical value, the vertical force does not have any influence on the horizontal capacity of the foundation. For circular foundations the critical angle is predicted to be approximately  $19^\circ$  by the numerical studies and from the modified expression of Bolton (1979), compared to  $13^\circ$  predicted by the conventional method of Vesic (1975). In Figure 3.5, the non-dimensional form of the failure envelope predicted by the finite element analyses is compared with those of Vesic (1975), Equation (3.1), Bolton (1979), Equation (3.4), Murff (1994), Equation (3.6), and Bransby and Randolph (1998), Equation (3.7). The shape of the failure locus predicted by the numerical analyses is closest to the modified expression of Bolton (1979). It can be seen that the conventional method gives a good approximation of the failure locus except for high values of horizontal loads. The failure locus presented by Murff (1994) gives a very conservative approximation of the other failure loci.

#### Vertical-Moment (V-M) Loading

For a circular foundation on an undrained clay subjected to pure moment, an ultimate capacity of  $M_u = 0.8A.D.s_u$  was predicted by the finite element analysis of Taiebat and Carter (2000). In Figure 3.6 the predicted failure envelope is compared with those of Murff, Equation (3.6), and Bransby and Randolph, Equation (3.7). The failure envelopes approximated by Murff (1994) and Bransby and Randolph (1998) are both conservative with respect to the failure envelope predicted by the numerical analyses. It is noted that the equations presented by Bransby and Randolph were suggested for strip footings, rather than the circular footing considered here.

#### Horizontal-Moment (H-M) Loading

The failure locus predicted for horizontal load and moment is plotted in Figure 3.7. A maximum moment capacity of  $M = 0.89A.D.s_u$  is coincident with a horizontal load of  $H = 0.71A.s_u$ . This is 11% greater than the capacity predicted for the foundation under pure moment.

A non-dimensional form of the predicted failure locus and the suggestions of Murff (1994) and Bransby and Randolph (1998) are plotted in Figure 3.8. It can be seen that the locus suggested by Murff (1994) is symmetric and the maximum moment coincides with zero horizontal loading, whereas the numerical analy-

ses show that the maximum moment is sustained with a positive horizontal load, as already described. The failure locus obtained from Murff's equation becomes non-conservative when  $M \times H \leq 0$ . Bransby and Randolph (1998) identified two different upper bound plasticity mechanisms for strip footings under moment and horizontal load, a scoop mechanism and a scoop-wedge mechanism (Figure 3.2). The latter mechanism results in greater ultimate moment capacity for strip footings, supporting the finite element predictions.

#### General Failure Equation

An accurate three-dimensional equation for the failure envelope in its complete form, which accounts for both the load inclination and eccentricity, is likely to be a complex expression. Some degree of simplification is essential in order to obtain a convenient form of this failure envelope. Depending on the level of the simplification, different classes of failure equations may be obtained.

In the previous section, the failure envelopes suggested by different methods were compared in two-dimensional loading planes. It was demonstrated that the failure equation presented by Murff (1994) has simplicity in its mathematical form, but does not fit the failure envelopes produced by the conventional and numerical analyses. The failure equation presented by Bransby and Randolph (1998) for strip footings matches the data for circular footings in two planes, but does not give a suitable answer in three-dimensional load space.

A new equation describing the failure locus in terms of all three components of the load has been proposed recently by Taiebat and Carter (2000a). In formulating this equation, advantage was taken of the fact that the moment capacity of the foundation is related to the horizontal load acting simultaneously on the foundation. The proposed approximate failure equation is expressed as:

$$f = \left( \frac{V}{V_u} \right)^2 + \left( \frac{M}{M_u} \left( 1 - \alpha_1 \frac{H.M}{H_u |M|} \right) \right)^2 + \left( \frac{H}{H_u} \right)^3 - 1 = 0 \quad (3.9)$$

where  $\alpha_1$  is a factor that depends on the soil profile. For a homogeneous soil a value of  $\alpha_1 = 0.3$  provides a good fit to the bearing capacity predictions from the numerical analysis. Perhaps inevitably, the three-dimensional failure locus described by Equation (3.9) will not tightly match the numerical predictions over the entire range of loads, especially around the abrupt changes in the failure locus that occur when the horizontal load is high. However, overall the approximation is satisfactory, conservative and sufficient for many practical applications. Equation (3.9) is shown as a contour plot in Figure 3.9.

#### 3.2.3 Bearing capacity under eccentrically applied loading

There is no exact expression to evaluate the effects of eccentricity of the load applied to a foundation. However, the effective width method is commonly used in the analysis of foundations subjected to eccentric loading (e.g., Vesic, 1973; Meyerhof, 1951, 1953). In this method, the bearing capacity of a foundation subjected to an eccentrically applied vertical loading is assumed to be equivalent to the bearing capacity of another foundation with a fictitious effective area on which the vertical load is centrally applied.

Studies aimed at determining the shape of the failure locus in ( $V-M$ ) space (e.g., Taiebat and Carter, 2000a, 2000b; Houslyby and Puzrin, 1999) are relevant, because this loading case is also directly applicable to the analysis of a footing to which vertical load is eccentrically applied.

Finite element modelling of the problem of the bearing capacity of strip and circular footings on the surface of a uniform homogeneous undrained clay layer, subjected to vertical load and moment was described by Taiebat and Carter (2000b). It was also assumed in this particular study that the contact between the footing and the soil was unable to sustain tension. The failure



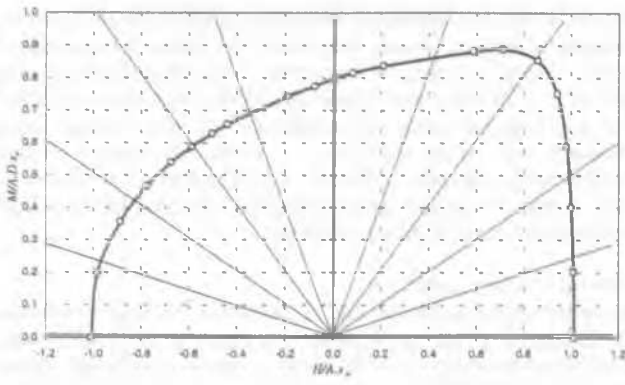


Figure 3.7. Failure loci in the  $M-H$  plane ( $V=0$ ).

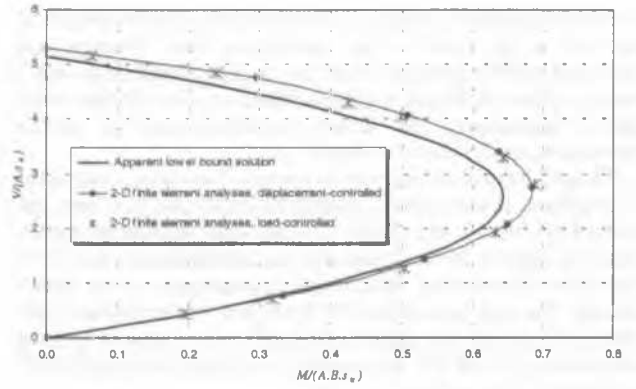


Figure 3.10. Failure loci for a strip footing under eccentric loading.

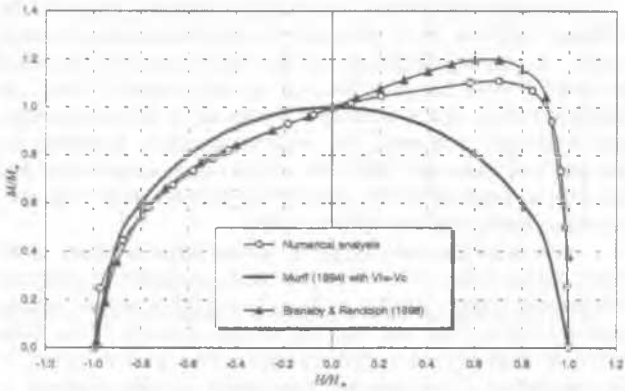


Figure 3.8. Non-dimensional failure loci in the  $M-H$  plane ( $V=0$ ).

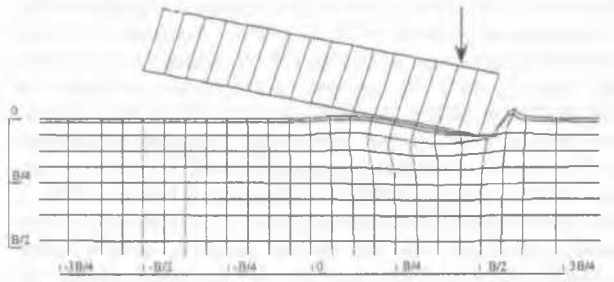


Figure 3.11. Deformed shape of the soil and the strip footing under an eccentric load.

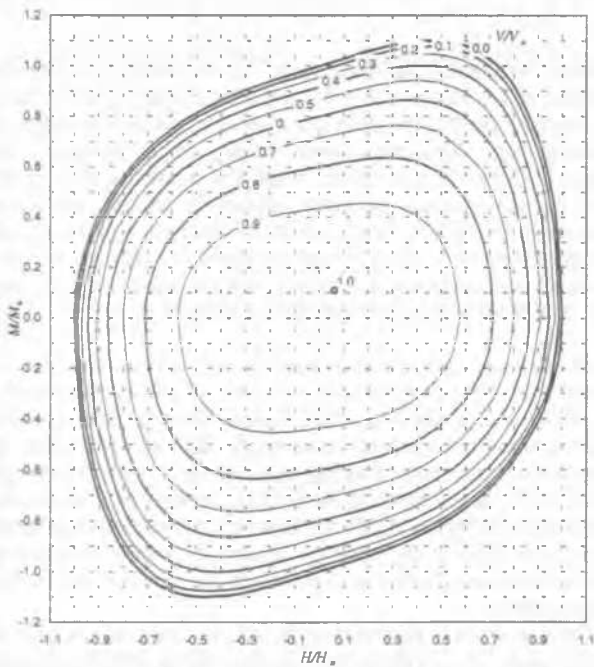


Figure 3.9. Representation of the proposed failure equation in non-dimensional  $V-M-H$  space.

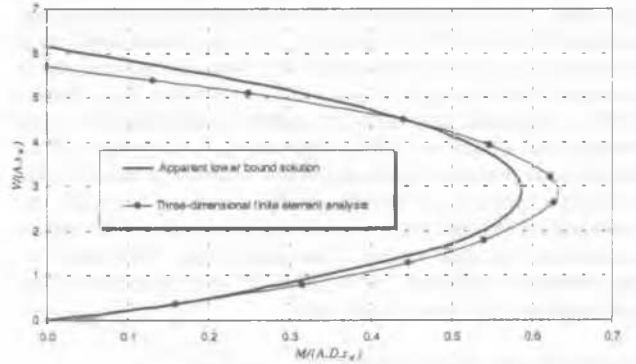


Figure 3.12. Failure loci for a circular footing under eccentric loading.

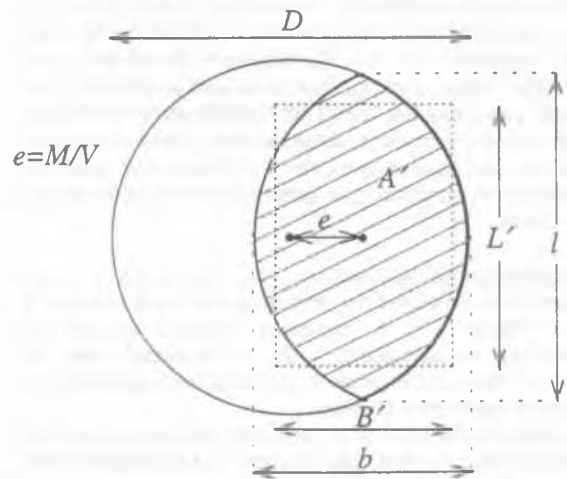


Figure 3.13. Effective area of a circular footing subjected to eccentric load.

envelopes predicted by Taiebat and Carter (2000b) have also been compared with the solutions obtained using the lower bound theorem of plasticity. The "lower bound" solutions satisfy equilibrium and do not violate the yield criterion. However, some of the solutions may not adhere strictly to all requirements of the lower bound theorem. For example, loss of contact at the footing-soil interface implies that the normality principle is not always obeyed. Therefore, the term "apparent lower bound" is used to describe these solutions, as suggested by Houlsby and Purzin (1999).

#### Strip footings

The failure envelope predicted by two-dimensional finite element analysis of a strip footing under both vertical load and moment is presented in Figure 3.10. Also shown in this figure is the failure envelope resulting from the apparent lower bound solutions of Houlsby and Purzin (1999), which is described by the following equation:

$$\frac{V}{A} = (\pi + 2) \left( 1 - \frac{2M}{VB} \right) s_u \quad (3.10)$$

where  $V$  is the vertical load,  $A$  is the area of the foundation, and  $M$  is the moment applied to the foundation. The failure envelope predicted by the finite element method is in good agreement with the envelope obtained from the apparent lower bound solutions. Figure 3.11 shows the deformed shape of the soil and the strip foundation under a vertical load applied with relatively large eccentricity.

#### Circular footings

The failure envelope predicted by three-dimensional finite element analyses and lower bound analyses of circular footings subjected to both vertical load and moment are presented in Figure 3.12. Good agreement between the two solutions is evident in this figure. It is noted that the apparent lower bound solution presented by Houlsby and Purzin (1999) is for conditions of plane strain only. For the three-dimensional case, the apparent lower bound solutions shown in Figure 3.12 have been obtained based on the following considerations.

A circular foundation, subjected to a vertical load applied with an eccentricity  $e = M/V$ , can be regarded as an equivalent fictitious foundation with a centrally applied load (Figure 3.13) as suggested by Meyerhof (1953) and Vesic (1973). For a circular footing the area of the fictitious foundation,  $A'$ , can be calculated as:

$$A' = \frac{D^2}{2} \left( \text{Arccos} \frac{2e}{D} - \frac{2e}{D} \sqrt{1 - \left( \frac{2e}{D} \right)^2} \right) \quad (3.11)$$

The aspect ratio of the equivalent rectangular area can also be approximated as the ratio of the lengths  $b$  and  $l$ , as shown in Figure 3.13, i.e.,

$$\frac{B'}{L'} = \frac{b}{l} = \sqrt{\frac{D-2e}{D+2e}} \quad (3.12)$$

Therefore, in this case the shape factor for the fictitious rectangular foundation is given by (Vesic, 1973):

$$\zeta_s = 1 + 0.2 \sqrt{\frac{DV - 2M}{DV + 2M}} \quad (3.13)$$

Hence, the bearing capacity of circular foundations subjected to eccentric loading can be obtained from the effective width method as:

$$V = \zeta_s A' (2 + \pi) s_u \quad (3.14)$$

Note that based on Vesic's recommendation the shape factor for circular footings under the pure vertical load is usually

adopted as  $\zeta_s = 1.2$ . However, exact solutions for the vertical bearing capacity of circular footings on uniform Tresca soil (Shield, 1955; Cox, 1961) suggest the ultimate bearing capacity of  $5.69 A \cdot s_u$  and  $6.05 A \cdot s_u$  for smooth and rough footings, respectively. Therefore, the appropriate shape factors are actually 1.11 and 1.18 for smooth and rough footings.

In summary, it is clear from the comparisons presented in this section that the effective width method, commonly used in the analysis of foundations subjected to eccentric loading, provides good approximations to the collapse loads. Its continued use in practice therefore appears justified.

#### 3.2.4 Bearing capacity of non-homogeneous soils

Progress has also been made in recent decades in predicting reliably the ultimate bearing capacity of foundations on non-homogeneous soils. A particular example is the important case that arises often in practice where the undrained shear strength of the soil varies approximately linearly with depth below the soil surface, i.e.,

$$s_u = c_0 + \rho z \quad (3.15)$$

or below a uniform crust, i.e.,

$$\begin{aligned} s_u &= c_0 & \text{for } z < \frac{c_0}{\rho} \\ s_u &= \rho z & \text{for } z > \frac{c_0}{\rho} \end{aligned} \quad (3.16)$$

in which  $c_0$  is the undrained shear strength of the soil at the surface,  $\rho$  is the strength gradient and  $z$  is the depth below the soil surface. Several theoretical approaches attempted to take account of this effect, most notably the work by Davis and Booker (1973) and Houlsby and Wroth (1983). Both used the method of stress characteristics from the theory of plasticity. Assuming the soil to obey the Tresca yield criterion, Davis and Booker's plane strain solution has been expressed as:

$$q_u = \frac{Q_u}{B} = F \left[ (2 + \pi) c_0 + \frac{\rho B}{4} \right] \quad (3.17a)$$

where  $F$  is a function of the soil strength non-homogeneity ( $\rho B/c_0$ ) and the roughness of the foundation-soil interface. Values of the bearing capacity factor  $F$  are reproduced in Figure 3.14 for two different undrained strength profiles. It is worth noting that the solutions of Davis and Booker (1973) can also be adapted to circular footings, at least approximately, by the replacement of Equation (3.17a) by:

$$q_u = \frac{Q_u}{B} = F \left[ 6c_0 + \frac{\rho B}{4} \right] \quad (3.17b)$$

Tani and Craig (1995) also investigated the case where the undrained shear strength is proportional to depth using plasticity theory. They made predictions of the bearing capacity of skirted offshore gravity structures with skirt length to diameter ratios of 0 to 0.3. They found that their results for surface and circular footings (for both smooth and rough interfaces) obtained using the method of stress characteristics agree very well with the solutions obtained by Davis and Booker (1973) and Houlsby and Wroth (1983). Tani and Craig's results for the computed bearing capacity of an embedded rough footing are reproduced here in Figure 3.15. In this figure  $c_{Df}$  is the undrained strength of the clay at the level of the footing base,  $k$  is the rate of increase of strength with depth,  $Df$  is the depth to the base of the footing, and  $B$  and  $D$  are the width and diameter of the strip and circle, respectively. Tani and Craig found that the ultimate bearing capacity of the foundation was governed largely by the strength of the soil at the skirt tip rather than at surface level. Soil above this level has little influence on the bearing capacity of the footing. It may be concluded from these results that the increase in

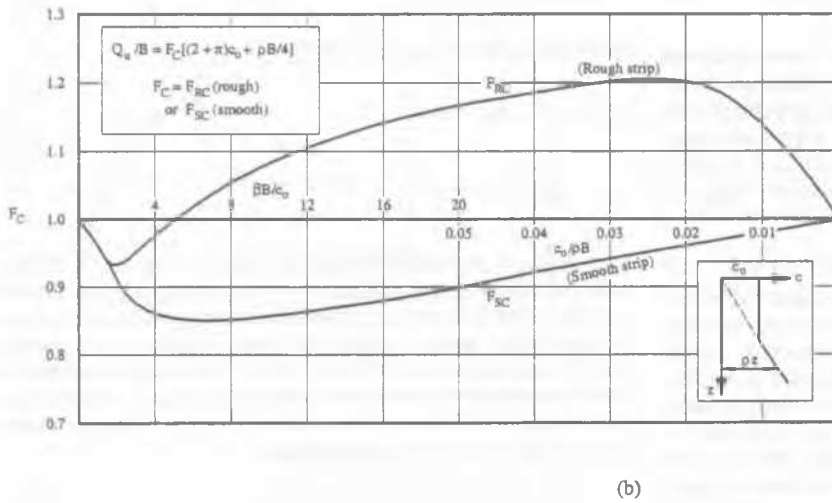
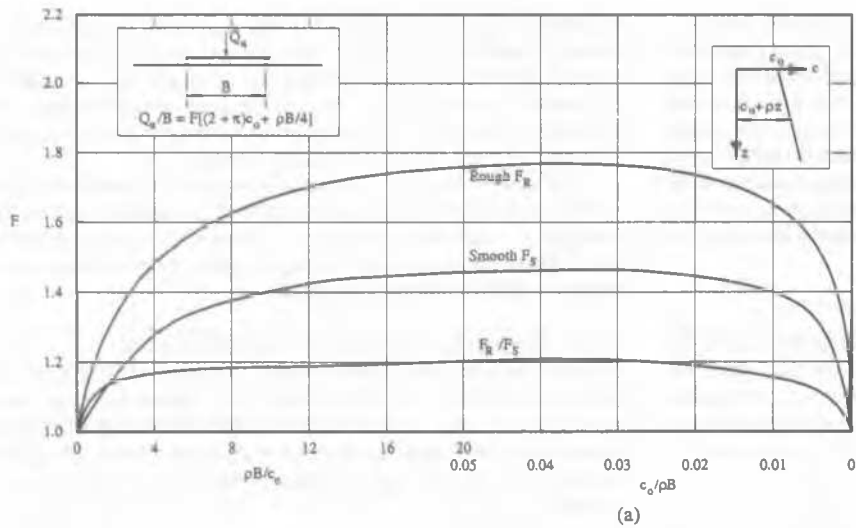


Figure 3.14. Bearing capacity of a strip footing on non-homogeneous clay (after Davis and Booker, 1973).

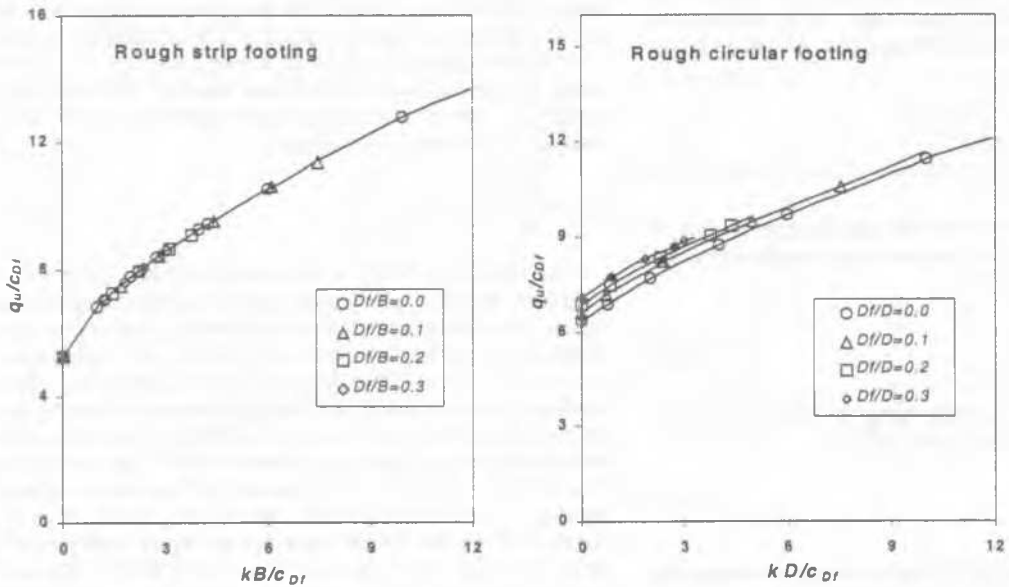


Figure 3.15. Bearing capacity of rough strip footing and circular footing on non-homogeneous clay (after Tani and Craig, 1995.)

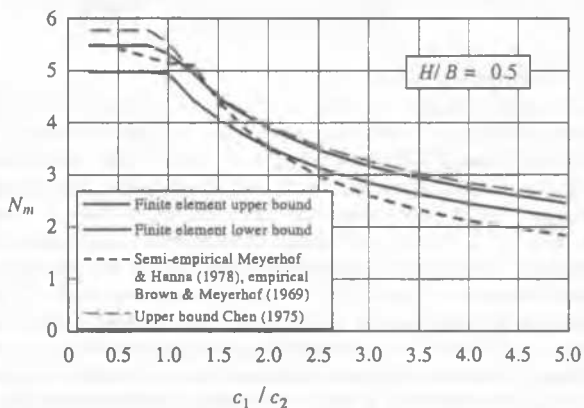
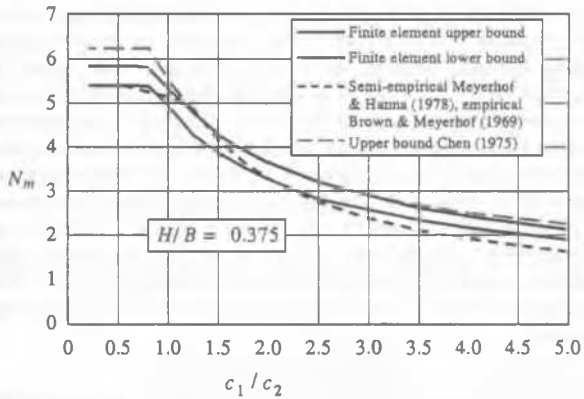
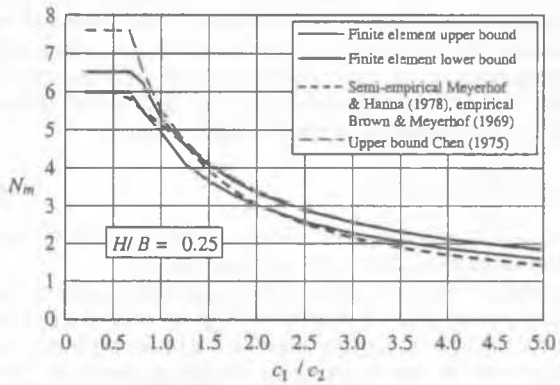
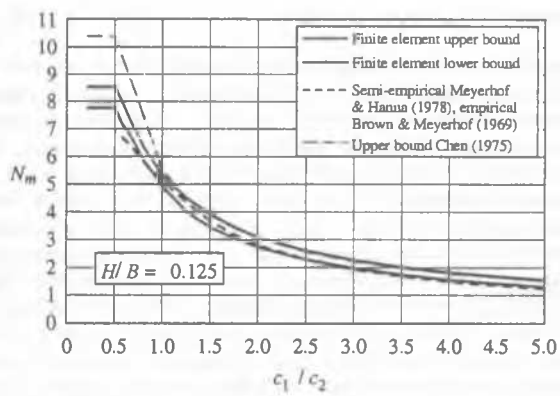


Figure 3.16. Bearing capacity factor  $N_m$  for a two-layered clay (after Merfield et al., 1999).

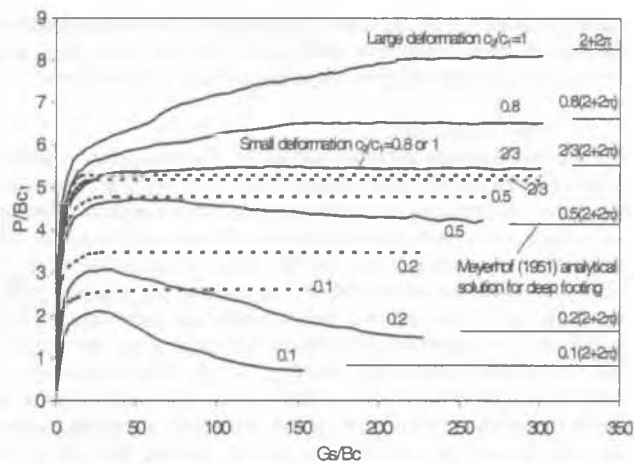
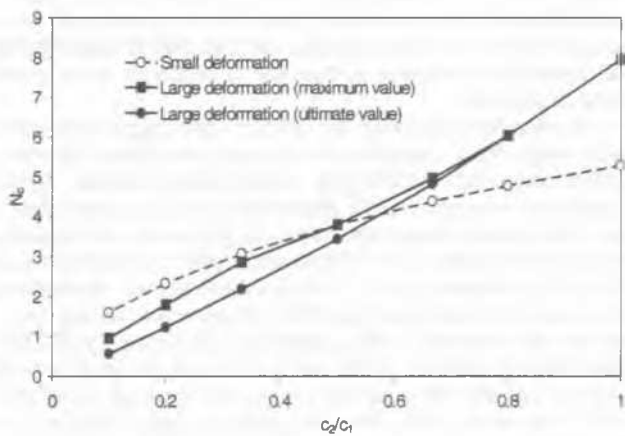
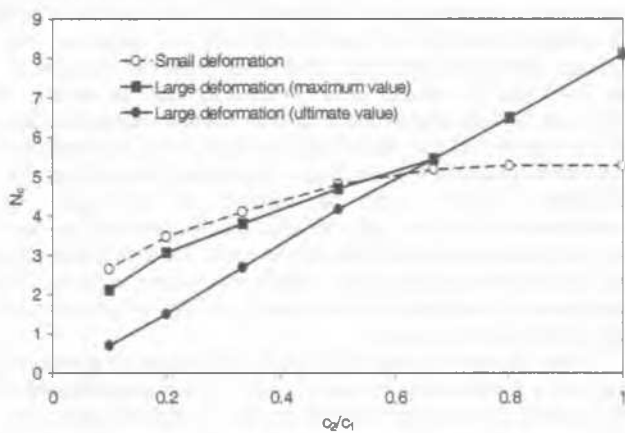


Figure 3.17. Normalised load-settlement curves for layered clay ( $G/c = 67$ ,  $H/B = 1$ ) (after Wang, 2000).



(a)  $H/B = 0.5$



(b)  $H/B = 1$

Figure 3.18. Bearing capacity factors for a rigid strip footing on a two-layered clay (after Wang, 2000).

bearing capacity with increasing embedment can be attributed to the higher shear strength at the tip level for the most part, and very little to the shearing resistance of the soil above tip level.

### 3.2.5 Two-layered soils

Natural soil deposits are often formed in discrete layers. For the purpose of estimating the ultimate bearing capacity of a foundation on a layered soil it is often appropriate to assume that the soil within each layer is homogeneous. If a footing is placed on the surface of a layered soil and the thickness of the top layer is large compared with the width of the footing, the ultimate bearing capacity of the soil and the displacement behaviour of the footing can be estimated to sufficient accuracy using the properties of the upper layer only. However, if the thickness of the top layer is comparable to the footing width, this approach introduces significant inaccuracies and is no longer appropriate. This is because the zone of influence of the footing, including the potential failure zone, may extend to a significant depth, and thus two or more layers within that depth range will affect the bearing behaviour of the footing. Examples include offshore foundations of large physical dimensions, and vehicle loads applied to unpaved roads over soft clay deposits.

The case of a footing on a stronger soil layer overlying a weaker layer is of particular interest because of the risk of punch-through failure occurring. Such failures are normally sudden and brittle, with little warning, and methods of analysis that can predict the likelihood of this type of behaviour are of great value in practice.

Methods for calculating the bearing capacity of multi-layer soils range from averaging the strength parameters (Bowles, 1988), using limit equilibrium considerations (Button, 1953; Reddy and Srinivasan, 1967; Meyerhof, 1974), to a more rigorous limit analysis approach based on the theory of plasticity (Chen and Davidson, 1973; Florkiewicz, 1989; Michalowski and Shi, 1995; Merifield, *et al.*, 1999). Semi-empirical approaches have also been proposed based on experimental studies (e.g., Brown and Meyerhof, 1969; Meyerhof and Hanna, 1978). The finite element method, which can handle very complex layered patterns, has also been applied to this problem. (e.g., Griffiths, 1982; Love *et al.*, 1987; Burd and Frydman, 1997; Merifield, *et al.*, 1999).

However, almost all these studies are limited to footings resting on the surface of the soil and are based on the assumption that the displacement of the footing prior to attaining the ultimate load is relatively small. In some cases, such as those where the underlying soil is very soft, the footings will experience significant settlement, and sometimes even penetrate through the top layer into the deeper layer. Penetration into the seabed of spud-can footings supporting a jack-up platform provides a particular example of this behaviour. For these cases, the small displacement assumption is no longer appropriate, and a large displacement theory should be adopted. In all cases, the consequences for the load-deformation response of a non-homogeneous soil profile should be understood, because such profiles can be associated with a brittle foundation response. The prediction of brittleness in these cases can only be made using a large deformation analysis.

A brief review of recent small and large deformation analyses applied to foundations on layered soils is therefore presented in this section. In particular, the behaviour of rigid strip and circular footings penetrating two-layered clays is discussed first, followed by the problem of a sand layer overlying clay. In most cases, the upper layer is at least as strong as the lower layer, so that the issue of punch-through failure can be explored.

#### Small deformation analysis

In the absence of surcharge pressure, the ultimate bearing capacity,  $q_u$ , of a strip or circular footing on a two-layered purely cohesive soil can be expressed as:

$$q_u = c_1 N_m \quad (3.18)$$

where  $N_m$  is the modified bearing capacity factor that will depend on the strength ratio of the two layers  $c_2/c_1$  and the relative thickness of the top layer,  $H/B$ .  $c_1$  and  $c_2$  denote the undrained shear strengths of the top and bottom layers, respectively,  $H$  is the thickness of the top layer and  $B$  is the foundation width (or diameter). Equation (3.18) is both a simplification and an extension to account for layering of the general bearing capacity Equation, (3.1). Several researchers have published approximate solutions for the bearing capacity factor  $N_m$  appearing in Equation (3.18). For strip footings, Button (1953) and Reddy and Srinivasan (1967) have suggested very similar values for  $N_m$ . These include both upper bound plasticity solutions to this problem, and at one extreme they return a bearing capacity factor for a homogeneous soil (considered as a special case of a two-layered soil) of 5.51, i.e., approximately 7% above Prandtl's exact solution of  $(2+\pi)$ . Brown and Meyerhof (1969) published bearing capacity factors based on experimental studies, and their recommendations are in better agreement with the value of  $(2+\pi)$  for the case of a homogeneous soil. The Brown and Meyerhof factors can be expressed by the following equation:

$$N_m = 1.5 \left( \frac{H}{B} \right) + 5.14 \left( \frac{c_2}{c_1} \right) \quad (3.19)$$

with an upper limit for  $N_m$  of 5.14 in this case.

Recently, Merifield *et al.* (1999) calculated rigorous upper and lower bound bearing capacity factors for layered clays under strip footings by employing the finite element method in conjunction with the limit theorems of classical plasticity. The results of their extensive parametric study have been presented in both graphical and tabular form. Some typical results are reproduced in Figure 3.16.

The number of published studies of circular footings on layered cohesive soil is significantly less than for strip footings. Bearing capacity factors for circular footings were given by Vesic (1970) for the case of a relatively weak clay layer overlying a stronger one. These factors were obtained by interpolation between known rigorous solutions for related problems, and they have been published in Chapter 3 of the text by Winterkorn and Fang (1975). Based on the results of model tests, Brown and Meyerhof (1969) suggested that for cases where a stronger clay layer overlies a weaker one, an analysis assuming simple shear punching around the footing perimeter is appropriate. The bearing capacity factors for this case are given by the following equation:

$$N_m = 1.5 \left( \frac{H}{B} \right) + 6.05 \left( \frac{c_2}{c_1} \right) \quad (3.20)$$

with an upper limit for  $N_m$  of 6.05 for a circular footing of diameter  $B$ .

#### Large deformation analysis

The bearing response of strip footings on a relatively strong undrained clay layer overlying a weaker clay layer has been examined by Wang (2000) and Wang and Carter (2000), who compared the results given by both small and large deformation analyses. Cases corresponding to  $H/B = 0.5$  and 1, and  $c_2/c_1 = 0.1, 0.2, 1/3, 0.5, 2/3$  and 1 (homogeneous soil) were investigated. Normalised load-displacement curves for weightless soil are shown in Figure 3.17, for cases where the width of the footing is the same as the thickness of the stronger upper clay layer, i.e.,  $H/B = 1$ . It is noted that predictions of the large deformation behaviour are also dependent on the rigidity index of the clay,  $G/c$ , where  $G$  is the elastic shear modulus of the clay. The curves shown in Figure 3.17 correspond to a value of  $G/c = 67$ .

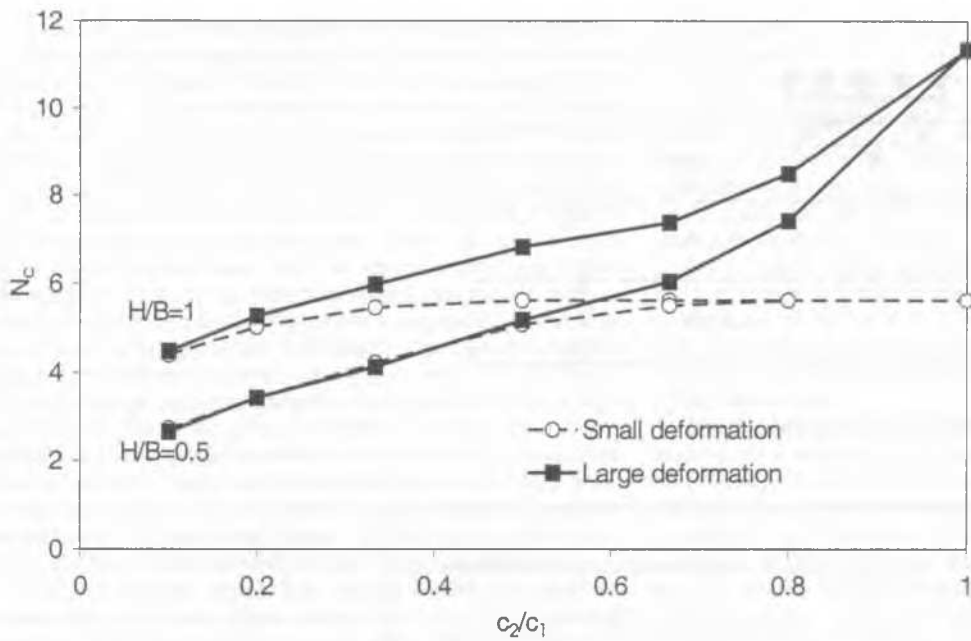


Figure 3.19. Maximum bearing capacity factors for a circular footing on a two-layered clay (after Wang, 2000).

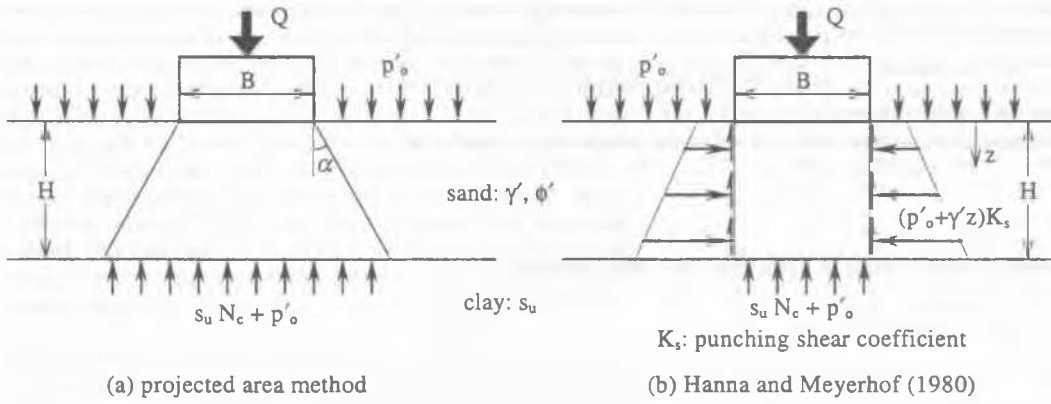


Figure 3.20. Failure mechanisms assumed in two methods of analysis of bearing capacity of a layer of sand over clay.

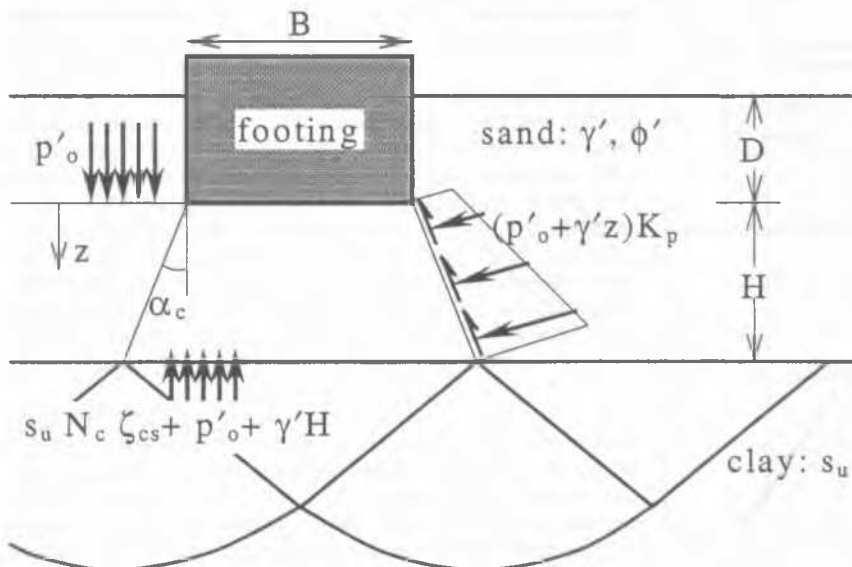


Figure 3.21. Failure mechanisms suggested by Okimura *et al.* (1998) for estimating the bearing capacity of a layer of sand over clay.

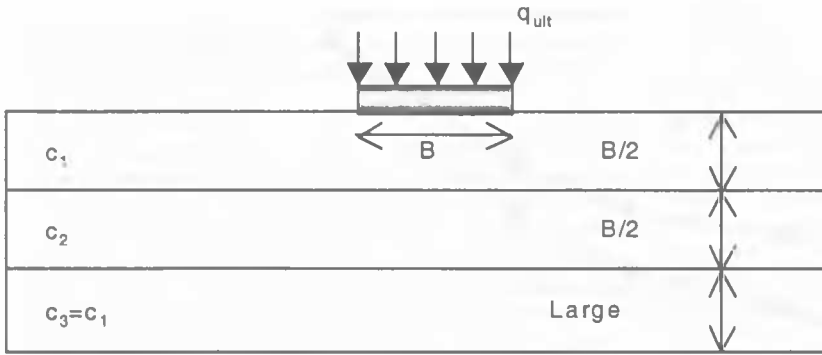


Figure 3.22. Bearing capacity of a strip footing on a layered soil deposit.

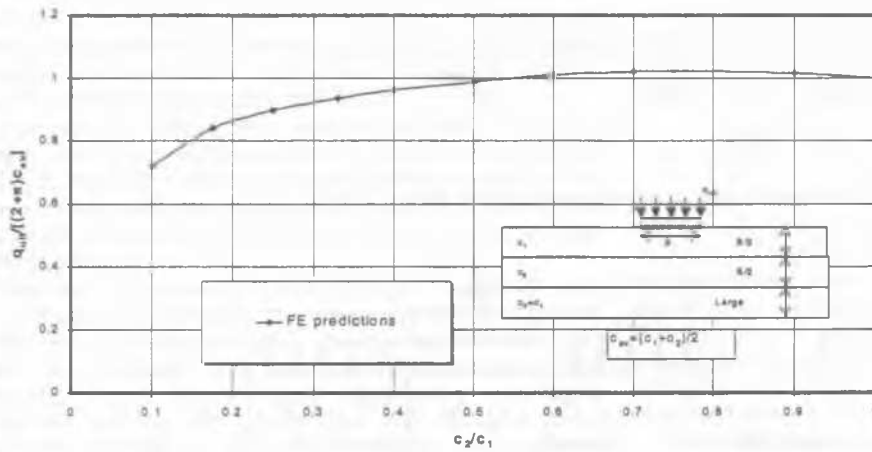


Figure 3.23. Bearing capacity charts for a strip footing on layered clay – soft centre “sandwich”.

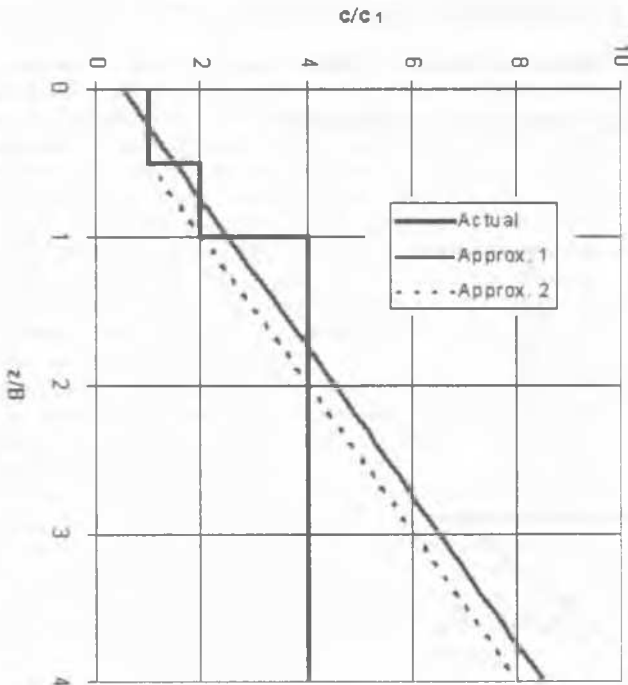


Figure 3.24. Strength profiles for layered clay.

Typically, the curve predicted by the small deformation analysis reaches an ultimate value after a relatively small footing penetration (settlement). Generally, the load-displacement curves predicted by the large deformation analyses are quite different from those given by the small displacement analysis. For cases where a stronger top layer overlies a much weaker bottom layer (e.g.,  $c_2/c_1 = 0.1, 0.2,$  and  $0.5$ ), the overall response is characterised by some brittleness, even though the behaviour of both component materials is perfectly plastic and thus characterised by an absence of brittleness. For these cases, the load-penetration curves given by the large deformation analysis rise to a peak, at which point the average bearing pressure is generally lower than the ultimate bearing capacity predicted by the small deformation analysis. With further penetration of the footing into the clay, it appears that the load-displacement curve approaches an asymptotic value. The peak values of average bearing pressure obtained from these large deformation curves define the maximum bearing capacity factor, and the values reached after large penetration are referred to as the ultimate bearing capacity factor. It is noted that in the small deformation analysis, the maximum and ultimate values of the bearing capacity factor are identical.

It is reasonable to expect that footings exhibiting a brittle response should ultimately behave much like a strip footing deeply buried in the lower clay layer, so that the ultimate value of the average bearing pressure should then be approximately  $(2+2\pi)c_2$ , where  $c_2$  is the undrained shear strength of the lower layer. These theoretical limits are also indicated on Figure 3.17, and it seems clear that the curves obtained from the large deformation finite element analysis approach closely these limiting values at deep penetrations. In Figure 3.18, values of the bearing capacity factors for cases where  $H/B = 0.5$  and  $H/B = 1$  have been plotted against the strength ratio,  $c_2/c_1$ . Also plotted in this figure are the bearing capacity factors predicted by the small deformation analysis. Wang (2000) has also demonstrated that large deformation effects appear to be even more significant for the case of a circular footing. In all the cases examined, the maximum bearing capacity factors obtained from the large deformation analysis were greater than those obtained from the small deformation analysis. Both sets of values are plotted in Figure 3.19.

#### Effect of soil self-weight during footing penetration

It is well known that for a surface footing on a purely cohesive soil, the ultimate bearing capacity given by a small strain undrained analysis is independent of the soil density. However, in large deformation analysis, the footing can no longer be regarded as a surface footing once it begins to penetrate into the underlying material, and in this case the self-weight of the soil will also affect the penetration resistance.

The results of the large deformation footing analyses presented in the previous section were obtained by Wang without considering soil self-weight. This was done deliberately in order to investigate the effects of the large deformation analysis exclusively on the bearing capacity factor  $N_m$ . However, if soil self-weight is included, the surcharge pressure becomes significant as the footing becomes buried. It was demonstrated by Wang (2000) that it is reasonable to approximate the mobilised penetration resistance for a ponderable soil as that for the corresponding weightless soil supplemented by the overburden pressure corresponding to the depth of footing penetration.

#### Sand overlying clay

Various theoretical and experimental studies have been conducted into the ultimate bearing capacity of a footing on a layer of sand overlying clay, e.g., Yamaguchi (1963), Brown and Paterson (1964), Meyerhof (1974), Vesic (1975), Hanna and Meyerhof (1980), Craig and Chua (1990), Michalowski and Shi (1995), Vinod (1995), Kenny and Andrawes (1997), Burd and Frydman (1997), Okamura *et al.* (1998). This is an important problem in foundation engineering, as this case often arises in practice and it is one in which punch-through failure may be a

genuine concern, particularly for relatively thin sand layers overlying soft clays.

Exact plasticity solutions for this problem have not yet been published, but a number of the existing analyses of the bearing capacity of sand over clay use limit equilibrium techniques. They can be broadly classified according to the shape of the sand block punching into the clay layer and the shearing resistance assumed along the side of the block. Two proposed failure mechanisms are illustrated in Figure 3.20. In each case the strength of the sand is analysed in terms of effective stress, using the effective unit weight ( $\gamma'$ ) and the friction angle ( $\phi'$ ), while the analysis of the clay is in terms of total stress, characterised by its undrained shear strength ( $s_u$ ). In the case of the "projected area" method an additional assumption about the angle  $\alpha$  (Figure 3.20a) is required.

Okamura *et al.* (1998) assessed the validity of these two approaches by comparing their predictions with the results of some 60 centrifuge model tests. This comprehensive series of tests included strip and circular footings on the surface of the sand and embedded in it. Significant differences between observed and calculated bearing capacities were noted and these were attributed to discrepancies in the shapes of the sand block or the forces acting on the sides of the block. To overcome these problems Okamura *et al.* proposed an alternative failure mechanism, which can be considered as a combination of the two mechanisms shown in Figure 3.20. Their new limit equilibrium mechanism is illustrated in Figure 3.21, in which it is noted that  $K_p$  is Rankine's passive earth pressure coefficient for the sand, i.e.,  $K_p = (1 + \sin\phi)/(1 - \sin\phi)$ . In this method it is assumed that a normal stress of  $K_p$  times the vertical overburden pressure acts on the inclined sides of the sand block. Consideration of equilibrium of the forces acting on the sand block, including its self-weight, provides the following bearing capacity formulae:

(i) for a strip footing;

$$q_u = \left( 1 + 2 \frac{H}{B} \tan \alpha_c \right) (s_u N_c + p'_o + \gamma H) + \left( \frac{K_p \sin(\phi' - \alpha_c)}{\cos \phi' \cos \alpha_c} \right) \times \left( \frac{H}{B} \right) (p'_o + \gamma H) - \gamma H \left( 1 + \frac{H}{B} \tan \alpha_c \right) \quad (3.21)$$

(ii) for a circular footing;

$$q_u = \left( 1 + 2 \frac{H}{B} \tan \alpha_c \right)^2 (s_u N_c \zeta_s + p'_o + \gamma H) + \left( \frac{4K_p \sin(\phi' - \alpha_c)}{\cos \phi' \cos \alpha_c} \right) \times \left\{ \left( \frac{H}{B} \right) \left( p'_o + \frac{\gamma H}{2} \right) + p'_o \tan \alpha_c \left( \frac{H}{B} \right)^2 + \frac{2}{3} \gamma H \tan \alpha_c \left( \frac{H}{B} \right)^2 \right\} - \frac{\gamma H}{3} \left\{ 4 \left( \frac{H}{B} \right)^2 \tan^2 \alpha_c + 6 \frac{H}{B} \tan \alpha_c + 3 \right\} \quad (3.22)$$

where  $\zeta_s$  is the shape factor for a circular footing, which is usually assigned a value of 1.2. In these equations the angle  $\alpha_c$  (Figure 3.21) is given as a function of the friction angle of the sand,  $\phi'$ , the geometry of the layer and footing and the undrained strength of the clay,  $s_u$ , i.e.,



$$\alpha_c = \tan^{-1} \left( \frac{(\sigma_{mc}/s_u) - (\sigma_{ms}/s_u)(1 + \sin^2 \phi')}{\cos \phi' \sin \phi' (\sigma_{ms}/s_u) + 1} \right) \quad (3.23)$$

where

$$\sigma_{mc}/s_u = N_c s_u \left( 1 + \frac{1}{\lambda_c} \frac{H}{B} + \frac{\lambda_p}{\lambda_c} \right) \quad (3.24)$$

and

$$\sigma_{ms}/s_u = \frac{\sigma_{mc}/s_u - \sqrt{(\sigma_{mc}/s_u)^2 - \cos^2 \phi' ((\sigma_{mc}/s_u)^2 + 1)}}{\cos^2 \phi'} \quad (3.25)$$

The parameters  $\lambda_p$  and  $\lambda_c$  are respectively the normalised overburden pressure and the normalised bearing capacity of the underlying clay, given by:

$$\lambda_p = \frac{p'_o}{\gamma B} \quad (3.26)$$

and

$$\lambda_c = \frac{s_u N_c}{\gamma B} \quad (3.27)$$

$N_c$  is the conventional bearing capacity factor for a strip footing on undrained clay ( $N_c = 2 + \pi$ ). Okamura *et al.* contended that Equations (3.21) and (3.22) are generally reliable for predicting the bearing capacity of a sand layer overlying clay for cases where  $\lambda_c < 26$  and  $\lambda_p < 4.8$ . However, it is most important to note that the method may not be applicable over the full range of these values, and indeed it may overestimate the capacity if used indiscriminately, without regard to its limitations. Indeed, one very important limitation was highlighted by Okamura *et al.* They recognized that the bearing capacity for a sand layer overlying a weaker clay cannot exceed that of a deep sand layer ( $H/B = \infty$ ). Hence, the bearing capacity values obtained from this method (Equations (3.21) and (3.22)) and from the formula for a deep layer of uniform sand (e.g., Equation (3.1)) must be compared, and the smaller value should be chosen as the bearing capacity of the layered subsoil.

Unlike the case of two clay layers, it seems that no finite element studies of the post-failure behaviour of footings on sand over clay have been published. However, it is expected that a brittle response may also be a possibility for this type of problem, particularly in cases where the self-weight and overburden effects do not dominate the influence of the clay strength.

### 3.3 Multiple layers

In nature, soils are often heterogeneous and in many cases they may be deposited in several layers. For such cases reliable estimation of the bearing capacity is more complicated. Of course, with modern computational techniques such as the finite element method, reliable estimates can ultimately be achieved. However, these methods usually require considerable effort, and the question arises whether simple hand techniques can be devised to provide realistic first estimates of the ultimate bearing capacity of layered soils. In particular, it would be useful to find answers to the following questions, in order to develop reasonably general guidelines for estimating the ultimate bearing capacity of layered soils.

- Can the bearing capacity be estimated by computing the average bearing capacity over a particular depth, e.g., 1 to 2B where B is the footing width?
- If the answer to the previous question is negative, is it possible to assess an average strength of the layers and then use that strength in the bearing capacity calculations for a homogeneous deposit to obtain a reliable estimate of the bearing capacity of the layered soil?

- If neither of the two previous approaches proves reliable, how can the practitioner solve the problem to obtain a reliable estimate of the ultimate bearing capacity?

In order to address some of these issues, consider now the idealised problem of a long strip footing on the surface of a soil deposit consisting of three different horizontal layers. The geometry of the problem is defined in Figure 3.22. The strength of each layer is characterised by the Mohr-Coulomb failure criterion and the conventional strength parameters  $c$  and  $\phi$ . Self-weight of the soil is defined by the unit weight,  $\gamma$ . Various cases of practical interest have been identified, as indicated in Table 3.2. In cases where self-weight of the soil has been considered, it has been assumed for simplicity that the initial stress state is isotropic. This assumption should not affect the calculation of the ultimate capacity of a strip footing on the surface of the soil, but of course it will have a significant influence on the computed load-displacement curve. Finite element solutions for the various cases are described in the following subsections.

#### 3.3.1 Clay "sandwich" - soft centre

Consider the case where the middle layer is weaker than the overlying and underlying clay layers. Undrained analyses have been conducted using the displacement finite element method and the results of a series of these analyses are presented in Figure 3.23. It is clear from this figure that the use of the simple average of the undrained shear strengths of the top and middle layer,  $c = (c_1 + c_2)/2$ , in the bearing capacity equation for a uniform undrained clay (Equation (3.1)) provides a reasonable estimate of the ultimate load, at least for most practical purposes and provided the strength ratio  $c_2/c_1$  is greater than about 0.5. If this average strength is used for cases where  $c_2/c_1$  is less than 0.5 the bearing capacity will be overestimated. The error for a very weak middle layer ( $c_2/c_1 = 0.1$ ) is approximately 33%. It is also worth noting that the two-layer approach suggested by Brown and Meyerhof (1969) and summarized in Equation (3.19) is generally reasonable for this case only when the strength ratio  $c_2/c_1$  is greater than about 0.7. For strength ratios less than 0.7, Equation (3.19) significantly underestimates the ultimate capacity, presumably because it ignores the higher strength of the bottom layer. It is worth noting that the upper bound solutions for a two-layer system published by Merifield *et al.* (1998) and illustrated in Figure 3.17, provide quite reasonable estimates (typically within 10 to 20%) of the ultimate capacity for this three-layer problem. It should be noted however, that these findings are relevant only for the particular geometry (layer thicknesses) indicated in Figure 3.22. Whether they could be extended to other situations requires further investigation.

#### 3.3.2 Clay "sandwich" - stiff centre

For this case the predicted ultimate bearing capacity is only slightly larger (1 to 2%) than the capacity predicted for a uniform clay layer with undrained strength equal to that of the top layer. Clearly, in this case the capacity is derived predominantly from the strength of the material of the top layer and is almost unaffected by the presence of a stronger underlying middle layer. It is expected that this result would not hold for cases where the layer thicknesses and strength ratios are different from those adopted in this example. A more complete description of the effects of layer thickness and strength ratio requires further research. The results presented by Merifield *et al.* (1998) also have significant application to this particular problem.

#### 3.3.3 Clay - strengthening with depth

The only significant difference between this case and the one discussed immediately above is that the strengths of the three layers increase monotonically with depth so that the bottom layer is even stronger than the middle layer. Within the accuracy of the finite element predictions the ultimate capacities are essentially the same, and in both cases the capacity is only 1 or 2% more than that of a uniform clay deposit having the same strength as the top layer.

Table 3.2. Bearing capacity cases for soils with three layers.

Case	Layer 1 (Top)			Layer 2 (Middle)			Layer 3 (Bottom)		
	$c_1$ (kPa)	$\phi_1$ (°)	$\gamma_1$ (kN/m <sup>3</sup> )	$c_2$ (kPa)	$\phi_2$ (°)	$\gamma_2$ (kN/m <sup>3</sup> )	$c_3$ (kPa)	$\phi_3$ (°)	$\gamma_3$ (kN/m <sup>3</sup> )
Clay "Sandwich" - Soft Centre	$c_1$	0	0	$< c_1$	0	0	$= c_1$	0	0
Clay "Sandwich" - Stiff Centre	$c_1$	0	0	$> c_1$	0	0	$= c_1$	0	0
Clay - Strengthening With Depth	$c_1$	0	0	$= 2c_1$	0	0	$= 4c_1$	0	0
Clay - Weakening With Depth	$c_1$	0	0	$= 0.5c_1$	0	0	$= 0.25c_1$	0	0
Clay "Sandwich" - Sand Centre	100	0	20	0	30	20	100	0	20
Sand "Sandwich" - Clay Centre	0	30	20	100	0	20	0	30	20

It is instructive to investigate whether the solutions presented by Davis and Booker (1973) for strengthening soil profiles can provide reasonably accurate predictions in this case. Two of the most obvious idealizations of the strength profile are:

$$s_u = 0.5c_1 + \left(\frac{2c_1}{B}\right)z \quad (3.28)$$

and

$$s_u = c_1 \quad \text{for } z < B/2$$

$$s_u = \left(\frac{2c_1}{B}\right)z \quad \text{for } z > B/2 \quad (3.29)$$

Equation (3.28) is an approximation assuming strength increasing linearly with depth from a finite value at the surface, while Equation (3.29) is the most obvious approximation for the case of a crust of constant strength overlying material whose strength increases linearly with depth. These profiles are illustrated in Figure 3.24.

For the strength profile indicated in Equation (3.28), Figure 3.14a together with Equation (3.17a) indicates an average value of the average bearing pressure at failure for a smooth strip footing, 1m wide, of approximately  $4.1c_1$ . This estimate is well below (approximately 80% of) the value predicted by the finite element analysis. A much closer match to the finite element prediction is given by the case depicted in Figure 3.14b, viz. approximately  $5.15c_1$ , indicating the dominant influence of the strength of the uppermost crustal layer and the relative insignificance in this case of the increase in strength beneath the crust.

### 3.3.4 Clay - weakening with depth

In this slightly unusual case, which could correspond in practice to a clay deposit with a thick desiccated or weathered crust overlying weaker but probably overconsolidated clay, the ultimate capacity predicted by the finite element analysis is approximately  $3.1c_1$ . This is more than 20% less than the finite element prediction for the case of a soft centre layer discussed in section 3.3.1. It is also approximately 10 to 15% less than the predictions by Brown and Meyerhof and Merifield *et al.* for a two-layered clay deposit. Clearly, in this case the weaker bottom layer has a significant influence on the overall capacity, but it is difficult to devise a simple approach for estimating the capacity of the footing for this type of strength variation.

### 3.3.5 Clay "sandwich" - sand centre

In this case the ultimate capacity computed by the finite element model is not much less than for a uniform clay layer with undrained shear strength of 100 kPa. The sand layer has only a small influence of the overall capacity of the footing.

### 3.3.6 Sand "sandwich" - clay centre

For this case the finite element prediction of the ultimate capacity,  $q_u$ , was approximately 98 kPa. This can be compared with the prediction of the bearing capacity for a uniform sand of 86 kPa, obtained using Equation (3.1) and the bearing capacity factors given in Table 3.1. It can be deduced from these results that the presence of the stiff clay beneath the sand has made a small contribution to the bearing capacity, taking it slightly above the value for sand alone.

For this case, it is also instructive to calculate what the capacity would be if the two-layer method proposed by Okamura *et al.*, Equation (3.21), were to be used. Application of Equation (3.21), which in this case is inappropriate, produces an ultimate capacity of 812 kPa., clearly far in excess of the values quoted previously for this problem. The reason for this discrepancy was explained by Okamura *et al.* themselves, when they pointed out that values estimated by their method must always be compared with predictions for a sand layer alone, and the smaller value should be chosen as the bearing capacity of the layered subsoil. This case therefore highlights the necessity of being aware of the limitations of all design methods, if very substantial errors in estimating the bearing capacity are to be avoided.

## 3.4 Summary

From the preceding discussion of the bearing capacity of shallow foundations, the following conclusions can be drawn.

1. The use of conventional theory, based on the original approach suggested by Terzaghi and extended by others such as Vesic, to calculate the bearing capacity of a foundation on homogeneous soil has stood the test of time, and is generally regarded as being reliable for use in engineering practice. Although this approach is approximate and makes a number of simplifying assumptions, as identified above, it is considered acceptable for most practical problems of shallow footings on relatively homogeneous soils. However, the use of the outdated and inaccurate information regarding some of the bearing capacity factors, particularly the factor  $N_q$ , should be discontinued. The factors set out in Table 3.1 are the most reliable values available, at least from a theoretical standpoint, and their use is therefore recommended.
2. Significant developments have been made in recent times concerning methods for estimating the ultimate load capacity of footings subjected to combinations of vertical, horizontal and moment loading. Failure loci such as those expressed by Equation (3.9) have been proposed, and should see increasing use in geotechnical practice. However, although some experimental justification has been provided for them, there is a need for more work of this type.
3. The effective width method, commonly used in the analysis of foundations subjected to eccentric loading, provides good

approximations to the collapse loads. Its continued use in practice therefore appears justified.

4. Improvements have also been made in the area of non-homogeneous and layered soils. Theoretically sound and relatively simple to use design methods are now available for cases involving the following:
  - (a) Clays where the undrained shear strength increases linearly with depth,
  - (b) Two layers of clay, and
  - (c) A layer of sand overlying relatively soft clay.
 The work of Booker and Davis (Figure 3.14), Merifield *et al.* (Figure 3.16) and Okamura *et al.* (Equations (3.21) and (3.22) and Figure 3.21) have been influential with regard to cases (a), (b) and (c) listed above, and the judicious use of their results in practical design is recommended.
5. Sophisticated experimental and theoretical studies have highlighted the brittle nature of footing system behaviour that can occur when relatively thin stronger soils, loaded by surface footings, overlie much weaker materials.
6. It would appear that to date the problem of predicting the bearing capacity of multiple layers of soil lying beneath a footing and within its zone of interest remains beyond the means of relatively simple hand calculation methods. The major reason that relatively little progress has been made to date seems to be the large number of different cases that may be encountered in practice and still require analysis. Some problems of this type were addressed in section 3.3, and only in the simplest case of three layers of clay could simple design rules be deduced. This problem area requires further investigation.

## 4 SETTLEMENT OF SHALLOW FOOTINGS

### 4.1 Introduction

The main objective of this section is to examine and evaluate some procedures for predicting the settlement of shallow foundations in the light of relatively recent research. Ideally, such an evaluation should consider both the theoretical "correctness" of the methods and also their applicability to practical cases. However, primary attention will be paid here to identifying the shortcomings and limitations of the methods when compared to modern theoretical approaches. Two common problems will be considered:

- Settlement of shallow foundations on clay
- Settlement of shallow foundations on sand.

In each case, an attempt will be made to suggest whether the prediction methods considered can be adopted, or alternatively, adapted to provide an improved prediction capability.

### 4.2 Shallow foundations on clay

Estimation of settlement and differential settlement is a fundamental aspect of the design of shallow foundations. For foundations on clay, Table 4.1 summarizes some of the available techniques and their capabilities. The traditional approach, first developed by Terzaghi, employs the one-dimensional method in which the settlement is assumed to arise from consolidation due to increases in effective stress caused by the dissipation of excess pore pressures. Because of its still widespread use, it is of interest to examine the capabilities and shortcomings of the method, when compared with more complete two- and three-dimensional methods.

The one-dimensional method has the following limitations:

1. It assumes that the foundation loading causes only vertical strains in the subsoil
2. It assumes that all the settlement arises from consolidation, and that settlements arising from immediate shear strains are negligible

3. It assumes that the dissipation of excess pore pressures occurs only in the vertical direction; any lateral dissipation of excess pore pressures is ignored.

Three-dimensional analyses involve, in one form or another, the integration of vertical strains to obtain the settlement of the foundation. In a three-dimensional situation employing the theory of elasticity, the vertical strain  $\epsilon_1$  may be obtained in terms of the increments of applied stress. Alternative forms of the strain versus stress increment relationship are as follows:

$$\epsilon_1 = (\Delta\sigma_v - \nu(\Delta\sigma_x + \Delta\sigma_y)) / E \quad (4.1a)$$

$$\epsilon_1 = 1/3[(\Delta q / G) + \Delta p' / K] \quad (4.1b)$$

where  $\Delta\sigma_v$  = increment in vertical stress;  $\Delta\sigma_x$ ,  $\Delta\sigma_y$  = increments in horizontal stresses in  $x$  and  $y$  direction;  $\Delta q$  = increment in deviator stress;  $\Delta p'$  = increment in mean principal effective stress;  $E$  = Young's modulus;  $G$  = shear modulus;  $K$  = bulk modulus.

In applying the above equations, the stress increments are usually computed from elasticity theory. Appropriate values of  $E$  and  $\nu$  must also be used in Equation (4.1): undrained values for immediate (undrained) strains and drained values for total (undrained plus consolidation) strains. In Equation (4.1b), for the undrained case in a saturated soil,  $K = \infty$ , while in a saturated soil,  $K$  can be related to the constrained modulus  $D$  by the following elasticity relationship:

$$K = (1 + \nu') D / [3(1 - \nu')] \quad (4.2)$$

where  $\nu'$  = drained Poisson's ratio of the soil.

The values of  $E$ ,  $G$  and  $K$  in the above equations can be related to stress or strain levels, as discussed in Section 8, so that non-linear soil behaviour can be accounted for in a simple manner. A fuller discussion of these procedures is given by Lehane and Fahey (2000).

### 4.2.1 One-dimensional versus three-dimensional settlement analysis

To examine the possible significance of the limitations of one-dimensional analysis, two very simple hypothetical examples are considered. The first involves a uniformly loaded circular footing resting on the surface of a homogeneous layer of overconsolidated clay, in which the soil stiffness is uniform with depth. The second involves the same footing on a layer of soft normally consolidated clay in which the soil stiffness increases linearly with depth, from a small initial value at the soil surface. The relationship between the one-dimensional compressibility,  $m_v$ , and drained Young's modulus,  $E'$ , (for three-dimensional analysis) is assumed to be that given by elasticity theory for an ideal two-phase elastic soil skeleton, as is the relationship between the undrained Young's modulus  $E_u$  and  $E'$ , i.e.

$$m_v = \frac{(1 + \nu')(1 - 2\nu')}{(1 - \nu')E'} \quad (4.3)$$

$$E_u = \frac{3E'}{2(1 + \nu')} \quad (4.4)$$

where  $\nu'$  = drained Poisson's ratio of soil skeleton.

Figure 4.1 shows the ratio of the one - dimensional settlement (excluding creep) to the correct three-dimensional total final settlement (Davis and Poulos, 1968). For the overconsolidated clay layer, the one-dimensional analysis gives a good approximation to the correct total settlement when the drained Poisson's ratio of the soil layer is less than about 0.35, even for relatively deep soil layers. The one-dimensional analysis tends to under-predict the settlement as the drained Poisson's ratio of the soil increases or the relative layer depth increases. For the soft clay layer, the one-dimensional analysis again gives a remarkably good approximation to the total final settlement if the drained Poisson's ratio of the soil layer is 0.35 or less.

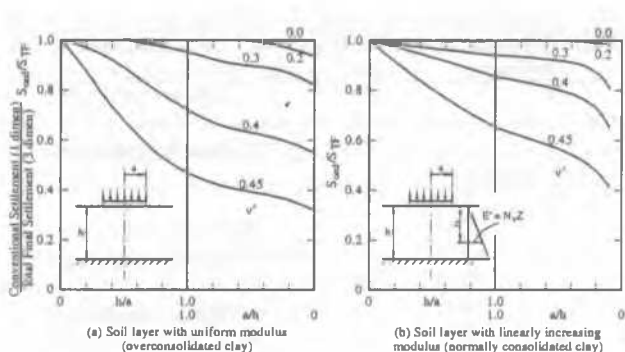


Figure 4.1. Theoretical ability of one-dimensional analysis to predict total final settlement.

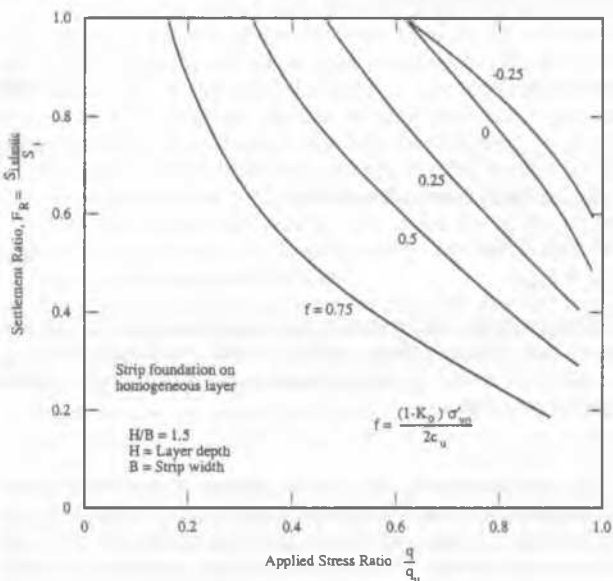


Figure 4.2. Local yield factor  $F_R$  for strip foundation on homogeneous layer (D'Appolonia et al, 1971).

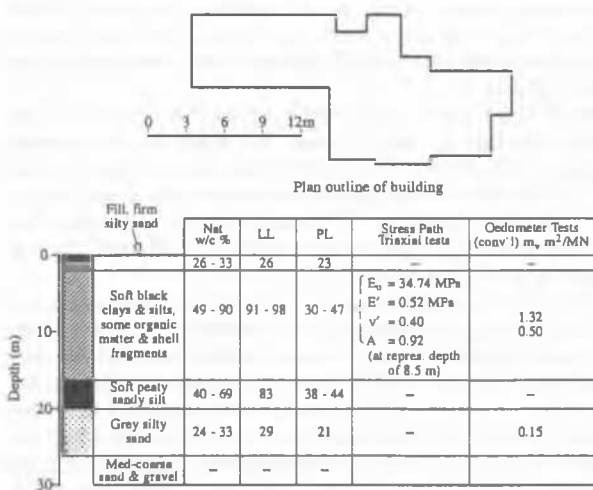


Figure 4.3. Boyd domestic college building, South Melbourne (after Moore & Spencer, 1969).

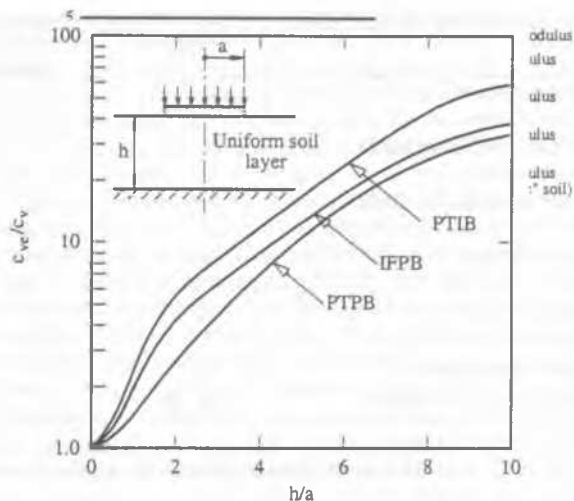


Figure 4.4. Equivalent coefficient of consolidation for 1-D analysis of rate of settlement - circular footing.

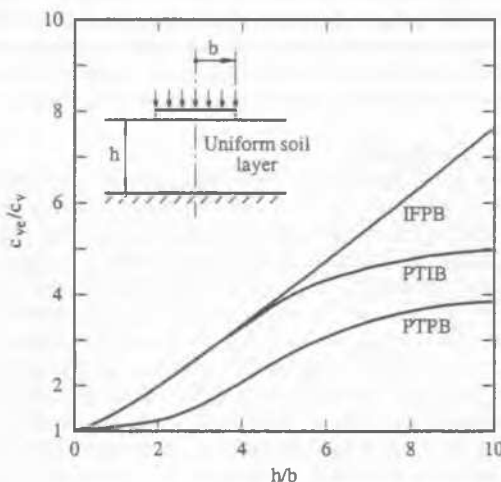


Figure 4.5. Equivalent coefficient of consolidation for 1-D analysis of rate of settlement - strip footings.

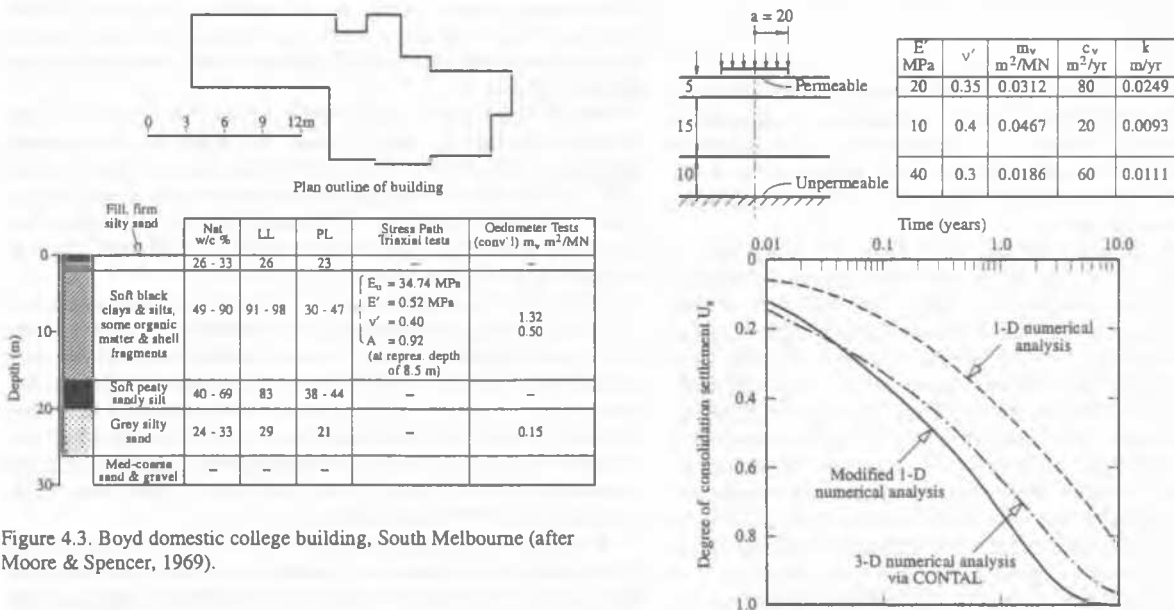


Figure 4.6. Example of comparison between 3-D & modified 1-D rate of settlement analysis.

Table 4.1. Some methods of settlement analysis for shallow foundations.

Method	Category	Immediate settlement	Consolidation settlement	Settlement rate	Creep settlement
One dimensional $S_{TF} = S_{CF} = S_{oed}$	2		✓	✓	(can be incorporated)
Modified One Dimensional $S_{TF} = S_i + S_{oed}$	2	✓	✓	✓	(can be incorporated)
Skempton & Bjerrum (1957) $S_{TF} = S_i + \mu S_{oed}$	1-2	✓	✓	✓	
Elastic Method $S_{TF} = S_i + (S_{TF} - S_i)$	2A	✓	✓	✓	(can be incorporated)
Modified Elastic $S_{TF} = S_i/F_R + (S_{TF} - S_i)$	2B	✓	✓	✓	(can be incorporated)
Elastic Finite Element	3A	✓	✓	✓	(can be incorporated)
Non-Linear Finite Element	3B, 3C	✓	✓	✓	(can be incorporated)

Note:  $S_{TF}$  = total final settlement;  $S_{oed}$  = one-dimensional settlement (from oedometer);  $S_i$  = immediate settlement  $\mu$  = correction factor (Skempton & Bjerrum, 1957);  $S_{CF}$  = final consolidation settlement;  $F_R$  = nonlinear correction factor (D'Appolonia *et al.*, 1971).

Burland *et al.* (1977) provide a detailed discussion of the ratio of one-dimensional settlement to total settlement, and demonstrate that soil anisotropy can have some influence on this ratio. They also argue that, while  $S_{oed}$  is a good approximation to  $S_{TF}$  for stiff clays, it is more likely to approximate the final consolidation settlement  $S_{CF}$  for normally consolidated clays, because of the yielding of such a soil and the consequent irrecoverable strains.

#### 4.2.2 Effects of local yield

The commonly used methods of settlement analysis implicitly assume elastic behaviour of the soil over the range of stress applied by the foundation. While some allowance is made for non-linear soil response by distinguishing between normally consolidated and over-consolidated states, and using different values of compressibility for each, no allowance is made for the development of local yield within the soil due to foundation loading. Davis and Poulos (1968) considered the conditions affecting the onset of local yield and showed that the applied loading at which local yield commenced was a function of both the factor of safety (i.e., the ratio of applied pressure  $q_u$  to ultimate bearing capacity  $q_u$ ) and also the initial stress state. D'Appolonia *et al.* (1971) extended these concepts and developed correction factors for the effects of local yield on immediate settlement. In their approach, the immediate settlement  $S_i$  was given as:

$$S_i = S_{elas} / F_R \quad (4.5)$$

where  $S_{elas}$  = immediate settlement computed from elasticity theory;  $F_R$  = yield correction factor, a function of  $q/q_u$  and the initial stress ratio  $f$ , which is a function both of coefficient of earth pressure at rest and undrained shear strength. Figure 4.2 plots  $F_R$  which is 1 for elastic conditions, and less than 1 when local yield occurs in the soil.

The effects of local yield on consolidation settlement and ratio of settlement do not appear to have been studied extensively. However, solutions presented by Small *et al.* (1976) and Carter *et al.* (1979a) suggest that both the consolidation settlement and the rate of settlement are not greatly affected by local yield within the soil, and that elasticity theory can be used with sufficient accuracy for their estimation. Thus, the main influence of local yield is on the immediate settlement  $S_i$ , and for Category 2 methods of calculation, Equation (4.5) can be used to estimate  $S_i$ .

In summary, it would appear that one-dimensional settlement theory can be adopted, but with some measure of adaptation. In particular, there is clear evidence that immediate settlements are important and cannot be ignored, especially for stiff clays. The effects of local yield on immediate settlement should also be considered. Based on the theoretical relationships discussed above, it would appear reasonable to adopt the following procedures if employing one-dimensional settlement theory:

1. for stiff overconsolidated clays:

$$S_{TF} = S_{oed} \quad (4.6a)$$

$$S_{CF} = S_{oed} - S_i \quad (4.6b)$$

2. for normally consolidated clays:

$$\begin{aligned} S_{TF} &= S_i + S_{oed} \\ S_{CF} &= S_{oed} \end{aligned} \quad (4.7)$$

The predicted settlement for the second case may be conservative, but since  $S_i$  is often relatively small in comparison to  $S_{oed}$ , the potential extent of over-estimation is unlikely to be significant in many cases.

#### 4.2.3 Case study

The performance of the various methods of settlement analysis, including the one-dimensional method, can be gauged by applying them to a real case history in which measurements of settlement are available. The case selected for consideration here is that published by Moore and Spencer (1969). This case involved a 2-storey brick structure erected in 1890 on a thick layer of compressible soil in South Melbourne. Figure 4.3 shows a plan of the building and a simplified representation of the soil profile. The average loading acting on the building was about 45kPa. Oedometer and laboratory stress path triaxial test data were obtained on the dominant clay and silt layer, and these data are also shown in Figure 4.3.

Moore and Spencer employed a number of methods of settlement calculation, ranging from one-dimensional settlement analysis to two different types of stress path analysis. Three types of oedometer test were carried out for use in the conventional oedometer analysis. The results of the calculations reported by Moore and Spencer are shown in Table 4.2, together with the measured settlement.

The effects of possible local yield have not been taken into account, and hence the immediate settlements are likely to have been under-estimated. It can be seen that the conventional one-dimensional analysis underestimates the settlement significantly, (depending on which type of oedometer data has been employed), as does also the Skempton and Bjerrum method. The elasticity method of Davis and Poulos (1968) underestimates the settlement by only about 10%, while the Lambe stress path method gives a 23% underestimate.

While this case study can in no way be used to imply that a three-dimensional settlement analysis is always necessary, it does indicate that caution should be exercised in applying one-dimensional settlement analysis to foundations on soft clay. On the other hand, the earlier studies of Skempton *et al.* (1955) and Skempton and Bjerrum (1957) provide evidence that one-dimensional analyses provide an adequate estimate of founda-

tions on relatively stiff clays. Thus, the one-dimensional method deserves to be retained, but adapted, as a means of estimating the settlement of shallow foundations on clay.

Table 4.2. Comparison of total settlements: Boyd Domestic College Building (after Moore and Spencer, 1969).

Method	Settlement mm
Observed	787
Conventional Oedometer	508
Oedometer with Back Pressure	404
Oedometer with Constant Rate of Strain	404
Skempton and Bjerrum (1975)	564
Davis and Poulos (1968)	709
Stress Path, Lambe (1964)	610

Note: Oedometer methods used stress distributions for 2-layer soil mass.

#### 4.2.4 Rate of settlement

It is well known that three-dimensional effects may significantly accelerate the rate of settlement of foundations on clay, primarily because of the ability of excess pore pressures to dissipate horizontally as well as vertically. A number of approaches have been developed for estimating the rate of settlement under two and three-dimensional conditions, including the following:

1. Category 2 design charts for strip and circular foundations on a homogeneous layer, e.g., Davis and Poulos (1972); Booker (1974), the former are derived from solutions of the simplified diffusion theory of consolidation, while the latter are based on the complete Biot theory.
2. Finite layer numerical solutions for strip, circular and rectangular footings on elastic clay layers, e.g., as implemented by the computer program CONTAL (Small, 1998). This would be classified as a Category 3A approach.
3. Finite element numerical analyses for linear and non-linear soil layers, e.g., Small *et al.* (1976); Sandhu and Wilson (1969).

From a practical viewpoint, it may not always be feasible to employ a full two- or three-dimensional consolidation analysis. However, it is possible to *adapt* a one-dimensional consolidation analysis to take account of this effect by using an equivalent coefficient of consolidation,  $c_{ve}$ , which is obtained by multiplying the actual coefficient of consolidation  $c_v$  by a geometrical rate factor  $R_f$ :

$$c_{ve} = R_f c_v \quad (4.8)$$

$R_f$  values can be derived from three-dimensional rate of settlement solutions, such as those derived by Davis and Poulos (1972). Figures 4.4 and 4.5 show values of  $R_f$  as a function of the layer depth to footing size ratio, for circular and strip foundations. In each case, three combinations of hydraulic boundary conditions at the top and base of the layer are considered: PTPB (permeable top, permeable base), PTIB (permeable top, impermeable base) and IFPB (impermeable top, permeable base). As the layer thickness increases relative to the footing size, the factor  $R_f$  increases, reflecting the acceleration of the rate of settlement due to lateral dissipation. It should be noted that for the case IFIB (impermeable footing, impermeable base), it is not possible to adapt a one-dimensional solution since the theoretical rate of settlement is always zero.

If the soil is anisotropic, then a further factor can be applied to the coefficient of consolidation, as presented by Davis and Poulos (1972).

An example of a comparison between solutions for the rate of settlement of a large flexible circular foundation (such as an oil tank) on a layered clay soil profile is shown in Figure 4.6. Three solutions are shown: a three-dimensional solution from a finite layer consolidation analysis using the program CONTAL (Small, 1998), a modified one-dimensional analysis in which the coefficients of consolidation have been multiplied by an  $R_f$  factor of 6 (see Figure 4.4 for the PTIB case), and a one-dimensional numerical analysis in which the original values of coefficient of

consolidation are used. The modified one-dimensional solution is in reasonable agreement with the three-dimensional solution (although it suggests a somewhat more rapid rate of consolidation at larger times). The conventional one-dimensional numerical analysis significantly under-predicts the rate of settlement.

The above approach has been used in several practical cases with good results, for example, for an embankment on clay (Davis and Poulos, 1975). A comparison between the measured rate of settlement and that calculated from a one-dimensional analysis using the equivalent coefficient of consolidation, shows quite reasonable agreement, certainly better than would have been obtained using a normal one-dimensional consolidation analysis. Thus, it would appear feasible in practical cases to adapt the one-dimensional consolidation analysis, as suggested above, if a proper three-dimensional analysis is either unwarranted or not available

#### 4.2.5 Creep and secondary consolidation

The existence of creep complicates the prediction of both the magnitude and rate of settlement of foundations on clay soils. Most practical methods of accounting for creep still rely on the early observations of Buisman (1936) that creep is characterised by a linear relationship between settlement and the logarithm of time. The gradient of this relationship is generally represented by the coefficient of secondary compression  $C_\alpha$ , where:

$$C_\alpha = \Delta e / \Delta \log t \quad (4.9)$$

and  $\Delta e$  = change in void ratio;  $t$  = time.

Mesri and Godlewski (1977) have found that  $C_\alpha$  is related to the compression index of a soil, as indicated in Table 4.3. It should be noted that, for overconsolidated clays, the ratios in Table 4.3 apply to the recompression index; thus, the creep settlement rate is significantly smaller for an overconsolidated soil than for the same soil in a normally consolidated state.

The difficulty with applying the ' $C_\alpha$ ' concept is that the time at which creep is assumed to commence is not well-defined. Considerable controversy exists on this point, with some researchers maintaining that creep only commences at the end of primary consolidation (e.g., Mesri *et al.*, 1994) while others contend that it takes place simultaneously with primary consolidation (e.g., Leroueil, 1996).

Table 4.3. Values of  $C_\alpha/C_c$  for geotechnical materials (Mesri *et al.*, 1994).

Material	$C_\alpha/C_c$
Granular soils, including rockfill	0.02 ± 0.01
Shale and mudstone	0.03 ± 0.01
Inorganic clays and silts	0.04 ± 0.01
Organic clays and silts	0.05 ± 0.01
Peat and muskeg	0.06 ± 0.01

While various creep laws can and have been incorporated into consolidation analyses (e.g., Gibson and Lo, 1961; Garlanger, 1972), it is very uncommon in practice for such analyses to be applied, even for one-dimensional problems.

From a practical viewpoint, the most convenient approach appears to be to add the creep settlement relationship to the conventional time-settlement relationship from consolidation theory, commencing at one of the following times:

1. a predetermined time after commencement of loading
2. after a predetermined degree of consolidation settlement
3. when the gradients of the primary settlement versus log time and the creep settlement versus log time relationships are equal.

Overall, it appears that, of all the aspects of settlement analysis, the issue of creep and secondary consolidation is the one in which least progress has been made in terms of fundamental understanding and in the incorporation of research into practice. In the absence of a more satisfactory approach, the method of

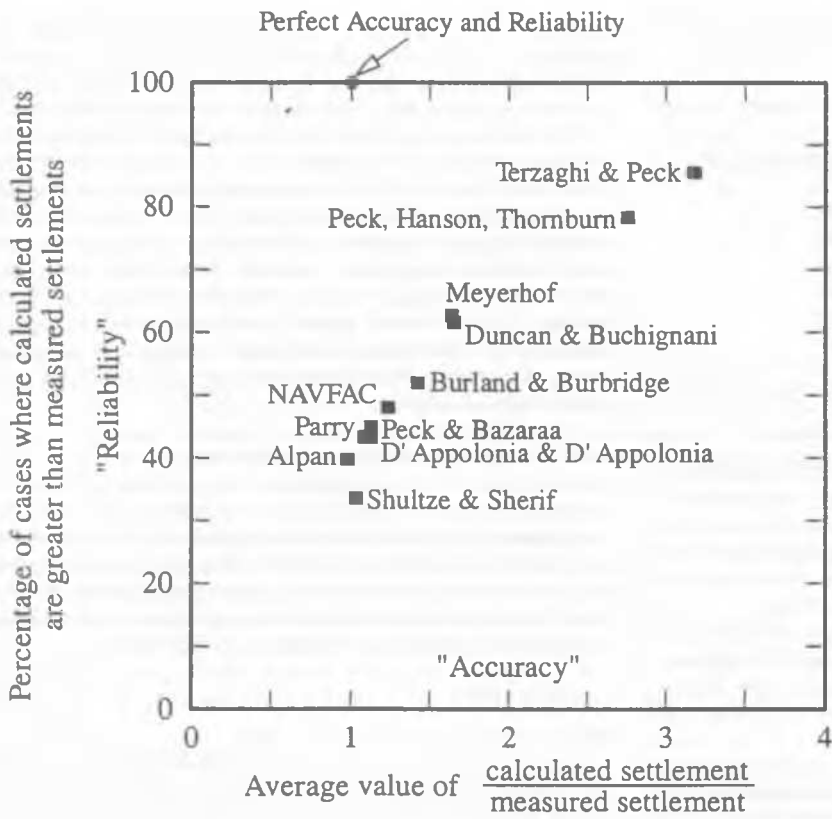


Figure 4.7. Relationships between accuracy and reliability for eleven methods based on SPT blow count (Tan and Duncan, 1991).

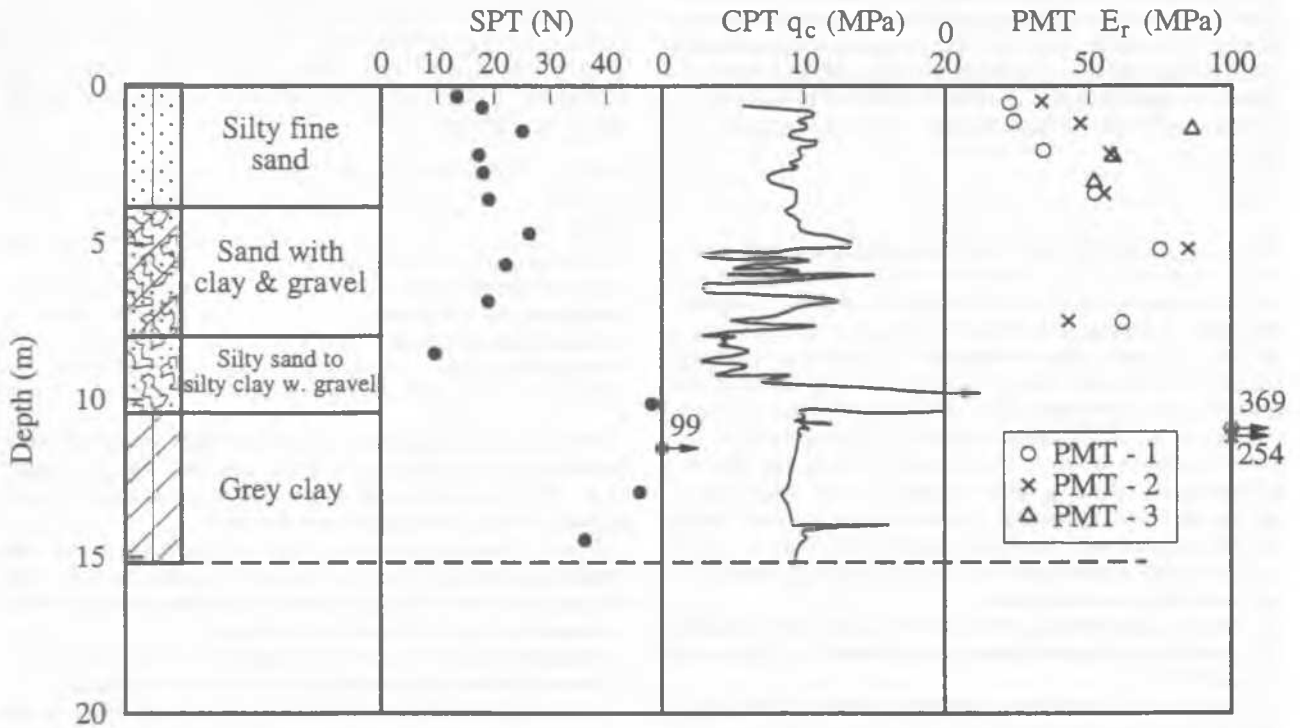


Figure 4.8. Summary of soil conditions near footing 1.

Table 4.4. Variables used in methods of estimating settlements of footings on sand (Tan and Duncan, 1991).

Method (reference)	Variables used											
	$N$	$N_{cor}$	$q_c$	$B$	$D_w$	$D_f$	$\gamma_t$	$L$	$T$	Soil type	Str. hist	Time
Alpan (1964)		✓		✓	✓	✓	✓				✓	
Burland and Burbridge (1985)	✓			✓	✓	✓	✓	✓	✓	✓	✓	✓
D'Appolonia & D'Appolonia (1970)	✓			✓	✓	✓			✓			
Duncan & Buchignani (1976)	✓			✓						✓		✓
Meyerhof (1956)	✓			✓								
NAVFAC (1982)	✓			✓	✓							
Parry (1971)	✓			✓	✓				✓			
Peck & Bazaraa (1969)		✓		✓	✓	✓	✓			✓		
Peck, Hanson, Thornburn (1974)		✓		✓	✓	✓	✓					
Schmertmann (1978)			✓	✓	✓	✓	✓					✓
Schultz & Sherif (1973)	✓			✓		✓			✓			
Terzaghi and Peck (1967)	✓			✓	✓					✓		

$N$  = SPT Blow Count;  $B$  = footing width;  $q_c$  = Cone Penetration Test tip resistance;  $\gamma_t$  = total unit weight of sand;  $D_f$  = depth of footing below ground surface; Soil Type = silty or clean sand;  $T$  = thickness of sand layer below footing;  $D_w$  = depth of water table; Time = duration of loading;  $L$  = footing length;  $N_{cor}$  = SPT Blow Count corrected for overburden pressure; Stress Hist. = max. prev. load.

Buisman may be adapted to provide a crude estimation of creep settlements.

### 4.3 Settlement of shallow foundations on sand

#### 4.3.1 Previous studies

A remarkable number of methods have been developed to estimate the settlement of shallow foundations on sand, yet consistent success in accurately predicting such settlements remains elusive. These methods range from purely empirical (Category 1) methods developed originally for conservative footing design (Terzaghi and Peck, 1967), to complex Category 3 nonlinear finite element methods.

Many of the methods rely on in-situ SPT or CPT data, and hence it is not possible to satisfactorily examine the theoretical relationship between the various methods. Assessments of the performance of various methods have therefore been made on the basis of comparisons with measured settlements. At least two significant studies have been reported, one by Jeyapalan and Boehm (1986), and the other by Tan and Duncan (1991).

The study by Jeyapalan and Boehm (1986) involved the statistical analysis of 71 case histories for which settlements of footings on sand were reported, and the assessment of the relative accuracy of nine methods of settlement estimation. The methods of Schultze and Sherif (1973) and Schmertmann (1978) appeared to among the more dependable approaches.

Tan and Duncan (1991) carried out an assessment of the reliability of twelve methods of estimating footing settlement on sands by comparing calculated and measured settlements for 76 cases. Each of the methods was evaluated in terms of (1) accuracy (the ratio of average calculated to measured settlement), (2) reliability (the percentage of cases in which the calculated settlement equalled or exceeded the measured settlement, and (3) ease of use (the length of time required to apply the method. Table 4.4 summarizes the methods considered and the parameters used in each method. Figure 4.7 summarizes the findings on accuracy and reliability. Values of "accuracy" range from 1.0 (the ideal value) for Alpan's method to 3.2 for Terzaghi and Peck's

method. Values of "reliability" varied from 34% for Schultze and Sherif's method to 86% for Terzaghi and Peck's method. In general, the methods which were less accurate (and more conservative) were more reliable in the sense that they underestimated the settlement relatively infrequently. Table 4.5 summarizes the hand computation times for a simple example. Those methods requiring correction of the SPT values generally involved the longer computation times. As concluded by Tan and Duncan, there is a tradeoff between accuracy and reliability in choosing a method of calculation.

#### 4.3.2 Case study

A comparison of the performance of a number of the methods has been made via a well-documented Prediction Symposium in which a number of people made "Class A" predictions of the settlement of footings on a natural sand profile (Briaud and Gibbons, 1994). The predictions were then compared with the actual settlement measurements.

Figure 4.8 summarizes the soil conditions near one of the footings tested (footing 1, nominally 3m by 3m in plan). The site consisted by layers of silty sand, underlain by a hard clay layer. A substantial amount of in-situ and laboratory data was obtained, some of which is shown in Figure 4.8.

In the Prediction Symposium, a total of 31 persons made predictions, using a wide variety of methods. However, for the present exercise, the authors have made their own application of a number of the methods to Footing 1, as well as presenting the original prediction made for this footing. An exception is the result of a finite element analysis, which was carried out by one of the other predictors.

Table 4.6 summarizes the results of the authors' calculations for the settlement at a load of 4000 kN (corresponding to a factor of safety against ultimate failure of about 2.5). The following observations can be made from Table 4.6:

1. all methods over-estimated the footing settlement
2. the elasticity-based methods, based on CPT, SPT and pressuremeter data, all give reasonable predictions



3. the Terzaghi and Peck method, which is meant to provide a conservative footing design to ensure a settlement less than 25mm, gives a predictably conservative settlement estimate
4. the authors' original prediction, based on an elasticity analysis with a strain-dependent Young's modulus, overpredicts the settlement significantly
5. the finite element method, using a nonlinear constitutive soil model, overpredicts the settlement substantially.

While it is again imprudent to draw firm conclusions on the basis of such limited comparisons, it does appear reasonable to suggest that the simple elasticity-based methods (including Schmertmann's method) appear capable of providing reasonable estimates of footing settlement. The key to success lies more in the appropriate choice of the shear or Young's modulus of the sand than in the details of the method employed. Such methods therefore deserve to be retained and adopted. On the other hand, the more complex finite element methods appear to require far more development before being able to be used with confidence. Indeed, from a practical viewpoint, there may be relatively few cases in which such analyses are warranted.

Table 4.5. Computation times for methods based on SPT Blow Count (Tan and Duncan, 1991).

Method	Computation time (minutes)
Alpan (1964)	29
Burland & Burbridge (1985)	14
D'Appolonia & D'Appolonia (1970)	8
Duncan & Buchignani (1976)	9
Meyerhof (1956)	6
NAVFAC (1982)	8
Parry (1971)	9
Peck & Bazaraa (1969)	25
Peck, Hanson, Thornburn (1974)	25
Schultze & Sherif (1973)	6
Terzaghi & Peck (1967)	11

Table 4.6. Summary of calculated & measured settlement of 3m square footing.

Method	Settlement for P = 4MN	Notes
Terzaghi & Peck (1967)	39	Av. N = 20
Schmertmann (1978)	28	
Burland & Burbridge (1985)	21	Average value (range 10-58 mm)
Elasticity Theory, using $E_s = 3N$ MPa	18	Decourt (1989)
Elasticity Theory, using PMT data	24	Reload modulus values
Strain-dependent modulus	32	Poulos (1996a), Class A prediction
Finite Element Analysis	75	Chang (1994), Class A prediction, using constitutive soil model
Measured	14	After 30 minutes

## 5 DEEP FOUNDATIONS

### 5.1 Design issues

The key design issues in relation to pile foundations include:

1. Selection of the type of pile and installation method;
2. Estimation of the pile size in order to satisfy the requirements of an adequate margin of safety against failure of both the supporting soil and the pile itself, both in compression and tension;

3. Estimation of the settlement of the foundation, and the differential settlement between adjacent foundations;
4. Consideration of the effects of any lateral loading, and the design of the piles to produce an adequate margin of safety against failure of the soil and the pile, and an acceptable lateral deflection;
5. Consideration of the effects of ground movements which may occur due to external causes (such as soil settlement and swelling), and the estimation of the movements and forces induced in the pile by such movements;
6. Evaluation of the performance of the pile from appropriate pile loading tests, and the interpretation of these tests to evaluate parameters which may be used to predict more accurately the performance of the pile foundation.

In this section, only items 2 to 6 will be addressed, but it must be emphasized that both pile type selection and pile load testing are crucial components of the design process which must be given careful consideration.

### 5.2 Axial load capacity

Pile foundation designers have employed both dynamic and static methods of analysis to estimate the ultimate axial load capacity of piles. Here, only static methods will be reviewed as they apply to all types of pile and, unlike dynamic methods, can be applied prior to the installation of the pile. However, it should be emphasized that dynamic methods of estimating pile axial capacity are used very widely in conjunction with the installation of driven piles and in load testing of both driven and bored piles.

It is almost universally accepted that the ultimate axial load capacity of a pile can be estimated by summation of the ultimate shaft capacity,  $P_{su}$ , and the ultimate base capacity,  $P_{bu}$ . The weight  $W_p$  of the pile is subtracted for the compressive load capacity, and added for the uplift capacity. In turn,  $P_{su}$  and  $P_{bu}$  are related to the ultimate shaft and base resistances,  $f_s$  and  $f_b$ . Thus, for compression, the ultimate load capacity,  $P_{uc}$ , is:

$$P_{uc} = \sum f_s C dz + f_b A_b - W_p \quad (5.1)$$

where  $f_s$  = ultimate shaft friction in compression,  $C$  = pile perimeter,  $dz$  = length of soil layer or sub-layer,  $f_b$  = ultimate base pressure in compression,  $A_b$  = area of pile base, and the summation for the shaft capacity is carried out over the entire embedded length of the pile shaft.

For uplift, the ultimate load capacity,  $P_{ur}$ , is

$$P_{ur} = \sum f_{st} C dz + f_{bt} A_b + W_p \quad (5.2)$$

where  $f_{st}$  = ultimate shaft friction in uplift and  $f_{bt}$  = ultimate base pressure in uplift.

Unless the pile has an enlarged base, the uplift resistance of the base is usually disregarded.

#### 5.2.1 Developments in total stress analysis for piles in clay

One of the traditional methods of estimating the ultimate shaft friction in compression,  $f_b$ , involves the use of the total stress ("alpha") method for piles in clay soils. This method relates  $f_s$  to the undrained shear strength  $s_u$  as:

$$f_s = \alpha s_u \quad (5.3)$$

where  $\alpha$  = adhesion factor.

The ultimate end bearing resistance  $f_b$  is given by:

$$f_b = N_c s_u \quad (5.4)$$

where  $N_c$  = bearing capacity factor.

Table 5.1 summarizes some of the approaches commonly adopted for estimating the adhesion factor  $\alpha$ . A number of modifications to these recommendations exist in various countries, for example, in Europe (De Cock, 1998).

The bearing capacity factor  $N_c$  is commonly taken as 9, provided that the pile length exceeds about 3-4 shaft diameters. Some modifications are applied in some countries (De Cock, 1998), including a reduction for large-diameter bored piles (Meyerhof, 1976).

One of the key difficulties in applying the total stress method is the estimation of the undrained shear strength  $s_u$ . Early correlations used laboratory unconfined compression test data, but it is now more common for  $s_u$  to be estimated from in-situ tests such as field vane tests or cone penetration tests. It is well-recognized that  $s_u$  values can vary considerably, depending on the test type and the method of interpretation; consequently, it is desirable to develop local correlations for  $\alpha$ , in relation to a defined method of measuring  $s_u$ .

Table 5.1. Total stress approaches for estimating  $f_s$  for piles in clay  $f_s = \alpha s_u$ .

Pile type	Remarks	Reference
Driven	$A = 1.0$ ( $s_u \leq 25$ kPa) $A = 0.5$ ( $s_u \geq 70$ kPa) Interpolate linearly between	API (1984)
Driven	$A = 1.0$ ( $s_u \leq 25$ kPa) $A = 0.5$ ( $s_u \geq 70$ kPa) Linear variation between. Length factor applies for $L/d \geq 50$ .	Sample & Rigden (1984)
Driven	$\alpha = (s_u/\sigma'_v)^{0.5} (s_u/\sigma'_v)^{-0.5}$ for $(s_u/\sigma'_v) \leq 1$ $\alpha = (s_u/\sigma'_v)^{0.5} (s_u/\sigma'_v)^{-0.25}$ for $(s_u/\sigma'_v) \geq 1$	Fleming <i>et al.</i> (1985)
Bored	$\alpha = 0.21 + 0.26 (p/s_u) (\leq 1.0)$	Kulhaway and Phoon (1993)
Bored	$\alpha = 0.7$ times value for driven displacement pile	Fleming <i>et al.</i> (1985)

### 5.2.2 Developments in effective stress analysis

The effective stress ("beta") method can be applied for piles in any soil type.  $f_s$  is related to the in-situ effective stresses as follows:

$$f_s = K_s \tan \delta \sigma'_v \quad (5.5a)$$

where  $K_s$  = lateral stress coefficient;  $\delta$  = pile-soil friction angle;  $\sigma'_v$  = effective vertical stress at level of point under consideration.

Several of the more recent effective stress methods have employed cavity expansion theories in an attempt to model the effects of installation and subsequent loading of the pile (for example, Randolph *et al.*, 1979; Carter *et al.*, 1979b). While the results of such studies have been illuminating and have indicated the important effects of initial installation and subsequent dissipation of excess pore pressures, they appear to have had relatively little impact on design practice, due largely to the need to have reasonably detailed knowledge of the initial stress conditions within the soil, as well as the soil strength and compressibility characteristics.

An alternative approach has been adopted by a number of researchers, in which attempts have been made to develop more reliable methods of estimating the lateral stress coefficient  $K_s$ . Among such methods are the following:

- Jardine and Chow (1996), who have related  $K_s$  to the cone resistance, the distance from the pile tip, and the dilatant increase in normal stress during pile loading. Different expressions have been derived for driven piles in sand and clay soils, and the case of open-ended piles has also been considered. These expressions have been based on carefully instrumented pile data and a close appreciation of the fundamental behaviour of soils and pile-soil interfaces;
- Go and Olsen (1993), who have related  $K_s$  to the SPT value for driven piles in sand;

- Yasufuku *et al.* (1997), who have related  $K_s$  to the relative depth along the pile, and the at-rest and passive pressure coefficients of the soil, for bored piles;
- Miller and Lutenegeger (1997), who have related  $K_s$  to the at-rest and maximum lateral stress ratio for a full displacement penetrometer, and also take into account the extent of plugging of a tube pile.

Table 5.2 summarises these approaches, together with the classic approaches of Burland (1973) and Meyerhof (1976).

A detailed and intensive discussion of effective stress approaches to estimating the ultimate shaft friction is given in a recent paper by O'Neill (2001).

### 5.2.3 Correlations with SPT data

Empirical correlations with the results of SPT data usually take the following form:

$$f_s = A_N + B_N N \quad (\text{kPa}) \quad (5.5b)$$

where  $A_N$  and  $B_N$  are empirical numbers, and depend on the units of  $f_s$ , and  $N$  = SPT value at the point under consideration.

$$f_b = C_N N_b \quad (\text{MPa}) \quad (5.5c)$$

where  $C_N$  = empirical factor;  $N_b$  = average SPT within the effective depth of influence below the pile base (typically 1 to 3 pile base diameters).

The most widely used correlations are those developed originally by Meyerhof (1956) for driven piles in sand, in which  $A_N = 0$ ,  $B_N = 2$  for displacement piles and 1 for small-displacement piles, and  $C_N = 0.3$ . Limiting values of  $f_s$  of about 100 kPa were recommended for displacement piles and 50 kPa for small displacement piles.

Some other correlations have included other soil types and both bored piles and driven piles. A number of these are summarized by Poulos (1989).

Decourt (1995) has developed more recent and extensive correlations between  $f_s$  and SPT, which take into account both the soil type and the methods of installation. For displacement piles,  $A_N = 10$  and  $B_N = 2.8$ , while for non-displacement piles,  $A_N = 5 - 6$  and  $B_N = 1.4 - 1.7$ . For the base, values of  $C_N$  are shown in Table 5.3. Correlations for piles in gravel are discussed by Rollins *et al.* (1997).

It must be emphasized that the correlations with SPT must be treated with caution as they are inevitably approximate, and are not of universal applicability. For example, different correlations are used in Hong Kong than those indicated above, but have been developed for use in the prevailing local geological conditions (GEO, 1996).

### 5.2.4 Correlations with CPT data

Empirical correlation with the results of CPT data often take the following form:

$$f_s = A_q q_c \quad (5.6)$$

where  $A_q$  = empirical number, and  $q_c$  = cone penetration resistance at the point under consideration, and

$$f_b = C_q q_{cb} \quad (5.7)$$

where  $C_q$  = empirical factor, and  $q_{cb}$  = average cone resistance around the pile tip.

In most practical methods of design, an upper limits are placed on the values of  $f_s$  ( $f_{st}$ ) and  $f_b$  ( $f_{bt}$ ), these being dependent on the type of soil and the type of pile.

A number of correlations appear in the literature, including those of Bustamante and Gianceselli (1982). These form the basis of correlations given by Poulos (1989), and appear to be the basis of the later correlations developed by MELT (1993). De Cock (1998) summarizes a number of approaches adopted in Europe,

Table 5.2. Effective stress approaches for estimating ultimate shaft friction  $f_t = \sigma'_r \tan \delta = K_s \tan \delta \cdot \sigma'_v$ .

Pile type	Soil type	Details	Reference
Driven	Sand	$\sigma'_r = \sigma'_{ro} + \Delta\sigma'_{rd}$ $\sigma'_{ro} = 0.029q_c (\sigma'_{vo}/p_a)^{0.13} (h/R)^{-0.38}$ $\Delta\sigma'_{rd} = 2G\delta h/R$ where $q_c$ = cone resistance $p_a$ = atmospheric pressure $h$ = distance from pile tip ( $h/R$ ) $\geq 8$ $R$ = pile radius = $d/2$ $G$ = soil shear modulus $\delta h$ = roughness parameter $\approx 2 \cdot 10^{-5}$ m $\delta$ = interface friction angle (crit.state) For open-ended piles, with inner radius $R_i$ and outer radius $R_o$ , $R$ is replaced by $R^* = (R_o^2 - R_i^2)^{0.5}$	Jardine & Chow (1996)
Driven	Clay (long-term case)	$\sigma'_r = 0.8K_s\sigma'_{vo}$ $K_s = [2 - 0.625I_{vr}]YSR^{0.42} (h/R)^{-0.20}$ , or $K_s = [2.2 + 0.016YSR^{-0.67} \Delta I_{vr}]YSR^{0.42} (h/R)^{-0.20}$ where $\Delta I_{vr} = \log S_i$ $YSR$ = yield stress ratio = $\sigma'_{vy}/\sigma'_{vo}$ $\sigma'_{vy}$ = vertical effective yield stress $S_i$ = soil sensitivity For open-ended piles, with inner radius $R_i$ and outer radius $R_o$ , $R$ is replaced by $R^* = (R_o^2 - R_i^2)^{0.5}$	Jardine & Chow (1996)
Driven & Bored	Sand	$K_s = A + BN$ where $N$ = SPT value $A = 0.9$ (displacement piles) Or $0.5$ (non-displacement piles) $B = 0.02$ for all pile types	Go and Olsen (1993)
Bored	Sandy soils	$K_s = \{1 - (z/L)^\alpha\} K_p + (z/L)^\alpha K_o$ where $z$ = depth below surface $L$ = pile length $K_p$ = passive pressure coefficient $K_o$ = at-rest pressure coefficient $\alpha = 0.2$ (typically)	Yasufuku <i>et al.</i> (1997)
Driven & Bored	Sand	$K_s = K_o (K_r/K_o)$ where $K_o$ = at-rest pressure coefficient $(K_r/K_o)$ depends on installation method; range is 0.5 for jetted piles to up to 2 for driven piles.	Stas & Kulhawy (1984)
Driven	Clay	$K_s = (1 - \sin \phi') (OCR)^{0.5}$ where $\phi'$ = effective angle of friction $OCR$ = overconsolidation ratio; Also, $\delta = \phi'$	Burland (1973); Meyerhof (1976)
Driven	Overconsolidated Clay	$K_s = (K_o - K_{cmax}) SRR + K_{cmax}$ where $K_{cmax}$ = lateral effective stress coefficient for full displacement penetrometer $SRR$ = specific recovery ratio $= 1.0$ for unplugged pile, & $0$ for plugged pile	Miller & Lutenegeger (1997)

while Bustamante and Gianeselli (1998) present correlations for screw piles in various soil types. Lee and Salgado (1999) have developed relationships between pile base resistance  $f_b$  and conepenetration resistance  $q_c$  for piles in sand, and have investigated the effects of the initial coefficient of earth pressure at rest,  $K_o$ , and the pile length. Table 5.4 summarizes some of the results of this study. The main conclusions are as follows:

- the ratio  $f_b/q_c$  increases with increasing relative settlement  $S/d$  of the pile, where  $S$  = settlement and  $d$  = pile diameter;
- $f_b/q_c$  is greater for displacement piles than for non-displacement piles, although the difference becomes less as the relative settlement increases; the effect of pile length is relatively insignificant;
- the value of  $K_o$  has a relatively small influence;
- $f_b/q_c$  tends to decrease with increasing relative density.

Table 5.3. Factor  $C_N$  for base resistance (Decourt, 1995).

Soil type	Displacement piles	Non-displacement piles
Sand	0.325	0.165
Sandy silt	0.205	0.115
Clayey silt	0.165	0.100
Clay	0.100	0.080

Table 5.4. Relationships between base capacity and CPT data for piles in sand (after Lee & Salgado, 1999).

Pile type	$f_b/q_c$ at $s/B = 5\%$	$f_b/q_c$ at $s/B = 10\%$
Displacement	0.14-0.25 (computed)	0.20-0.35 (computed)
	0.27-0.43 (test data)	0.32-0.47 (test data)
Non-displacement	0.09-0.18 (test data)	0.20-0.26 (test data)

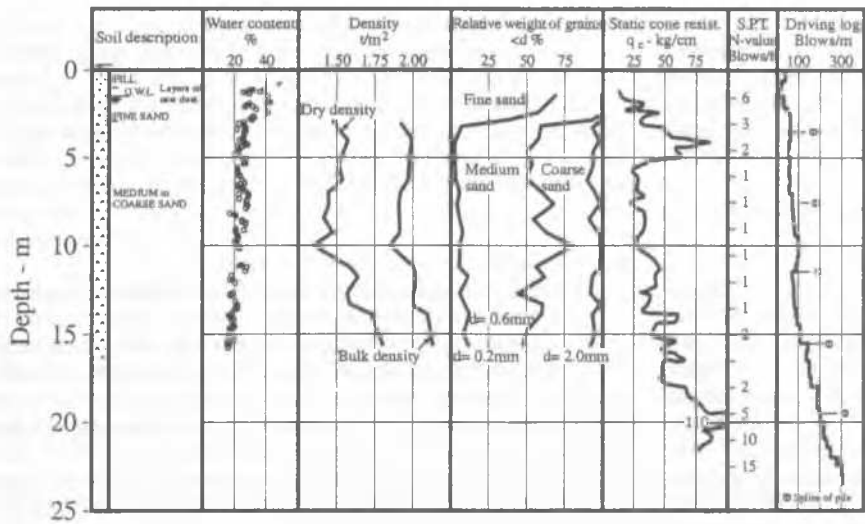


Figure 5.1. Soil data for driven piles (Gregersen et al, 1973).

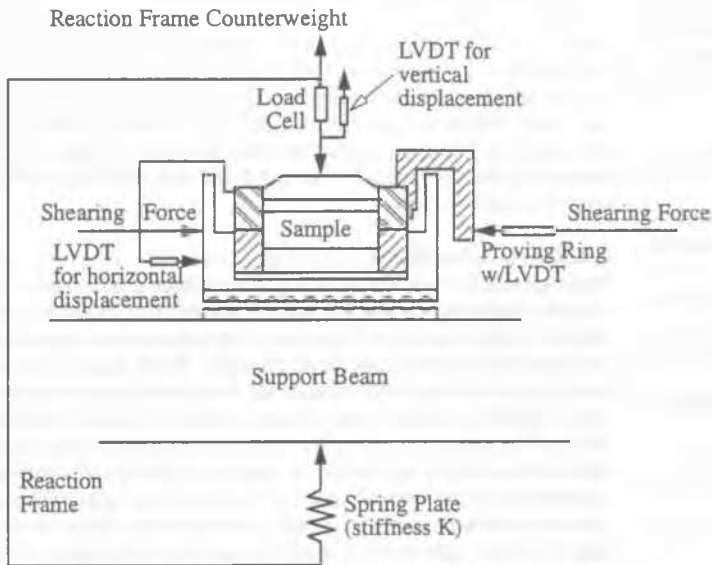


Figure 5.2. Schematic diagram of CNS shear box apparatus (Tabucanon et al, 1995).

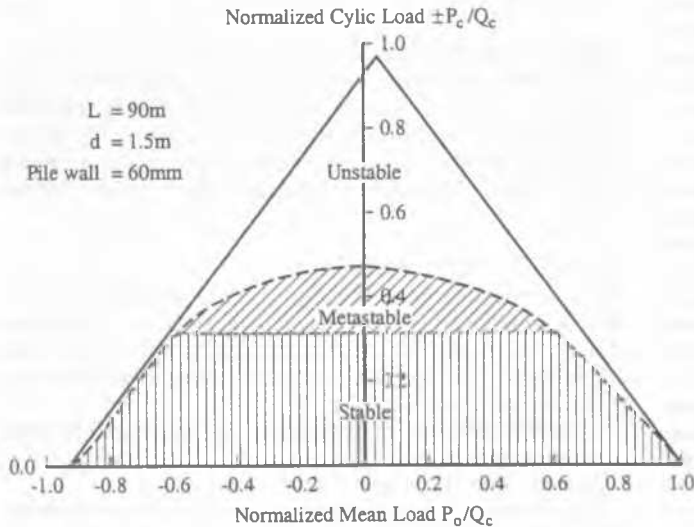


Figure 5.3. A cyclic stability diagram for a driven steel tube in clay;  $N = 100$  cycles (Poulos, 1988).

Improved correlations with CPT data have had considerable influence on design practice for estimating ultimate shaft resistance. Of particular interest is the work of Jardine, Lehane and their co-workers (e.g., Jardine and Chow, 1996; Lehane and Jardine, 1994), who have carried out tests on carefully instrumented piles in both sand and clay. On the basis of these data, and measurements of CPT in the soil, design procedures have been developed for both sands and clays. These methods are summarized in Table 5.5 and cover both open-ended and closed-ended piles.

### 5.2.5 Comparison between various methods

It is instructive to compare some of the commonly used methods of assessing the ultimate capacity with methods developed more recently. The case of two driven precast concrete piles in sand, described by Gregersen *et al.* (1973) is considered here. Figure 5.1 shows the soil conditions. A series of 0.28m diameter precast piles was driven and tested, some being 8m long and others being a total of 16m in length. Table 5.6 shows the ultimate shaft, base and total capacities computed by various methods, together with the values deduced from the load tests. It can be seen that there is some variability in the predictions from the various methods employed, with the method of Poulos (1989) seriously over-estimating the shaft capacity. For both pile lengths considered, the methods of Jardine and Chow (1996) and MELT (1995) agree well, and provide comfortably conservative estimates of shaft capacity, although they tend to over-predict the base capacity. The approach of Lee and Salgado (1999) appears to give reasonable base capacity predictions for both pile lengths.

### 5.2.6 Some issues relating to estimation of ultimate shaft resistance

A number of issues remain somewhat mysterious to many practical pile designers in relation to the ultimate shaft friction on piles. Such issues include the following:

- Does a limiting value of  $f_s$  actually exist, especially for piles in sandy soils?
- How does the value of  $f_s$  in uplift compare to the value of  $f_s$  for compression?
- Can laboratory testing be used to provide a more reliable estimate of  $f_s$ ?
- How does cyclic loading influence  $f_s$ ?

The results of recent research over the past decade or so can shed some light on these issues.

#### Limiting $f_s$ values for piles in sandy soils

The concept of limiting ultimate shaft resistance in sandy soils was developed by Kerisel (1961), Vesic (1967) and BCP (1971). It arose from tests on instrumented piles in which it appeared that the average ultimate shaft friction reached a limiting value for depths in excess of between 5 and 20 pile diameters from the top of the pile. This was attributed to an arching phenomenon around the shaft, and led to the adoption of a common practice of specifying limiting  $f_s$  values in design (e.g., Vesic, 1969; Meyerhof, 1976; Poulos and Davis, 1980).

The existence of such a limiting value has been questioned critically by a number of authors subsequently (e.g., Kulhawy, 1984; Fellenius, 1984). The apparent limiting values of  $f_s$  have been attributed to at least two factors:

- the existence of residual stresses in the piles before the measurements of shaft resistance were made. This leads to the shaft friction in the lower part of the pile appearing to be lower than the true value;
- the overconsolidation of the soil near the surface, which gives rise to higher values of in-situ lateral stress, and hence values of shaft resistance. The effects of overconsolidation become less with increasing depth, and hence the rate of increase of shaft resistance with depth becomes less.

Attempts to reproduce theoretically the apparent limiting shaft friction have been unsuccessful, although a reduction in the rate of increase of shaft resistance has been obtained by consideration of the effects of compressibility of the soil, and the re-

duction of the soil friction angle (and hence the interface friction angle) with increasing effective pressure and depth. The conclusion to be drawn from research into this aspect is that a limiting value of  $f_s$  probably does not exist, although the rate of increase of  $f_s$  with depth is not linear. However, from the viewpoint of practical design, the adoption of a suitable limiting value of  $f_s$  is a conservative approach which at least avoids predicting unrealistically large shaft friction values at great depths within a sandy soil.

### Shaft resistance in uplift and compression

It is generally accepted that the uplift shaft resistance for piles in clay is similar to that for compressive loading. However, there is conflicting evidence in relation to piles in sand, with some early researchers indicating similar values for both compression and uplift, while others found the values in uplift to be less than in compression. A significant advance in understanding of this problem was made by de Nicola and Randolph (1993) who showed that the ratio of the uplift resistances in uplift and compression,  $f_{su} / f_{sc}$ , was dependent on the relative compressibility of the pile, via the Poisson effect. The relationship they derived is as follows:

$$f_{su} / f_{sc} = \{1 - 0.2 \log_{10}[100/(L/d)]\} (1 - 8\eta + 25\eta^2) \quad (5.8)$$

where  $L$  = pile length;  $d$  = pile diameter;  $\eta$  = dimensionless compressibility factor =  $v_p \tan \delta \cdot (L/d) \cdot (G_{av}/E_p)$ ;  $v_p$  = pile Poisson's ratio;  $\delta$  = pile-soil interface friction angle;  $G_{av}$  = average soil shear modulus along pile shaft;  $E_p$  = Young's modulus of pile material. For typical piles in medium dense to dense sands, this ratio typically ranges between 0.7 and 0.9, but tends towards unity for relatively short piles.

### Laboratory testing for $f_s$

It has generally been accepted by practitioners that there is no suitable laboratory test which can be used reliably to measure the ultimate shaft friction  $f_s$ . However, there has been a significant development over the past 10-15 years in direct shear testing of interfaces, with the development of the "constant normal stiffness" (CNS) test (Ooi and Carter, 1987; Lam and Johnston, 1982). The basic concept of this test is illustrated in Figure 5.2, and involves the presence of a spring of appropriate stiffness against which the normal stress on the interface acts. This test provides a closer simulation of the conditions at a pile-soil interface than the conventional constant normal stress direct shear test. The normal stiffness  $K_n$  can be "tuned" to represent the restraint of the soil surrounding the pile, and is given by:

$$K_n = 4G_s / d \quad (5.9)$$

where  $G_s$  = shear modulus of surrounding soil;  $d$  = pile diameter.

The effects of interface volume changes and dilatancy can be tracked in a CNS test, and the results are particularly enlightening when cyclic loading is applied, as they demonstrate that the cyclic degradation is due to the reduction in normal stress arising from the cyclic displacements applied to the interface (see below).

### The Effects of Cyclic Loading on $f_s$

Cyclic or repeated axial loading can arise from the action of wave or wind forces and can be an important factor in the design of piles for offshore structures, transmission towers, and some tall buildings. The application of cyclic loading to piles can have at least two detrimental effects:

1. a possible reduction or "degradation" of pile resistance, especially shaft resistance
2. accumulation of permanent displacements.

If the loading is applied rapidly, there may be a counterbalancing effect of loading rate, that tends to increase pile resistance.

Table 5.5. Calculation of pile base capacity via CPT (after Jardine *et al.*, 1996).

Case	Expression	Notes
Closed – ended piles in sand	$f_b = q_{cav}[1-0.5 \log(d/d_{CPT})]$	$q_{cav}$ is averaged CPT value 1.5 pile diameters above and below pile toe. Lower bound $f_b=0.13q_{cav}$ applies for $d>2m$ .
Open-ended piles in sand – fully plugged piles	$f_b = q_{cav}[0.5-0.25 \log(d/d_{CPT})]$	Fully plugged piles occur only if $d<0.02[D_r-30]$ , where $d$ is in metres and $D_r$ is sand relative density (%). Develop 50% lower resistance than comparable closed-ended piles for $S/d=10\%$ . $d$ = pile diameter, $d_{CPT}$ = diameter of CPT probe.
Open-ended piles in sand – unplugged piles	$f_b = q_{cav}$	Lower bound for unplugged piles and large open-ended piles. End bearing acts only on annular base area of steel. No contributions from internal shear stresses
Closed-ended piles in clay	$f_b = 0.8q_{cav}$ (undrained loading) $f_b = 1.3q_{cav}$ (drained loading)	$q_{cav}$ is averaged 1.5 pile diameters above and below tip.
Open-ended piles in clay – fully plugged piles	$f_b = 0.4q_{cav}$ (undrained loading) $f_b = 0.65q_{cav}$ (drained loading)	Fully plugged pile occurs if $[d/d_{CPT}+0.45q_{cav}/p_a] < 36$ , where $d_i$ = inner diameter of pile, $d_{CPT}$ = diameter of CPT, $p_a$ = atmospheric pressure
Open-ended piles in clay – unplugged piles	$f_b = q_{cav}$ (undrained loading) $f_b = 1.6q_{cav}$ (drained loading)	End bearing on annular area of steel only. $q_{cav}$ = average CPT at the founding depth. No contributions from internal shear stresses

Table 5.6. Comparison between predicted ultimate capacity for driven piles in sand tests of Gregersen *et al.* (1973).

Method	Ultimate resistance for 8m long piles kN			Ultimate shaft resistance for 16m long piles kN		
	Shaft	Base	Total	Shaft	Base	Total
Jardine & Chow (1996)	152	120	272	320	217	537
MELT (1995)	146	118	264	313	196	509
Lee & Salgado (1999)	-	56	-	-	117	-
Poulos (1989)	315	-	-	676	-	-
Stas & Kulhawy (1984)	154	-	-	468	-	-
Effective Stress (Poulos & Davis, 1980)	202	136	338	428	136	564
Measured Values	206 & 240	60 & 35	266 & 275	373 & 397	108 & 74	481 & 471

The degradation of shaft resistance has been found to be a function of the cyclic displacement and the number of cycles (Mallock and Foo 1980; Poulos 1988a, 1988b). It arises from the reduction in normal stress as a consequence of volume reduction due to repeated cyclic shear strains. Using a simplified characterisation of shaft resistance degradation, it is possible to analyse the axial response of a pile subjected to various combinations of mean and cyclic loading. The results of such an analysis can be represented in the form of a cyclic stability diagram, that is a normalised plot of mean load  $P_o$  versus cyclic load  $P_c$  each normalised with respect to the ultimate compressive load capacity  $Q_c$  (Poulos, 1988a). A typical cyclic stability diagram is shown in Figure 5.3 for a driven offshore pile in clay. Three main regions can be identified:

- a cyclically stable region (A), in which cyclic loading has no influence on the axial pile capacity
- a cyclically metastable region (B), in which cyclic loading causes some reduction of axial capacity, but the pile does not fail within the specified number of cycles
- a cyclically unstable zone, in which cyclic loading causes sufficient reduction of axial capacity for the pile to fail within the specified number of cycles of load. Figure 5.4 summarises data from field and model cyclic load tests on piles in clay. Also shown are three computed relationships for the metastable/unstable boundary, covering a wide range of pile geometry and soil conditions. Reasonable agreement can be seen between the predicted combinations of cyclic and mean axial load for failure, and those actually measured.

A useful estimate of the cyclic load representing the boundary between the stable and metastable zones of the cyclic stability diagram may be obtained from the following expression developed by Randolph (1983):

$$P_{cl} / P_{su} \leq 1 / \sqrt{\Pi_3} \quad (5.10)$$

where  $P_{cl}$  is the cyclic load which just avoids slip between the pile and soil,  $P_{su}$  is the ultimate shaft load capacity, and

$$\Pi_3 = \frac{8}{\lambda \zeta} (L/d)^2 \quad (5.11)$$

in which  $\lambda$  and  $\zeta$  are defined in Equation (5.12) below, and  $L$  and  $d$  are the pile length and diameter respectively.

$$\zeta = 1n\{[0.25 + (2.5\rho(1-\nu) - 0.25)\xi]2L/d\} \quad (5.12a)$$

$$\lambda = E_p / G_l \quad (5.12b)$$

$$\xi = G_l / G_b \quad (5.12c)$$

$$\rho = G_m / G_l \quad (5.12d)$$

$\nu$  = soil Poisson's ratio;  $L$  = pile length;  $d$  = pile diameter;  $E_p$  = pile Young's modulus;  $G_l$  = soil shear modulus at level of pile tip;  $G_m$  = average soil shear modulus along shaft;  $G_b$  = shear modulus of bearing layer below pile tip.

### 5.2.7 Some issues related to the estimation of ultimate base resistance

#### Limiting end bearing resistance of piles in sand

As for ultimate shaft resistance, it is common in design practice to assign limiting values of ultimate base resistance, to piles in sand based largely on the research of Vesic (1969) and others. The existence of such a limiting value in reality has been questioned, and as for ultimate shaft resistance, the apparent limiting ultimate base resistance may be due to the presence of residual stresses in the pile, together with the reduction in friction angle of a sandy soil with increasing effective stress. The compressibility of the soil also plays an important role in determining the ultimate bearing capacity (Vesic, 1972), and the values for relatively compressible sands, such as marine carbonate sands, have been found to be considerably smaller than those for less compressible quartz sands (Poulos *et al.*, 1984; Poulos and Chua, 1985; Nauroy *et al.*, 1986). While there is a diminishing rate of increase of end bearing resistance with depth in sands, it remains

- 1 Theoretical lower boundary of unstable zone for model piles ( $N=100$ )
  - 2 Theoretical lower boundary of unstable zone for typical field piles ( $N=100$ )
  - 3 Theoretical lower boundary of unstable zone for example offshore pile ( $N=100$ )
  - Test with no failure for  $N > 10000$
  - △ Test with failure at  $N=564$
  - Test of Puesch (1982) - no failure
  - × Stevens (1978) - no settlement
  - + Stevens (1978) - continuing settlement
  - Stevens (1978) - "plunging failure"
  - ▼ Poulos (1981) - model tests, failure after 3-180 cycles
  - Karlsrud et al (1986) - failure after 100 cycles
- } McAnoy et al (1982)

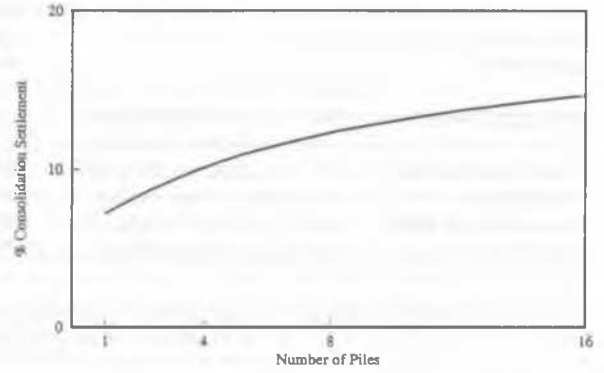
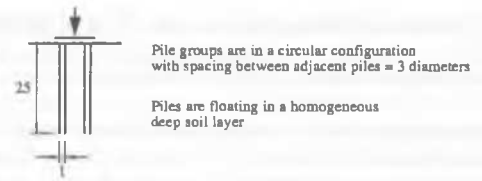


Figure 5.6. Group effect on proportion of consolidation settlement.

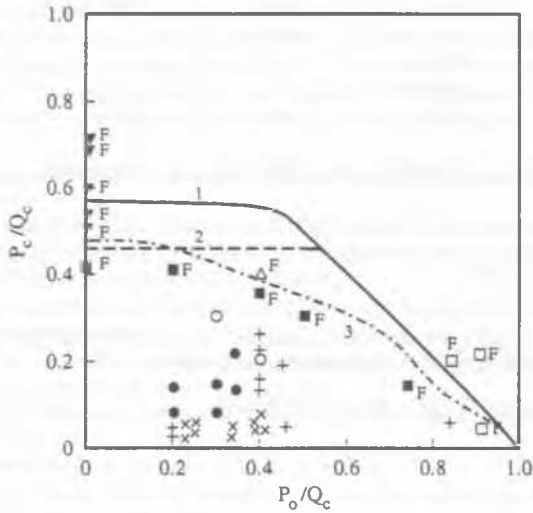
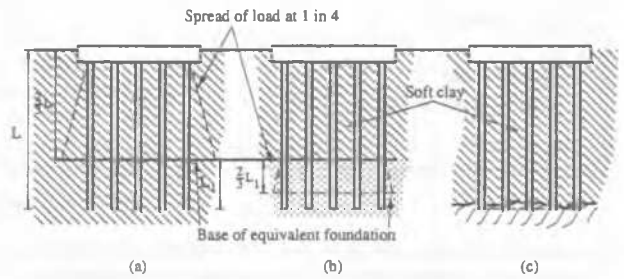


Figure 5.4. Comparison between field test data and theory.



- (a) Group of piles supported mainly by skin friction
- (b) Group of piles driven through weak clay to combined skin friction and end-bearing in stratum of dense granular soil
- (c) Group of piles supported in end-bearing on hard incompressible stratum. (After Tomlinson, 1986)

Figure 5.7. Equivalent raft approach.

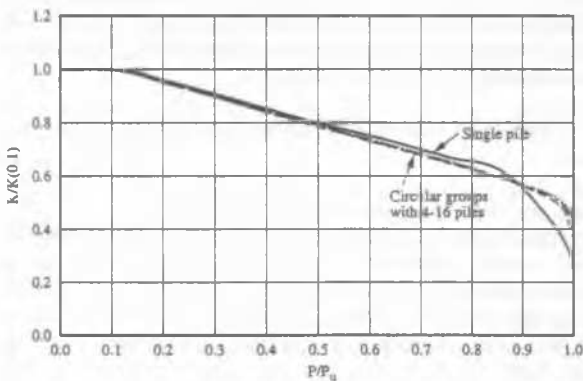
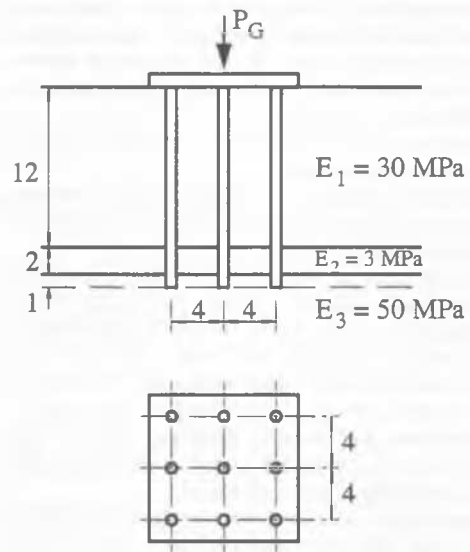


Figure 5.5. Effect of grouping on relative pile stiffness.



DEFPIG vs. equivalent raft analysis

Figure 5.8. Example of pile group with soft layer about tip.

convenient from a design viewpoint to impose an upper limit to the design value of  $f_b$ , and it would appear unlikely that this common practice will be easily discarded.

#### End bearing capacity of piles in a layered soil profile

This very important problem was addressed by Meyerhof (1976) and subsequently by Meyerhof and Sastry (1978). In the latter paper, it was recommended that the effects of a softer layer underlying the founding layer in which the pile base was situated should be taken into account if the ratio  $h/d_b$  was less than 6, where  $h$  = depth between pile base and the lower layer,  $d_b$  = diameter of pile base. Subsequent work by Matsui (1993) has indicated that the earlier recommendations may have been rather conservative, and that the weaker underlying layer only affected end bearing capacity if  $h/d_b$  is less than 3.

#### Effects of cyclic loading

There is only limited information on cyclic loading effects on end bearing capacity of piles, but the indications from the work of van Weele (1979) and Poulos and Chua (1985) are that, while there may be some accumulation of settlement, the ultimate end bearing capacity does not appear to reduce significantly after the application of cyclic loading.

#### 5.2.8 Group effects on ultimate load capacity

It is convenient to define a pile group efficiency  $Y$  for ultimate capacity as follows:

$$Y = P_{ug} / \Sigma P_u \quad (5.13)$$

where  $P_{ug}$  = ultimate capacity of group;  $\Sigma P_u$  = sum of ultimate capacities of individual piles in group.

Early methods of estimating  $Y$  were often based purely on geometry, e.g., the Converse Labarre formulae and Feld's rule (Poulos and Davis, 1980), but it is now recognised that such approaches are deficient in not considering the soil and pile characteristics. Table 5.7 summarises recommendations for the estimation of  $Y$  for various situations. There appears to have been relatively little research into group effects on pile capacity over the past two decades, and the approach suggested by Terzaghi and Peck (1948) continues to be widely used for groups in clay, while empirical approaches such as those in Table 5.7 are used for groups in sand.

#### 5.2.9 Summary

It is difficult to recommend any single approach as being the most appropriate for estimating ultimate axial pile capacity. In principle the effective stress approach provides the most acceptable methods, and the recent adaptations by Jardine and his co-workers appear to be valuable for driven piles. However, from a practical viewpoint, methods relying on SPT and CPT data are attractive and can provide adequate estimates of pile capacity, especially if load correlations are employed. The traditional approach of Terzaghi and Peck (1948) still appears to provide a useful basis for estimating the capacity of pile groups in clay.

### 5.3 Settlement of piles and pile groups

#### 5.3.1 Methods of Analysis

Methods of estimating the settlement of single piles usually fall into three groups:

- Load transfer ( $t$ - $z$ ) methods
- Elasticity-based methods
- Numerical methods such as the finite element or finite difference methods.

Of particular practical value is the approach originally developed by Randolph and Wroth (1978), which falls within the second of the above groups. It is expressed in closed form and is therefore very convenient for spreadsheet or mathematical programming. This approach however has a number of limitations:

- The soil is assumed to be elastic;

- The soil stiffness is assumed to increase linearly with depth along the pile shaft;
- The pile shaft is of uniform diameter.

Subsequent work by Chin and Poulos (1992), Guo and Randolph (1997) and Guo (1999) has removed some of the restrictions of the original work by Randolph and Wroth.

Poulos (1989) has compared some of the methods (boundary element, load transfer, closed-form and finite element) and found that most of the methods are capable of giving similar results for single pile settlement, despite differences in the fundamental basis of the analyses. The key to successful settlement prediction lies therefore not in the method of analysis used, but in the selection of appropriate soil-pile parameters, and in quantifying the relationship between the settlement of a single pile and a pile group.

Table 5.7. Recommendations for pile group efficiency estimation.

Case	Group Efficiency $Y$	Remarks
Driven piles in loose to medium dense sand	1.0	$Y$ may be considerably greater than 1: adopt 1 for design
End-bearing piles on rock, dense sand, or gravel	1.0	Base resistance is not much effected by group action, even at small spacings (Meyerhof, 1976)
Bored friction piles in sand	0.67	For "customary spacings": i.e., 3 " 1 diameters (Meyerhof, 1976)
Friction piles in clay - cap above surface	Lesser of $P_B/\Sigma P_u$ , or 1.0	Terzaghi and Peck (1967). Make allowance for any soft layers below base.
		Poulos and Davis (1980). Make allowance for any soft layers below base

Note:  $P_B$  = ultimate load capacity of block containing piles and soil;  $\Sigma P_u$  = sum of ultimate capacities of individual piles.

It is now well recognized that the settlement of a pile group can differ significantly from that of a single pile at the same average load level. There are a number of approaches commonly adopted for the estimation of the settlement of pile groups:

- Methods which employ the concept of interaction factors and the principle of superposition (e.g., Poulos and Davis, 1980);
- Methods which involve the modification of a single pile load-settlement curve, to take account of group interaction effects;
- The settlement ratio method, in which the settlement of a single pile at the average load level is multiplied by a group settlement ratio  $R_s$ , which reflects the effects of group interaction;
- The equivalent raft method, in which the pile group is represented by an equivalent raft acting at some characteristic depth along the piles;
- The equivalent pier method, in which the pile group is represented by a pier containing the piles and the soil between them. The pier is treated as a single pile of equivalent stiffness in order to compute the average settlement of the group.
- Numerical methods such as the finite element method and the finite difference method (such as FLAC). While earlier work employed two-dimensional analyses, it is now less uncommon for full three-dimensional analyses to be employed (e.g., Katzenbach *et al.*, 1998).



Because of the limitations of space, it is not possible to review fully the various methods available for analysis of piles and pile groups. Therefore, in the following subsections, some issues relating to the practical application of theories for pile settlement prediction will be considered. These include:

1. Developments in the interaction factor method for pile groups
2. The applicability of the equivalent raft method
3. The applicability of the equivalent pier method
4. The effects of dissimilar or defective piles within the group
5. The effects of compressible underlying layers
6. Differential settlements within a group
7. The significance of non-linearity in pile settlement prediction
8. The time-dependency of settlement of pile foundations
9. Interaction between adjacent groups
10. Assessment of soil stiffness for pile settlement calculation.

### 5.3.2 Significance of non-linearity

For piles which derive the majority of their resistance from shaft friction, it is found that the load-settlement behaviour at normal design working loads is quasi-linear and dependent largely on the stiffness provided by the pile shaft. As a consequence, linear settlement theory is often adequate to predict the settlement. Non-linearity may become more significant under the following circumstances:

- For piles which derive a significant amount of their resistance from the base; in such a case, the full shaft resistance of the pile may be fully mobilized at the working load, and the load-settlement relationship is then dependent on both the shaft stiffness and the base stiffness.
- For piles which are operating at a relatively low overall factor of safety.
- For piles which are slender and relatively compressible; in such cases, pile-soil slip commences near the pile head at relatively low load levels, and progressively works its way down the pile, thus giving rise to a distinctly non-linear load-settlement behaviour, even at normal working load levels.
- For piles in soils which exhibit strain-softening characteristics.

Non-linear pile-soil behaviour can be taken into account in many methods of analysis, and may also be readily incorporated into hand methods of calculation. Such a method has been described by Poulos and Davis (1980), and requires a knowledge only of the elastic stiffness of the pile, the proportion of load carried by the base under elastic conditions, and the ultimate shaft and base capacities. A more sophisticated approach has been developed by Fleming (1992), in which the shaft and base behaviours have been represented by hyperbolic relationships between settlement and load level. In this way, it has been possible to obtain remarkably good agreement between computed and measured load-settlement behaviour of piles, for a very wide range of geometries and soil types.

Poulos (1989) has found that a simple representation of non-linearity is often adequate to model non-linear pile settlement behaviour, and this contention has been supported by more recent work by Guo and Randolph (1997). They have indicated that a simple elastic-plastic nonlinear behaviour can give a good representation of load-settlement behaviour, and have developed closed-form solutions for the estimation of this behaviour.

As an example of the significance of non-linearity for single piles and pile groups, Figure 5.5 shows the variation of stiffness with applied load level, for a single pile, a 4-pile group, an 8-pile group, and a 16-pile group, the group piles being in a circular configuration with a spacing of 3 diameters between adjacent piles. These results have been obtained from a boundary element analysis in which each of the piles is divided into 20 elements, and hyperbolic shaft and base responses are assumed. The stiffness is presented in dimensionless form in terms of the initial stiffness at an applied load level of 0.1 times the ultimate load capacity. It can be seen that, for the case considered, the effects

of non-linearity are similar for the single pile and the pile groups, except near failure, when the single pile behaviour is more severely affected than that of the group.

### 5.3.3 Time-dependency of pile settlements

Time-dependency of settlement of foundations (under constant loading) usually arises from two sources:

1. Consolidation settlements due to dissipation of excess pore pressures, usually in clay or silty soils;
2. Settlements arising from creep of the soil under constant loading.

For an ideal elastic clay soil, the relative importance of consolidation settlement can be computed by comparing the immediate settlement (computed by using the undrained deformation parameters of the soil) and the total final settlement (computed using the drained deformation soil parameters). As an example, Figure 5.6 shows the proportion of consolidation settlement for the same cases as shown in Figure 5.5. The solutions from an elastic boundary element analysis have been used. It can be seen that, for the single pile, the consolidation settlement comprises only about 7% of the total settlement. This occurs because the majority of the deformation of a single pile is from shear deformation, rather than volumetric deformations. Thus, for single piles, consolidation settlements are relatively minor and time-settlement calculations are rarely necessary. The vast majority of pile loading tests on single piles support the above theoretical conclusion that consolidation settlements are small at normal working loads.

As the number of piles in the group increases, the proportion of consolidation settlement also increases, because of the greater proportion of load carried by the pile bases, and the consequent greater amount of volumetric deformation. However, even for the 16-pile group, the computed consolidation settlement accounts for only about 15% of the final settlement. In general, the consolidation settlement is likely to be significant only if the group is relatively large, and/or there is a relatively deep layer of compressible material within the zone of soil influenced by the group. This issue is explored further in Section 5.3.8.

Settlements due to soil creep are generally not significant at normal working loads, but may become important at load levels of 70% or more of the ultimate. Practical methods for estimating creep settlements are not well developed, Booker and Poulos (1976) have demonstrated that a time-dependent Young's modulus of the soil may be used, but it is not easy to estimate the modulus-time relationship from the data obtained from conventional site characterization data. Guo (2000) has developed a closed-form expression for the load transfer characteristics, taking into account both non-linearity and visco-elastic behaviour. His approach shows good agreement with the earlier Booker and Poulos solutions. A method of back-calculating the required creep parameters is also described by Guo.

### 5.3.4 Developments in the interaction factor method for pile groups

One of the common means of analyzing pile group behaviour is via the interaction factor method described by Poulos and Davis (1980). In this method, the settlement  $w_i$  of a pile  $i$  within a group of  $n$  piles is given as follows:

$$w_i = \sum_{j=1}^n (P_{av} S_1 \alpha_{ij}) \quad (5.14)$$

where  $P_{av}$  = average load on a pile within the group;  $S_1$  = settlement of a single pile under unit load (i.e., the pile flexibility);  $\alpha_{ij}$  = interaction factor for pile  $i$  due to any other pile ( $j$ ) within the group.

In the original approach, the interaction factors were computed from boundary element analysis and plotted in graphical form. They were also applied to the total flexibility  $S_I$  of the pile, including both elastic and non-elastic components of the single pile settlement.

In recent years, significant improvements have been made to the original interaction factor method, among the most important being:

1. The application of the interaction factor to only the elastic component of the single pile flexibility (e.g., Randolph, 1994);
2. The incorporation of non-linearity of single pile response within the interaction factor for the effect of a pile on itself (Mandolini and Viggiani, 1997);
3. The development of simplified or closed-form expressions for the interaction factors, thus enabling a simpler computer analysis of group settlement behaviour to be obtained.

In relation to item 1 above, the settlement of a pile  $i$  in the group is then given by:

$$w_i = \sum_{j=1}^n (P_{av} S_{1e} \alpha_{ij}) \quad (5.15)$$

where  $S_{1e}$  is the elastic flexibility of the pile.

By assuming that the load-settlement behaviour of the pile is hyperbolic, Mandolini and Viggiani (1997) express the interaction factor,  $\alpha_{ii}$ , for a pile  $i$  due to its own load as:

$$\alpha_{ii} = 1/(1 - R_f P/P_u)^q \quad (5.16)$$

where  $R_f$  = hyperbolic factor (taken as unity);  $P$  = load on pile  $i$ ;  $P_u$  = ultimate load capacity of pile  $i$ ;  $q$  = analysis exponent = 2 for incremental non-linear analysis and 1 for equivalent linear analysis. Randolph and Wroth (1979) have developed the following closed-form approximation for the interaction factor for a pile in a deep layer of soil whose modulus increases linearly with depth:

$$\alpha_{ij} = \frac{1 - s/(d/\pi + s) + \pi(1 - \nu)\rho\Lambda(1/\gamma - 1/\Gamma)}{1 + \pi(1 - \nu)\rho\Lambda/\gamma} \quad (5.17)$$

where  $s$  = centre-to-centre spacing between piles  $i$  and  $j$ ;  $\rho$  = ratio of soil modulus at mid-length of pile to that at the level of the pile tip (=1 for a constant modulus soil and 0.5 for a "Gibson" soil);  $\gamma = \ln(2r_m/d)$ ;  $\Gamma = \ln(2r_m^2/ds)$ ;  $r_m = 2.5(1 - \nu)\rho L$ ;  $\nu$  = soil Poisson's ratio;  $L$  = pile length;  $d$  = pile diameter;  $\Lambda = L/d$ .

Mandolini and Viggiani (1997) have developed simple expressions for the interaction factor, in one of the following forms:

$$\alpha = k_1 (s/d)^{k_2} \quad (5.18a)$$

$$\alpha = \{k_3 + k_4 \ln(s/d)\} \quad (5.18b)$$

where  $k_1 - k_4$  = fitting parameters.

For four typical field cases analyzed by Mandolini and Viggiani, the values of  $k_1$  ranged between 0.57 and 0.98, while the range of  $k_2$  was -0.60 to -1.20. For one other case, values of  $k_3 = 1.0$  and  $k_4 = -0.26$  were computed.

It was also assumed that no interaction occurred for spacings greater than a limiting value  $s_{max}$  where:

$$s_{max} = [0.25 + (2.5\rho(1 - \nu) - 0.25)E_{sL}/E_b]L + r_g \quad (5.19)$$

where  $E_{sL}$  = soil modulus at mid-length of the pile;  $E_b$  = modulus of bearing stratum below pile tip;  $r_g$  = a group distance defined by Randolph and Wroth (1979), and the other parameters are defined above.

The presence of a hard layer at the base of a soil layer can substantially reduce the interaction factor and "damp out" its effect at relatively small pile spacings. The use of solutions for a deep layer may thus lead to significant over-estimates of pile interactions and hence, pile group settlements. Mylonakis and Gazetas 1998) and Guo and Randolph (1999) have developed closed-form expressions for the interaction factor, in which the important effect of the finite thickness of a soil layer can be taken into account.

Costanzo and Lancellotta (1998) have developed an analytical expression for the interaction factor, taking into account the soil non-linear response. The case of floating piles is considered, with a linear variation of soil shear modulus with radial distance from the pile shaft.

### 5.3.5 Applicability of the equivalent raft method

The equivalent raft method has been used extensively for estimating pile group settlements. It relies on the replacement of the pile group by a raft foundation of some equivalent dimensions, acting at some representative depth below the surface. There are many variants of this method, but the one suggested by Tomlinson (1986) appears to be a convenient and useful approach. As illustrated in Figure 5.7, the representative depth varies from  $2L/3$  to  $L$ , depending on the assessed founding conditions; the former applies to floating pile groups, while the latter value is for end bearing groups. The load is spread at an angle which varies from 1 in 4 for friction piles, to zero for end bearing groups. Once the equivalent raft has been established, the settlement can be computed from normal shallow foundation analysis, taking into account the embedment of the equivalent raft and the compression of the piles above the equivalent raft founding level (Poulos, 1993).

Van Impe (1991) has studied a number of case histories, and related the accuracy of the equivalent raft method to the parameter  $\omega$ , where:

$$\omega = \frac{\text{Sum of pile cross-sectional areas in the group}}{\text{Plan area of pile group}} \quad (5.20)$$

Van Impe has concluded that the equivalent raft method should be limited to cases in which  $\omega$  is greater than about 0.10, i.e., the pile cross-sections exceed about 10% of the plan area of the group.

Poulos (1993) has examined the applicability of the equivalent raft method to groups of friction piles and also end bearing pile groups. He concluded that the equivalent raft method gives a reasonably accurate prediction of the settlement of groups containing more than about 16 piles (at typical spacing of 3 pile diameters centre-to-centre). This is consistent with the criterion developed by van Impe (1991). Thus, at the very least, the equivalent raft method is a very simple and useful approach for a wide range of pile group geometries, and also provides a useful check for more complex and complete pile group settlement analyses.

Much of the success of the equivalent raft method hinges on the selection of the representative depth of the raft and the angle of load spread. Considerable engineering judgement must be exercised here, and firm rules cannot be employed without a proper consideration of the soil stratigraphy. As an example, the case shown in Figure 5.8 has been analyzed using the equivalent raft method (following the general approach outlined by Poulos, 1993), and compared with a less approximate analysis using the computer program DEFFIG. In the case examined, a 2m deep soft layer exists just above the level of the pile tips. In employing the equivalent raft method, the following variants of the equivalent raft method have been used:

1. The equivalent depth of the raft has been taken at  $2L/3$  below the pile head, i.e., above the soft layer, with a 1:4 spread of the load
2. The equivalent depth has been taken at the base of the soft layer, with no dispersion of load above that level
3. The equivalent depth has been taken at the base of the soft layer, with dispersion of the load only to  $2L/3$ .

Table 5.7 shows the results of the calculations, and it can be seen from the table that option 1 above gives a severe over-estimate of the settlement compared to the DEFFIG result. Option 2 over-estimates the settlement by about 34%, while option 3 slightly under-estimates the settlement (by about 10%). Table 5.7 also shows the results of the calculations when no soft layer is present. In that case, the equivalent raft gives a very good es-

imate of the settlement. From this simple example, it may be concluded that the equivalent raft method provides a useful approach to estimating pile group settlements and can be adapted, as long as appropriate judgement is exercised in the selection of the equivalent depth (to mirror the actual load transfer mechanisms), and the degree of dispersion along the pile shafts.

### 5.3.6 Applicability of the equivalent pier method

In this method, the pile group is replaced by a pier of similar length to the piles in the group, and with an equivalent diameter,  $d_e$ , estimated as follows (Poulos, 1993):

$$d_e \equiv (1.13 \text{ to } 1.27) \cdot (A_G)^{0.5} \quad (5.21)$$

where  $A_G$  = plan area of pile group.

The lower figure is more relevant to predominantly end bearing piles, while the larger value is more applicable to predominantly friction or floating piles.

Poulos (1993) and Randolph (1994a) have examined the accuracy of the equivalent pier method for predicting group settlements, and have concluded that it gives good results. Randolph (1994a) has related the accuracy to the aspect ratio  $R$ , of the group, where:

$$R = (ns/L)^{0.5} \quad (5.22)$$

where  $n$  = number of piles;  $s$  = pile centre-to-centre spacing;  $L$  = pile length.

The equivalent pier method tends to over-predict stiffness for values of  $R$  less than about 3, but the values appear to be within about 20% of those from a more accurate analysis for values of  $R$  of 1 or more, provided that the pile spacing is not greater than about 5 diameters. It would appear that the equivalent pier approach can be adopted for preliminary estimates of group settlement.

An attractive feature of the equivalent pier method is the ability to employ the closed-form equations of Randolph and Wroth (1978), and also to develop a non-linear load-settlement curve, for example, using the simple approach described by Poulos and Davis (1980). It is also possible to estimate the rate of consolidation settlement, using solutions from consolidation theory for a pier within a two-phase poro-elastic soil mass.

Table 5.7. Computed settlement for pile group example.

Analysis	Equivalent depth of raft (m)	Assumed load dispersion	Computed settlement (mm)	Remarks
DEFPIG	-	-	7.1	Soft layer present
Equivalent Raft - Case 1)	10	1:4	16.5	"
Equivalent Raft - Case 2)	14	None	9.6	"
Equivalent Raft - Case 3)	14	1:4 (only to 10m)	6.4	"
DEFPIG	-	-	7.0	No soft layer present
Equivalent Raft - Case 1)	10	1:4	7.2	"

### 5.3.7 Effects of dissimilar or defective piles within a group

Most of the available methods of pile group settlement analysis assume that all the piles within the group are identical and that the soil profile does not vary over the plan area of the group. In practice, piles are often dissimilar, especially with respect to length, and may also contain structural defects such as necked sections and sections of poor concrete, and/or geotechnical defects such as a soft toe or a section along which the skin friction is reduced because of poor construction practices. The possible consequences of dissimilar or defective piles within a group have been explored by Poulos (1997a), who has found the following indications from theoretical analyses of defects in a single pile:

- Defects within a single pile can reduce the axial stiffness and load capacity of the pile.
- Structural defects such as "necking" can be characterized by a structural integrity factor, to which the reduction in axial stiffness can be approximately related.
- Geotechnical defects, such as a soft toe, lead to a reduction in pile head stiffness which becomes more severe as the applied load level increases. Failure, or apparent failure, of a pile is more abrupt in piles with structural defects than for piles with geotechnical defects.

For groups containing one or more defective piles, it has been found that the reduction in axial stiffness of a group becomes more marked as the proportion of defective piles, and/or the applied load level, increases. Importantly, the presence of defective piles can result in induced lateral deflection and cap rotation in the group, and additional moments in the piles. This induced lateral response, which can occur under purely axial applied loading, becomes more severe as the location of the defective piles becomes more asymmetric, and can compromise the structural integrity of the sound piles. It is not yet feasible to employ simple methods of calculation to examine the behaviour of groups with defective or dissimilar piles, and even computer methods of group settlement analysis should have the ability to consider both axial and lateral responses, rather than only axial response. In computer programs employing the interaction factor method, modifications need to be made to account for the interaction between dissimilar piles. Such approximations have been explored by Xu (2000).

### 5.3.8 The effects of compressible underlying layers

It has been recognized for some time that the presence of soft compressible layers below the pile tips can result in substantial increases in the settlement of a pile group, despite the fact that the settlement of a single pile may be largely unaffected by the compressible layers. Some examples of such experiences include the chimney foundation reported by Golder and Osler (1968) and the 14 storey building described by Peaker (1984).

To emphasize the potential significance of compressible underlying layers, a simple hypothetical problem has been analyzed. Square pile groups founded in a stiffer layer, overlying a softer layer have been analyzed, using the computer program DEFPIG, and assuming that the pile-soil response remains elastic. The settlement of the group is expressed as a proportion of the settlement of the group if the compressible layer was not present, and is related to the number of piles in the group (with the spacing between adjacent piles remaining constant). The results of the analysis are shown in Figure 5.10. It can be seen that, as might be expected, the larger the group (and therefore the width of the pile group), the greater is the effect of the underlying compressible layer on settlement. It is clear that if the presence of such compressible layers is either not identified, or is ignored, the pile group settlements can be several times those which would be predicted for the group bearing on a continuous competent stratum.

### 5.3.9 Differential settlements within a group

Most analyses of pile group settlement make one of the two following extreme assumptions:

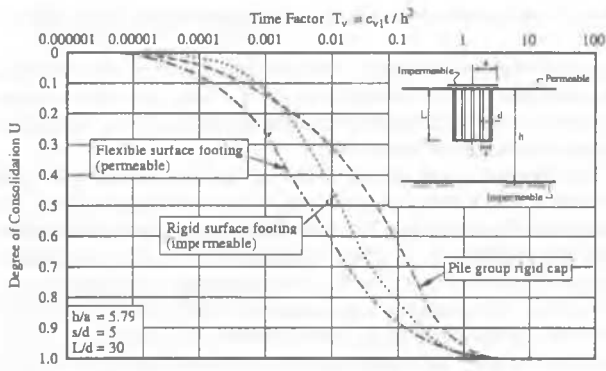


Figure 5.9. Rate of consolidation of 5 x 5 pile group.

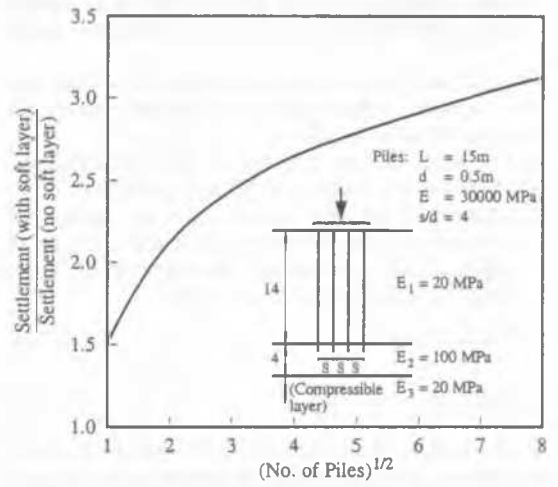


Figure 5.10. Effect of underlying compressible layer on group settlement.

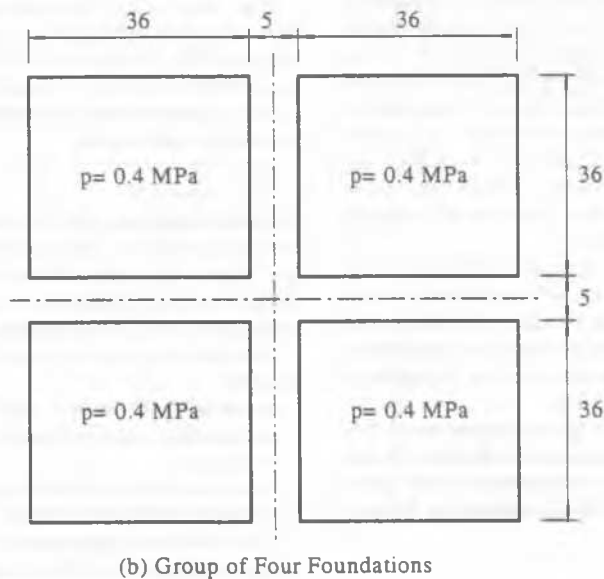
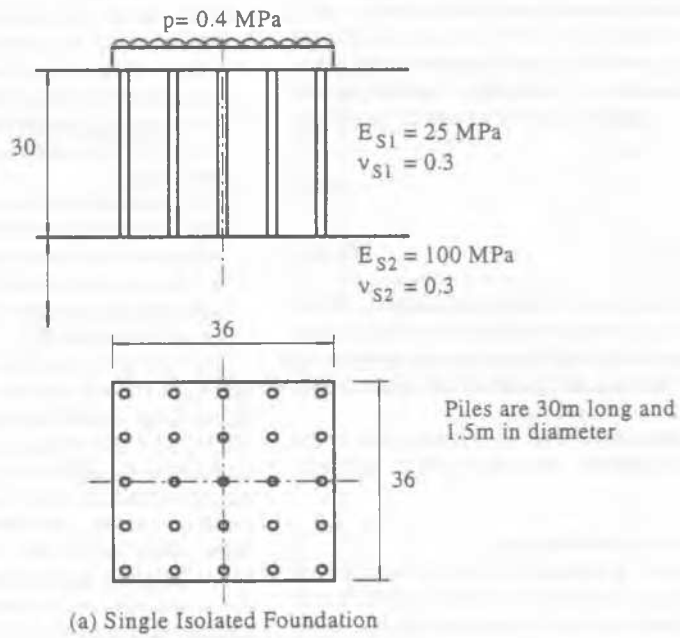


Figure 5.11. Example of 4 interacting structures.

1. The pile cap is perfectly rigid so that all piles settle equally (under centric load) and hence there is no differential settlement.
2. The pile cap is flexible, so that the distribution of load onto the piles is known; in this case, the differential settlements within the group can be computed.

In reality, the situation is usually between these two extremes. Randolph (1994a) has developed useful design guidelines for assessing the differential settlement within a uniformly loaded pile group. For a flexible pile cap, Randolph has related the ratio of differential settlement  $\Delta S$  to the average group settlement,  $S_{av}$ , to the ratio  $R$  defined in Equation (5.22), as follows:

$$\Delta S / S_{av} = fR / 4 \text{ for } R \leq 4 \quad (5.23a)$$

$$\Delta S / S_{av} = f \text{ for } R > 4 \quad (5.23b)$$

where  $f = 0.3$  for centre-to-midside, and  $0.5$  for centre-to-corner.

For pile caps with a finite rigidity, the differential settlements will reduce from the above values (which are for perfectly flexible pile caps), and Randolph suggests that the approach developed by Randolph and Clancy (1993) be adopted. This approach relates the normalized differential settlement to the relative stiffness of the pile cap (considered as a raft). Mayne and Poulos (1999) have developed a closed-form approximation for the ratio of corner to centre settlement of a rectangular foundation, and from this approximation, a rigidity correction factor,  $f_R$  can be derived:

$$f_R = 1 / (1 + 2.17 K_F) \quad (5.24a)$$

$$\text{where } K_F = (E_c / E_{sv})(2t / d)^3 \quad (5.24b)$$

is the foundation flexibility factor;  $E_c$  = Young's modulus of pile cap;  $E_{sv}$  = representative soil Young's modulus beneath the cap (typically within a depth of about half the equivalent diameter of the cap);  $t$  = thickness of pile cap;  $d$  = equivalent diameter of pile cap (to give equal area with the actual cap).

The factor  $f_R$  from Equation (5.24a) is then applied to the maximum differential settlement estimated from Equation (5.23).

### 5.3.10 Interaction between adjacent groups

It is often assumed that, when a structure is founded on piles, its settlement will be dependent only on the loading applied to that structure. However, if there are other structures nearby, there will be some interaction between the foundations, and as a consequence, the settlement of each of the structures will be greater than that of an isolated structure. To assess the possible consequences of such interaction, the case shown in Figure 5.11 has been analyzed, using the computer program DEFPIG. The case involves four identical structures on four identical foundations, each consisting of 25 equally loaded piles which bear on a stiffer stratum and are connected by a flexible cap. For simplicity, the soil layers are assumed to be linearly elastic. While this case is hypothetical, it is not dissimilar to some high-density housing developments in cities such as Hong Kong.

Figure 5.12 shows the variation of computed settlement of the foundations. The settlement of an isolated foundation is also shown. It will be seen that the settlement taking interaction into account is significantly greater than the settlement of the isolated foundation, with the maximum settlement of the foundations being increased by almost 150% in this case.

An important consequence of inter-group interaction is that each of the foundations suffers an induced tilt, despite the fact that the ground conditions are identical beneath all four structures. This tilt can be substantial when the underlying bearing stratum is relatively compressible.

### 5.3.11 Assessment of soil stiffness for pile settlement calculation

Section 8 will deal in detail with the assessment of soil stiffness for estimates of the deformation of various foundation types. However, some comments specifically related to the estimation of pile settlement are given below.

For estimations of pile settlement, the key geotechnical parameter is the stiffness of the soil. If the analysis is based on elastic continuum theory, the soil stiffness can be expressed by a Young's modulus  $E_s$  or shear modulus  $G_s$ . Both the magnitude and distribution of these moduli are important. It is clear that  $E_s$  (or  $G_s$ ) are not constants, but depend on many factors, including soil type, initial stress state, stress history, the method of installation of the pile, the stress system and stress level imposed by the pile and the pile group, and whether short-term or long-term conditions are being considered.

It should also be recognized that, in conventional analyses (including those presented herein), the assumption of lateral homogeneity of the soil is generally made. However, in reality, there are at least four stress regimes operative within the soil surrounding a group of vertically loaded piles, as shown in Figure 5.13. Hence, the following four different values of Young's modulus can be distinguished:

1. The value  $E_s$  for the soil in the vicinity of the pile shaft. This value will tend to influence strongly the settlement of a single pile and small pile groups.
2. The value  $E_{sb}$  immediately below the pile tip. This value will also tend to influence the settlement of single pile and small pile groups.
3. The small-strain value,  $E_{si}$  for the soil between the piles. This will reflect the small strains in this region and will affect the settlement interaction between the piles.
4.  $E_s$  for the soil well below the pile tips ( $E_{sd}$ ). This value will influence the settlement of a group more significantly as the group size increases.

The first and third values ( $E_s$  and  $E_{si}$ ) reflect primarily the response of the soil to shear, while the second and fourth values ( $E_{sb}$  and  $E_{sd}$ ) reflect both shear and volumetric strains.  $E_s$  and  $E_{sb}$  will both be influenced by the installation process, and would be expected to be different for bored piles and for driven piles. On the other hand,  $E_{si}$  and  $E_{sd}$  are unlikely to be affected by the installation process, but rather by the initial stress state and the stress history of the soil. As a corollary, the method of installation is likely to have a more significant effect on the settlement of a single pile (which depends largely on  $E_s$  and  $E_{sb}$ ) than on the settlement of a pile group, which may depend to a large extent on  $E_{si}$  and  $E_{sd}$ .

The issue of the estimation of the soil modulus values has been discussed at length by Randolph (1994), Poulos (1994), Mayne (1995), Mandolini and Viggiani (1997), and Yamashita *et al.* (1998). The latter suggest that, for a purely elastic analysis, a typical value of modulus of about 0.25 to 0.3 times the small-strain value can be used.

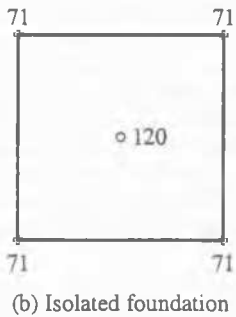
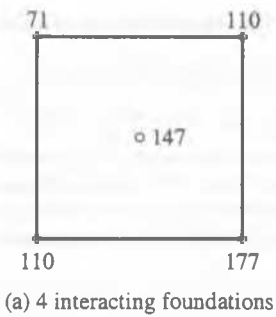
### 5.3.12 Summary

Elasticity-based methods for estimating the settlement of a single pile can be adopted, as can load-transfer methods in which the "t-z" curves are appropriately selected. Methods based on consolidation theory generally do not mirror the correct load transfer process and should be discarded.

For pile groups, one or more of the following methods can be adopted:

1. methods based on an elasticity analysis of pile-soil-pile interaction; these enable detailed response of the pile group to be completed,
2. the equivalent raft method, and
3. the equivalent pier method.

The latter two approaches are best used for estimates of the overall settlement but are not suitable for predicting the detailed distributions of settlement and pile load within the group.



Note: Settlements in mm

Figure 5.12. Computed settlements for example of interacting and isolated foundations.

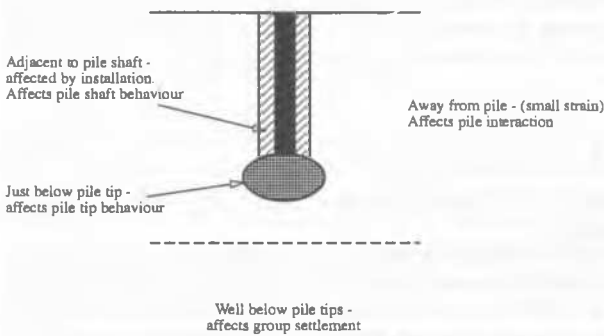
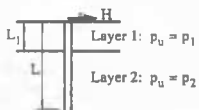


Figure 5.13. Different soil modulus values in various regions around piles.



$H_u$  (homog) is for pile in homogeneous layer with  $p_u = p_2$

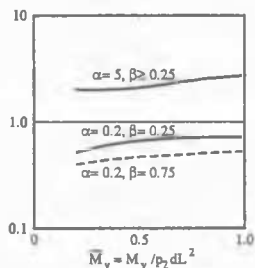
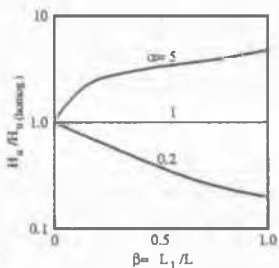


Figure 5.14. Effect of soil layering on ultimate lateral capacity of pile in clay.

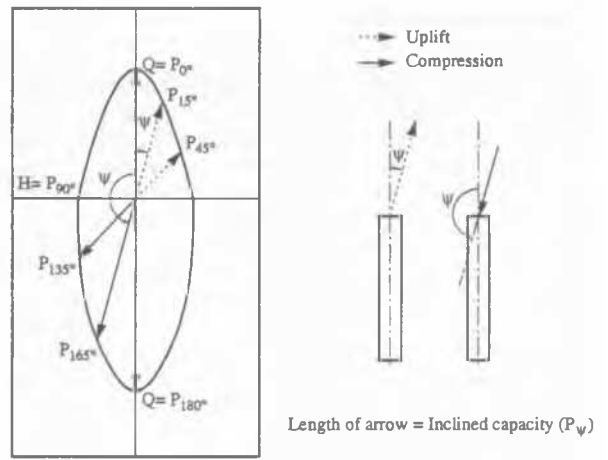


Figure 5.15. Schematic of polar capacity diagram and load inclination definition (Cho and Kulhawy, 1995).

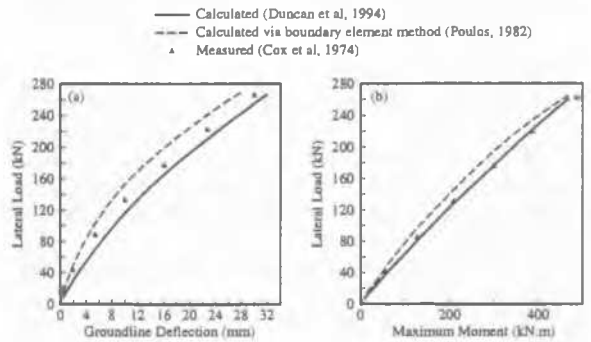


Figure 5.16. Comparison of measured and calculated deflections and moments for pipe pile in sand (a) deflection; (b) moment.

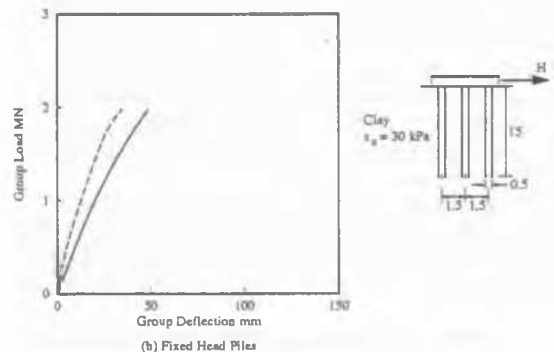
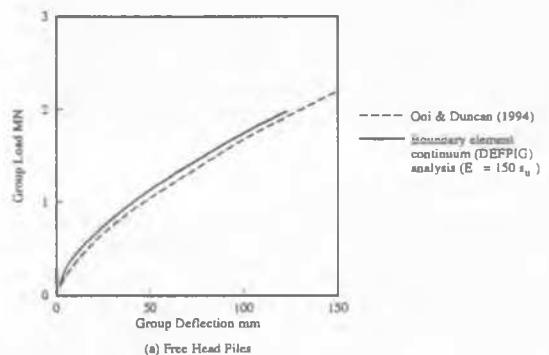


Figure 5.17. Comparison of load-deflection curves for 9-pile group in clay.

## 5.4 Lateral response of piles

### 5.4.1 Introduction

The lateral response of piles can be an important consideration in the design of foundations subjected to horizontal forces and overturning moments, for examples, marine and offshore structures, retaining structures and tall buildings subjected to wind and seismic loadings. As with vertical loading, consideration must be given in design to both the ultimate lateral resistance of piles and the lateral deflections under the design serviceability loadings. It is not common for the ultimate lateral resistance to be the governing factor in design unless the piles or piers are relatively short or have a low flexural strength. Nevertheless, it is important to consider the ultimate lateral capacity and the ultimate lateral resistance of the soil, since the latter is an important component of a non-linear analysis of lateral response.

This Section will address some of the important issues in relation to the estimation of lateral response of piles and pile groups. The ultimate lateral capacity of piles and groups will be reviewed, and then methods of estimating the lateral deflections of piles and groups will be outlined. As with axial loading, a number of the issues which may be of concern to practitioners will be discussed.

### 5.4.2 Ultimate lateral capacity of piles

The calculation of the ultimate lateral capacity of piles usually involves the consideration of the statics of a pile under lateral loading. This requires specification of the distribution of ultimate lateral pile-soil pressure with depth, the structural strength of the pile in bending, and the postulated failure mode of the pile-soil system. The conditions usually examined are:

- Failure of the soil supporting the pile (termed "short-pile failure by Broms (1964a, 1964b)
- Structural failure of the pile itself (termed "long-pile failure by Broms).

In addition, the two pile head conditions usually considered are a free (unrestrained) head and a fixed head (restrained against rotation).

The classical work in this area has been published by Broms (1964a, 1964b), and this work continues to be the cornerstone of many practical assessments today. Meyerhof (1995b) has provided a summary of an alternative approach to the estimation of ultimate lateral capacity, that incorporates the effects of load eccentricity and inclination.

#### Assessment of Broms' Theory

Kulhawy and Chen (1993) have carried out an assessment of the applicability of Broms' method, based on comparisons with the results of a number of laboratory and field tests on bored piles. For both undrained and drained lateral load capacities, Broms' method tended to underestimate the ultimate lateral load by about 15 - 20%. They concluded that, while Broms' method was conservative overall, it provided as good an approach as any other method, and could give good results if empirical adjustments were made to the values computed from the theory. It should be re-stated that Broms himself acknowledged that his assumed ultimate lateral pressure distributions were conservative.

Despite the apparent success of Broms' method, it must be recognized that it has a number of practical limitations, among which are the following:

1. It assumes that the soil layer is homogeneous with depth;
2. It considers only a pure sand (frictional soil), or a clay under undrained conditions having a constant strength with depth;
3. It considers only a single pile, and not a group of piles directly.

Because of these limitations, the practitioner must exercise considerable judgement in applying Broms' theory, and indeed, the theory cannot strictly be applied directly to the following problems:

1. Layered soil profiles
2. Profiles containing both sand and clay layers

3. Uniform and profiles in which the water table is not at the surface or below the pile tip
4. Groups of piles.

#### Layered and non-homogeneous soils

Some extensions to Broms' theory have been made in an attempt to overcome some of the above limitations. For example, Poulos (1985) has developed a general solution for piles in a two-layer cohesive soil. This solution involves the solution of a quadratic equation of the form:

$$aH^2 + bH + c = 0 \quad (5.25)$$

where  $H^* = H/p_y dL$ ,  $p_y$  = ultimate lateral pile-soil pressure,  $L$  = pile length,  $d$  = pile diameter or width. The coefficients  $a$ ,  $b$  and  $c$  depend on the relative thickness of the two layers, the relative strength of the layers, the eccentricity of loading, and the characteristics of the pile. Figure 5.14 shows some typical results derived from Poulos' analysis. The ratio of the lateral capacity for the two-layer soil to that for a homogeneous layer is plotted against the relative thickness of the upper layer, for both the short pile and long pile failure modes. This figure highlights that the near-surface layer has a very important effect on the ultimate lateral capacity.

For multi-layered soil profiles, closed-form solutions and design charts are not feasible, and a simple computer-based analysis is required. Such an analysis is based on the simple principles of statics used by Broms and others, and requires the estimation of the ultimate lateral pile-soil pressures.

#### Estimation of ultimate lateral pile-soil pressures

Following the work of Broms (1964a, 1964b), it has been common for the ultimate lateral pressure,  $p_y$ , to be estimated as follows:

- For clays,

$$p_y = N_c \cdot s_u \quad (5.26)$$

where  $N_c$  = a lateral capacity factor;  $s_u$  = undrained shear strength.

Various solutions have been developed for  $N_c$ , but in general, it is found to increase from 2 at the ground surface to about 9 to 12 at a depth of 3 to 4 diameters, then remaining constant for greater depths. In many practical applications, a value of 9 is adopted (as for the undrained end bearing capacity of piles in clay).

- For sands,

$$P_y = N_s p_p \quad (5.27)$$

where  $N_s$  = a multiplying factor;  $p_p$  = Rankine passive pressure.

$N_s$  is usually within the range 3 to 5, with 3 being a common design value.

A number of alternative approaches are available, and Kulhawy and Chen (1993) have compared three of the available distributions. They have concluded that Broms' approach appears to be very conservative at depth, but that conversely, the approach of Reese *et al.* (1974) appears to be quite bold.

#### Effects of inclined loading

Meyerhof (1995b) has given detailed consideration to the effects of inclined loading on a pile, and has developed practical procedures for combining axial and lateral capacities in such cases. A simple alternative approach has been suggested by Cho and Kulhawy (1995), who have obtained correction factors based on the results of undrained load tests on bored piles (drilled shafts) in clay, to modify the axial and lateral pile capacities. The notation adopted by these authors is illustrated in Figure 5.15, and the following expressions were developed for the vertical and horizontal components of the inclined failure load:

1. For inclined uplift,

$$\text{Vertical component: } P_o = Q_m(1 - \Psi/90) + W, \quad (5.28a)$$

$$\text{Horizontal component: } P_{90} = H_u (\sin \Psi)^{0.5} \quad (5.28b)$$

2. For inclined compression,

$$\text{Vertical component: } P_{180} = Q_{sc} (\Psi/90 - 1) + Q_{bc} [(\Psi/90) - 1]^{7.3} \quad (5.28c)$$

$$\text{Horizontal component: } P_{90} = H_u (\sin \Psi)^{0.5} \quad (5.28d)$$

where  $Q_{su}$  = uplift capacity of shaft,  $W_s$  = weight of pile,  $H_u$  = ultimate lateral load capacity,  $Q_{sc}$  = ultimate shaft capacity in compression,  $Q_{bc}$  = ultimate base capacity in compression,  $\Psi$  = angle of inclination of load to vertical, in degrees.

#### Pile groups

For practical purposes, the ultimate lateral capacity of a pile group can be estimated as the lesser of:

- The sum of the ultimate lateral capacities of the individual piles in the group
- The ultimate lateral capacity of an equivalent block containing the piles and the soil.

In the latter case, only the "short-pile" case need be considered. Care should be exercised when applying Broms' theory to groups in clay, as it implicitly assumes that there is a "dead" zone from the surface to a depth of 1.5 diameters in which the soil contributes no lateral resistance. This assumption may be inappropriate for large-diameter blocks, and it is therefore recommended that the block analysis be carried out from a consideration of statics, using a "dead" zone of 1.5 times the diameter of an individual pile.

#### 5.4.3 Lateral load-deflection prediction

##### Lateral load-deflection prediction

Methods of estimating the lateral deflection and rotation of a laterally loaded pile usually rely on either the theory of subgrade reaction (Broms, 1964a, 1964b) or on elastic continuum theory (Poulos, 1971a, 1971b; Randolph, 1981; Budhu and Davies, 1987, 1988). For a soil having a constant modulus with depth, the linear solutions for pile groundline deflection,  $\rho$ , and rotation,  $\theta$ , may be expressed as follows:

$$\rho = I_{uH} \cdot H / (E_s d) + I_{uM} \cdot M / (E_s d^2) \quad (5.29)$$

$$\theta = I_{\theta H} \cdot H / (E_s \cdot d^2) + I_{\theta M} \cdot M / (9 E_s d^3) \quad (5.30)$$

where  $H$  = applied load at groundline,  $M$  = applied moment at groundline,  $E_s$  = soil Young's modulus,  $d$  = pile diameter of width,  $I_{uH}$ ,  $I_{uM}$ ,  $I_{\theta H}$  and  $I_{\theta M}$  are influence factors which depend on the ratio  $K$  of pile modulus to soil modulus and the relative length of the pile.

Similar expressions hold for a pile in a soil whose modulus increases linearly or via a power law with depth, and some of these solutions are summarised by Poulos (2000b).

Solutions for the influence factors are available from several sources, including the references cited above. For piles which are "flexible", (i.e., their embedded length is longer than the critical length), comparisons show that the various solutions from elastic continuum theory generally agree well, but that the subgrade reaction theory tends to over-predict the deflection influence factors for piles having a low ratio of pile to soil modulus. While such differences in the solutions may be of some concern, it is possible to allow for these differences by "calibration" of the analyses with field data, and appropriate choice of the soil parameters. The assessment of parameters for continuum analysis of laterally loaded piles has been discussed by Poulos (1982a) who has collected recommendations from various sources for both linear and non-linear analyses.

The estimation of the Young's modulus for estimation of lateral pile deflection is discussed further in Section 8.

#### Non-linear analyses

Of more practical significance than the differences in linear solutions is the major effect of soil non-linearity on the lateral response of piles. Non-linearity leads to increased lateral deflection and pile head rotation, and these increases may become very great (compared to the initial linear response) at relatively modest applied load levels. This effect was recognised early in the pioneering work of Reese and his co-workers, who developed the "p-y" method. The "p-y" curves in their method are essentially non-linear spring characteristics, and the p-y method itself can be considered as a non-linear subgrade reaction approach. On the basis of carefully instrumented field pile tests, a series of p-y curves was developed for various types of soil, and these form the basis of much common practice today. Details of these empirical curves are summarised by Sullivan *et al.* (1980) while Murchison and O'Neill (1984) and Bransby (1999) have developed alternative approaches to the development of p-y curves via the use of analytical solutions. An alternative procedure to account for non-linearity has been proposed by Prakash and Kumar (1996) who have assumed that the modulus of subgrade reaction at any depth is dependent on the level of shear strain adjacent to the pile at that depth.

It is also possible to develop non-linear lateral response solutions from elastic continuum theory, by imposing the condition that the lateral pile-soil pressure cannot exceed the ultimate lateral pile-soil pressure,  $p_y$ . The results of such theory can be expressed in terms of correction factors to the elastic solutions (such as those in Equations (5.29) and (5.30)), for example, Poulos and Davis, 1980; Budhu and Davies, 1987, 1988; Poulos and Hull, 1989). These correction factors depend on both the applied load level and the relative flexibility of the pile. It has been shown by Poulos (1982) that good agreement can be obtained by this approach, and also with the use of simple representations of p-y curves (e.g., hyperbolic or elastic-plastic), rather than the relatively complex curves commonly used.

In summary, the research on the behaviour of single laterally loaded piles leads to the following conclusions:

1. There are some differences between the linear solutions from elastic continuum theory and subgrade reaction theory, but these differences can be accommodated in practice via calibration of the analysis with field data and the use of appropriate values of the relevant soil deformation parameters;
2. Non-linear pile-soil response is a most important aspect of behaviour. Failure to allow for this behaviour may lead to grossly inaccurate (and unconservative) predictions of lateral deflection and rotation.
3. It is not necessary to employ complex representations of non-linear soil behaviour in order to obtain reasonable predictions of lateral pile response. Even a simple elastic-plastic or hyperbolic response may often be adequate to capture the main non-linear effects.
4. As with most foundation problems, the key to successful prediction is more the ability to choose appropriate geotechnical parameters rather than the details of the analysis employed.

#### Practical procedure for load-deflection estimation

A very useful practical procedure for estimating the load-deflection behaviour of single piles was presented by Duncan *et al.* (1994) and Brettmann and Duncan (1996). They introduced the concept of the "characteristic load", and used dimensional analysis to characterize the non-linear behaviour of piles via relationships between dimensionless variables. These variables are defined as follows:

- Characteristic Load:

(i) for clay:

$$H_c = 7.34 d^2 (E_p R_1) \cdot [s_u / (E_p R_1)]^{0.68} \quad (5.31a)$$

(ii) for sand:

$$H_c = 1.57 d^2 (E_p R_1) \cdot [\gamma' d \phi' K_p / (E_p R_1)]^{0.57} \quad (5.31b)$$



- Characteristic Moment:

(i) for clay:

$$M_c = 3.86d^3 (E_p R_1) \cdot [s_u / (E_p R_1)]^{0.46} \quad (5.31c)$$

(ii) for sand:

$$M_c = 1.33d^3 (E_p R_1) \cdot [\gamma' d \phi' K_p / (E_p R_1)]^{0.40} \quad (5.31d)$$

where  $P_c$  = characteristic load,  $M_c$  = characteristic moment,  $d$  = pile diameter or width,  $E_p$  = pile modulus,  $R_1$  = ratio of moment of inertia of pile section to that of a solid circular cross-section (=1 for a solid circular pile),  $s_u$  = undrained shear strength of clay,  $\gamma'$  = effective unit weight of sand,  $\phi'$  = effective stress friction angle for sand (degrees),  $K_p$  = Rankine passive pressure coefficient.

For applied horizontal loading, the lateral load – deflection relationship can be approximated as follows (Brettmann and Duncan, 1996):

$$(\rho_h / d) = a_h (H / H_c)^{b_h} \quad (5.32a)$$

while for applied moment loading, the corresponding relationship is:

$$(\rho_h / d) = a_m (M / M_c)^{b_m} \quad (5.32b)$$

The relationship between maximum moment induced in the pile and the applied horizontal loading can similarly be expressed as:

$$(H / H_c) = a_x (M_{\max} / M_c)^{b_x} \quad (5.32c)$$

In the above equations, where  $\rho_h$  = groundline deflection,  $a_h$ ,  $b_h$  = constants for applied horizontal loading,  $a_m$ ,  $b_m$  = constants for applied moment loading,  $a_x$ ,  $b_x$  = constants for maximum pile moment,  $H$  = applied lateral load at top of pile,  $M$  = applied moment at top of pile,  $H_c$  = characteristic load (Equations (5.31a) and (5.31b)),  $M_c$  = characteristic moment (Equations (5.31c), (5.31d)).

Values of the various constants in the above equations are given in Table 5.8.

When both horizontal load and moment are applied simultaneously, the following procedure is followed:

1. Compute the deflections which would be caused by the load acting alone ( $\rho_{hh}$ ) and the moment acting alone ( $\rho_{hm}$ ).
2. Compute the value of load ( $H_m$ ) that would cause the same deflection as the moment and the value of moment ( $M_h$ ) that would cause the same deflection as the load.
3. Compute the ground-line deflection,  $\rho_{h1}$ , that would be caused by the sum of the real load and the equivalent load ( $H + H_m$ ), and the deflection,  $\rho_{h2}$ , that would be caused by the sum of the real moment and the equivalent moment ( $M + M_h$ ).
4. The estimated value of deflection due to both load and moment is taken as the average of the two values computed above, i.e.

$$\rho_h = 0.5(\rho_{h1} + \rho_{h2}) \quad (5.33)$$

As pointed out by Duncan *et al.* (1994), the characteristic load method (CLM) has some limitations. It applies only to "long" piles that have a length greater than the critical or active length, and it applies only to uniform soils which are sand or clay along the critical length. However, only the soil within the critical depth (usually the upper 8 diameters or so) is important for estimating lateral response, and where ground conditions vary, average properties of the ground profile within this depth can be assumed for the analysis.

To compare the predictions from this approach with that from other methods, the field tests for a pipe pile in sand (Cox *et al.*, 1974) have been analyzed. Figure 5.16 shows the comparison for both the head load – deflection relationships and the applied load

versus maximum pile moment relationship. Also shown are the relationships predicted from a non-linear boundary element analysis by Poulos (1982b). It can be seen that both the Duncan *et al.* approach and the boundary element analysis give results which are comparable and in good agreement with the test data.

Table 5.8. Constants for lateral load-deflection estimation (Brettmann and Duncan, 1996).

Con- stant	Clay		Sand	
	Free head	Fixed head	Free head	Fixed head
$a_h$	50.0	14.0	119.0	28.8
$b_h$	1.822	1.846	1.523	1.500
$a_m$	21.0	-	36.0	-
$b_m$	1.412	-	1.308	-
$a_x$	0.85	0.78	4.28	2.64
$b_x$	1.288	1.249	1.384	1.300

#### Group effects

A group of piles will generally deflect more than a single pile under the same load per pile, due largely to the effects of pile-soil-pile interaction. At the same time, the restraining effects of the pile cap connecting the piles may considerably modify the pile behaviour as compared to a single free-headed pile. Therefore, considerable caution must be exercised in applying the theory for a single pile to pile groups.

Various procedures have been developed to estimate the lateral deflection of pile groups, and these generally fall into the following categories:

- Interaction factor approaches: these were introduced by Poulos (1971b) and involve the consideration of the additional lateral deflections and rotations caused by a loaded pile on adjacent piles. The soil mass is taken to be an elastic continuum, and use is made of the classical equations of Mindlin to compute the various interaction factors. Randolph (1981) has developed extremely useful approximations for these interaction factors, for soils whose stiffness is either constant or else increases linearly with depth.
- Hybrid approach, combining the p-y method for single piles with elastic continuum analysis to estimate interaction effects (Focht and Koch, 1973; O'Neill *et al.*, 1977).
- Equivalent pier approach, in which the group is represented by an equivalent single pier (Bogard and Matlock, 1983; Poulos, 1975a)
- Group reduction factor method. A version of this approach was developed by Davisson (1970), based on model pile tests by Prakash (1962). This approach reduced the sub-grade reaction modulus to account for group interaction.
- Group deflection ratio method. This been used by Poulos (1987), and uses elasticity theory to derive group factors which are applied to the response of a single pile to allow for group effects. This approach is analogous to the use of a group settlement ratio for estimating pile group settlements.
- Elastic continuum boundary element analysis, such as used by Banerjee and Driscoll (1976) and Xu (2000).
- Finite element analysis, using either a plane strain model (e.g., Desai, 1974) or a full three-dimensional model (Kimura *et al.*, 1998).

A useful practical procedure has been developed by Ooi and Duncan (1994), based on the results of extensive parametric studies using the method of Focht and Koch (1973). Their approach, the "group amplification procedure", can be summarized as follows:

1. The group deflection,  $\rho_g$ , is given by:

$$\rho_g = C_y \rho, \quad (5.34)$$

2. The maximum bending moment,  $M_g$ , in a pile within a group is given by:

$$M_g = C_m M, \quad (5.35)$$

where  $\rho_s$  = single pile deflection under the same load per pile;  $M_s$  = maximum moment in a single pile under the same load;  $C_y$  = deflection amplification factor ( $\geq 1$ );  $C_m$  = moment amplification factor ( $\geq 1$ ).

In applying Equation (5.34), the pile head condition for the single pile should reflect the conditions of restraint at the pile cap. For a cap which provides little or no restraint,  $\rho_s$  is computed for a free-head pile, while for pile caps that provide restraint, it is appropriate to compute  $\rho_s$  for a fixed head pile.

The following expressions were derived from parametric studies by Ooi and Duncan:

$$C_y = (A + N_{pile}) / (B(s/d + P_s / CP_N)^{0.5}) \quad (5.36a)$$

$$C_m = (C_y)^n \quad (5.36b)$$

where  $A = 16$  for clay, and  $9$  for sand;  $N_{pile}$  = number of piles in group;  $B = 5.5$  for clay and  $3.0$  for sand;  $s$  = average spacing of piles;  $d$  = diameter of single pile;  $P_s$  = average lateral load on pile in group;  $C = 3$  for clay and  $16$  for sand;  $P_N = (s_u d^2)$  for clay and  $(K_p \gamma d^3)$  for sand;  $\gamma$  = average total unit weight of sand over the top  $8$  diameters;  $K_p$  = Rankine passive pressure;  $s_u$  = average undrained shear strength within the top diameters;  $n = (P_s / 150 P_N) + 0.25$  for clay, and  $(P_s / 300 P_N) + 0.30$  for sand.

Ooi and Duncan (1994) have found satisfactory agreement between their approach and the results of a number of field measurements. However, they point out that their method has a number of limitations, including the following:

- It has been developed for uniformly spaced piles which are vertical (not raked);
- The load distribution within the group cannot be obtained;
- The results do not depend on the arrangement of the piles in the group;
- The method is restricted to piles whose embedded length exceeds the critical length.

A simple approach has been suggested by Poulos (2000a) in which the group lateral deflection  $\rho_g$  is estimated as follows:

$$\rho_g = R_p \rho_s \quad (5.37)$$

where  $R_p$  = group deflection ratio =  $(N_{pile})^{\omega_1}$ ;  $\rho_s$  = deflection of single pile at the same lateral load;  $N_{pile}$  = number of piles;  $\omega_1$  = exponent depending on the critical length of the pile and the pile spacing.

From Equations (5.34) and (5.37), it can be seen that Ooi and Duncan's factor  $C_y$  has the same meaning as the group deflection ratio  $R_p$ .

Figure 5.17 compares load – deflection curves for a typical pile group in clay, computed from Ooi and Duncan's approach, and also via the computer program DEFPIG. For the free-headed pile group, the agreement is good, but for a fixed head group, Ooi and Duncan's approach predicts a stiffer response than the elasticity-based DEFPIG analysis.

#### 5.4.4 Summary

For assessing the ultimate lateral capacity of single piles in relatively uniform soil deposits, the theory of Broms (1964a, b) can be adopted. For layered soils, however, substantial engineering judgement is required to adapt Brom's theory.

For estimating the lateral load-deflection response of piles non-linear soil behaviour plays a crucial role. Provided that this nonlinear behaviour is allowed for, both the  $p$ - $y$  and elastic continuum approaches give comparable results and can be adopted. For pile groups, an elastic-based analysis of pile-soil-soil interaction can be adopted, as can the simplified procedure developed by Ooi and Duncan (1994).

## 5.5 Effects of ground movements on piles

### 5.5.1 Introduction

There are many circumstances in which pile foundations may be subjected to loadings arising from vertical and/or lateral movements of the surrounding ground. In such cases, at least two important aspects of pile foundation design must be considered:

1. the movements of the piles caused by the ground movements
2. the additional forces and/or bending moments induced in the piles by the ground movements, and their effect on the structural integrity of the piles.

These two aspects will be considered below for some selected cases of ground movement. It should be emphasized that, in general, the geotechnical axial and lateral load capacities of a pile are unlikely to be seriously affected by ground movements.

### 5.5.2 Negative friction

It has long been recognised that pile foundations located within a settling soil layer will be subjected to negative friction stresses caused by the downward movement of the soil relative to the pile. As a consequence, an additional "downdrag" force will be developed within the pile and the pile head will experience additional settlement.

There is a misconception among some practitioners that negative friction leads to a reduction in ultimate axial load capacity of piles, and indeed, some methods of design attempt to compute a reduced axial load capacity in which the downdrag load caused by negative friction is subtracted from the original load capacity. The allowable axial load is then assessed on the basis of this reduced load capacity. Such a concept, although convenient, is not strictly valid, since a pile can only fail geotechnically if the pile moves past the soil, whereas negative friction requires the soil to move past the pile.

Computer analyses of the effects of negative friction can be carried out by incorporating the 'free field' ground movements into an analysis of pile-soil interaction (e.g., Poulos and Davis 1980). However, for simpler practical applications, approximate methods of calculation can be used (e.g., Fellenius 1989; Poulos 1997b). Figure 5.18 illustrates the approach adopted in the latter reference. A pile of length  $L$  is located in a soil profile consisting of a consolidating layer, of thickness  $L_1$ , that is underlain by a stable non-consolidating layer. It is assumed that the settlement of the consolidating layer decreases linearly with depth, from  $S_0$  at the surface to zero at depth  $L_1$ . The neutral plane is the location along the pile where the pile friction changes from negative to positive, and is located at a depth  $z_n$ . The location of the neutral plane may be computed via the procedure outlined by Fellenius (1989, 1991).

To compute the maximum force in the pile and the pile head movement, the following procedure may be followed:

1. the maximum force  $P_{max}$  in the pile is the force at the location of the neutral plane, and is the sum of the applied load and the maximum downdrag force;
2. the pile head movement is the larger of the following two values:
  - a) the elastic compression of the pile above the neutral plane, plus the settlement of that portion of the pile below the neutral plane; the latter component may be estimated from pile settlement theory, assuming a pile length  $(L - z_n)$  subjected to the computed maximum axial force  $P_{max}$ ;
  - b) the "free-field" vertical movement of the soil at the level of the neutral plane.

These two "options" are illustrated in Figure 5.18.

In summary the hand calculation procedure is as follows:

1. compute the maximum possible value of  $z_n$  ( $z_{nmax}$ )
2. compute the maximum axial force in the pile as follows:

$$P_{nmax} = P_0 + f_s cz' \quad (5.38)$$

where  $z_N$  is determined as follows: if  $z_{nmax} > L_1$ ,  $z_N = L_1$ ; and if  $z_{nmax} < L_1$ ,  $z_N = z_{nmax}$

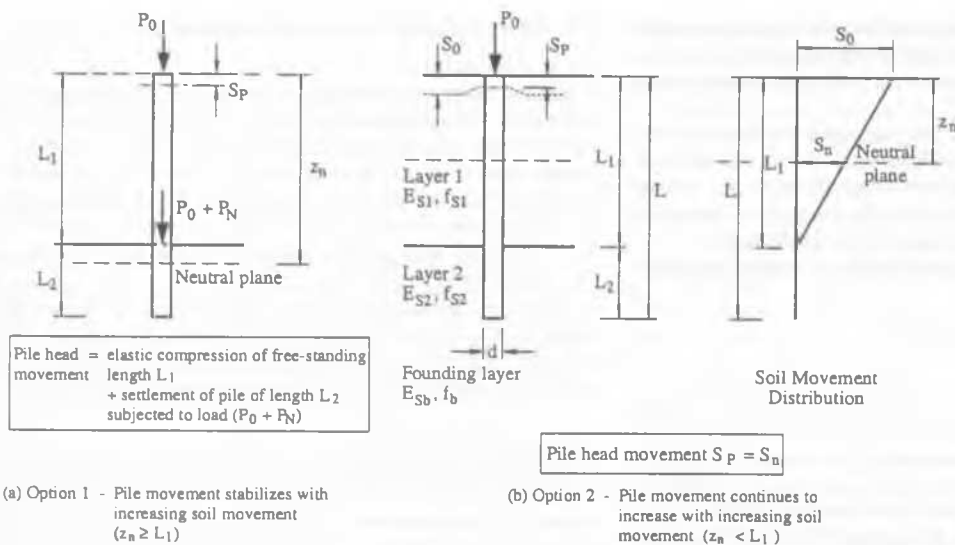


Figure 5.18. Simplified approaches to estimating pile head movement due to negative friction.

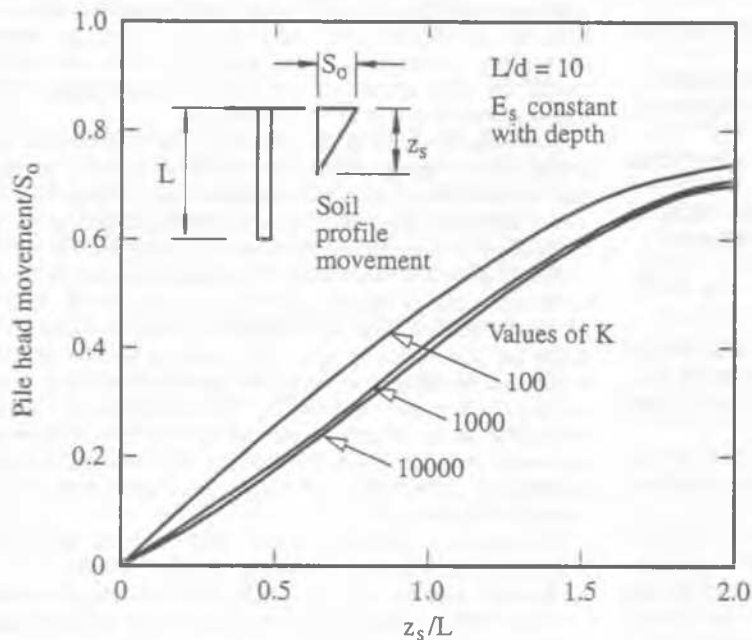


Figure 5.19. Elastic solutions for pile movements in expansive soil - uniform pile diameter (Poulos, 1989).

- compute the pile head settlement, using Options (a) and (b) shown in Figure 5.18, and adopt the larger value.

The above approach assumes implicitly that full mobilization of the negative skin friction above the neutral plane occurs. While this may be reasonable for piles in soft clays, it is not necessarily accurate for piles in stiffer clays, where the ground movements may be small. It may also not be valid for pile groups.

For piles subjected to externally-imposed soil movements, group effects have a beneficial influence on the pile behaviour. The pile movements tend to be reduced and the induced axial forces are also reduced, especially for piles near the centre of a larger pile group, since the effects of pile-soil-pile interaction tend to inhibit the development of pile-soil slip along inner piles of the inner group. In such cases, analyses considering pile-soil

interaction are preferable (e.g., Chow *et al.*, 1990; Kuwabara and Poulos 1989) if an accurate assessment of the pile forces is required. However, from a simple design viewpoint, the consideration of a single isolated pile provides a conservative assessment of the settlement and axial forces developed within the pile group.

The detrimental effects of negative friction can be reduced by the application of suitable coatings along the pile in the settling portion of the soil profile. Bitumen is the most commonly used coating material.

### 5.5.3 Expansive soils

Piles in expansive soils may be subjected to alternating heave and settlement of the ground in response to environmentally-induced moisture changes in the soil. The design of piles in ex-

pansive soils again involves two main issues: the maximum axial force induced in the piles by the ground movements, and the amount of pile head movement. In principle, the same approach may be adopted for pile design as with negative friction.

However, there are at least three practical difficulties that may arise:

1. the soil may be stiff and the ground movements may not be sufficient to cause full mobilisation of the ultimate shaft resistance;
2. assessment of the ultimate shaft resistance of piles in expansive soils is generally more difficult than in soft clays because the expansive soils are often only partly saturated;
3. tensile forces are induced in the pile by swelling movements and these forces may cause concrete piles to crack if not properly reinforced.

As an aid to the assessment of pile head movement in relation to ground surface movement, Figure 5.19 shows theoretical elastic solutions developed by Poulos (1989). These have been found to give useful indications of the movement of model piles in laboratory tests (Challa and Poulos, 1991). Charts for the estimation of pile forces are given by Nelson and Miller, (1992). The development of any pile-soil slip will tend to reduce the induced axial movement of the pile, compared to the purely elastic case.

#### 5.5.4 Piles subjected to lateral ground movements

The response of piles subjected to lateral ground movements may be analysed by an extension of the techniques employed to analyse the behaviour of piles subjected to lateral loads (e.g., Poulos and Davis, 1980; Maugeri and Motta, 1991). A key aspect of such analyses is the estimation of the 'free field' ground movements, since these movements play a major role in determining the pile behaviour.

If the distribution with depth of free-field movements can be simplified, it is possible to develop useful design charts to enable approximate assessment of the pile head deflection and the maximum bending moment in the pile. Chen and Poulos (1997) have presented two series of such charts, one for a pile in a soil subjected to a uniform movement with depth (to a depth  $z_f$  below the surface), and the other for a soil in which the horizontal movement decreases linearly with depth, from a maximum at the surface to zero at a depth  $z_f$ . The first movement profile may be relevant to piles in unstable soil slopes, while the linear profile may be relevant for piles adjacent to embankment construction.

For the linear soil movement profile, Figures 5.20 and 5.21 present charts for pile head movement and maximum moment, for a homogeneous (uniform) soil, and a "Gibson" soil whose modulus increases linearly with depth. The pile head is unrestrained.

As discussed by Chen and Poulos (1997), these solutions assume that the soil remains elastic, and they therefore generally give an upper bound estimate of the pile moment and deflection. The extent of the possible over-estimation increases with increasing lateral soil movements, due to the progressive departure from elastic conditions that results from the development of plastic flow of the soil past the pile.

As an example of the application of both a theoretical computer analysis and the design charts, the case reported by Kalteziotis *et al.* (1993) can be considered. Two rows of piles were used to stabilise a sliding slope on which a semi-bridge structure had been built. The soil conditions consisted mainly of lacustrine deposits, with a thickness of more than one hundred metres, overlying bedrock of Triassic marl. Among the piles were three steel pipe piles instrumented with strain gauges, aiming to study the lateral reaction mechanism in a landslide; results were presented only for one of these. All the piles had a length of 12m and the steel piles had an external diameter of 1.03m, a wall thickness of 18mm and a flexural stiffness  $E_p I_p$  of 1540 MN.m<sup>2</sup>. The centre-to-centre spacing of the piles was 2.5m.

In the theoretical analysis reported by Chen and Poulos (1997), a triangular soil movement profile, with a maximum

movement of 3.5mm at the soil surface and zero at a depth of 6m below the surface, was adopted on the basis of the reported inclinometer data. Based on the results of the pressuremeter tests reported by the authors, the limiting soil pressure was taken to be 0.9 MPa and 3.2 MPa for the moving soil layer and the stable soil layer, respectively, while the corresponding soil Young's modulus values were taken to be 15 MPa and 70 MPa.

The predicted results agreed reasonably well with those measured, with reasonable agreement being observed between the predicted and the measured distributions of bending moment and deflection. The maximum bending moment was developed at about 6.2m below the soil surface, which is very close to the assumed sliding surface. The design charts were also used to estimate the maximum moment and deflection, and were found to give results which were in good agreement with the measurements also.

#### 5.5.5 Specific applications

There are a number of important specific applications of the analysis of piles subjected to lateral soil movements. Four of these are listed below.

##### *Piles in unstable slopes*

There are two important aspects of piles in unstable slopes: first, the effect on the piles of the ground movements (i.e., the induced bending moments and deflections) and second, the effect, on the slope, of the shear resistance provided by the piles, (i.e., the reinforcing effect of the piles.)

Lee *et al.* (1991) discuss how the effect of the slope on the piles can be assessed and describe the various possible modes of behaviour. In addition, the design charts presented by Chen and Poulos (1997) provide a simple approach for preliminary assessment. Viggiani (1981) and Poulos (1995, 2000a) discuss means by which an assessment can be made of the stabilising effect of the piles on the slope.

##### *Piles near an excavation*

The ground movements caused by excavation may induce substantial bending moments in nearby piles, as well as axial down-drag forces. Failure of existing piles may result (e.g., Poulos 1997a). Simplified design charts to enable approximate estimate of pile deflection and bending moment have been presented by Poulos and Chen (1996) for unsupported excavations, and Poulos and Chen (1997) for supported excavations. In the latter reference, factors are presented to take account of distance from the excavation, the excavation depth, the pile stiffness, the soil strength, and the stiffness and spacing of the struts supporting the excavation.

##### *Piles in and near embankments*

The construction of road embankments and fills causes lateral and vertical soil movement which can have an adverse effect on the adjacent piles supporting structures, bridges or utilities. A number of instrumented case studies have been reported (e.g., Heyman, 1965; Leussink and Wenz, 1969), and centrifuge studies have also been undertaken in recent years (e.g., Stewart *et al.*, 1994).

A number of methods of design have been employed, several of which are based on assumed pressure distributions and which are unreliable, as discussed by Poulos (1996b). Stewart *et al.* (1994) have developed a useful empirical approach, based on the results of centrifuge tests, while some design charts have been developed by Poulos (1994c), based on theoretical boundary element analyses. More recently, Goh *et al.* (1997) have undertaken analyses via an approach similar in principle to that described by Poulos (1994c). They have derived the following useful approximations for the maximum bending moment  $M_{max}$  induced in a pile by embankment loading:

$$M_{max} = \lambda \exp[\beta(q/s_u)] s_u dh_s^2 \quad (5.39)$$

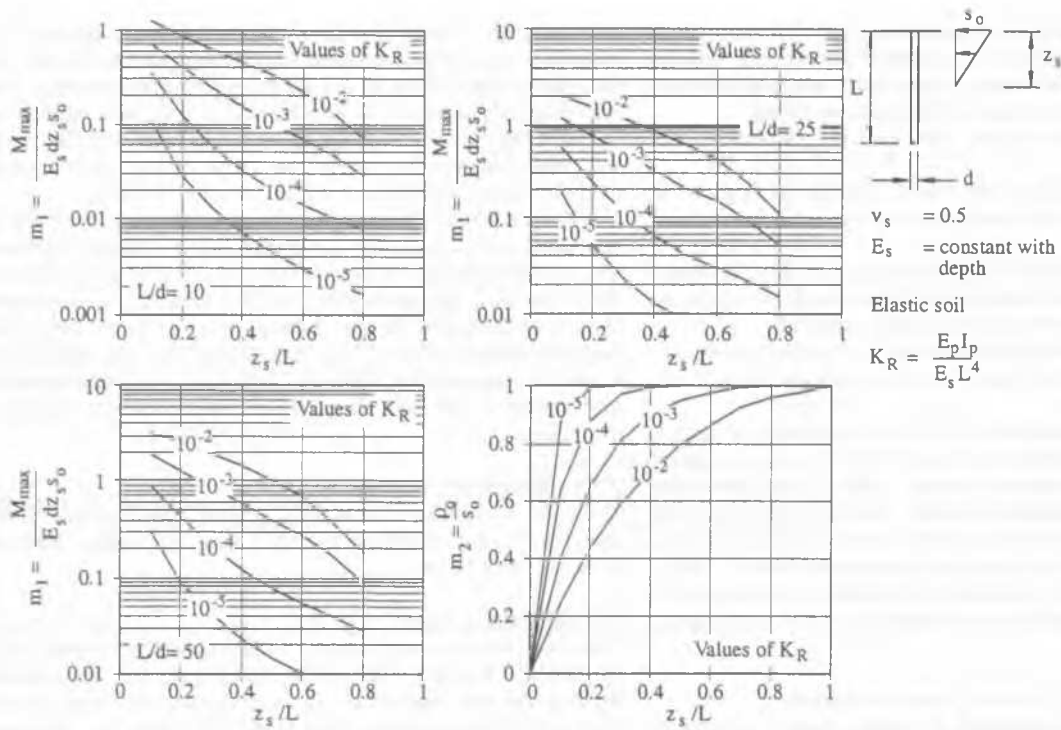


Figure 5.20. Elastic solutions for unrestrained free-head pile in uniform soil (linear soil movement profile) (Chen & Poulos, 1997).

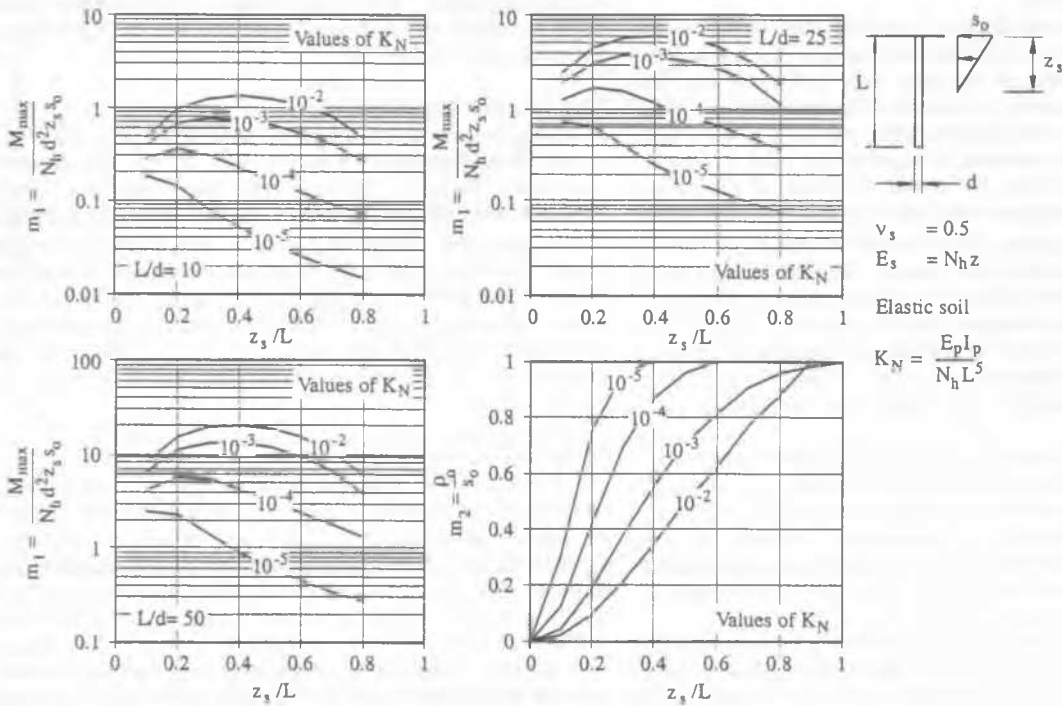


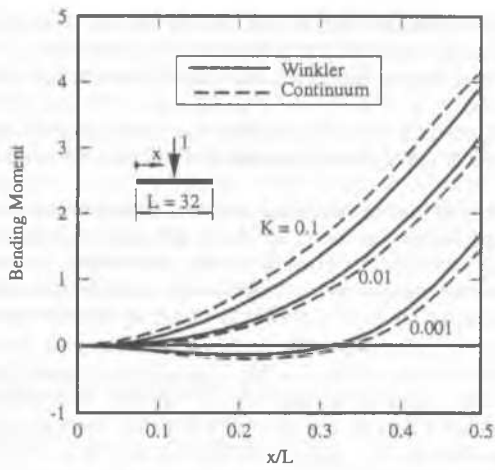
Figure 5.21. Elastic solutions for unrestrained free-head pile in Gibson soil (linear soil movement profile) (Chen & Poulos, 1997).

$$\lambda = 1.88(K_R)^{0.3} \quad (5.40)$$

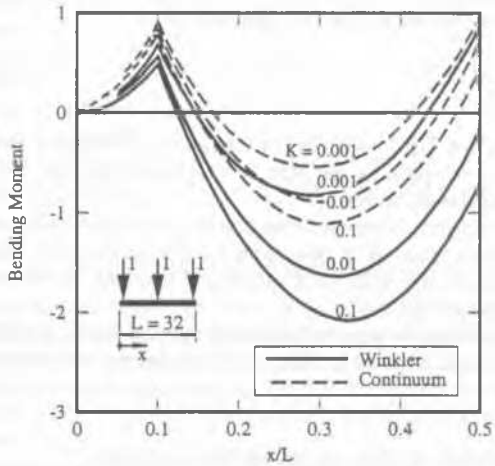
$$\beta = 0.18(K_R)^{-0.1} \quad (5.41)$$

$$K_R = E_p I_p / E_s h^4 \quad (5.42)$$

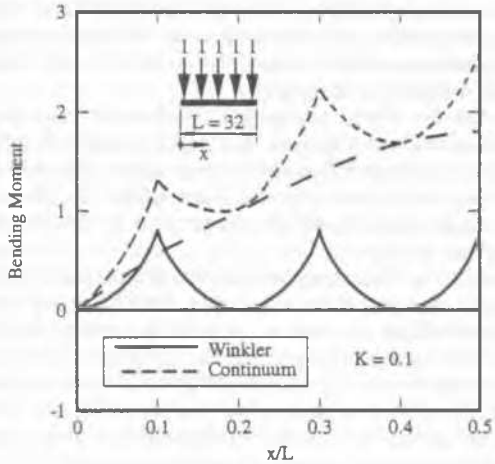
where  $s_u$  = undrained shear strength of clay;  $d$  = pile diameter;  $h_s$  = depth of clay layer;  $q$  is the applied embankment loading. Comparisons between the bending moments computed from the above equations and the design charts produced by Poulos (1994c) suggest that these equations tend to give conservative estimates of the bending moments for relatively flexible piles.



(a)



(b)



(c)

Figure 6.1. Moments in strip raft calculated for continuum and spring models.

### Piles near tunnelling operations

Design charts for the axial and lateral responses of piles adjacent to tunnelling operations were developed by Chen *et al.* (1999). They found that the pile responses depended on a number of factors, including tunnel geometry, ground loss ratio, soil strength and stiffness, pile diameter, and the ratio of pile length to tunnel cover depth. They also showed that the lateral pile behaviour was different for “long” piles whose tip was below the tunnel axis level, and “short” piles, whose tip lay above the tunnel axis level. Application of the results to a published case history gave fair agreement between the measured and calculated lateral pile deflections. Further verification of the applicability of

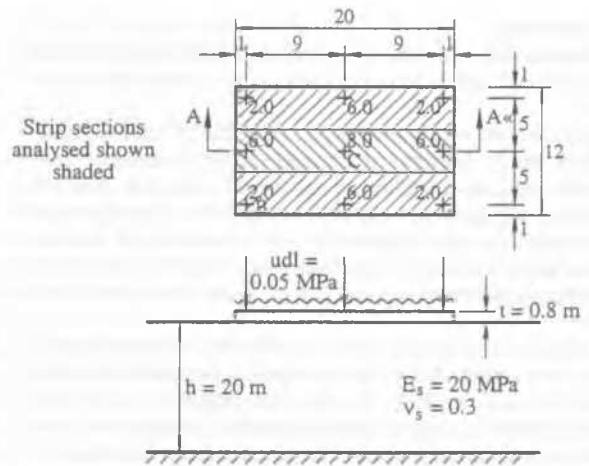


Figure 6.2. Raft on soil of finite depth.

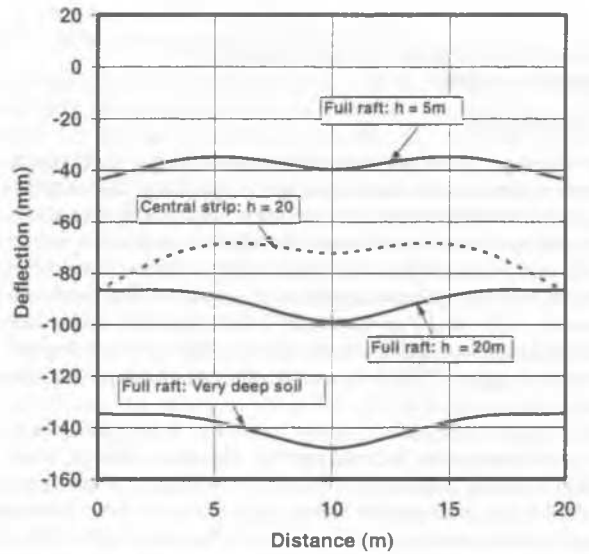


Figure 6.3. Vertical deflection along section A-A'.

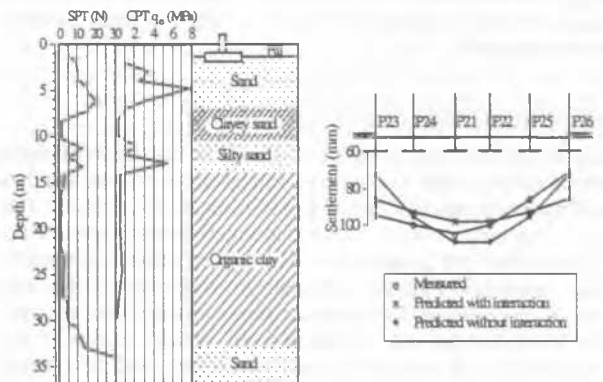


Figure 6.4. Settlement of building computer with and without interaction.

theory to this problem has been obtained via the centrifuge model tests described by Loganathan *et al.* (2000).

### 5.5.6 Summary

The subject of pile response to ground movements is still evolving, but it would appear that the following recommendations can be made:

1. design methods which attempt to reduce the ultimate capacity of piles due to negative friction, should be discarded. Negative friction causes additional settlement and axial stress in the piles, but does not generally influence the geotechnical capacity of the piles. Relatively simple methods of analysis which assume the full mobilization of shaft friction can be adopted to estimate the increases in axial stress and settlement
2. In relation to lateral ground movements, extreme caution should be exercised with pressure-based methods which represent the soil loading via assumed distribution of lateral pressure. Such methods can be misleading and may not properly reflect the complex pile-soil interaction mechanisms
3. In general, the effects of non-linear soil behaviour and group interaction are beneficial and tend to reduce the deflection and induced forces in piles, compared to a single isolated pile. Analyses which ignore group effects are therefore likely to provide conservative estimates of pile response.

## 6 ANALYSIS OF RAFT AND PILED RAFT FOUNDATIONS

### 6.1 Introduction

Raft or piled raft foundations are often used where it is necessary to improve the bearing capacity or to reduce the differential deflections in the foundation of a structure. Many different methods of analysis have been devised in order to predict the behaviour of such foundations, and these range from simple hand based methods up to more complex approaches. The books by Selvaduri (1979) and Hemsley (1998) discuss some of the analytic techniques that may be used for the analysis of raft foundations and Hemsley (2000) discusses raft and piled raft foundations.

Approximate methods that have been used for the analysis of piled raft foundations include spring (Winkler) models, two-dimensional finite element models and strip models where only a strip of the raft is analysed. These simple models have become popular because analysis of a piled raft foundation involves a problem that is essentially three-dimensional, and to carry out full three-dimensional analyses is time consuming even with the software and speed of computers available today.

However, the use of quick hand methods or simplified analytic approaches may lead to significant errors, and it is of interest to know the advantages and disadvantages of these methods before using them.

### 6.2 Winkler foundations vs elastic continua

Often, structural designers prefer to represent the soil underneath a slab or raft foundation as a series of springs (commonly known as a Winkler foundation). Although this is a simple approach that is quick and easy to use, it can lead to incorrect results because:

1. The springs are independent and do not interact. Therefore the compression of one spring does not influence other parts of the foundation. To illustrate this, consider the case of a uniformly loaded raft. Such a raft will undergo a uniform displacement and therefore there will be no bending moment predicted in the raft. This is obviously wrong, as it is observed that such a loading would make a rectangular raft (for example) deform into a dished shape, and the raft would then carry bending moments.
2. It is difficult to establish the stiffness values for the springs that are used in analysis because the spring constants are dependent on the scale of the foundation. For example, if a modulus of subgrade reaction is determined from a plate loading test, the load-deflection behaviour is specific to the

size of plate used in that test. It should not be applied to loaded areas that are different in size to that of the plate.

3. A Winkler or spring model cannot directly take account of soil layering.
4. A vertical loading on a foundation may cause lateral displacements. A spring model cannot be used for such predictions.

Because of the limitations listed above, it is desirable to use continuum models for the soil (i.e., treat it as being an elastic or elasto-plastic material). An example of the differences in solutions obtained by using a spring model and a continuum model has been presented by Brown (1977) to illustrate the difference in the choice of soil model. The problem involves unit point loads applied to a strip raft ( $L/B = 10$ ). In order to compare the two models, the modulus of elasticity of the soil (continuum model) and of the subgrade reaction (spring model) were chosen so that the settlements of a rigid strip foundation with a central point load are equal. Figure 6.1 shows the computed moments in the raft, where the raft stiffness is defined as  $K$

$$K = \frac{16El(1-\nu_s^2)}{\pi E_s L^4} \quad (6.1)$$

and where  $El$  = bending stiffness of the raft;  $\nu_s$  = Poisson's ratio of the soil;  $L$  = length of the raft;  $B$  = width of the raft;  $E_s$  = Young's modulus of the soil.

From the figures, it may be seen that the calculated moments in the raft show reasonable agreement for the central point load only. For the multiple point load cases there is a large difference in the calculated moments.

It may therefore be concluded that the use of spring models may lead to large errors and should not be used for raft foundation design.

### 6.3 The analysis of a raft as a series of strip footings

It is common design practice to analyse a raft foundation by dividing it up into strips, and analysing each strip individually. Each strip is then considered to be only subjected to the loads that are applied to that particular strip.

To illustrate the effects of doing this, the raft foundation shown in Figure 6.2 was analysed. The problem involves a raft foundation on a uniform soil layer of finite depth. The column loads are treated as a series of point loads in the analysis. All dimensions, loads and material properties used in the analysis are shown on the figure.

Firstly the full raft was analysed by using the program FEAR (Finite Element Analysis of Rafts – Small, 1998) that treats the soil as a layered elastic material and uses finite element analysis for the raft. The solution obtained for the deflection of the full raft along the section A-A' is shown in Figure 6.3 where it can be seen that the deflection under load C is about 98.7mm. The deflected shape of the raft is such that the raft has a bowl shape with the deflection being largest at the centre and smallest at the edges.

However, when the central strip alone is analysed, the deflected shape is completely different (see Figure 6.3) and this leads to errors in predicted moments as well as deflections.

Shown in Table 6.1 are the moments and deflections calculated from FEAR using the full raft and using the individual strips. Values are given for the points C (at the centre of the raft) and B (at the corner column) for the finite layer depth of 20m. It may also be seen from Table 6.1 that if individual strips are used, the deflections and moments that are computed in the raft are not accurate with deflections being lower for the strip than for the full raft.

### 6.4 Effect of layer depth

It is also of interest to see what the values of deflection and moment would be if the only available analysis was for an infi-



nately deep soil, and these values are also shown in Table 6.1. If the layer is assumed to be very deep, the computed deflections are larger as should be expected (see Figure 6.3), but the moments per unit length are only very slightly in error because the curvatures in the raft are similar to those of the 20m deep case.

If the soil layer is only 5m deep instead of 20m deep, then for the full raft, the deflection profile along A-A' is very different again with the deflections at the edges greater than at the centre (see Figure 6.3). The values for the shallow soil layer are also shown in Table 6.1. Although the deflections are again significantly affected by layer depth, the table shows that the moments in the raft are not as greatly affected.

Table 6.1. Moments and deflections in raft.

Quantity	Full raft $h = 20\text{m}$	Single strip $h = 20\text{m}$	Full raft $h = 5\text{m}$	Full raft $h = \infty$
Settlement at C (mm)	98.8	72.5	39.8	148
Settlement at B (mm)	76	45	35	125
$M_{xx}$ at C MNm/m	2.8	2.4	2.4	2.8
$M_{yy}$ at C MNm/m	2.3	1.9	1.9	2.3
$M_{xx}$ at B MNm/m	0.24	0.3	0.2	0.22
$M_{yy}$ at B MNm/m	0.31	0.39	0.3	0.31

### 6.5 The effects of structure-foundation-soil interaction

The examples above have been given for a raft alone without the stiffening effect of any structure that is supported by the raft. Methods of incorporating the stiffness of a structure into a raft analysis has been examined by several authors including Lee and Brown (1972), Lee (1975), Poulos (1975b) and Brown and Yu (1986).

Fraser and Wardle (1975) presented results for a 2 bay portal frame where they showed that the differential deflections in the frame depended on the stiffness of the frame. Brown (1975) has also shown, for a strip raft beneath a 2-dimensional frame, that the relative stiffness of the structure has an effect on differential displacement in the raft. Zhang and Small (1994) analysed 3-dimensional framed buildings on raft foundations, and demonstrated that the larger the relative stiffness of the building frame, the smaller the differential deflections in the raft.

Brown and Yu (1986) also showed that as a building is constructed, the stiffness of the overall structure increases and this affects the differential displacement in the raft. Gusmau Filho and Guimaraes (1997) have also looked at construction sequence and have noted that the loads in columns reach a maximum (or minimum) value as more stories are added to the building, leading to the idea of the building reaching a "limit stiffness".

An example showing how incorporation of the stiffness of the structure into the analysis can improve the predicted behaviour of a foundation has been presented by Lopes and Gusmao (1991). For a 15 story structure in Brazil supported by a system of strip footings, the settlement distribution was shown to be predicted more closely if the stiffness of the structure is included in the settlement analysis (see Figure 6.4).

Although all of the authors mentioned above have found that the structural stiffness does have an effect on the raft's behaviour, Yao and Zhang (1985) concluded that this was not so. They carried out analyses of two-dimensional building frames on raft foundations where the raft and soil were analysed using finite element techniques. They found that as the "rigidity" of the frame members increased, that it had only a marginal effect on the differential settlement and forces in the raft.

It may therefore be concluded that the stiffness of a structure will influence the calculated settlements of a raft foundation, but this depends on the stiffness of the structure relative to the raft. For buildings with rigid shear walls, the stiffening effect on the

raft will be significant. However for flexible light framed structures, the effect of the structure on a thick raft, will be small.

### 6.6 Piled raft foundations

Where loads on a foundation are excessively large for a raft alone, the raft can be used in conjunction with piles. Both the raft and the piles transfer load to the soil in this case, and the piles can be designed to carry loads that are well below their failure load, or can be designed to fail so that they are carrying maximum load or close to maximum load (Hansbo and Källström 1983).

Piles do not need to be placed uniformly over the whole raft, but can be judiciously placed so as to limit differential deflections in the foundation. For example, Horikoshi and Randolph (1997) have shown that the optimum design of a piled raft carrying a uniform load would involve piles placed over the central 16 to 25% of the raft area.

Piled raft foundations may be designed using simple techniques or more complex techniques (as for raft foundations), and again it is necessary to know whether these techniques are providing reasonable estimates of the behaviour of the foundation.

### 6.7 Soil treated as elastic continua

In order to analyse piled rafts in a simplified fashion, many researchers have treated the soil as an elastic continuum and computed the interaction between the raft, the soil and the piles through the use of the theory of elasticity. For example, Poulos (1994a) assumed that the forces acting down the shaft of a pile could be treated as a series of uniform shear stresses acting over sections of the pile shaft. The base load was treated as a uniform load over a circular region. The effects of these loads on other piles was computed using the theory of elasticity and Mindlin's solution for a subsurface load.

Hain and Lee (1978), Ta and Small (1996) and Chow (1986) have used similar techniques to compute the interaction that occurs between the elements of a piled raft foundation, treating the soil as a continuum.

It is of interest to note the accuracy of these techniques, because they treat the forces along the pile shaft as being forces applied to a continuum (i.e., they do not consider the presence of the pile when calculating the soil displacements). To examine this, a 3-dimensional finite element analysis was undertaken using the layout shown in Figure 6.5a. Only one quarter of the problem needs to be considered (as shown in the figure) due to symmetry, and the side boundaries need to be far enough away so as not to affect the results.

The problem involves a raft supported by nine piles in a soil having a uniform elastic modulus of 20 MPa. The modulus of the raft and piles is taken as 20,000 MPa respectively, and the Poisson's ratios of the soil, raft and piles are taken as 0.4, 0.2 and 0.2, respectively. The raft is 3.9 m square in plan and its thickness is 0.3 m. The pile length was chosen to be 15 m and the thickness of the soil layer was taken as 65 m. The overhang of the raft (around the perimeter) is one pile diameter and the raft is in full contact with the soil.

The problem was analysed firstly by use of the 3-dimensional finite element program, and then with a finite layer based program that uses finite element analysis for the raft and piles and finite layer theory (for layered elastic continua) for the soil (Zhang and Small, 2000).

Loads of 100 kPa are applied to the raft over two areas as shown in Figure 6.5b as this is a more severe test of the program with the piles being subjected to lateral loads as well as vertical loads. For the finite element method, the pile sections are assumed to be 0.3 m square, whereas for the finite layer method, the pile sections are assumed to be circular with an equivalent pile diameter (D) of 0.3385 m. The ratio of the centre-to-centre spacing to the equivalent pile diameter is 4.43.



Comparison of results from the two analyses show that the continuum approach (finite layer method) overestimates the deflection of the piled raft although the deformed shape is the same along section A-A' (see Figure 6.6). Because the deformed shape is the same, the moments per unit length in the raft are very similar. This may be seen from Figure 6.7 where the moment in the  $x$ -direction and in the  $y$ -direction are shown for the section A-A'. ( $M_x = I_{Mx}P$ ,  $M_y = I_{My}P$  where  $P$  is the total vertical load).

It may therefore be concluded that if the soil is treated as an elastic continuum, the errors introduced are not large when compared to more rigorous solutions such as those computed using the finite element method.

### 6.8 A simplified method of estimating load-settlement behaviour of a piled raft

For preliminary estimates of piled raft behaviour, a convenient method of estimating the load-settlement behaviour may be developed by combining the approaches described by Poulos and Davis (1980) and Randolph (1994). As a consequence, the method to be described below will be referred to as the Poulos-Davis-Randolph (PDR) method. The method involves two main steps:

1. Estimation of the ultimate load capacity of the foundation.
2. Estimation of the load-settlement behaviour via a simple tri-linear relationship.

For assessing vertical bearing capacity of a piled raft foundation using simple approaches, the ultimate load capacity can generally be taken as the lesser of the following two values:

- The sum of the ultimate capacities of the raft plus all the piles
- The ultimate capacity of a block containing the piles and the raft, plus that of the portion of the raft outside the periphery of the piles.

For estimating the load-settlement behaviour, an approach similar to that described by Poulos and Davis (1980) can be adopted, but extending it by using the simple method of estimating the load sharing between the raft and the piles, as outlined by Randolph (1994). The definition of the pile problem considered by Randolph is shown in Figure 6.8. Using his approach, the stiffness of the piled raft foundation can be estimated as follows:

$$K_{pr} = (K_p + K_r(1 - \alpha_{cp})) / (1 - \alpha_{cp}^2 K_r / K_p) \quad (6.2)$$

where  $K_{pr}$  = stiffness of piled raft;  $K_p$  = stiffness of the pile group;  $K_r$  = stiffness of the raft alone;  $\alpha_{cp}$  = raft - pile interaction factor.

The raft stiffness  $K_r$  can be estimated via elasticity theory, for example using the solutions of Fraser and Wardle (1976) or Mayne and Poulos (1999). The pile group stiffness can also be estimated from elasticity theory, using approaches such as those described by Poulos and Davis (1980), Fleming *et al.* (1992) or Poulos (1989). In the latter cases, the single pile stiffness is computed from elasticity theory, and then multiplied by a group stiffness efficiency factor, which is estimated approximately from elasticity solutions.

The proportion of the total applied load carried by the raft is:

$$P_r / P_t = K_r(1 - \alpha_{cp}) / (K_p + K_r(1 - \alpha_{cp})) = X \quad (6.3)$$

where  $P_r$  = load carried by the raft;  $P_t$  = total applied load.

The raft - pile interaction factor  $\alpha_{cp}$  can be estimated as follows:

$$\alpha_{cp} = 1 - \ln(r_c / r_0) / \zeta \quad (6.4)$$

where  $r_c$  = average radius of pile cap, (corresponding to an area equal to the raft area divided by number of piles);  $r_0$  = radius of pile;  $\zeta = \ln(r_m / r_0)$ ;  $r_m = 0.25 + \xi [2.5 \rho (1 - \nu) - 0.25] * L$ ;  $\xi = E_{st} / E_{sb}$ ;  $\rho = E_{sav} / E_{st}$ ;  $\nu$  = Poisson's ratio of soil;  $L$  = pile length;  $E_{st}$  = soil Young's modulus at level of pile tip;  $E_{sb}$  = soil Young's modulus of bearing stratum below pile tip;  $E_{sav}$  = average soil Young's modulus along pile shaft.

The above equations can be used to develop a tri-linear load-settlement curve as shown in Figure 6.9. First, the stiffness of the piled raft is computed from Equation (6.2) for the number of piles being considered. This stiffness will remain operative until the pile capacity is fully mobilized. Making the simplifying assumption that the pile load mobilization occurs simultaneously, the total applied load,  $P_t$ , at which the pile capacity is reached is given by:

$$P_t = P_{up} / (1 - X) \quad (6.5)$$

where  $P_{up}$  = ultimate load capacity of the piles in the group;  $X$  = proportion of load carried by the piles (Equation (6.3)).

Beyond that point (Point A in Figure 6.9), the stiffness of the foundation system is that of the raft alone ( $K_r$ ), and this holds until the ultimate load capacity of the piled raft foundation system is reached (Point B in Figure 6.9). At that stage, the load-settlement relationship becomes horizontal.

The load - settlement curves for a raft with various numbers of piles can be computed with the aid of a computer spreadsheet or a mathematical program such as MATHCAD. In this way, it is simple to compute the relationship between the number of piles and the average settlement of the foundation. Such calculations provide a rapid means of assessing whether the design philosophies for creep piling or full pile capacity utilisation are likely to be feasible.

### 6.9 Comparison of simple methods

Some simple models are able to produce accurate solutions that are particularly useful in the design concept stage, particularly at working load levels. It is of interest to evaluate the accuracy of these simple models, and this was carried out by analysis of the problem of a piled raft shown in Figure 6.10 by using 3 simplified methods.

1. The Poulos-Davis-Randolph (PDR) method - as described above
2. GASP Analysis (strip on continuum). In this analysis, the raft was divided into three strips in each direction. A pseudo-three-dimensional analysis is then carried out by considering the free field movements of the other strips on the strip being analysed. The stiffness of the piles is computed by using the equations of Randolph and Wroth (1978).
3. GARP analysis (Plate on continuum). A finite difference solution is used to evaluate the behaviour of the raft that is treated as a thin plate using 273 nodes in the grid. The stiffness of the piles and the pile-pile interaction factors are calculated using the program DEFPIG that is based on a boundary element analysis.

The results of the three simplified analyses are presented in Figure 6.12, where it can be seen that the simplified methods give a load deflection behaviour that is similar for each of the methods. The elastic part of the load deflection curve is also in good agreement with the results of a full 3-dimensional analysis (that is described in the following section) but the simple techniques deviate from the 3-D results once plastic failure begins to dominate at higher load levels.

### 6.10 Two-dimensional analysis

Some designers in the past have treated a piled raft as being two dimensional, and have carried out finite element analysis of the piled raft with the rows of piles treated as a continuous strip. The piles are given equivalent elastic properties so as to approximate the stiffness of the actual row of piles.

This approach was used by Desai *et al.* (1974) for the design of a gravity lock constructed on piles. These authors used a stiffness in the two dimensional model that was equal to the total of the axial stiffnesses of the individual piles, and they reported reasonable correlations between predicted and measured settlements and average load in the piles. Lin *et al.* (1999) also used

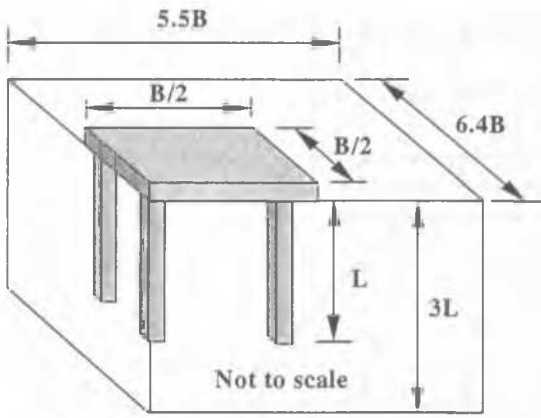


Figure 6.5a. One quarter of raft analysed by finite element technique.

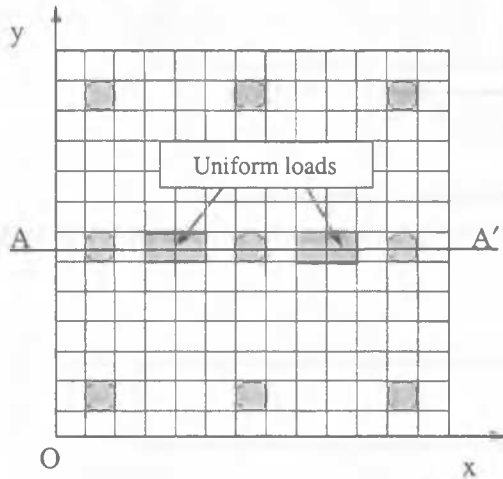


Figure 6.5b. Nine pile group showing loaded regions.

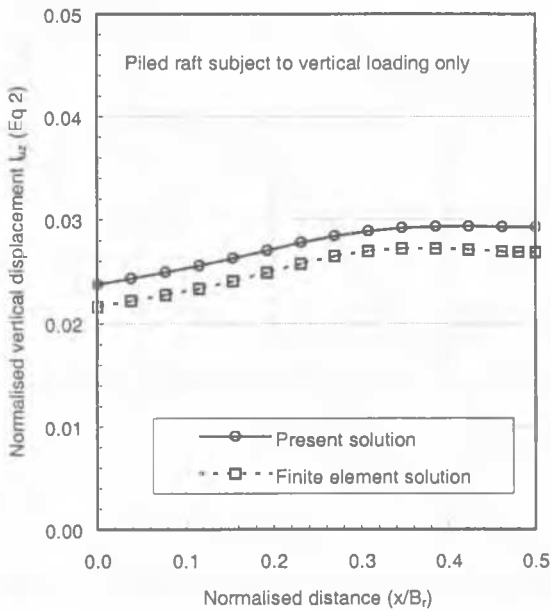


Figure 6.6. Vertical deflection along section A-A'.

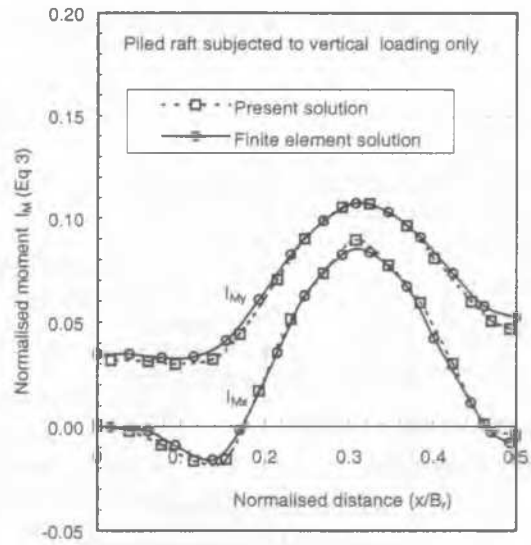


Figure 6.7. Moment/unit length along section A-A'.

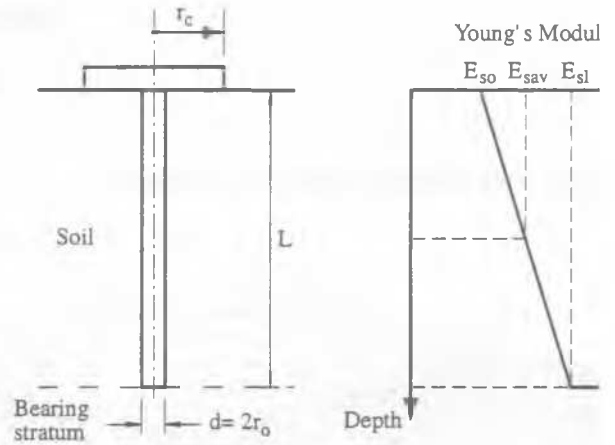


Figure 6.8. Simplified representation of pile-raft unit.

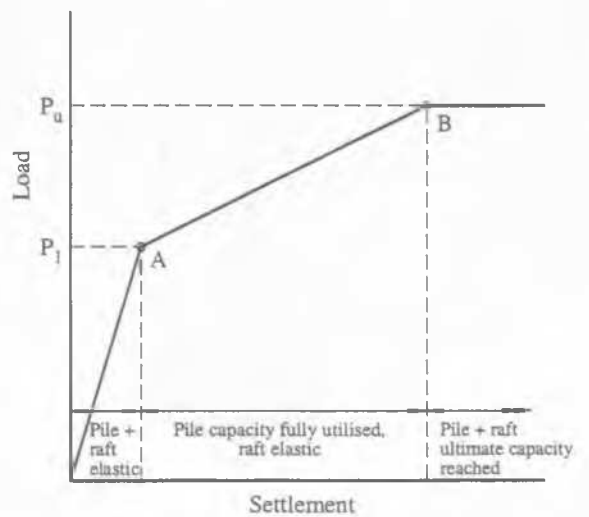


Figure 6.9. Tri-linear load-deflection behaviour for piled raft.

Case	$P_1$	$P_2$	No. of Piles	Remarks
A	2.0	1.0	15	—
B	2.5	1.25	15	—
C	2.0	1.0	9	Piles A are not present

Bearing capacity of raft = 0.3 MPa

Load capacity of each pile

= 0.786 MN (Tension)

= 0.873 MN (Compression)

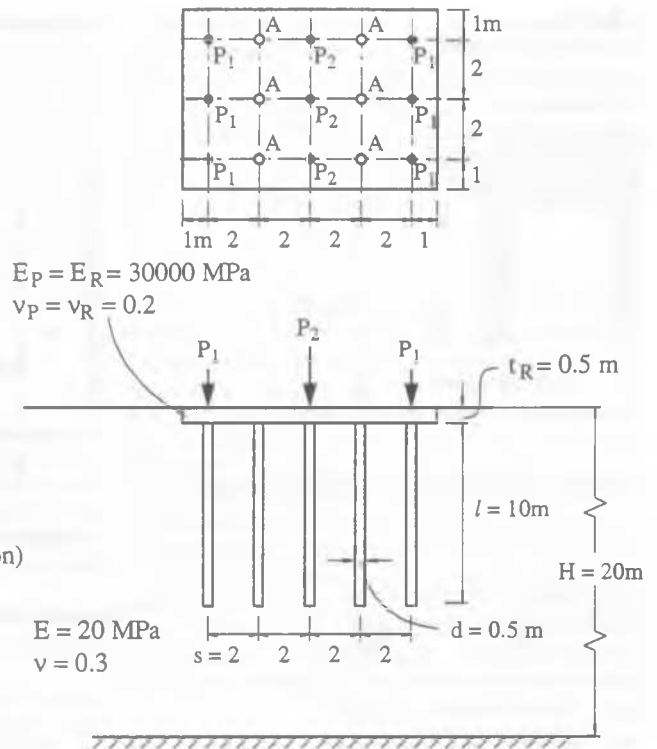


Figure 6.10. Simple example analysed by various methods.

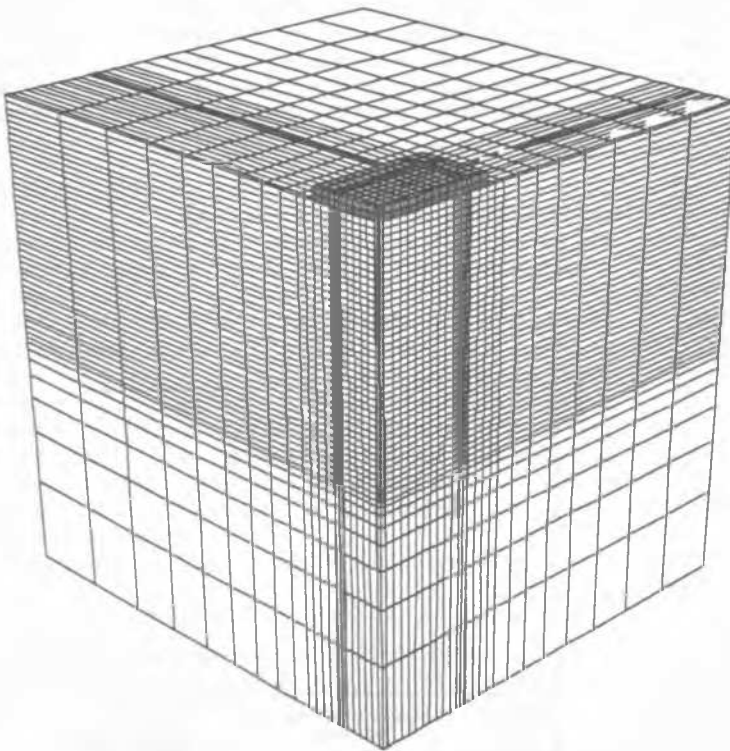


Figure 6.11. Grid used for FLAC 3D analysis of pile groups.

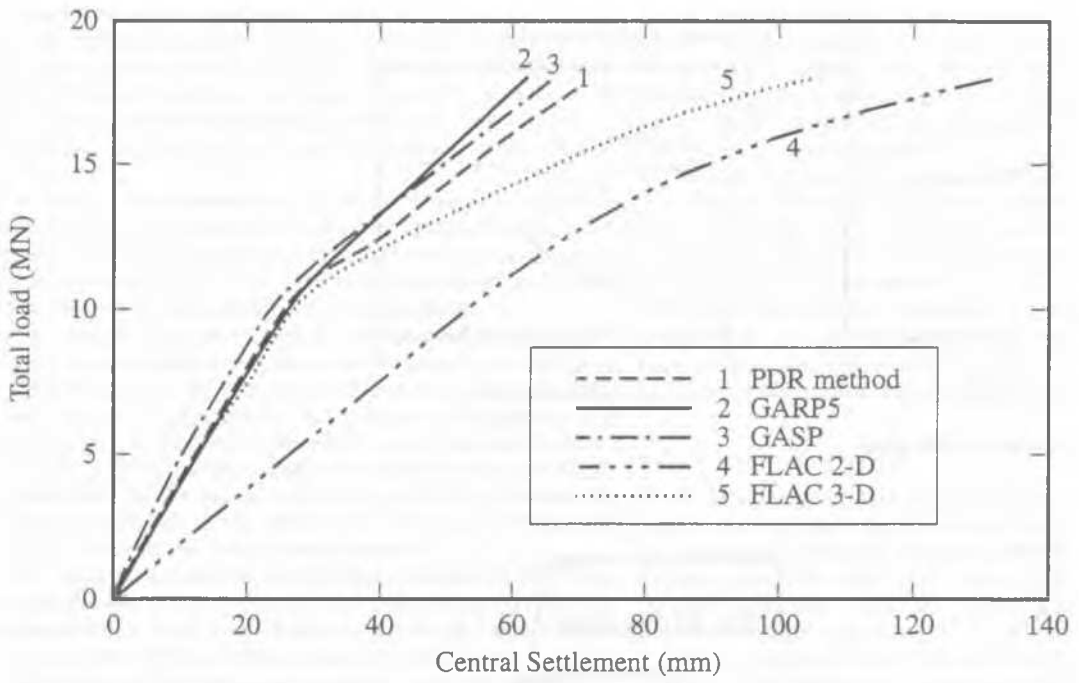


Figure 6.12. Settlement of piled raft computed by various methods.

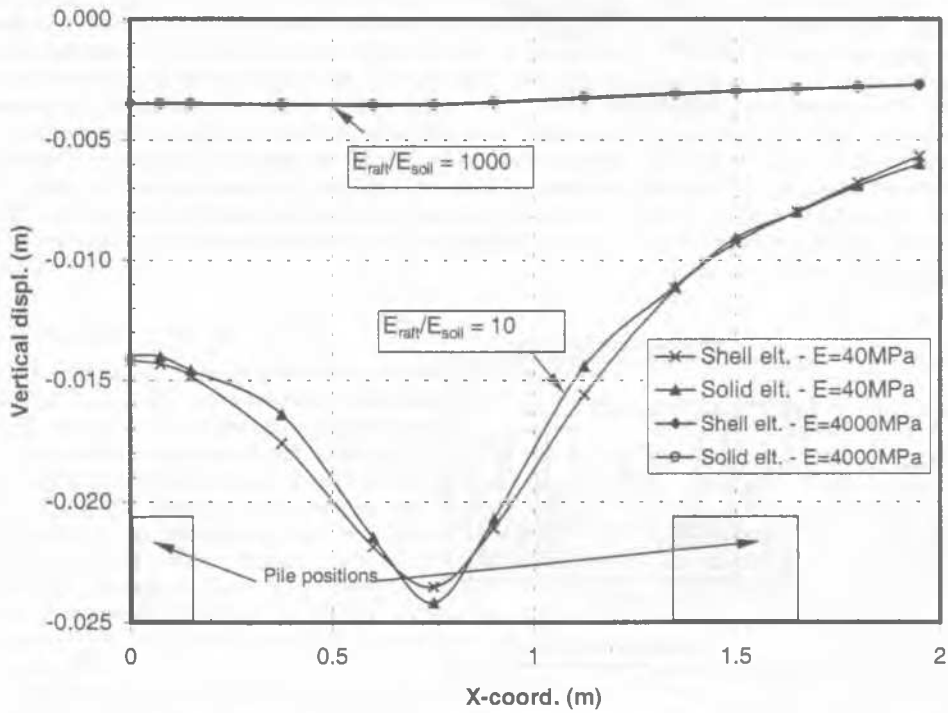


Figure 6.13. Deflection along centre line computed using thick and thin shell theory for raft.

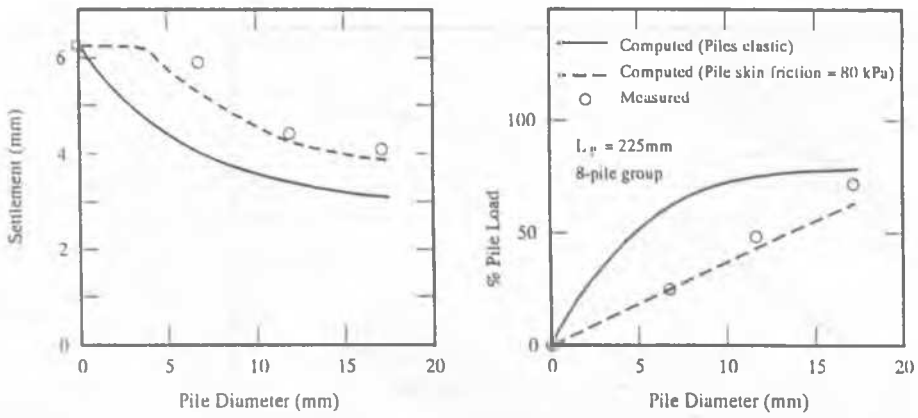


Figure 6.14 Centrifuge test results for 8 pile group.

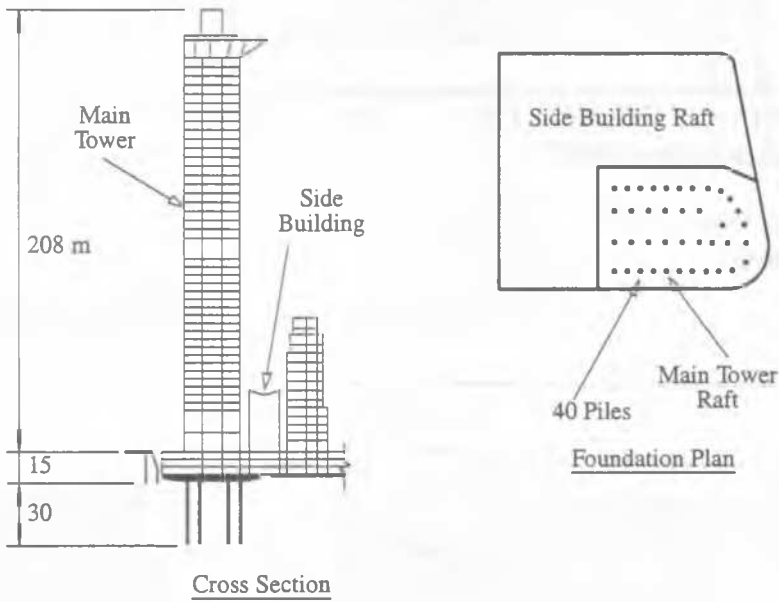


Figure 6.15. Westend Street 1 Tower, Frankfurt.

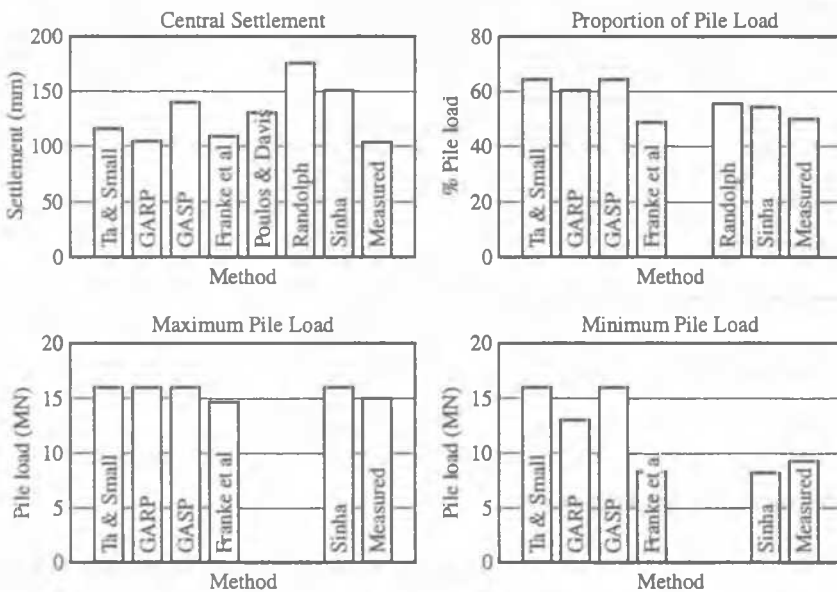


Figure 6.16. Comparison of computed and measured results – Westend Street 1 Tower.

this approach for the analysis of piled raft foundations. They used the commercially available finite difference code FLAC<sup>2D</sup> to analyse a raft supported by 25 piles where slip of the piles was allowed through the use of interface elements. The authors do not compare their two-dimensional results with results from 3-dimensional analyses, so the degree of accuracy cannot be determined.

In order to demonstrate the differences between a full three dimensional analysis and a 2-dimensional analysis, the problem that was used for the simple models in the previous section was re-analysed (see Figure 6.10). The raft is supported by 9 piles and carries point loads applied at the pile locations.

- 3-D analysis. The commercially available program FLAC<sup>3D</sup> was used to compute the piled raft behaviour, and the finite difference grid used is shown in Figure 6.11. The grid consists of 40,026 grid points, and because of symmetry, only one quarter of the mesh is shown. The soil was modelled as a Mohr-Coulomb material using the undrained shear strength parameters for the soil ( $s_u = 50$  kPa,  $\phi_u = 0$ ). Slip between the piles and the raft is not specifically modelled, although the soil is treated as an elasto-plastic material.
- 2-D analysis. In this case, the computer program FLAC<sup>2D</sup> was used to carry out the analysis. The soil-raft-pile system was discretised in the longer direction of the raft using 39 grid lines in the horizontal direction and 34 grid lines in the vertical direction. The soil was modelled as a Mohr-Coulomb material, and again slip was not modelled at the pile soil interface. To obtain the equivalent pile properties, the axial stiffness of the piles was made the same for the 2-D model and the actual row of piles. The concentrated loads were "smeared" in a similar manner.

Figure 6.12 shows the computed load-deflection curves for the central point of the raft as the total load is increased up to a value of 18 MN. As can be seen from the plot, the load deflection behaviour of the raft is quite different, even in the elastic range, with the deflection from the 2-D analysis being much larger than the deflection from the 3-D analysis.

Care therefore needs to be taken in using the two-dimensional approach, especially if the loads on the raft are not uniform or if the loads are applied laterally. Localised behaviour cannot be predicted by such methods, and so it is advisable to use methods that take the three-dimensional nature of the problem into account.

### 6.11 Analysis of the raft

Many analyses of piled rafts are based on the raft being treated as a thin plate, and it is of interest to see what the effect of using thick plate theory is on the numerical predictions.

The problem involves a raft supported by a 3x3 pile group subjected to 2 loaded regions in between the piles on the centre line of the raft. Details of the analysis are: Dimensions of raft 4.5 m by 3.9 m; modulus of raft and piles 40 or 4000 MPa, modulus of soil 4 MPa, Poisson's ratio of the soil 0.4, thickness of raft 0.3 m, length of piles 15 m, depth of soil 45 m, spacing of piles 5 diameters. Loadings of 950 kPa were applied over two regions 0.3 m by 0.3 m in plan, in the same manner as shown in Figure 6.5b.

The problem was analysed using a three dimensional finite element program where the raft was firstly modelled using thin shell theory, and then modelled again making the raft 0.3 m thick, and assigning the raft modulus to that part of the finite element mesh representing the raft. It was assumed in the analysis that there was no slip between the raft and the soil or between the piles and the soil.

The results of the analysis are shown in Figure 6.13 where the deflections along the centre line are plotted. For both the thick raft analysis and the thin plate analysis, there is not a great deal of difference in the computed deflections for the raft because it is relatively thin. This is true for both the stiff raft and the flexible raft. The analysis also showed that when the thick raft was used

in the analysis, then the stress from the concentrated load is spread onto the foundation through the thickness of the raft. For the thick raft analysis (and the flexible raft  $E_{raft}/E_{soil} = 10$ ), a contact stress reduction (at the contact between the raft and the soil) of from 123 to 83kPa (i.e., about 48%) was computed beneath the concentrated load.

The authors have also analysed rafts with thicknesses of up to 2m, and have obtained very similar deflections and moments in the raft from both the solid elements and the shell elements.

It may be concluded therefore, that the use of thin shell elements to represent the raft will lead to reasonable estimates of deflections and therefore moments as long as the raft is not extremely thick. Stresses in the soil will be higher for the thin shell analysis, and this effect may become important if yield of the soil due to concentrated loads is of concern.

### 6.12 Non-linear behaviour

If piles are designed to reach their maximum load, or are designed to carry a high proportion of their maximum load, then slip of the piles becomes important and non-linear behaviour of the piles should be taken into account. This type of behaviour becomes important if piles are used to control differential deflections and are designed to yield or fail.

Full 3-dimensional finite element analyses have been used to allow non-linear behaviour of piled raft foundations (Katzenback *et al.* 1997), but simpler techniques have been developed. Clancy and Randolph (1993) have presented a non-linear analysis for piles and this is incorporated into the computer program HyPR (Hybrid Piled Raft Analysis), and Bilotta *et al.* (1991) have presented two methods for computing the behaviour of piled rafts where the pile may have a non-linear load-displacement relationship. The latter authors stress the point that if piles are designed to yield, then a non-linear analysis of the piles is essential.

Poulos (1994a) has demonstrated the need to take pile non-linearity into account in analysis of centrifuge tests on piled rafts (Thaier and Jessburger 1991). Shown in Figure 6.14 are the settlement and pile load predictions made for a piled raft with 8 piles. If the pile is not allowed to fail, then the results of the analysis do not match the observed behaviour. However, if the skin friction on the piles is limited to 80 kPa so that the piles can yield, then the predicted values are much closer to the measured values for both settlement and percentage load carried by the piles.

### 6.13 Case study

In order to gauge whether some of the numerical methods that have been mentioned can be applied with confidence in practice, the case of the Westend Street 1 Tower in Frankfurt Germany was examined. The building is 51 stories high (208m) and has been described by Franke *et al.* (1994) and Franke (1991). The foundation for the building was a piled raft with 40 piles that were 30m long as shown in Figure 6.15.

The foundation was constructed in a deep deposit of the Frankfurt clay 120m thick, and using pressuremeter tests reported by Franke *et al.* (1994), the modulus of the clay was assessed to be 62.4 MPa.

The ultimate load capacity of each pile was computed to be 16 MN and a total load of 968 MN was assumed to be applied to the foundation (this is greater than the ultimate capacity of the individual piles).

Six methods were used to predict the performance of the piled raft foundation:

1. The boundary element approach of Poulos and Davis (1980).
2. Randolph's (1983) method.
3. The strip on springs approach using the program GASP (Poulos, 1991).
4. The raft on springs approach using the program GARP (Poulos, 1994a).

5. The Finite element and finite layer method of Ta and Small (1996).
6. The finite element and boundary element method of Sinha (1997).

Measured values were available for the settlement of the foundation, the percentage of load carried by the piles, the maximum load carried by a pile in the group and the minimum load carried by a pile in the group. The results of the six different analysis methods are shown in the bar chart of Figure 6.16 compared with the measured values and the values reported by Franke *et al.* (1994).

From the figure, it may be seen that:

1. Most of the methods over-predicted the settlement of the foundation. However this depends on the soil modulus chosen, and it can only be concluded that most of the methods gave a reasonable estimate of the settlement for the adopted soil stiffness.
2. Most of the methods over-predicted the percentage of load carried by the piles, although the calculated values are acceptable from a design point of view.
3. All of the methods that are able to give a prediction of pile load, suggest that the most heavily loaded pile is almost at its ultimate capacity, and this is in agreement with the measured value.
4. For the minimum pile load, there is a considerable variation in the calculated results, with three of the methods indicating a much larger value than was measured.

These results show that when some of the piles are carrying loads close to their capacity, there can be significant variability in the computed results, especially for simple methods and methods based on the theory of elasticity.

#### 6.14 Summary

Some of the many schemes for analysis of raft and piled raft foundations have been discussed, and the following conclusions made:

1. Spring models are highly undesirable for use in the design of raft (and piled raft) foundations as they do not allow for interaction between various parts of the foundation. Continuum models allow the soil to be treated in a far more realistic manner and whether linear or non-linear, yield vastly improved solutions over spring models.
2. Analytic techniques that are based on just analysing one strip of a continuous raft can lead to error. Modern methods that employ the full raft in the analysis are preferable.
3. Inclusion of the depth of the soil in a raft or piled raft foundation problem is desirable, as treating the soil as an infinitely deep layer will generally lead to overestimates of settlements. Moments are generally not as greatly affected by the soil depth as are settlements.
4. The structure above a raft or piled raft foundation will stiffen the raft and generally lead to less differential settlements. This effect will obviously depend on the stiffness of the structure. Shear walls will have a large stiffening effect, but flexible frames have only a minor effect.
5. For piled rafts, simple models can yield reasonably good first stage design approximations to pile behaviour. Two-dimensional models can be inaccurate, and should be used with caution.
6. The use of thin shell theory for the raft in analysis yields results that are in good agreement with those obtained using thick shell theory. It is therefore acceptable to use thin shell theory for analysis of rafts.
7. Ideally, slip along the pile shafts should be allowed for in piled raft analyses, especially if the loads on the foundation are large enough to cause yield of some of the piles.
8. Application of some current methods of analysis to field cases show that a reasonably good prediction of performance can be made with some of the analytic techniques presented.

However, there is great scope for improvement in these predictive techniques, and some of the areas where improvement may be achieved are non-linear behaviour, lateral loading and the inclusion of the structure in the analysis.

## 7 EARTH RETAINING STRUCTURES

A fundamental component of all engineering design is the complete identification of situations which may make a structure, or a component of a structure, unfit for the purpose it is intended to serve. In many applications in civil engineering this may involve identification of a number of "limit states" including possible failure mechanisms or conditions under which unacceptable displacements may occur. It is important to note that collapse of the structure is not usually the sole consideration. Behaviour of the structure in service, usually well before the collapse condition is approached, is also of significant concern.

In principle, the design of earth retaining structures is no different to the design of most other engineered structures. However, in the execution of the design process it has been common practice to place far greater emphasis on assessments of the limit condition corresponding to collapse of the retaining structure, rather than its behaviour in service. With a few important exceptions, estimation of the behaviour of the retaining structure prior to the development of a collapse mechanism has traditionally received very little attention. The exceptions include various (now classical) methods to estimate strut loads for braced excavations (e.g., Terzaghi and Peck, 1967), but even these studies only focused on estimating loads and paid little attention to actually quantifying displacements. The increasing use of numerical modelling over the past few decades, coupled with careful observations of the behaviour of retaining structures in the laboratory and field, has begun to alter this former emphasis on the collapse limit state. Design methods that make use of sophisticated numerical modelling to estimate the importance of soil-structure interaction, as well as field observations to calibrate and validate these models, are currently under development. In these newer methods, much greater emphasis is placed on estimation of the movements behind relatively flexible retaining walls after excavation.

In order to review the current status of the methods available for the design of flexible retaining systems, it is necessary first to provide a brief review of the techniques available for estimating the earth pressures that may act on the retaining structure under the most commonly prevailing conditions. The review will then address the methods currently under development, i.e., those that take into account the movements of the retained soil and the retaining structure. The emphasis here is placed clearly on relatively flexible retaining systems, i.e., ones for which the structural interaction between the retained soil and the retaining system is significant in terms of estimating wall and soil movements and wall loadings. For these cases the construction sequence, including wall placement, will be important considerations.

### 7.1 Assessment of earth pressures

Informative reviews of the development of earth pressure theory have been provided in several texts (e.g., Heyman, 1972; Clayton, *et al.*, 1993). In these we are reminded that it was developments of fortifications and defence systems around the turn of the 18<sup>th</sup> century that resulted in the construction of structures with deep excavations in soil with near-vertical faces retained by walls. Although a number of authors appear to have worked on the problem of estimating the loads on such walls at about that time, it was Coulomb (1776) who was to make the most lasting impression in this field. He divided the strength of soil into two components, i.e., "cohesion" and "friction". He then analysed the statics of an assumed failure mechanism, involving movement

("failure") of a triangular wedge of soil behind the retaining wall, developing what we now know as a "limit equilibrium" technique. Both "active" and "passive" conditions were considered using this approach. Later, Rankine (1857) derived a solution to a related problem, namely that of a complete soil mass in a state of failure. Formulations of the Coulomb and Rankine theories may be found in most basic texts on Soil Mechanics, so it is unnecessary to repeat them here.

The early analyses performed by Coulomb and Rankine and others were formulated in terms of total stress. However, following the work of Terzaghi in the early 1920s on the concept of effective stress as the controlling influence on strength and compression of soils, the Coulomb and Rankine formulations have been extended in terms of effective stress in order to include the influence of pore water pressures.

## 7.2 Classical and plasticity solutions for earth pressures

As indicated by Clayton *et al.* (1993), work continued during the 20<sup>th</sup> century on refining and extending the available analytical solutions for earth pressures, following reassessment of their underlying assumptions and in response to observations that indicated pressure distributions which did not increase linearly with depth, as implied by Coulomb. In particular, Prandtl (1921), Hencky (1923) and Sokolovsky (1960) obtained a range of active and passive pressure solutions for a  $c, \phi, \gamma$  soil. Solutions for limiting earth pressures were also developed using the bound theorems of plasticity. It should be noted, however, that upper and lower bound solutions bracket the correct solution only for a material with an associated plastic flow rule.

### 7.2.1 Kinematics

Coulomb's original solution implied a particular mode of wall movement, namely rotation about the base of the wall. Terzaghi (1936), reasoning on the basis of analysis and observations of retaining structures, concluded that other modes of wall movement could lead to different pressure distributions. In particular if the wall exists before soil is placed behind it, or if the wall could be placed with minimal disturbance to the soil, then before any wall movement occurs, the pressures on the wall would be the earth pressures at rest. In an attempt to extend the theory of earth pressures, Terzaghi considered not only rotation of the wall about its toe, but also translation away from the retained soil, as well as the at-rest condition.

Application of the Rankine solution to retaining walls has also been criticised by Terzaghi (1936), among others, who indicated that such a stress state could never exist behind a rigid wall, principally because of the kinematic constraint against lateral expansion required in the soil beneath the wall in order to develop the Rankine active condition throughout the entire soil mass. The Rankine solution is also inapplicable if significant shear stresses are developed along the interface between the retained soils and the back of the retaining wall. Other limitations of the Rankine solution have been clearly summarised by Clayton *et al.* (1993) and Lee *et al.* (1983). In particular they note that if the retained soil has an inclined ground surface, the Rankine passive condition must not be used since the resultant force on the vertical plane will be inclined in the wrong direction relative to the normal to the back of the wall. Despite these criticisms, a reinforced cantilevered retaining wall provides at least one situation where the Rankine active earth pressure solution is relevant, e.g., see page 84 of Clayton *et al.* (1993).

### 7.2.2 Earth pressures on rigid retaining walls

The above limitations notwithstanding, research, mainly in the latter part of the 20<sup>th</sup> century, has confirmed that active earth pressures computed using Coulomb's limit equilibrium method are, for all practical purposes, quite acceptable and are applicable to the design of rigid retaining structures. In this case, it is therefore unnecessary for geotechnical engineers to reject the Coulomb approach in favour of the more rigorous plasticity theory.

Expressions for the total thrust that must be resisted by the rigid wall in the active case are usually given in terms of relevant earth pressure coefficients. Often, these are in a generalised form expressing the lateral pressure on the wall as:

$$p_{AN} = K_A \gamma z - K_{AC} c \quad (7.1)$$

for the active condition, and

$$p_{PN} = K_P \gamma z - K_{PC} c \quad (7.2)$$

for the passive case, in which  $p_{AN}$  and  $p_{PN}$  are the normal pressures acting on the wall at depth  $z$ ,  $\gamma$  is the unit weight of the soil and  $c$  is the cohesion assigned to the soil mass. For many design problems a value of zero is assigned to  $c$ .

Tabulated values of the coefficients  $K_A$  may be found in numerous text books and design codes and manuals, e.g., Lee *et al.* (1983), Clayton *et al.* (1993), Caquot and Kerisel (1948, 1953), Kerisel and Absi (1990), so there is no need to reproduce comprehensive listings here. However, it is instructive to present a comparison of selected earth pressure coefficients obtained using the Coulomb analysis (C) assuming a planar failure surface, rigorous plasticity analysis (P), and the lower bound theorem of the theory of plasticity (L). Such a comparison has been provided by Chen (1975) and reproduced in Lee *et al.* (1983). It is also reproduced here in Table 7.1. The symbol  $\delta$  is used in this table to indicate the angle of friction relevant to the interface between the back of the wall and the retained soil.

The values in Table 7.1 reveal several important features. The Coulomb limit analysis and the lower bound plasticity values are, for most practical purposes, equal in the active case. Thus the planar failure surface assumed in the Coulomb analysis provides reasonable predictions of the wall loads, despite the fact that the actual failure surface may not be planar. This situation should be contrasted with the passive case, where it is quite evident that a planar surface is inadequate; indeed it is completely incompatible with observation.

For the passive case, the most complete set of rigorous solutions for the thrust on a rigid wall appear to be those produced by Lee and Herrington (1972a, 1972b). They expressed the horizontal and vertical components of the overall wall thrust in the following form,

$$P_{HP} = H(cN_{cHP} + qN_{qHP} + \gamma HN_{\gamma HP}) \quad (7.3)$$

$$P_{VP} = H(cN_{cVP} + qN_{qVP} + \gamma HN_{\gamma VP}) \quad (7.4)$$

in which  $q$  is the vertical surcharge applied to the surface of the retained soil and  $H$  is the wall height. Components of the thrust factors  $N_{cP}$  and  $N_{\gamma P}$  are given in Table 7.2. These values were obtained by Lee and Herrington (1972a) using the lower bound theorem of plasticity, for a material with an associated plastic flow rule. It is worth noting that they are also exact solutions for the case where the wall translates and rotates about the base. The angle  $\beta$ , indicating the slope of the surface of the retained soil is positive when the backfill surface slopes up from the retaining wall. The angle  $\alpha$  indicates the slope of the back of the wall, i.e., the included angle between the back face and the horizontal leading away from the retained soil.

### 7.2.3 Progressive failure

Both the Coulomb and Rankine analyses, as well as those based on the theory of plasticity, imply a solid, which behaves as a rigid, perfectly plastic material, so that it is assumed the peak strength is mobilised throughout the failing soil mass at the same instant. Further, it is implied that failure of this type occurs after only infinitesimal movement. It is well known that some real soils are compressible and most exhibit some strain hardening, followed by plastic failure which could also be associated with a reduction in strength (strain softening or progressive failure) as the wall movement and the strains in the soil increase. Since real soils are compressible and can strain soften, there are many



situations where the peak strength will not be mobilised simultaneously along the entire potential failure surface, or throughout the entire region of failing soil. The most important practical implication of this type of real soil behaviour arises in the case of passive wall failure. For example, Rowe and Peaker (1965) demonstrated quite clearly in their experiments that the maximum force exerted by the wall, and sustained by the retained soil, is much less than is calculated on the basis of the available peak strength, if strain softening occurs.

#### 7.2.4 Soil-structure interaction

As indicated previously, classical solutions for wall pressures assume that the wall itself is a perfectly rigid structural member. In practice, many walls, particularly those constructed using sheet piling or concrete diaphragm walls, will not behave rigidly, but will flex significantly under the influence of the earth pressures acting on them. This problem was studied extensively by Rowe (1952), who provided a method for estimating the effects of soil-structure interaction on the maximum bending moments induced in the wall section (see also CIRIA, 1974). Wall-soil structural interaction has also been the topic of much recent research, particularly involving the use of sophisticated numerical modelling, mostly making use of finite element methods. These more recent advances will be reviewed separately below.

#### 7.2.5 Construction details

In general, earth pressures at rest are reduced to limiting active values by movement of the wall away from the soil. Movements of the wall towards the soil of much larger magnitude are needed to increase the at rest pressure to limiting passive values. The extent of wall movement relative to the retained soil therefore determines the proportion of the limit pressure that applies. As noted by Pullar (1996), this movement may be derived from a variety of sources including deflection of the wall itself, compression or translation of the support system (e.g., shoring or anchors), movements needed to mobilise a sufficient proportion of the passive soil resistance in front of a wall to maintain equilibrium at an intermediate stage of excavation, or simply rigid body rotation or translation of the wall relative to the soil. Significant influences on these possible sources of wall and soil movement are the method and sequence of construction

Some particular examples of the significance of construction sequence on the earth pressures acting on retaining walls have been identified by several workers, including Potts and Fourie (1984) and Clayton *et al.* (1993). Increasingly, the construction of excavations and retaining systems in urban environments requires that lateral wall displacements must be minimized in order to prevent damage to adjacent buildings. If lateral movements must be kept small then it is likely that the wall will be required to support earth pressures that are much higher than those corresponding to the active condition. This effect is particularly significant for overconsolidated clays, in which values of the at-rest earth pressure coefficient may be as large as 2. Thus if it is assumed that at rest conditions are sustained in the longer term, as might be the case for a relatively rigid support system, then prop forces and bending moments which are many times those calculated on the basis of active pressures will be required (Potts and Fourie, 1984).

Despite the fact that few designers have, until recently, taken the (initial) in situ earth pressures into account, many walls have not failed. This apparent discrepancy between the conventional design assumptions and reality has been attributed to the effects of the wall installation process (Clayton *et al.*, 1993), which are particularly significant for excavation walls. This type of wall usually involves the excavation of a hole (often supported by bentonite slurry) prior to placement of concrete and reinforcing steel. The total horizontal stress on the boundary of this hole will be reduced as a result of excavation, and the initial value may not be reinstated by the placement of concrete, even in the long term. As a consequence, many walls constructed in this manner may not experience full at rest earth pressure conditions.

Finite element analyses of retaining walls have also shown the significant implications of construction details and installation sequence. Potts and Fourie (1984, 1985) and Fourie and Potts (1989) have demonstrated such effects for a propped cantilever wall in clay. They showed that sophisticated numerical analyses can provide predictions of the depths of embedment required for equilibrium that agree remarkably well with those calculated using simple limit equilibrium solutions, regardless of the initial value of the horizontal total stress assumed to act in the soil. However, in contrast, the values of the prop force and maximum bending moment are much higher than values predicted by the limit equilibrium methods whenever the assumed initial horizontal stresses are relatively large.

Finite element analyses reported by various authors, e.g., Kutmen (1986), Higgins *et al.* (1989) and Gunn *et al.* (1992), have shown the sensitivity of the bending moments calculated for the wall to the details of the construction procedure.

### 7.3 Design approaches

The first stage in the design process for an earth retaining structure is usually an assessment of which type of structure is most appropriate for the problem at hand. This is followed by identification of the possible ways in which the structure may fail to perform satisfactorily. As mentioned previously, collapse of the structure is not usually the sole consideration. Its behaviour in service, often well before the collapse condition is approached, is also of significant concern. The design process may proceed through various iterations and stages, from preliminary to final design. Throughout this process calculations are usually required to identify the limit states of the proposed structure, and the design adjusted so that these conditions are satisfactorily avoided. As noted by Clayton *et al.* (1993) and others, the following conditions need to be considered:

- moment equilibrium must be satisfied, i.e., the structure should not overturn,
- horizontal force equilibrium must be satisfied, i.e., the structure should not slide,
- vertical force equilibrium must be satisfied, e.g., bearing capacity of the soils on which the structure is founded should be adequate,
- earth pressures should not overstress any part of the structure, e.g., in bending or shear,
- the general stability of the soil around the structure must be maintained, e.g., slope failure, base failure and overall instability must be avoided, and
- deformations of the structure should be acceptable.

Some of these conditions are illustrated in Figure 7.1.

It should be clear from the above list of important design considerations that earth retaining structures must be analysed for many different conditions, and therefore in many different ways. Traditionally, hand calculations have generally been carried out using limit equilibrium methods, i.e., where it is assumed that the wall is at a state of failure or collapse. However, with the increasing need to restrict displacements of the retaining structure itself as well as the ground adjacent to the structure, more complex computer analyses have been developed.

#### 7.3.1 Limit equilibrium methods

The limit equilibrium techniques include methods based on simple active and passive earth pressure distributions for cantilever wall, and others such as those known as the "free earth support method" and the "fixed earth support method" for propped or anchored walls. Each of the latter methods also involves particular assumptions about the earth pressures acting on the wall. A comprehensive review of these methods is included in many texts, e.g., Clayton *et al.* (1993).

For relatively small earth retaining structures, the limit analysis techniques are widely used for design. In most analyses it is assumed that the wall moves sufficiently to reduce the initial *in*

Table 7.1. Comparison of Coulomb (C), Plasticity (P) and Lower Bound (L) Solutions for earth pressures behind a vertical wall with horizontal soil surface ( $c = 0$ ) (after Chen, 1975).

$\phi^\circ$	$\delta^\circ$	Active, $K_A$			Passive, $K_P$		
		C <sup>*</sup>	P <sup>#</sup>	L <sup>†</sup>	C <sup>*</sup>	P <sup>#</sup>	L <sup>†</sup>
20	0	0.490	0.490	0.490	2.04	2.04	2.04
	10	0.426	0.446	0.450	2.52	2.64	2.55
	20	0.350	0.426	0.440	2.93	3.52	3.04
30	0	0.333	0.333	0.330	3.00	3.00	3.00
	10	0.290	0.307	0.320	3.96	4.15	
	20	0.247	0.297	0.300	5.06	6.15	
40	30	0.297	0.302	0.310	10.80	9.80	6.55
	0	0.217	0.217	0.220	4.60	4.60	4.60
	20	0.199	0.200	0.200	11.80	10.10	9.69
	30	0.201	0.203	0.200	21.60	14.80	
	40	0.210	0.214	0.200	70.90	20.90	18.60

\* Plane surface of failure; # Log-spiral failure surface; † Shape of failure surface determined by numerical analysis

Table 7.2. Values of passive thrust factors for cohesion and self-weight (after Lee and Herrington, 1972a).

$\beta$	$\alpha$	$\phi$	$N_{cVP}$	$N_{cHP}$	$K_{PV}=2N_{cVP}$	$K_{PH}=2N_{cHP}$
0	90	22.5	3.15	5.10	1.40	3.45
		30	5.00	6.95	3.30	5.65
		40	11.1	12.1	12.0	14.2
		45	18.0	17.0	26.0	26.0
	80	22.5	2.05	4.65	0.65	3.00
		30	3.20	6.05	1.80	4.95
		40	6.85	10.1	6.55	11.0
		45	10.9	14.0	13.2	18.8
	70	22.5	1.15	4.10	0.15	2.75
		30	1.85	5.30	0.75	4.25
		40	4.05	8.60	3.20	8.80
		45	6.00	11.3	6.55	14.2
-20	90	22.5	2.35	3.20	0.60	1.35
		30	3.40	4.10	1.30	2.25
		40	6.15	6.10	3.95	4.70
		45	9.00	8.00	7.50	7.50
	80	22.5	1.60	2.85	0.25	1.15
		30	2.30	3.50	0.70	1.90
		40	3.95	5.10	2.10	3.60
		45	5.50	6.40	3.80	5.40
	70	22.5	1.05	2.45	0.05	1.10
		30	1.45	3.00	0.30	1.55
		40	2.35	4.15	1.00	2.80
		45	3.20	5.10	1.85	4.00
20	90	22.5	4.15	7.85	2.30	5.60
		30	7.65	11.45	6.45	11.20
		40	20.1	22.8	29.6	35.0
		22.5	2.50	7.00	1.20	5.20
	80	30	4.05	10.05	3.60	9.60
		40	12.2	19.5	15.8	27.4
		22.5	1.25	6.30	0.25	4.80
		30	2.60	8.85	1.50	8.50
	70	40	6.80	16.1	8.00	21.7

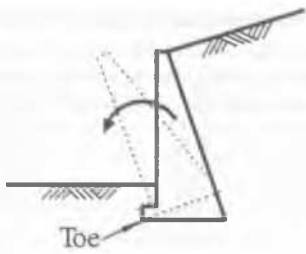
situ earth pressures to their active limits. Typically, passive pressures are factored down to provide both a margin of safety and as a means of restricting displacements. Earth pressures are normally assessed using published tables, graphical techniques or analytical expressions often programmed in a computer spreadsheet.

Numerous manuals have been produced to assist designers, especially where approaches based on the limit equilibrium techniques are to be used in the design. Examples include those developed in Europe (Padfield and Mair, 1984; Clayton *et al.*, 1993), USA (e.g., US Army Corps of Engineers, 1994; NAVFAC – DM7, 1982), and Hong Kong (GCO, 1982). Complicating issues such as lateral pressures acting on retaining structures due to external surface load and compaction of back-fill can also be taken into account in these design procedures, e.g., see Clayton *et al.* (1993).

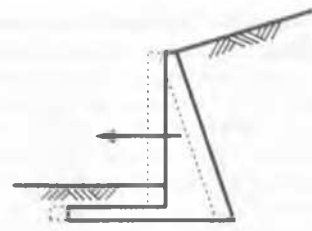
### 7.3.2 Computer methods

A significant number of computer programs are available commercially to assist with the design of retaining structures. These vary from programs that simply assist in computing earth pressures for simple to quite complex soil profiles, that automate analyses using the limit equilibrium technique, to those that attempt to take into account the interaction of the soil with the retaining structure.

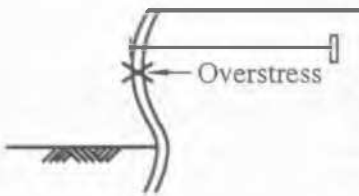
The more sophisticated computer models assume either a Winkler or a continuum soil model in an attempt to deal adequately with the issue of structure-soil interaction. In the Winkler approach the soil is modelled as a series of discrete, usually unconnected and linear, horizontal springs. However, most programs adopting this approach will allow the user to impose active or passive limits on the pressures applied to the wall. The wall is represented as by a series of structural beam or beam-column elements. For an excavated wall an estimate of the in situ stress state is also required and the analysis commences with



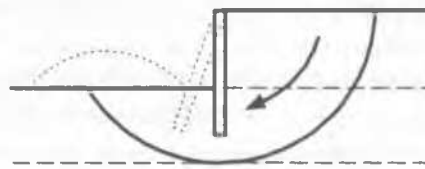
**(a) Overturning**  
Check moment equilibrium



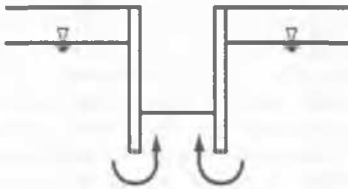
**(b) Sliding**  
Check force equilibrium



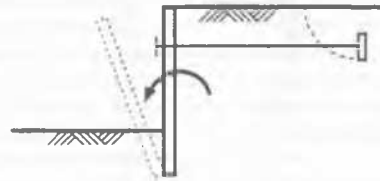
**(a) Overstress**  
Check bending and shear stresses



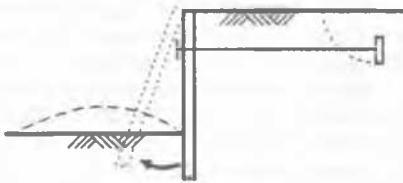
**(d) General stability**  
Carry out overall (slope) stability analysis



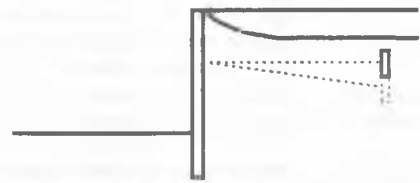
**(e) Granular soil, associated with excessive upward seepage**



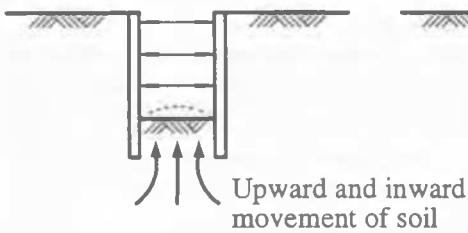
**(f) Failure of anchor system**



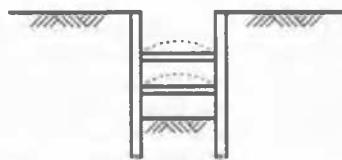
**(g) Bottoms of piles move outward (passive resistance not sufficient)**



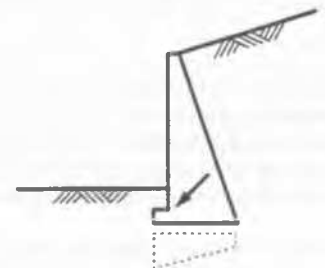
**(h) Settlement behind the wall**



**(i) Bottom heave**



**(j) Buckled struts**



**(k) Overstress of foundations**

Figure 7.1. Failure state for earth retaining structures (after Clayton et al., 1993).

balanced horizontal forces applied to the wall. Top down excavation in front of the wall is simulated by setting spring forces progressively to zero until the final depth of excavation is reached, and at the same time the spring stiffnesses are progressively halved, to model the reduction in support on the excavated side of the wall. As a result of the load imbalance, horizontal wall displacement and bending take place. Various stages of the construction sequence are usually analysed, and propping or anchoring is simulated by the addition of further discrete springs at the required stiffnesses and levels.

The major criticism of this approach is that a Winkler model for the soil may not be reasonable, as it cannot capture some of the more important aspects of soil behaviour. Although the model can be extended by assuming non-linear springs, there is still the difficulty of specifying the precise nature of the spring behaviour in practice, and the very serious limitation that such a spring model does not adequately represent shear transfer through the soil. With a Winkler spring representation of the soil, the wall is the only component providing distribution of forces. It is well known, for example, that by judicious choice of the spring constants this type of model can be made to provide adequate predictions of soil-structure interaction when the loading is highly concentrated, but generally it provides poor estimates of the structural behaviour for more highly distributed forms of loading. Earth pressure loading on the wall is generally distributed in nature, so the use of the Winkler-type models must be used with caution. Several investigators, e.g., Brooks and Spence (1992) and Yang (1997), have compared predictions obtained using the Winkler approach with others based on a continuum representation of the soil. These studies indicate that generally lower stiffnesses must be used in the Winkler springs models to achieve displacements comparable with those predicted by the continuum models.

More sophisticated and complex analyses, based on either the finite element or finite difference methods and continuum models of soil behaviour, are now used commonly in the design of larger retaining walls, particularly in cases where displacements around the excavation may be critical. A variety of commercial and proprietary (in-house) computer codes exist for this purpose. A brief review of some of the commercially available computer codes has been given in chapter 11 of Clayton *et al.* (1993). They provide a list of the major issues in modelling of this type and discussion on the important choices to be made in terms of constitutive models to represent the soil behaviour and parameter determination. The more complex computer methods are normally used for particular case studies, and as such it has not been usual to present the results of such studies in the form of generally applicable design charts. An exception, that has significant relevance to geotechnical practice, is described in the following section.

### 7.3.3 Design methods based on displacement control

Field data, particularly for soft and medium clays show that the movements of excavation support systems are not a constant proportion of excavation depth. Generally, yielding is induced in the soil mass beneath and surrounding an excavation as it is deepened. One of the early attempts to take account of soil yielding and the consequent movements in the soil and the structural support system in the design of support systems was suggested by Peck (1969) who correlated the observed movements against the stability number, defined as:

$$N = \frac{\gamma H}{c} \quad (7.5)$$

in which  $H$  is the depth of the excavation,  $\gamma$  is the unit weight of the soil and  $c$  is the undrained shear strength of the clay. It will be recognized that the parameter  $N$  is inversely related to the factor of safety against basal heave in an excavation in undrained clay. An example of the type of design guidance provided by such correlations is indicated in Figure 7.2.

More recently, a semi-empirical procedure for estimating movements of excavation support systems in clays, using the factor of safety against basal heave,  $F$ , as a principal element, was proposed by Mana and Clough (1981). As a first step, they correlated wall movements with  $F$  for excavations supported by braced sheetpile walls of average stiffness. The correlation was based on both observed field data and finite element results. Modification factors were provided through a series of charts to account for the effects of parameters such as wall stiffness, strut stiffness, width of excavation and preload. Figure 7.3 (taken from Clough *et al.*, 1989) presents an extension of the ideas of Mana and Clough, where the maximum lateral wall movement,  $\delta_{LM}$ , is linked to both  $F$  and a term defining the stiffness of the support system stiffness and the average vertical spacing between the lateral props.

Clough *et al.* (1989) made the important point that the results in Figure 7.3 are based upon average conditions and good workmanship. They are also based on the assumption that movements that develop when the wall is in the cantilever stage before supports are applied to the wall are a small portion of the total movements. If this is not true then, according to Clough *et al.* the chart will underestimate the actual movement.

Clough and others, including Goldberg *et al.* (1976) have also examined movement around supported excavations and developed design charts allowing preliminary estimates of ground movements to be made. Examples of these design charts for clays are given in Figures 7.4 and 7.5. Settlement envelopes behind walls in sand suggested by Goldberg *et al.* (1976) are shown in Figure 7.6.

It is important to realise that design methods such as contained in Figures 7.3 to 7.6 should only be used to provide preliminary estimates of ground and support movements. They do not replace the need for monitoring in construction of this type, in order to provide early warning of difficulties and to allow time for design adjustments to be enacted, as required in the observational method. Potentially, better estimates of ground and wall movements should be possible using complex numerical techniques such as the finite element method. However, with these sophisticated prediction tools, great care in their use is also required. Further, meaningful and useable guidelines for their use in practice are still not available. This importance of this issue is illustrated in the following section.

### 7.4 Validation and calibration of computer models

The importance of soil-structure interaction in problems involving excavated retaining structures is now widely recognised. Addressing the interaction problem almost invariably requires the use of numerical models employing load-path techniques in order to follow the excavation and installation process and to keep track of the developing non-linear behaviour and consequently the changing nature of the soil-structure interaction. However, to date, relatively little attention has been paid in the literature to the important issue of validation and reliability of these numerical models, and in particular the specific software that enables their implementation. The work by Schweiger (1991, 1997, 1998, 2000) forms one of the limited studies on the subject of model validation. There is now a strong need to define procedures and guidelines to arrive at reliable numerical methods and, more importantly, input parameters which represent accurately the strength and stiffness properties of the ground *in situ*.

Benchmarking is of great importance in geotechnical engineering, probably more so than in other engineering disciplines, such as structural engineering. This issue has been addressed recently in the literature (e.g., Carter *et al.*, 2000). Obviously, there is currently considerable scope for developers and users of numerical models to exercise their personal preferences when tackling geotechnical problems. From a practical point of view, it is therefore very difficult to prove the validity of many calculated results because of the numerous modelling assumptions required. So far, no clear guidelines exist, and thus results for a

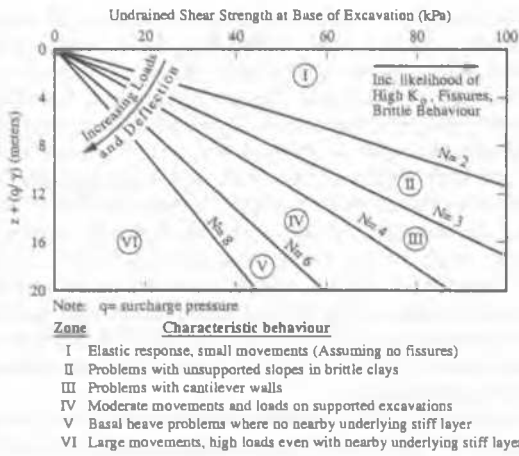


Figure 7.2. Classification of behaviour of excavations in clay (after Peck, 1969).

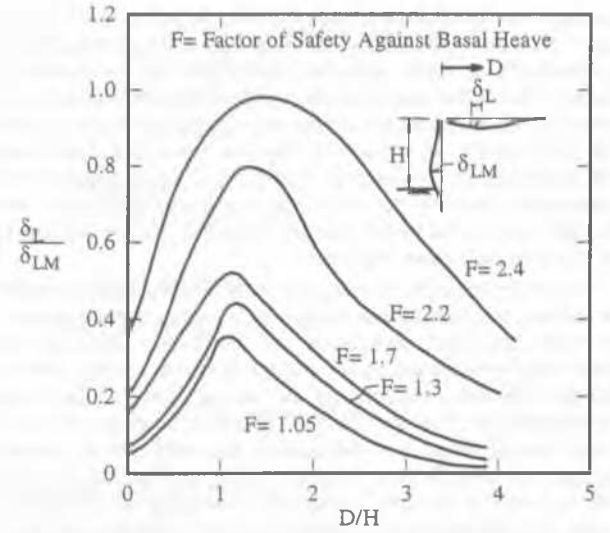


Figure 7.5. Lateral surface movement profiles behind retaining walls in clay (after Clough et al., 1989).

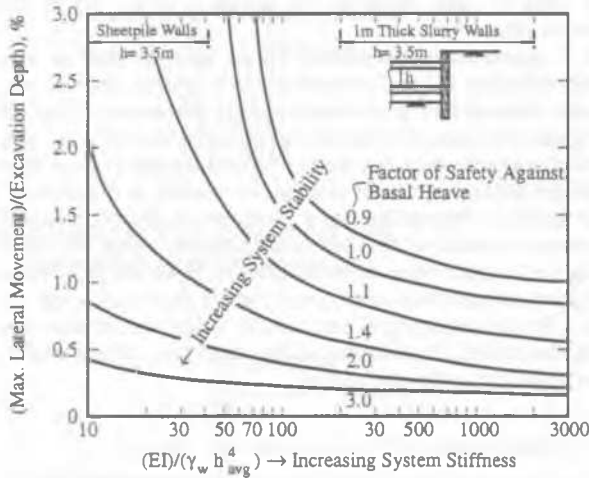


Figure 7.3. Design chart for estimating maximum lateral wall movements (after Clough et al., 1989).

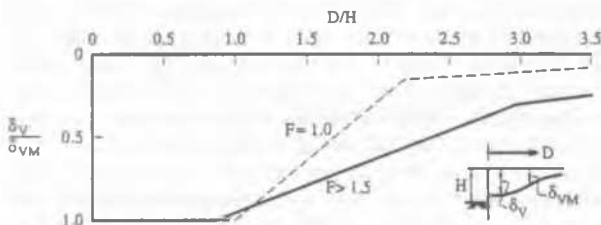


Figure 7.4. Settlement envelope behind retaining walls in clay (after Mana and Clough, 1981).

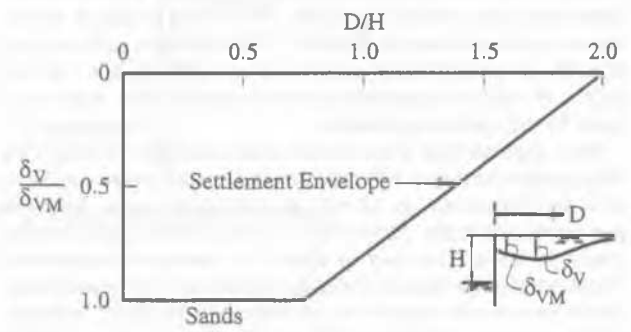


Figure 7.6. Settlement envelopes behind retaining walls in sand (after Goldberg, et al., 1976).

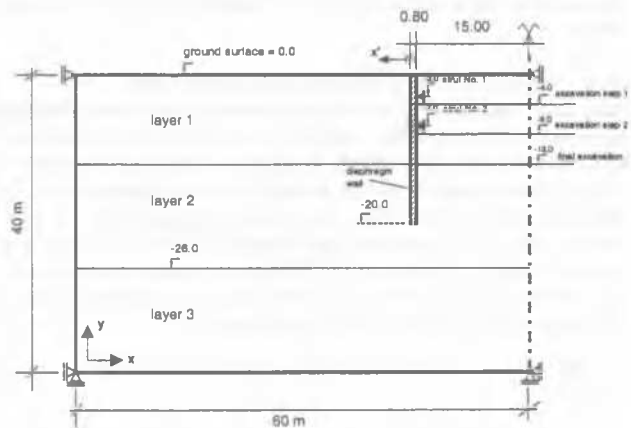


Figure 7.7. Geometry of the deep excavation example (after Schweiger, 1997, 1998).

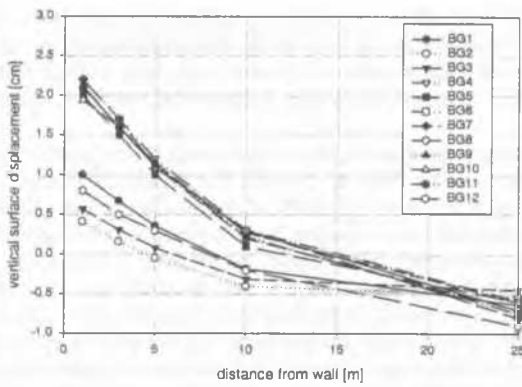


Figure 7.8. Vertical displacement of surface behind wall: construction stage 1 (after Schweiger, 1997, 1998).

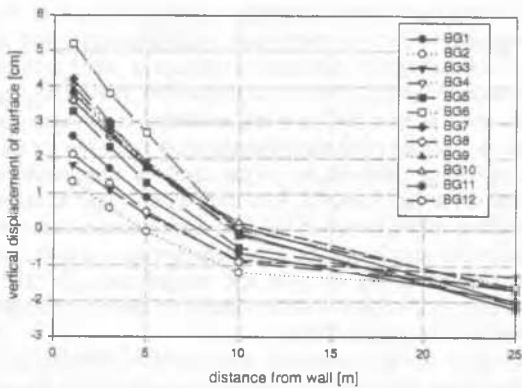


Figure 7.9. Vertical displacement of surface behind wall: final construction stage (after Schweiger, 1997, 1998).

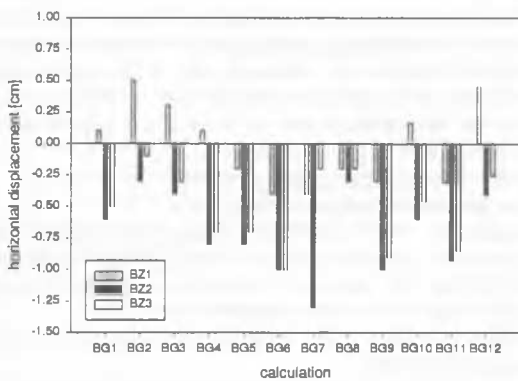


Figure 7.10. Horizontal displacement of head of wall (after Schweiger, 1997, 1998).

particular problem may vary significantly if analysed by different users, even for reasonably well-defined working load conditions.

Difficult issues such as these have been addressed by various groups, including recently Technical Committee 12 of ISSMGE and also a working group of the German Society for Geotechnics. It is the aim of both groups eventually to provide recom-

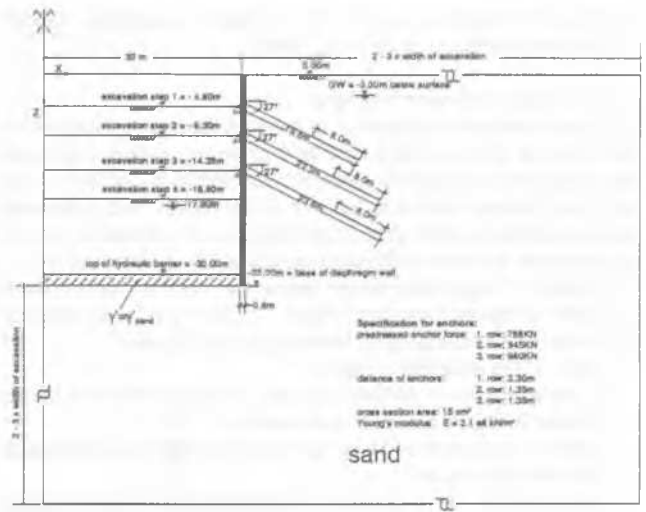


Figure 7.11. Geometry and excavation stages for the ties back excavation (after Schweiger, 2000).

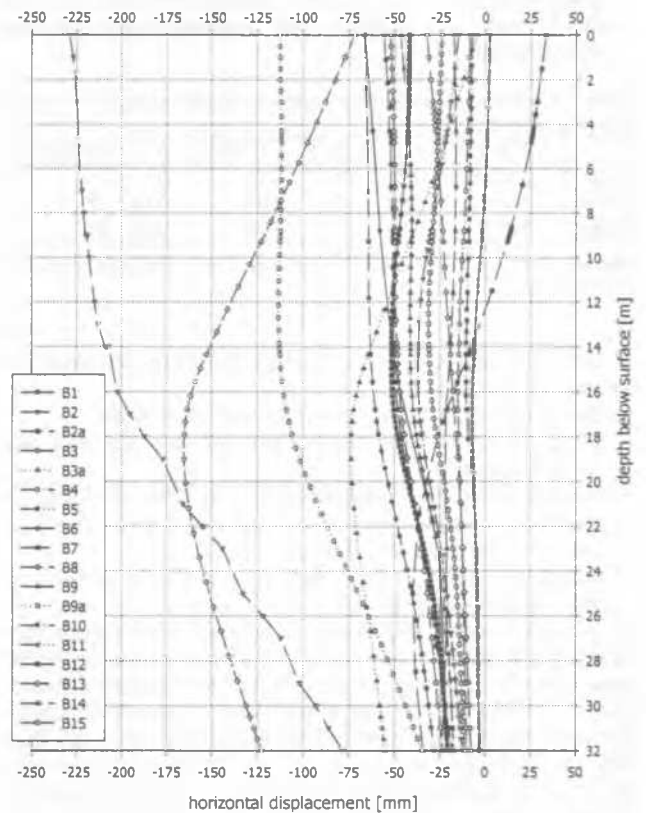


Figure 7.12. Wall deflection all solutions submitted: tied back excavation (after Schweiger, 2000).

mendations for numerical analyses in geotechnical engineering. So far the German group has published general recommendations (Meissner, 1991), recommendations for numerical simulations in tunnelling (Meissner, 1996) and it is expected that recommendations for deep excavations will also be published shortly.

In addition, benchmark examples have been specified by the German group and the results obtained by various users employing different software have been compared. Some of this work on retaining structures is summarised here, and greater de-

tail may be found in a recent review paper on computer modelling in geotechnics (Carter *et al.*, 2000).

#### 7.4.1 Deep excavation example

The first example considered involves a deep open excavation problem. It was a highly idealised problem, with a very tight specification so that little room for interpretation was left to the analysts. Despite the simplicity and the rather strict specifications, significant differences in the results were obtained, even in cases where the same software was utilised by different users.

Figure 7.7 illustrates the geometry and the excavation stages analysed in this problem, and Table 7.3 lists the relevant material parameters. Additional specifications are as follows.

- plane strain conditions apply,
- a linear elastic - perfectly plastic analysis with the Mohr-Coulomb failure criterion was required,
- perfect bonding was to be assumed between the diaphragm wall and the ground,
- struts used in the excavation were modelled as rigid members (i.e., the horizontal degree of freedom was fixed),
- any influence of the diaphragm wall construction could be neglected, i.e., the initial stresses were established without the wall, and then the wall was “wished-in-place”, and
- the diaphragm wall was modelled using either beam or continuum elements, with 2 rows of elements over the cross section if continuum elements with quadratic shape functions were adopted.

Table 7.3. Material parameters for “deep excavation” example (data from Schweiger, 2000).

	$E$ (kN/m <sup>2</sup> )	$\nu$	$\phi$ (°)	$c$ (kN/m <sup>2</sup> )	$K_o$	$\gamma$ (kN/m <sup>3</sup> )
Layer 1	20000	0.3	35	2.0	0.5	21
Layer 2	12000	0.4	26	10.0	0.65	19
Layer 3	80000	0.4	26	10.0	0.65	19

Diaphragm wall ( $d = 800$  mm): linear elastic  $E = 21\,000$  MPa,  $\nu = 0.15$ ,  $\gamma = 22$  kN/m<sup>3</sup>

The following computational steps had to be performed by the various analysts:

- the initial stress state was set to  $\sigma_v = \gamma H$ ,  $\sigma_h = K_o \gamma H$ ,
- all deformations were set to zero and then the wall was “wished-in-place”,
- construction stage 1: excavation step 1 to a level of -4.0 m,
- construction stage 2: excavation step 2 to a level of -8.0 m, and strut 1 installed at -3.0 m, and
- construction stage 3: final excavation to a level of -12.0 m, and strut 2 installed at -7.0 m.

It is worth mentioning that 5 out of the 12 calculations submitted for comparison were made by different analysts using the same computer program. Figure 7.8 compares surface displacements for construction stage 1 and shows 2 groups of results. The lower values for the heave from calculations BG1 and BG2 may be explained because of the use of interface elements, which were employed in these two analyses despite the fact that the specification did not require them. The results of BG3 and BG12 could not be explained in any detail. There were indications though that for the particular program used a significant difference in vertical displacements was observed depending whether beam or continuum elements were used for modelling the diaphragm wall. This emphasises the significant influence of different modelling assumptions and the need for evaluating the validity of these models under defined conditions. It may be worth mentioning that this effect was not observed to the same extent in the other programs used. Figure 7.9 shows the same displacements for the final excavation stage, and the results are now almost evenly distributed between the limiting values.

It is apparent from Figures 7.8 and 7.9 that simple linear elastic-perfectly plastic constitutive models are not well suited for analysing the displacement pattern around deep excavations, especially for the surface behind the wall because the predicted

heave is not realistic. However, it was not the aim of this exercise to compare results with actual field observation, but merely to see what differences are obtained when using slightly different modelling assumptions within a rather tight problem specification.

It is interesting to compare predictions of the horizontal displacement of the head of the wall for excavation step 1 (Case BZ1 in Figure 7.10). Only 50% of the analyses predict displacements towards the excavation (+ve displacement in Figure 7.10) whereas the other 50% predict movements towards the soil, which would appear to be not very realistic for a cantilever situation. Significant differences were not found in the predictions for the horizontal displacements of the bottom of the wall, the heave inside the excavation and the earth pressure distributions. Calculated bending moments varied within 30% and strut forces for excavation step 2 varied from 155 to 232 kN/m. A more detailed examination of this example can be found in Schweiger (1997, 1998).

#### 7.4.2 Tied-back deep excavation example

The second example represents a real application (a tied back diaphragm wall in Berlin sand – see Figure 7.11), for which the model specification was modified slightly in order to reduce computational effort. In particular, modifications were introduced in modelling the construction sequence, most notably the groundwater lowering, which was performed in various steps in the field, but was specified as being modelled in one step prior to excavation. Limited field measurements are available for this example, providing information on the order of magnitude of the deformations to be expected. It is important to realise however, that a perfect match between the field measurements and any of the predictions should not be expected, because of the simplifications adopted in the analysis and imperfections in the field measurement procedures. Further details of these limitations are described by Schweiger (2000).

Whereas in the first example, the constitutive model and the parameters were pre-specified, in this second example the choice of constitutive model was left to the user and the parameter values had to be selected either from the literature, on the basis of personal experience, or determined from laboratory tests which were made available to the analysts. Some basic material parameters were available from the literature and additional results from one-dimensional compression tests on loose and dense samples were given to the participants, together with the results of triaxial tests on dense samples. Thus the exercise represents closely the situation that is often faced in practice. Inclimometer measurements made during construction provided information of the actual behaviour *in situ*, although due to the simplifications mentioned above a one-to-one comparison is not possible. Of course, the measurements were not disclosed to the participants prior to them submitting their predictions.

Additional specifications for this example are as follows:

- plane strain conditions could be assumed,
- any influence of the diaphragm wall construction could be neglected, i.e., the initial stresses were established without the wall, and then the wall was “wished-in-place” and its different unit weight incorporated appropriately,
- the diaphragm wall could be modelled using either beam or continuum elements,
- interface elements existed between the wall and the soil, the domain to be analysed was as suggested in Figure 7.11, the horizontal hydraulic cut-off that existed at a depth of -30.00 m was not to be considered as structural support, and
- the pre-stressing anchor forces were given as design loads.

The following computational steps had to be performed by the various analysts:

- the initial stress state was given by  $\sigma_v = \gamma H$ ,  $\sigma_h = K_o \gamma H$ ,
- the wall was “wished-in-place” and the deformations reset to zero,
- construction stage 1: groundwater-lowering to -17.90 m,

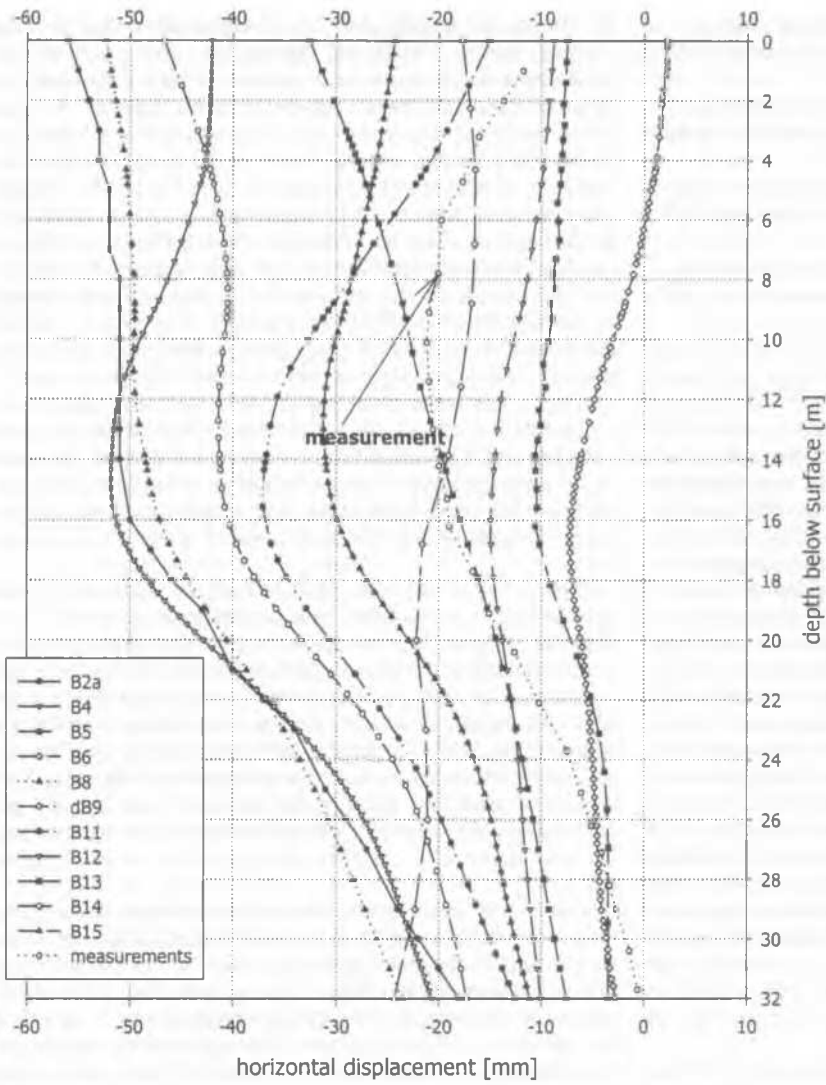


Figure 7.13. Wall deflection for selected solutions and inclinometer measurements: tied back excavation (after Schweiger, 2000).

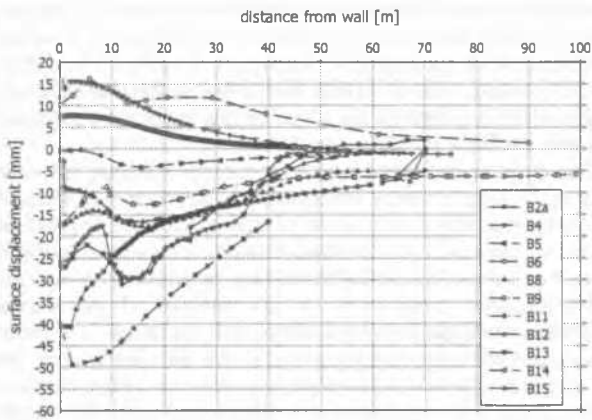


Figure 7.14. Predictions of surface settlement (after Schweiger, 2000).

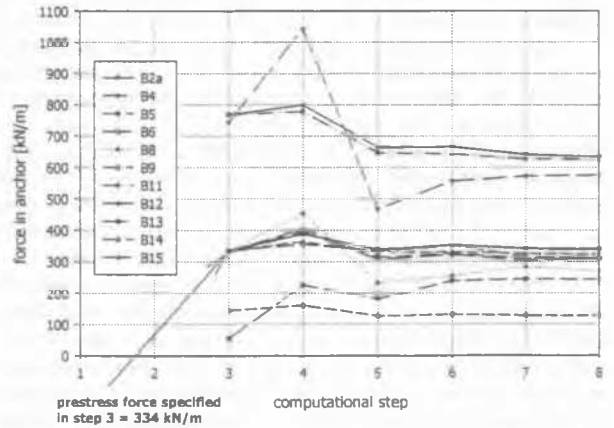


Figure 7.15. Forces in first layer of anchors for selected solutions: tied back excavation (after Schweiger, 2000).



- construction stage 2: excavation step 1 (to level -4.80 m),
- construction stage 3: activation of anchor 1 at level -4.30 m and prestressing,
- construction stage 4: excavation step 2 (to level -9.30 m),
- construction stage 5: activation of anchor 2 at level -8.80 m and prestressing,
- construction stage 6: excavation step 3 (to level -14.35 m),
- construction stage 7: activation of anchor 3 at level -13.85 m and prestressing, and
- construction stage 8: excavation step 4 (to level -16.80 m).

The length of the anchors and their prestressing loads are indicated in Figure 7.10.

A wide variety of computer programs and constitutive models was employed to solve this problem. Details may be found in Schweiger (2000) and Carter *et al.* (2000). Only a limited number of analysts utilised the laboratory test results provided in the specification to calibrate their models. Most of the analysts used data from the literature for Berlin sand or their own experience to arrive at input parameters for their analysis. Only marginal differences exist in the assumptions made about the strength parameters for the sand (everybody believed the laboratory experiments in this respect), and the angle of internal friction  $\phi'$  was taken as  $36^\circ$  or  $37^\circ$  and a small cohesion was assumed by many authors to increase numerical stability. A significant variation was observed however in the assumption of the dilatancy angle  $\psi$ , with values ranging from  $0^\circ$  to  $15^\circ$ . An even more significant scatter was observed in the assumption of the soil stiffness parameters. Although most analysts assumed an increase with depth, either by introducing some sort of power law, similar to the formulation presented by Ohde (1951), which in turn corresponds to the formulation by Janbu (1963), or by defining different layers with different Young's moduli. Additional variation was introduced by different formulations for the interface elements, element types, domains analysed and modelling of the prestressed anchors. Some computer codes and possibly some analysts may have had problems in modelling the prestressing of the ground anchors, and actually part of the force developed due to deformations occurring in the ground appears lost.

A total of 15 organisations (comprising University Institutes and Consulting Companies from Germany, Austria, Switzerland and Italy), referred to as B1 to B15 in the following, submitted predictions. Figure 7.12 shows the deflection curves of the diaphragm wall for all entries. It is obvious from the figure that the results scatter over a very wide range, which is unsatisfactory and probably unacceptable to most critical observers of this important validation exercise. For example, the predicted horizontal displacement of the top of the wall varied between  $-229$  mm and  $+33$  mm (-ve means displacement towards the excavation). Looking into more detail in Figure 7.12, it can be observed that entries B2, B3, B9a and B7 are well out of the "mainstream" of results. These are the ones that derived their input parameters mainly from the oedometer tests provided to all analysts, but it should be remembered that these tests showed very low stiffnesses as compared to values given in the literature. Some others had small errors in the specific weight, but these discrepancies alone cannot account for the large differences in predictions.

As mentioned previously, field measurements are available for this project and although the example here has been slightly modified in order to facilitate the calculations, the order of magnitude of displacements is known. Figure 7.13 shows the measured wall deflections for the final construction stage together with the calculated results. Only those calculations that are considered to be "near" the measured values are included. The scatter is still significant. It should be mentioned that measurements have been taken by inclinometer, but unfortunately no geodetic survey of the wall head is available. It is very likely that the base of the wall did not remain fixed, as was assumed in the interpretation of the inclinometer measurements, and that a parallel shift of the measurement of about 5 to 10 mm would probably reflect the *in situ* behaviour more accurately. This has been confirmed

by other measurements under similar conditions in Berlin. If this is true a maximum horizontal displacement of about 30 mm can be assumed and all entries that are within 100% difference (i.e., up to 60 mm) have been considered in the diagram. The predicted maximum horizontal wall displacements still varied between 7 and 57 mm, and the shapes of the predicted curves are also quite different from the measured shape. Some of the differences between prediction and measurements can be attributed to the fact that the lowering of the groundwater table inside the excavation has been modelled in one step whereas in reality a stepwise drawdown was performed (the same has been assumed by calculation B15). Thus the analyses overpredict horizontal displacements, the amount being strongly dependent on the constitutive model employed, as was revealed in further studies. In addition, it can be assumed that the details of the formulation of the interface element have a significant influence on the lateral deflections of the wall, and arguments similar to those discussed in the previous section for implementing constitutive laws also hold, i.e., no general guidelines and recommendations are currently available. A need for them is clearly evident from this exercise.

Figure 7.14 depicts the calculated surface settlements, again only for the same solutions that are presented in Figure 7.13. These key displacement predictions vary from settlements of up to approximately 50 mm to surface heaves of about 15 mm. Considering the fact that calculation of surface settlements is one of the main goals of such an analysis, this lack of agreement is disappointing. It also highlights again the pressing need for recommendations and guidelines that are capable of minimising the unrealistic modelling assumptions that have been adopted and consequently the unrealistic predictions that have been obtained. The importance of developing such guidelines should be obvious.

Figure 7.15 shows predictions of the development of anchor forces for the upper layer of anchors. Maximum anchor forces for the final excavation stage range from 106 to 634 kN/m. As mentioned previously, some of the analyses did not correctly model the prestressing of the anchors because they do not show the specified prestressing force in the appropriate construction step. Predicted bending moments, important from a design perspective, also differ significantly from 500 to 1350 kNm/m.

Taking into account the information presented in Figures 7.12 to 7.15, it is interesting to note that no definitive conclusions are possible with respect to the constitutive model or assumptions concerning element types and so on. It is worth mentioning that even with the same finite element code and the same constitutive model significant differences in the predicted results are observed. Clearly these differences depend entirely on the personal interpretation of the stiffness parameters from the information available. Again, it is noted that a more comprehensive coverage of this exercise is beyond the scope of this paper but further details may be found in Schweiger (2000).

The exercise presented here very clearly indicates the need for guidelines and training for numerical analysis in geotechnical engineering in order to achieve reliable solutions for practical problems. However, at the same time these examples demonstrate the power of numerical modelling techniques provided experienced users apply them. A full analysis of the second benchmark problem discussed above will be given in a forthcoming report of the working group of the German Society, and the problem will be further dealt with also by Technical Committee 12 (TC 12 – Validation of Computer Simulations) of the International Society for Soil Mechanics and Geotechnical Engineering (ISSMGE).

## 7.5 Summary

This limited review of retaining structures has identified a number of issues of major significance to geotechnical practitioners, and some areas where our knowledge and design methods are incomplete or imperfect. These are identified as follows.

1. For rigid retaining structures, the classical solution for active earth pressure suggested by Coulomb, based on a simple wedge failure mechanism, provides reasonable predictions of wall loads, and its continued use is therefore recommended.
2. Solutions proposed by Lee and Herrington (1972a, 1972b) for the passive thrusts acting on rigid retaining structures appear to be the most rigorous and complete solutions to date. Their use in practice is therefore recommended, and in particular the use of the Coulomb solution for this form of loading should be abandoned.
3. Progressive failure in soils can reduce the maximum passive thrusts acting on rigid walls below the value that would be calculated if the peak friction angle is assumed. This will be important for cases where passive resistance is required for wall stability, and should be allowed for in design.
4. Recent studies of relatively flexible retaining structures have indicated the importance of construction details and sequence, and the structural interaction between the retained soil and the retaining system, on the loads acting on the retaining system and its movements.
5. Increasingly, computer-based methods are being adopted for the analysis and design of flexible retaining structures. They can be broadly classified into those that assume a Winkler-type soil model, and those that represent the soil as a continuum.
6. Computer methods that adopt the Winkler-type soil model should be used with great caution, as it has been demonstrated that lower stiffnesses must be adopted for the Winkler soil springs to achieve wall displacements comparable with those predicted by the more rigorous continuum models.
7. The more rigorous and complex continuum models are normally used for particular case studies, and it has not been common for them to be used to generate general design charts. Exceptions include the work of Clough and co-workers, who have provided useful chart solutions for the preliminary design of retaining systems, based on the philosophy of restricting wall movements.
8. Recent research has also indicated the need for caution in the use of the more complex continuum models, and has highlighted the pressing need for reliable procedures to validate these types of models. Work in this area is currently in only its early stages of development.

## 8 ASSESSMENT OF GEOTECHNICAL PARAMETERS

### 8.1 Introduction

The assessment of geotechnical parameters is a vital component of geotechnical design, and almost invariably involves some form of soil testing. Atkinson and Salfors (1991) define five purposes for soil tests:

1. Tests to evaluate soil parameters
2. Profiling (in-situ testing)
3. Tests to determine basic soil behaviour
4. Tests to discover unusual behaviour
5. Validation of analyses.

From a practical viewpoint, the first two applications are of key importance. The tests to evaluate soil parameters may seek to obtain purely empirical parameters (for example, for Category 1 analyses), relatively simple properties (for Category 2 analyses) or tests for parameters which depend on the state, the stress history and the stress path (Category 3 analyses). Profiling tests usually rely on some form of penetration test which does not specifically measure soil properties, but which may be used with empirical correlations to assess required strength and deformation parameters.

The assessment of geotechnical parameters cannot be considered in isolation from the method of analysis employed. The two are tied together intimately, and it is both dangerous and inap-

propriate to attempt to report simplified parameters for a soil profile without clearly stating the intended application and associated method of analysis. For example, when a value of Young's modulus of a soil layer is quoted, it must be made clear whether it is a tangent or secant value, whether it is to be used with linear or nonlinear theory, and whether it is intended to be applied to a shallow foundation or to a deep foundation.

Attention will be focussed below on the practical assessment of parameters for the estimation of the deformation of foundations and retaining structures. The parameters which will be considered will be appropriate to the use of elasticity theory, linear or non-linear, and for both undrained and drained conditions.

### 8.2 Deformation parameters – shear modulus

Research into the strain-dependency of soil strains has elucidated some of the earlier confusion which prevailed in relation to the stiffness of soils. Key findings of this research are as follows:

1. The stiffness at very small strains (characterized by the small-strain shear modulus  $G_{max}$ ) is the same for static and dynamic loading conditions (Jamiolkowski *et al.*, 1994).
2.  $G_{max}$  is independent of drainage, and therefore applies to deformations under both undrained and drained conditions.
3.  $G_{max}$  is relatively insensitive to the overconsolidation ratio of both sands and natural clays.

Thus, as pointed out by Mayne (1995),  $G_{max}$  provides a universal reference or benchmark value of stiffness for deformation problems, which can be applied to foundation systems, retaining structures, tunnels and pavement subgrades. Methods of measuring  $G_{max}$  include careful laboratory triaxial testing with localized strain measurement, dynamic laboratory testing (for example, using the resonant column device) and field testing using shear wave velocity measurements. A discussion of these methods is given by Atkinson and Salfors (1991).  $G_{max}$  has also been correlated with the results of SPT and CPT tests, and a typical correlation for sands between  $G_{max}/q_{cl}$  and  $q_{cl}$  is shown in Figure 8.1 (Fahey, 1999).  $q_{cl}$  is a normalized cone resistance, defined as:

$$q_{cl} = (q_c / p_a)(p_a / \sigma'_v)^{0.5} \quad (8.1)$$

where  $q_c$  = measured cone resistance;  $\sigma'_v$  = vertical effective stress;  $p_a$  = atmospheric pressure.

Larsson and Mulabdic (1991) suggest the following relationship between  $G_{max}$  and undrained shear strength  $s_u$  for clays of medium to high values of plasticity index  $I_p$ :

$$G_{max} / s_u \approx 20000 / I_p + 250 \quad (8.2)$$

Atkinson (2000) has expressed  $G_{max}$  in the following manner:

$$G_{max} / p_a = A(p' / p_a)^n R_o^m \quad (8.3)$$

where  $p_a$  = reference pressure, taken here as 1 kPa;  $p'$  = current vertical effective stress;  $R_o$  = overconsolidation ratio;  $A$ ,  $m$ ,  $n$  = material parameters dependent on plasticity index.

Values of  $A$ ,  $m$  and  $n$  are plotted in Figure 8.2.

Because the stress-strain-strength behaviour of soils is highly nonlinear, true elastic behaviour is observed only at very small strain levels (typically  $10^{-3}$  % or less). The nonlinear shear stiffness of soils is usually described via the concept of modulus degradation. This describes the variation of normalized secant shear modulus ( $G/G_{max}$ ) with either shear strain or shear stress level, and this relationship can be measured via careful laboratory testing or via in-situ testing. For example, Fahey (1999) has also shown how the modulus degradation characteristics can be estimated from in-situ pressuremeter tests.

While shear strain may be the more fundamental parameter, from a practical viewpoint, it is often more convenient to use the shear stress level as the controlling parameter. Fahey and Carter (1993) have adopted the modified hyperbolic relationship:

$$G/G_{max} = 1 - f(\tau/\tau_{max})^g \quad (8.4)$$

where  $\tau$  = shear stress;  $\tau_{max}$  = limiting shear stress, and  $f$  and  $g$  are fitting parameters. For sands, Mayne (1995) suggests typical values of  $f = 1$  and  $g = 0.3$ .

Lee and Salgado (1999) have generalized Equation (8.4) for three dimensional stress states and have assumed that the shear modulus depends on the mean principal stress. They give the following expression:

$$G/G_{max} = 1 - f[(q - q_i)/(q_{max} - q_i)]^g (p'/p'_o)^{n_g} \quad (8.5)$$

where  $q_i$  = initial deviator stress;  $q$  = deviator stress;  $q_{max}$  = maximum deviator stress at failure;  $n_g$  is a constant with a typical value of 0.5.

The tangent shear modulus  $G_t$  may be derived from the above equation by differentiation, to give:

$$G_t/G_{max} = (G/G_{max})2(p'/p'_o)^{n_g} / [1 - f(1 - g)(q - q_i)/(q_{max} - q_i)]^g \quad (8.6)$$

Mayne (1995) demonstrates how the simple nonlinear relationship shown in Equation (8.4) can be used with simple elastic solutions to predict the load-settlement behaviour of shallow footings on sand and pile foundations a residual sandy soil. Despite the apparent success achieved by Mayne, there is still some potential difficulty in expressing the secant shear modulus in terms of stress level, in that the strain level for different foundation types may be different, despite the fact that the stress level may be similar. For this reason, it may be preferable to consider the degradation relationship for shear modulus in terms of strain level, rather than stress level.

It is possible to express the non-linearity of soil stiffness in terms of strain, rather than stress level (for example, Tatsuoka and Shibuya (1991); Michaelidis *et al.*, 1997; Atkinson, 2000). Lehane and Fahey (2000) suggest the following relationship for the secant Young's modulus  $E$  (and also shear modulus  $G$ ) of a soil in terms of strain:

$$E/E_{max} = 1/[1 + \{(\epsilon - \epsilon_{el})/(\epsilon_r - \epsilon_{el})\}^n] \quad (\text{for } \epsilon \geq \epsilon_{el}) \quad (8.7)$$

where  $E_{max}$  = very small strain value of Young's modulus;  $\epsilon_{el}$  = elastic limit strain (typically  $10^{-5}$ );  $\epsilon_r$  and  $n$  are empirical parameters used to alter the shape of the stiffness - strain relationship.

The relationship for tangent modulus may also be derived by differentiation of the above expressions. Equation (8.6) will be used subsequently in Section 3.4 to derive typical values of secant shear modulus for various types of foundation on clay.

### 8.3 Deformation parameters - undrained and drained Young's modulus

While the shear modulus is relevant to both undrained and drained conditions, for drained conditions, consideration must also be given to strains arising from volume changes. These are usually described via a bulk modulus, which relates volumetric stress and volumetric strain, or via a constrained modulus, which describes the relationship between vertical stress and vertical strain in a one-dimensional test. The theory of elasticity provides the following relationships between the various parameters, for an isotropic material:

$$E = 9G/(3 + G/K) \quad (8.8)$$

$$E = 9G/[3 + G(1 + \nu)/3D(1 - 2\nu)] \quad (8.9)$$

where  $G$  = shear modulus;  $E$  = Young's modulus;  $K$  = bulk modulus;  $D$  = constrained modulus;  $\nu$  = Poisson's ratio.

For the case of undrained loading of a saturated clay, the above equations give the following familiar result for the undrained Young's modulus  $E_u$ :

$$E_u = 3G \quad (8.10)$$

The non-linearity of  $E_u$  is reflected directly by the non-linearity of the shear modulus  $G$  (Equation (8.4)).

For drained conditions, the drained Young's modulus is given by Equation (8.9), with  $\nu = \nu'$ , the drained Poisson's ratio of the soil. Typical values of  $\nu'$  range between 0.25 and 0.4. Also, the constrained modulus  $D$  may be related to the compression ratio  $CR (= C_c / (1 + e_0))$  of a soil as follows (for relatively small stress increments):

$$D = 2.3\sigma'_{vo} / CR \quad (8.11)$$

where  $e_0$  = initial void ratio;  $\sigma'_{vo}$  = initial vertical stress on soil.

Substitution of the above values into Equation (8.8) gives the following result:

$$E' = 9G/[3 + b(G/\sigma'_{vo})CR/2.3] \quad (8.12)$$

where the factor  $b$  ranges between about 0.55 and 0.78.

The non-linearity of the shear modulus  $G$  may be taken into account via Equation (8.3), so that the drained modulus can be expressed as:

$$E' = \frac{9G_{max}(1 - f(\tau/\tau_{max})^g)}{3 + b(G_{max}/\sigma'_{vo}(1 - f(\tau/\tau_{max})^g)CR/2.3)} \quad (8.13)$$

Figure 8.3 plots the variation of normalized drained modulus,  $E'/G_{max}$ , versus stress level for a typical case in which  $b = 0.62$  (representing  $\nu' = 0.3$ ),  $f = 1.0$ ,  $g = 0.3$  and  $G_{max}/\sigma'_{vo} = 500$ , and various values of the compression ratio  $CR$ . Also shown in this figure is the relationship for an ideal two-phase elastic soil, in which the relationship between  $E'$  and  $E_u$  is given by equation  $E' = 1.5E_u/(1 + \nu')$ .

The following useful conclusions can be drawn from this figure:

1. The normalized undrained modulus is more sensitive to stress level than the drained modulus.
2. The more compressible the soil, i.e., the larger the value of  $CR$ , the smaller is the drained modulus ratio. For very compressible soils, the drained modulus may be only 10% or less of the undrained value, at the corresponding stress level.
3. As the compressibility decreases ( $CR$  decreases) the normalized drained modulus becomes larger, but more sensitive to the shear stress level.

Figure 8.3 demonstrates behaviour that is consistent with experience. For soft compressible clays, the ratio of the drained to the undrained modulus is small, while for stiffer overconsolidated clays, the ratio of the drained and undrained modulus is more consistent with that derived from elasticity theory.

Many of the commonly used solutions for foundation deformations are derived from elasticity theory and are expressed in terms of the Young's modulus of the soil. Equation (8.13) therefore provides a relatively simple means of estimating the drained Young's modulus of a soil to use in such solutions, and its variation with shear stress level, once the values of small strain shear modulus  $G_{max}$  and compression ratio  $CR$  are known. Since a number of correlations exist for both  $G_{max}$  and  $CR$  with other more easily measurable soil characteristics, the opportunity also exists to develop corresponding correlations for the drained and undrained values of Young's modulus.

### 8.4 Typical values of secant modulus for undrained loading of foundations on clay

In the application of elasticity theory to a non-linear material such as soil, a critical factor is the selection of an appropriate modulus to represent the soil deformation behaviour over a range of stress appropriate to the problem in hand. One of the difficulties in expressing the secant shear modulus in terms of stress level is that the strain level for different foundation types may be

different, despite the fact that the stress level may be similar. For this reason, it may be preferable to consider the degradation relationship for shear modulus in terms of strain level, rather than stress level.

It is possible to develop a more rational approach than the empirical approaches now usually adopted, by making use of the recent research on strain-dependency of modulus. By estimating typical values of strain within the soil due to various types of foundations loadings, assessments can be made of the relevant secant modulus of the soil, as a function of the maximum modulus for very small strains. The following paragraphs develop such assessments for three foundation loadings:

- Shallow footings subjected to vertical loading
- Piles subjected to axial loading
- Piles subjected to lateral loading.

#### 8.4.1 Shallow footings subjected to vertical loading

The simple case considered here is that of a rigid circular footing on a homogeneous saturated clay layer. From the theory of elasticity, the immediate (undrained) settlement is given by:

$$S = qBI / E_u \quad (8.14)$$

where  $q$  = average applied pressure;  $B$  = footing width;  $I$  = displacement influence factor;  $E_u$  = undrained secant modulus of soil.

The above expression can be re-stated as follows:

$$S / B = (q / q_u) N_c I . 1 / (G_{max} / s_u) . 1 / (G / G_{max}) . 1 / 2(1 + \nu_u) \quad (8.15)$$

where  $q_u$  = ultimate bearing capacity =  $N_c s_u$ ;  $N_c$  = bearing capacity factor  $\approx 6$  for a circular footing;  $s_u$  = undrained shear strength;  $G$  = secant shear modulus;  $G_{max}$  = maximum shear modulus value (for small strain);  $\nu_u$  = undrained Poisson's ratio = 0.5 for saturated soil.

For a typical case in which the soil layer is  $2B$  deep, the influence factor  $I \approx 1$ , and if the average axial strain is taken as  $S/2B$ , and  $G_{max}/s_u$  is taken as 1000, the average axial strain below the footing can be approximated as follows:

$$\epsilon_1 = (q / q_u) / [1500(G / G_{max})] \quad (8.16)$$

Use may now be made of the degradation function ( $G/G_{max}$  versus  $\epsilon_1$ ) in Equation (8.7), and this may be solved in conjunction with Equation (8.16) to obtain the average strain level and the corresponding value of  $G/G_{max}$  for the specified value of  $q/q_u$ , which is of course the inverse of the factor of safety against undrained failure.

Atkinson (2000) derives an alternative expression for the secant modulus for a shallow footing, using the observation that the settlement divided by the footing width is about 2 to 3 times the axial strain in a triaxial sample at the same average stiffness.

#### 8.4.2 Axially loaded pile

In this case, it will be assumed, for simplicity, that the pile shaft takes all the applied load. In this case, following the simple approach developed by Randolph and Wroth (1978), the shear strain  $\gamma$  along the shaft can be expressed as:

$$\gamma = \tau / G \quad (8.17)$$

where  $\tau$  = shaft shear stress;  $G$  = secant shear modulus.

By following a similar approach to that adopted for a surface footing, the above equation can be re-cast in the following form:

$$\gamma = \tau_f / [F . G_{max} (G / G_{max})] \quad (8.18)$$

where  $\tau_f$  = maximum shaft friction value (ultimate skin friction);  $F$  = factor of safety against failure.

Again, the degradation function in Equation (8.7) can be used to express ( $G/G_{max}$ ) as a function of  $\gamma$ , and the equation solved with (8.18) for  $\gamma$  and  $G/G_{max}$  for a specified value of  $F$ .

#### 8.4.3 Laterally loaded pile

The simple case of a relatively rigid pile subjected only to horizontal loading will be considered here. The lateral displacement of the pile head is given by (Poulos and Davis, 1980):

$$\rho_h = H . I_{\rho H} / E_s . L \quad (8.19)$$

where  $H$  = applied load;  $I_{\rho H}$  = displacement influence factor;  $E_s$  = secant Young's modulus;  $L$  = embedded pile length.

The applied load  $H$  can be expressed as a fraction of the ultimate load  $H_u$  for lateral soil failure, which for a relatively rigid pile in homogeneous clay, is  $0.414 s_u$ , where  $s_u$  = undrained shear strength. A typical value of  $I_{\rho H}$  is about 4. Also,  $E_s$  can be expressed in terms of the secant shear modulus  $G$ , which in turn can be related to the maximum shear modulus and the ratio ( $G/G_{max}$ ). Following the approximation presented by Prakash and Kumar (1996), the average shear strain  $\gamma$  around the laterally loaded pile is:

$$\gamma = (1 + \nu) \rho_h / 2.5d \quad (8.20)$$

where  $d$  = pile diameter or width;  $\nu$  = soil Poisson's ratio.

From Equations (8.19) and (8.20), the following expression may be derived for the average shear strain:

$$\gamma \approx 3.0[(H / H_u) . 1 / (G_{max} / s_u) . 1 / (G / G_{max})] \quad (8.21)$$

Once again using a modulus degradation function such as that given in Equation (8.7), solutions may be obtained for  $g$  and ( $G/G_{max}$ ) as a function of  $H/H_u$ , which is the inverse of the factor of safety against short-pile failure" (Broms, 1964 a).

#### 8.4.4 Secant modulus as a function of factor of safety

The relationships developed above for typical shear strain and shear modulus degradation factor have been solved via a MATHCAD worksheet. The shear modulus degradation is assumed to follow that of Lehane and Fahey (2000) in Equation (8.6), with  $\epsilon_r = 0.0008$  and  $n = 0.55$ . The relationships so derived are plotted in Figures 8.4a and 8.4b, for the three types of foundations, and for values of  $G_{max}/s_u$  of 1000 and 500 respectively. Also shown in these figures is the relationship in Equation (8.4) derived by Fahey and Carter (1993), assuming that the factor of safety is equal to  $\tau/\tau_{max}$ . The following observations can be made:

1. The secant shear modulus decreases with decreasing factor of safety, as expected.
2. For a given factor of safety, the secant shear modulus for the shallow footing is the lowest value, while that for the axially loaded pile is the highest. The difference in secant modulus values reflects the differences in induced strain in the soil by the different foundations.
3. For a typical safety factor of 3, and for  $G_{max}/s_u = 500$ , the secant modulus is about  $0.39 G_{max}$  for the axially loaded pile,  $0.25 G_{max}$  for the laterally loaded pile, and about  $0.18 G_{max}$  for the footing. These values imply a ratio of secant shear modulus to undrained shear strength of 195 for the axially loaded pile, 125 for the laterally loaded pile, and 90 for the footing.
4. The degradation relationship of Fahey and Carter (1993), which is dependent on stress level (factor of safety) and not on strain level, lies below the derived relationship for  $G_{max}/s_u = 1000$ , but well above it for  $G_{max}/s_u = 500$ . Also, it does not directly account for the differences in foundation performance because of the differences in strain level. The rate of reduction of secant modulus with decreasing factor of safety is generally consistent with those derived from the strain level assessments.

It must be emphasized that the curves in Figure 8.4 are for simple cases only, and involve several approximations in the derivation of the typical strain levels. The curves are meant to be for illustration and rough guidance only, and should not be treated as universal correlations. However, it can be mentioned

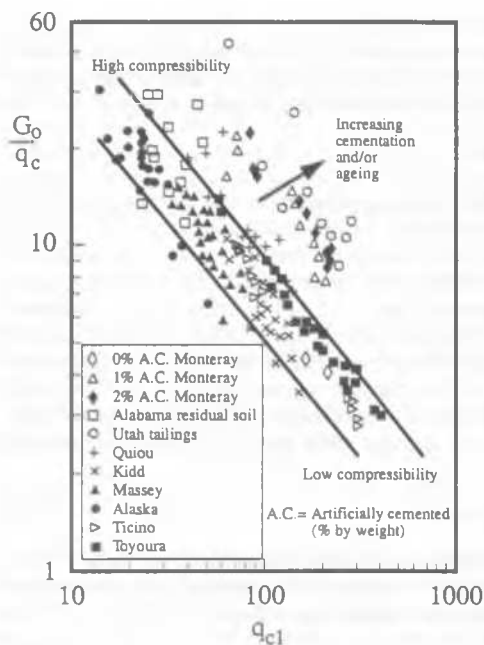


Figure 8.1. Plot of  $G/G_c$  versus  $q_{c1}$  for various sands (after Robertson, 1997 & Fahey, 1999).

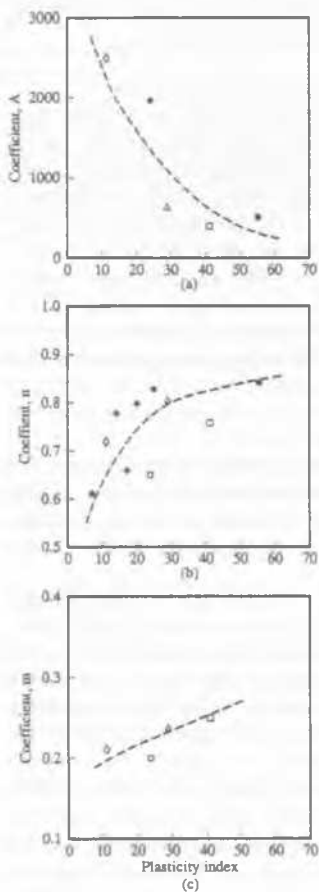


Figure 8.2. Material parameters for  $G_{max}$  (Atkinson, 2000).

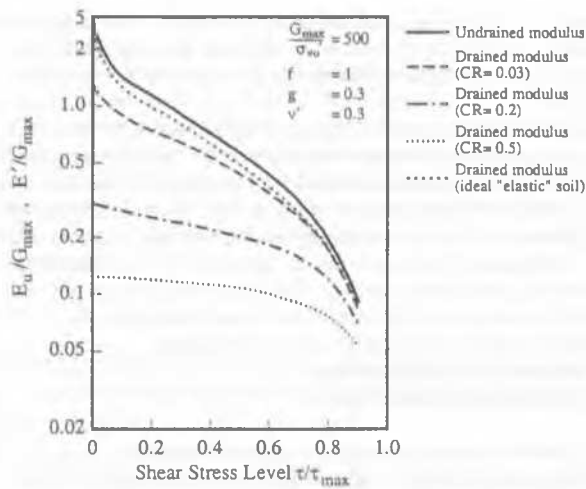


Figure 8.3. Computed relationships between normalized undrained and drained Young's modulus and shear stress level.

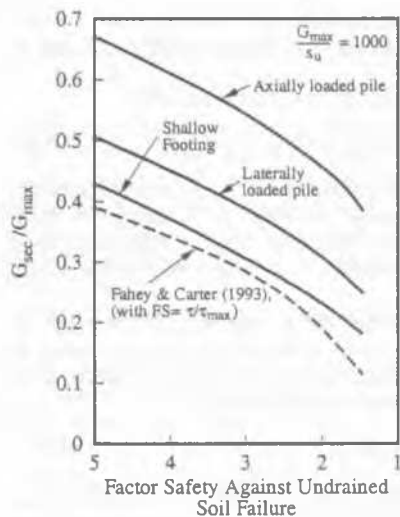


Figure 8.4(a). Secant modulus ratio for typical foundations on clay.  $G_{max}/s_u = 1000$ .

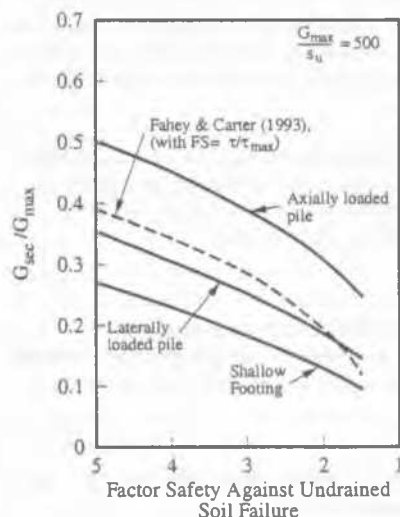


Figure 8.4(b). Secant modulus ratio for typical foundations on clay.  $G_{max}/s_u = 500$ .

that the results shown in this figure support, both qualitatively and quantitatively, prior experience, which has found that different values of secant modulus must be applied to different foundations on the same soil in order to match observed foundation movements. The typical values quoted in item (3) above are reasonably consistent with recommendations made in the literature. Figure 8.4 also emphasizes the importance of selecting the secant modulus for the appropriate applied load level.

## 9 FUTURE DIRECTIONS

Despite the fact that foundation engineering is a relatively mature aspect of geotechnical engineering, there still remain a considerable number of areas where uncertainty abounds. Among these areas are the following:

1. More appropriate characterisation of the ground conditions, both with respect to the geological aspects and the quantification of the relevant engineering properties. This remains an enduring challenge, not only in foundation engineering, but in all aspects of geotechnics. The aspects which continue to demand attention include:
  - The delineation of the ground conditions below the site in question, based on a limited number and extent of boreholes. The continuing development of geophysical techniques deserves encouragement;
  - The development of improved methods of in-situ assessment of geotechnical parameters of the ground;
  - The development of methods of laboratory testing, which can be carried out efficiently, to examine details of ground behaviour which are difficult to obtain from in-situ tests;
  - Continuing work to relate engineering deformation parameters for routine design to small-strain soil parameters
2. Much of the research in foundation engineering has focussed on the design and construction of new foundations. Increasingly, engineers are being asked to assess the condition of existing foundations and the extent to which such foundations can be used to support additional loadings, for example, because of an extension or heightening of a structure, or because of a change in the usage of the structure. It would therefore be appropriate for some re-direction of research effort to be made towards the better solution of such problems. Specific examples of relevant research topics include:
  - The identification in-situ of the nature of an existing foundation; this may involve the application of micro-geophysical techniques to identify pile length, diameter and modulus,
  - The assessment of the performance of an existing foundation via in-situ testing. Such testing is usually complicated by the difficulty of obtaining unobstructed access to the foundation in order to apply load, and also by the fact that an in-service foundation cannot be loaded to failure in order to assess its existing ultimate capacity.
  - The assessment of the performance of an existing foundation after it has been upgraded, for example, a large bored pile which has been enhanced by the addition of additional piles to increase the capacity and stiffness it can provide.
3. Consideration of interaction between the project being investigated and existing adjacent projects. For example, it is a common practice to ignore activities on sites other than the one being investigated, but such activities as dewatering, excavation, foundation construction, or the presence of another adjacent heavily-loaded structure, can have a major impact on the behaviour of the ground and the structure being constructed. In particular, the interaction among closely-spaced buildings deserves close attention, as the consequent tilts and differential settlements.
4. In-situ correction of deficient foundations. The Pisa Tower provides an outstanding example of the application of fundamental soil mechanics and innovative technology to the correction of foundation tilting. Similar techniques can be developed for structures supported by piles, and a proper

understanding of the consequences and risks of such techniques that can result from research.

## 10 CONCLUSIONS

This paper has reviewed various aspects of foundation engineering and has attempted to assess the capabilities of conventional methods of analysis and design in the light of more modern methods developed from research over the past two to three decades. Based on this review, it has been suggested that the conventional methods of analysis and design should be adopted, adapted or discarded. The results of this assessment may be summarized as follows:

- (i) Methods which may be adopted –
  - the effective width method, commonly used in the analysis of the bearing capacity of foundations subjected to eccentric loading in the case of undrained loading,
  - relatively new solutions for bearing capacity for cases involving the following:
    - clays where the undrained shear strength increases linearly with depth (Booker and Davis, 1973),
    - two layers of clay, Merifield *et al.* (1999),
    - a layer of sand overlying relatively soft clay (Okamura *et al.*, 1998),
  - Failure loci for combined loading of shallow foundations, such as those expressed by Equation (3.9),
  - Schmertmann's method for settlement of shallow footings on sands,
  - the elastic method for settlement of shallow footings on sands,
  - equivalent pier analysis for pile groups,
  - analyses for rafts or piled rafts that treat the soil as an elastic or elasto-plastic continuum,
  - the use of thin plate theory for rafts and piled rafts (except in areas where very stiff structural elements exist, e.g., shear walls), and
  - active earth pressures on rigid retaining structures as suggested by Coulomb and based on a simple wedge failure mechanism.
- (ii) Methods which should be adapted –
  - conventional bearing capacity theory, based on the original approach suggested by Terzaghi and extended later by others such as Vesic, to calculate the bearing capacity of a foundation on homogeneous soil, with the proviso that the use of the outdated and inaccurate information regarding some of the bearing capacity factors, particularly the factor  $N_c$ , should be discontinued. The factors set out in Table 3.1 are considered to provide the best values available and their use is therefore recommended,
  - one-dimensional settlement analysis of shallow footings on clay (make allowance for immediate settlement),
  - one-dimensional rate of settlement analysis for shallow footings (make allowance for three-dimensional geometry and soil anisotropy),
  - linear creep/secondary settlement versus log time relationship (need to consider carefully when creep commences),
  - strip analysis for rafts (allow for loaded areas outside the strip section analyzed),
  - simplified methods based on the Poulos-Davis-Randolph method, may be used to obtain preliminary estimates of load-settlement behaviour for piled raft foundations, and
  - solutions proposed by Lee and Herrington (1972a, 1972b) for the passive thrusts acting on rigid retaining structures. In particular, the use of the Coulomb solution for this form of loading should be abandoned.
- (iii) Methods which may need to be discarded –
  - methods for shallow foundations based on subgrade reaction concepts; while they may sometimes give satisfactory results for isolated loadings, they can be misleading for uniform loadings and may also create difficulties with the selection of

- modulus of subgrade reaction because of its dependence on the foundation dimensions,
- the use of Winkler springs for analysis of rafts and piled raft foundations,
- analysis of isolated strips as a simplified method of analysing rafts, and
- solutions proposed by Coulomb for the passive pressures acting on rigid retaining structures.

It is also noted that the inclusion of the structural stiffness in the analysis of rafts and piled rafts is desirable, as is the inclusion of soil layering and finite soil depth in analyses of rafts and piled rafts. Such inclusions are now quite feasible and relatively easily implemented in the more sophisticated analysis tools (Category 2 and 3 methods listed in Table 2.6).

It must be stated that the above assessments contain a certain element of subjectivity. Also, it is vital to recognize that the ultimate success of analysis and design calculations depends as much (if not more) on appropriate modelling and parameter selection than on the method of analysis used.

In conclusion, it is sobering to recall the following comments of Terzaghi (1951):

"...foundation engineering has definitely passed from the scientific state into that of maturity.....one gets the impression that research has outdistanced practical application, and that the gap between theory and practice still widens".

The gap to which Terzaghi referred is far greater now, almost fifty years later, and it would seem appropriate that a major effort be mounted for the beginning of the new millennium to assess the current state of practice in various aspects of foundation engineering, and incorporate relevant aspects of modern research and state of the art knowledge into practice.

## ACKNOWLEDGEMENTS

Some of the original work of the authors described in this paper was funded by grants from the Australian Research Council. The efforts of the following people, who provided valuable assistance in the preparation of this paper, are gratefully acknowledged: C. Bredillet, M. Domadenik, T.S. Hull, M.D.F. Liu, K. Pham, S.W. Sloan, H. Taiebat, C.X. Wang and K. Xu.

## REFERENCES

Alpan, I. 1964. Estimating Settlements of Foundations on Sands. *Civ. Eng. And Public Works Review*.

API 1984. *API RP2A, recommended practice for planning, designing and constructing fixed offshore platforms*. 14<sup>th</sup> Ed., Dallas, American Petroleum Institute.

Atkinson, J.H. & Salfors, G. 1991. Experimental determination of stress-strain-time characteristics in laboratory and in situ tests. *Proc. 10<sup>th</sup> Eur. Conf. Soil Mechs. Foundn. Eng.*, Florence, 3: 915-956.

Atkinson, J.H. 2000. Non-linear soil stiffness in routine design. *Géotechnique*, 50 (5): 487-508.

Banerjee, P.K. and Driscoll, R.M. 1976. Three-dimensional analysis of raked pile groups. *Proc. Instn. Civ. Engrs.*, 2(61): 653-671.

Barker, R.M., Duncan, J.M., Rojiani, K.B., Ooi, P.S.K., Tan, C.K. & Kim, S.G. 1991. Manuals for the design of bridge foundations. *NCHRP Rept. 343*, Transp. Res. Board, Washington.

BCP Committee 1971. *Field tests on piles in sand. Soils and Foundns.*, 11(2): 29.

Becker, D.E. 1996. Eighteenth Canadian geotechnical colloquium: limit states design for foundations. Part 1. An overview of the foundation design process. *Can. Geot. Jnl.*, 33: 956-983.

Bilotta, E., Caputo, V. & Viggiani, C. 1991. Analysis of Soil-structure interaction for piled rafts. Deformation of Soils and Displacements of Structures, *Proceedings of the Tenth European Conference on Soil Mechanics and Foundation Engineering, Florence, May 1991*.

Bjerrum, L. 1963. Discussion on compressibility of soils. *Proc. Eur. Conf. S.M. & Found. Eng.*, Wiesbaden, 2: 16-17.

Bogard, D. & Matlock, H. 1983. Procedures for analysis of laterally loaded pile groups in soft clay. *Geot. Practice in Offshore Enigneering*, Ed. S. C. Wright, ASCE, New York, 499-535.

Bolton, M. 1979. *A guide to soil mechanics*, MacMillan Publishers, London.

Booker, J.R. 1974. The consolidation of a finite layer subject to surface loading. *Int. J. Solids and Structs.*, 10: 1053-1065.

Booker, J.R. & Poulos, H.G. 1976. Analysis of creep settlement of pile foundations. *Jnl. Geot. Eng. Divn., ASCE*, 102(1): 1-14.

Boone, S.T. 1996. Ground-movement-related building damage. *Jnl. Geotech. and Geoenv. Eng., ASCE*, 122(11): 886-896.

Boscardin, M.D. & Cording, E.J. 1989. Building response to excavation-induced settlement. *Jn. Geotech. Eng., ASCE*, 115(1): 1-21.

Bowles, J.E. 1988. *Foundation analysis and design*. McGraw Hill, New York.

Bransby, M.F. & Randolph, M.F. 1998. Combined loading of skirted foundations, *Géotechnique*, 48: 637-655.

Bransby, M.F. 1999. Selection of p-y curves for the design of single laterally loaded piles. *Int. Jnl. Num. Anal. Methods in Geomechs.*, 23: 1909-1926.

Brettman, T. & Duncan, J.M. 1996. Computer applications of CLM lateral load analysis to piles and drilled shafts". *Jnl. Geotech. Eng., ASCE*, 122(6): 496-498.

Briaud, J-L. & Gibbens, R.M. 1994. Test and Prediction Results for Five Large Spread Footings on Sand. *Geot. Spec. Pub. 41, ASCE*, 92-128.

Brinch Hansen, J. 1961. Ultimate resistance of rigid piles against transversal forces. *Bull. 12, Danish Geotech. Inst., Copenhagen*, 5-9.

Broms, B.B. 1964a. Lateral resistance of piles in cohesive soils. *Jnl. S.M. & Foundns. Div., ASCE*, 90(SM2): 27-63.

Broms, B.B. 1964b. Lateral resistance of piles in cohesionless soils. *Jnl. S.M. & Foundns. Div., ASCE*, 90(SM3): 123-156.

Broms, B.B. 1966. Methods of calculating the ultimate bearing capacity of piles - a summary. *Sols Soils*, 18-19: 21-32.

Brooks, N.J. & Spence, J.F. 1992. Design and recorded performance of a secant retaining wall in Croydon. *Proc. Int. Conf. Retaining Structures*, Cambridge.

Brown, J.D. & Meyerhof, G.G. 1969. Experimental study of bearing capacity in layered clays. *Proc., 7th Int. Conf. on Soil Mechanics and Foundation Engineering, Mexico*, 2: 45-51.

Brown, J.D. & Paterson, W.G. 1964. Failure of an oil storage tank founded on a sensitive marine clay. *Can. Geotech. Jnl.*, 1: 205-214.

Brown, P.T. & Yu, S.K.R. 1986. Load sequence and structure-foundation interaction. *Journal of Structural Engineering, ASCE*, 112(1): 481-488.

Brown, P.T. 1975. The significance of structure-foundation interaction. *Proc. 2<sup>nd</sup> Australia-New Zealand Conf. on Geomechanics*, Brisbane, IEAust, 1.1: 79-82.

Brown, P.T. 1977. Strip Footings. *Geotechnical Analysis and Computer Applications; Lecture 7*, University of Sydney.

Budhu, M. & Davies, T.G. 1987. Nonlinear analysis of laterally loaded piles in cohesionless soils. *Can. Geot. Jnl.*, 24: 21-39.

Budhu, M. & Davies, T.G. 1988. Analysis of laterally loaded piles in soft clays. *J. Geot. Eng., ASCE*, 114(1): 21-39.

Buisman, A.S. 1936. Results of long duration settlement tests. *Proc. 1<sup>st</sup> ICSMFE, Cambridge, Mass.*, 1: 103-106.

Burd, H.J. & Frydman, S. 1997. Bearing capacity of plane-strain footings on layered soils. *Can. Geotech. Jnl.*, 34: 241-253.

Burland, J.B. 1973. Shaft friction on piles in clay-a simple fundamental approach. *Ground Eng.*, 6(3): 30-42.

Burland, J.B., Broms, B.B. & de Mello, V.F.B. 1977. Behaviour of foundations and structures. *Proc. 9<sup>th</sup> Int. Conf. Soil Mechs. Found. Eng.*, Tokyo, 1:495-546.

Burland, J.B. & Burbridge, M.C. 1985. Settlements of foundations on sand and gravel. *Proc. I.C.E.*, 1: 1325-1381.

Burland, J.B. & Wroth, C.P. 1974. Settlement of buildings and associated damage. *Settlement of Structures*, Pentech Press, London, 611-654.

Bustamante, M. & Gianceselli, L. 1982. Pile bearing capacity prediction by means of static penetrometer CPT. *Proc. ESOPT II, Amsterdam*, 2: 492-500

Bustamante, M. & Gianesselli, L. 1998. Installation parameters and capacity of screwed piles. *Deep Foundations on Bored and Auger Piles*, van Impe and Haegeman (eds, Balkema, Rotterdam, 95-108.



- Butterfield, R., Housby, G.T. & Gottardi, G. 1997. Standardized sign conventions and notation for generally loaded foundations. *Géotechnique*, 47: 1051-1054.
- Button, S.J. 1953. The bearing capacity of footings on a two-layer cohesive subsoil. *Proc., 3rd Int. Conf. on Soil Mechanics and Foundation Engineering*, Zurich, 1: 332-335.
- Caquot, A. & Kerisel, J. 1948. *Tables for the calculation of passive pressure, active pressure and bearing capacity of foundations*. Gauthier-Villars, Paris.
- Caquot, A. & Kerisel, J. 1953. *Traité de mécanique des sols*. Gauthier-Villars, Paris.
- Carter, J.P., Booker, J.R. & Small, J.C. 1979a. The analysis of finite elasto-plastic consolidation. *Int. J. Num. and Anal. Methods in Geomechanics*, 3: 107-129.
- Carter, J.P., Randolph, M.F. & Wroth, C.P. 1979b. Stress and pore pressure changes in clay during and after the expansion of a cylindrical cavity. *Int. J. Num. and Anal. Methods in Geomechanics*, 3: 305-322.
- Carter, J.P., Desai, C.S., Potts, D.M., Schweiger, H.M. & Sloan, S.W. 2000. Computing and Computer Modelling in Geotechnical Engineering. *GeoEng2000*; Nov. Melbourne, Australia. Lancaster, Pa. USA: Technomic Publishing Co. 157-252.
- Challa, P. & Poulos, H.G. 1991. Behaviour of single pile in expansive clay. *Geot. Eng.*, 22(2): 189-216.
- Chang, C.S. 1994. Compressibility for sand under one-dimensional loading condition. *Vertical and Horizl. Deformn. of Foundns. and Embankments Geot. Spec. Pub. 40*, ASCE, 2: 1298-1311.
- Chen, L.T. & Poulos, H.G. 1997. Piles subjected to lateral soil movements. *J. Geot. & Geoen. Eng.*, ASCE, 123(9): 802-811.
- Chen, L.T., Poulos, H.G. & Loganathan, N. 1999. Pile responses caused by tunneling. *Jnl. Geotech and Geoen. Eng.*, ASCE, 125(3): 207-215.
- Chen, W.F. 1975. *Limit analysis and soil plasticity*. Elsevier, New York.
- Chen, W.F., & Davidson, H.L. 1973. Bearing capacity determination by limit analysis. *J. Soil Mech. Found. Div. ASCE*, 99: 433-449.
- Chen, W.F. & McCarron, W.O. 1991. *Foundation Engineering Handbook*, Ed. Fang, 2<sup>nd</sup> Edition, Van Nostrand Reinhold, New York, 144-165.
- Chin, J.T. & Poulos, H.G. 1992. Cyclic axial pile loading analyses. A comparative study. *Computers and Geotechnics*, 13(3): 137-158.
- Cho, N.-J. & Kulhawy, F.H. 1995. The undrained behaviour of drilled shaft foundations subjected to static inclined loading. *Jnl. Korean Geot. Society*, 11(3): 91-111.
- Chow, Y.K. 1986. Analysis of vertically loaded pile groups. *Int. J. for Numerical and Analytical Methods in Geomechanics* 10: 59-72.
- Chow, Y.K., Chin, J.T. & Lee, S.L. 1990. Negative skin friction on pile groups. *Jnl. Num. and Anal. Meths. In Geomechs.*, 14(1): 75-91.
- Chua, K.M., Xu, L., Pease, E. & Tamare, S. 1994. Settlement of test footings: Predictions from the University of New Mexico. *Geot. Spec. Pub. 41*, ASCE, 240-244.
- CIRIA 1974. *A comparison of quay wall design methods*. Report No. 54, Construction Industry Research and Information Association, London.
- Clancy, P. & Randolph, M.F. 1993. An approximate analysis procedure for piled raft foundations. *Int. J. for Numerical and Analytical Meths. in Geomechanics*, 17(12): 849-869.
- Clayton, C.R.I., Milititsky, J. & Woods, R.I. 1993. *Earth pressure and earth-retaining structures*. 2<sup>nd</sup> edn. Blackie Academic & Professional, London.
- Clough, G.W., Smith, E.M. & Sweeney, B.P. 1989. Movement control of excavation support systems by iterative design. *Proc. ASCE, Foundation Engineering: Current Principles and Practices*, 2: 869-884.
- Costanzo, D. & Lancellotta, R. 1998. A note on pile interaction factors. *Soils and Foundations*, 38(4): 251-253.
- Coulomb, C.A. 1776. Essai sur une application des règle de maximis et minimis à quelques problèmes de statique relatifs à l'architecture. *Mémoires de Mathématique et de Physique présentés à l'Académie des Sciences*, Paris, 1773, T: 343-382.
- Cox, A.D. 1961. Axially-symmetric plastic deformation in soils - II. Indentation of ponderable soils. *Int. J. Mech. Sci.*, 4: 371-380.
- Cox, W., Reese, L.C. & Grubbs, B.R. 1974. Field testing of laterally loaded piles in sand. *Proc. 6<sup>th</sup> Offshore Tech. Conf.*, Dallas, Texas, 459-472.
- Craig, W.H. & Chua, K. 1990. Deep penetration of spud-can foundations on sand and clay. *Géotechnique*, 40(4): 541-556.
- D'Appolonia, D.J. & D'Appolonia, E. 1970. Closure to settlement of spread footings on sand. *JSMFED, ASCE*, 96(SM2): 754-762.
- D'Appolonia, D.J., Poulos, H.G. & Ladd, C.C. 1971. Initial Settlement of Structures on Clay. *JSMFD, ASCE*, 97(SM10): 1359-1397.
- Davis, E.H. & Booker, J.R. 1971. The bearing capacity of strip footings from the standpoint of plasticity theory. *Proc. First Australia-New Zealand Conference on Geomechanics*, 1: 276-282.
- Davis, E.H. & Booker, J.R. 1973. The effect of increasing strength with depth on the bearing capacity of clays. *Géotechnique*, 23: 551-563.
- Davis, E.H. & Poulos, H.G. 1968. The use of elastic theory for settlement prediction under three-Dimensional conditions. *Géotechnique*, 18(1): 67-91.
- Davis, E.H. & Poulos, H.G. 1972. Rate of settlement under three dimensional conditions. *Géotechnique*, 22(1): 95-114.
- Davis, E.H. & Poulos, H.G. 1975. Predicted and measured behaviour of an embankment on Boston Blue Clay. *Aust. Geomechs. Jnl.* G5(1): 1-9.
- Davissou, M.T. 1970. Lateral load capacity of piles. *High. Res. Record* 333: 104-112.
- Day, R.W. 2000 *Geotechnical engineer's portable handbook*. New York, McGraw Hill.
- De Cock, F. 1998. Design of axially loaded bored piles – European codes, practice and experience. *Deep Foundations on Bored and Auger Piles*, van Impe and Haegeman (eds, Rotterdam, 63-74. Balkema.
- De Nicola, A. & Randolph, M.F. 1993. Tensile and compressive shaft capacity of piles in sand. *Jnl. Geot. Eng.*, ASCE, 119(12): 1952-1973.
- Decourt, L. 1989. SPT – State of the Art Report. *Proc. 12 ICSMFE, Rio de Janeiro*, 4: 2405-2416.
- Decourt, L. 1995. Prediction of load-settlement relationships for foundations on the basis of the SPT-T. *Ciclo de Conferencias Intern. "Leonardo Zeevaert"*, UNAM, Mexico, 85-104.
- Dennis, N.D. & Olsen, R.E. 1984. Axial capacity of steel pipe piles in clay. *Proc. ASCE Spec. Conf. on Geotech. Practice in Offshore Eng.*, Austin, 370-388.
- Desai, C.S. 1974. Numerical design-analysis for piles in sands. *Jnl. Geot. Eng. Div.*, ASCE, 100(GT6): 613-635.
- Desai, C.S. & Christian, J.T. 1977. *Numerical methods in geotechnical engineering*. New York, McGraw-Hill.
- Desai, C.S., Johnson, L.D. & Hargett, C.M. 1974. Analysis of pile supported gravity lock. *Jl. Geotechnical Division*, ASCE 100(GT9): 1009-1029.
- Duncan, J.M. & Buchignani, A.L. 1976. An engineering manual for slope stability analysis. *Department of Civil Engineering, University of California*, Berkeley.
- Duncan, J.M., Evans, L.T. & Ooi, P.S.K. 1994. Lateral load analysis of single piles and drilled shafts. *Jnl. Geotech. Eng.*, ASCE, 120(5): 1018-1033.
- Fahey, M. 1999. Determining the parameters of a non-linear elastic model for prediction of ground deformation. *Australian Geomechanics*, March, 34(1): 39-59.
- Fahey, M. & Carter, J.P. 1993. A finite element study of the pressure-meter test in sand using a non-linear elastic plastic model. *Can. Geot. Jnl.* 30: 348-362.
- Fellenius, B. 1984. Negative skin friction and settlement of piles. *Proc. 2<sup>nd</sup> Intl. Geotech. Seminar, Pile Foundations*, Nanyang Tech. Inst., Singapore.
- Fellenius, B.H. 1989. Unified design of piles and pile groups. *Transp. Res. Board*, Washington, *TRB Record* 1169, 75-82.
- Fellenius, B. 1991. *Pile foundations*. Ch. 13 of *Foundation Engineering Handbook* (2<sup>nd</sup> Ed.), Ed. H-Y Fang, New York, Van Nostrand Reinhold, 511-536.
- Fleming, W.G.K. 1992. A new method of single pile settlement prediction and analysis. *Géotechnique*, 42(3): 411-425.
- Fleming, W.G.K., Weltman, A.J., & Randolph, M.F. 1992. *Piling Engineering*. 2<sup>nd</sup> Ed, New York, Halsted Press.
- Fleming, W.G.K., Weltman, A.J., Randolph, M.F. & Elson, W.K. 1985. *Piling engineering*. New York, Surrey University Press, Halsted Press.
- Fleming, W.G.K., Weltman, A.J., Randolph, M.F. & Elson, W.K. 1992. *Piling engineering*. 2<sup>nd</sup> Ed., New York, Halsted Press.
- Florkiewicz, A. 1989. Upper bound to bearing capacity of layered soils. *Can. Geotech. Jnl.*, 26: 730-736.



- Focht, J.A. & Koch, 1973. Rational analysis of the lateral performance of offshore pile groups. *Proc. 5<sup>th</sup> Offshore Tech. Conf.*, Houston, 2 OTC 1896: 701-708.
- Fourie, A.B. & Potts, D.M. 1989. Comparison of finite element and limiting equilibrium analyses for an embedded cantilever retaining wall. *Géotechnique*, 39: 175-188.
- Franke, E. 1991. Measurements beneath piled rafts. Keynote lecture *ENPC Conf. Paris*. 1-28.
- Franke, E., Lutz, B. & El-Mossallamy, Y. 1994. Measurements and numerical modelling of high-rise building foundations on Frankfurt clay. *Vert and Horiz. deformation of foundations and embankments, ASCE Geot. Spec. Pub. No. 40*. 2: 1325-1336.
- Fraser, R.A. & Wardle, L.J. 1975. A rational analysis of shallow footings considering soil-structure interaction *Australian Geomechanics Journal* 20-25.
- Fraser, R.A. & Wardle, L.J. 1976. Numerical analysis of rectangular rafts on layered foundations. *Géotechnique*, 26(4): 613-630.
- Garlanger, J.E. 1972. The consolidation of soils exhibiting creep under constant effective stress. *Geotechnique*, 22(1): 71-78.
- GCO 1982. *Guide to retaining wall design. Geoguide 1*, Geotechnical Control Office, Engineering Development Dept. Hong Kong.
- GEO 1996. Pile design and construction. *Pub. No. 1/96, Geot. Eng. Office*, Hong Kong.
- Gibson, R.E. & Lo, K.Y. 1961. A theory of consolidation for soils exhibiting secondary consolidation. *Acta Polytech. Scand.*, p. 296.
- Go, V. & Olsen, R.E., 1993. Axial load capacity of untapered piled in sand. *Proc. 11<sup>th</sup> S.E. Asian Geot. Conference*, Singapore, 517-521.
- Goh, A.T.C., The, C.I. & Wong, K.S. 1997. Analysis of piles subjected to embankment induced lateral soil movements. *J. Geot. & Geoenv. Eng.*, ASCE, 123(9): 792-801.
- Goldberg, D.T., Jaworski, W.E. & Gordon, M.D. 1976. Lateral support systems and underpinning, *Report FHA-RD-75-128, Federal Highway Administration*, Washington, D.C., Vol. 1.
- Golder, H.Q. & Osler, J.C. 1968. Settlement of a furnace foundation, Sorel, Quebec. *Can. Geot. Jnl.*, 5(1): 46-56.
- Grant, R. Christian, J.T. & Vanmarke, E.H. (1974). Differential settlement of buildings. *Jnl. Geot. Eng. Divn.*, ASCE, 100(GT9): 973-991.
- Gregersen, O.S., Aas, G. & Dibiagio, E. 1973. Load tests on friction piles in loose sand. *Proc. 8<sup>th</sup> Int. Conf. Soil Mechs. Found. Eng.*, Moscow, 2: 109-117.
- Griffiths, D.V. 1982. Computation of bearing capacity on layered soils. *Proc., 4th Int. Conf. on Num Meth. In Geomechanics*, 1: 163-170.
- Gudehus, G. 1998. Limit state design of structural parts at and in the ground. *Ground Eng.*, October, 42-45.
- Gunn, M.J., Satkunanathan, A. & Clayton, C.R.I. 1992. Finite element modelling of installation effects. *Proc. I.C.E. Conf. on Retaining Structures*, Cambridge.
- Guo W.D. & Randolph, M.F. 1997. Vertically loaded piles in non-homogeneous soils. *Int. Jnl. Num. Anal. Methods in Geomechs.*, 21: 507-532.
- Guo, W.D. & Randolph, M.F. 1999. An efficient approach for settlement prediction of pile groups. *Géotechnique*, 49(2): 161-179.
- Guo, D. 2000. Visco-elastic load transfer models for axially loaded piles. *Int. Jnl. Num. Anal. Methods in Geomechs.*, 24: 135-163.
- Gusmao Filho, J.A. & Guimaraes, L.J.N. 1997. Limit stiffness in soil-structure interaction of buildings. *Proc. 14<sup>th</sup> Int. Conf. on soil mechs and Found Eng.*, Hamburg 2: 807-808.
- Hain, S. & Lee, I.K. 1978. The analysis of flexible raft-pile systems. *Géotechnique* 28(1): 65-83.
- Hain, S.J. & Lee, I.K. 1974. Rational analysis of raft foundations. *Jnl. Geot. Div.*, ASCE, 100(GT7).
- Hanna, A. & Meyerhof, G.G. 1980. Design charts for ultimate bearing capacity of sand overlying soft clay. *Can. Geotech. Jnl.*, 17: 300-3-3.
- Hansbo, S. & Källström, R. 1983. A Case Study of Two Alternative Foundation Principles. *Väg-och Vattenbyggnaden* 7-8: 23-27.
- Hemsley, J.A. 1998. *Elastic Analysis of Raft Foundations*. Thomas Telford, London.
- Hemsley, J.A. (ed) 2000. *Design Applications of Raft Foundations*. Thomas Telford, London.
- Hencky, H. 1923. Über einige statisch bestimmte Fälle Gleichgewichts in plastischen Körpern. *Zeitschrift für Angewandte, Mathematik und Mechanik*, 3(4): 241-251.
- Heyman, 1965. Measurement of the influence of lateral earth pressure on piles. *Proc. 6<sup>th</sup> Int. Conf. S.M. & Found. Eng.*, Montreal, 2: 257-260.
- Heyman, J. 1972. *Coulomb's memoir on statics. An essay in the history of civil engineering*. Cambridge University Press, Cambridge.
- Higgins, K.G., Potts, D.M. & Symons, I.F. 1989. *Comparison of predicted and measured performance of the retaining walls of the Bell Common tunnel*. Transport Road Research Laboratory, Contractor Report 124.
- Horikoshi, K. & Randolph, M.F. 1997. Optimum design of piled raft foundations. *Proceedings of the 14<sup>th</sup> Int Conf. on Soil Mechs and Found Eng.*, Hamburg. 2: 1073-1076.
- Houlsby, G.T. & Purzin, A.M. 1999. The bearing capacity of strip footing on clay under combined loading. *Proc. Royal Society*, 455A: 893-916.
- Houlsby, G.T. & Wroth, C.P. 1983. Calculation of stresses on shallow penetrometers and footings. *Proc. IUTAM Symposium*, 107-112.
- Jamiolkowski, M. & Lo Presti, D.C.F. 1994. Validity of in-situ tests related to real behaviour. *Proc. 13<sup>th</sup> Int. conf Soil Mechs. Found. Eng.*, New Delhi, 5: 51-55.
- Janbu, N. 1963. Soil compressibility as determined by oedometer and triaxial tests, *European Conf. On Soil Mechanics and Foundation Engineering*, Wiesbaden, Germany, 19-25.
- Jardine, R.J. & Chow, F. 1996. New design methods for offshore piles. *MTD Pub. 96/103, Marine Technology Directorate*, London, UK.
- Jeyapalan, J.K. & Boehm, R. 1986. Procedures for Predicting Settlements in Sands. *Proc. Spec. Conf. On Settl. Of Shallow Foundns. on Cohesionless Soils*, Geot. Spec. Pub. 5 ASCE, 1-22.
- Kalteziotis, N., Zervogiannis, F.R., Seve, G. & Berche, J-C., 1993. Experimental study of landslide stabilization by large diameter piles. *Geot. Eng. of Hard Soils-Soft Rocks*, Ed. A. Anagnostopoulos et al, Balkema, Rotterdam, 1115-1124.
- Katzenbach, R., Arslan, U., Gutwald, J., Holzhäuser, J. & Quick, H. 1997. Soil-structure-interaction of the 300m high Commerzbank in Frankfurt am Main – Measurements and Numerical studies. *Proc. 14<sup>th</sup> Int. Conf. on Soil Mechs. Found. Eng.*, Hamburg. 2: 1081-1084.
- Kenny, M.J. & Andrawes, K.Z. 1997. The bearing capacity of footings on a sand layer overlying soft clay. *Géotechnique*, 47: 339-345.
- Kerisel, J. 1961. Fondations profondes en milieu sableux. *Proc. 5<sup>th</sup> Int. Conf. Soil Mechs. Found. Eng.*, Paris, 2: 73-83.
- Kerisel, J. & Absi, E. 1990. *Active and passive earth pressure tables* (3rd edition). Balkema, Rotterdam.
- Kimura, M., Zhang, F. & Inoue, T. 1998. Investigation of the behaviour of pile foundation undergone cyclic lateral loading by three dimensional finite element analysis. *Deep Foundations on Bored and Auger Piles*, Ed. W.F. van Impe, Rotterdam, 145-150, Balkema.
- Kulhawy, F.K. 1984. Limiting tip and side resistance: fact or fallacy? *Anal. and Des. of Pile Foundns.*, Ed. J.R. Meyer, ASCE, 80-98.
- Kulhawy, F.H. & Chen, Y-J. 1993. A thirty year perspective on Broms' lateral loading models, as applied to drilled shafts. *Proc. Broms Symposium*, Nanyang Univ. of Technology, Singapore.
- Kulhawy, F.K. & Phoon, K. K. 1993. Drilled shaft side resistance in clay soil to rock. *Des. & Perf. of Deep Foundns.*, ASCE, Spec. Pub. 38, 172-183.
- Kulhawy, F.H., Trautmann, C.H., Beech, J.F., O'Rourke, T.D. & McGuire, W. 1984. Transmission line structure foundations for uplift-compression loading. *Report EL-2870, Electric Power Research Institute*, Palo Alto, California, 412p.
- Kutmen, G. 1986. The influence of the construction process of bored piles and diaphragm walls: a numerical study. *M.Phil Thesis*, University of Surrey.
- Kuwabara, F. & Poulos, H.G. 1989. Downdrag forces in a group of piles. *J. Geot. Eng. Divn.*, ASCE, 115(6): 806-818.
- Lam, T.S.K. & Johnston, I.W. 1982. A constant normal stiffness direct shear machine. *Proc. 7<sup>th</sup> S.E. Asian Conf on Soil Eng.*, Hong Kong, 805-820.
- Lambe, T.W. 1964. Methods of Estimating Settlement. *Jnl. SMFD*, ASCE, 90(SM5): 47-71.
- Larsson, R. & Mulabdic, M. 1991. Shear moduli in Scandinavian clays. *Swedish Geot. Inst. Rep. No. 40, SGI*, Linköping.
- Lee, C.Y., Poulos, H.G. & Hull, T.H. 1991. Effect of seafloor instability on offshore pile foundations. *Can. Geot. Jnl.*, 28(5): 729,737.
- Lee, I.K. 1975. Structure-foundation-supporting soil interaction analysis. S. Valliappan, S. Hain and I.K. Lee Eds. *Soil Mechanics, Recent Developments*, Univ. of NSW 255-294.
- Lee, I.K. & Brown, P.T. 1972. Structure-foundation interaction analysis. *Jl. Structs. Div.*, ASCE. 98 (ST11): 2413-2430.

- Lee, I.K. & Herrington, J.R. 1972a. A theoretical study of the pressures acting on a rigid wall by a sloping earth or rock fill. *Géotechnique*, 22(1): 1-26.
- Lee, I.K. & Herrington, J.R. 1972b. Effect of wall movement on active and passive pressures. *Proc. Soil Mech. & Fndn Divn, ASCE*. 98(SM6): 625-640.
- Lee, I.K., White, W. Ingles, O.G. 1983. Geotechnical engineering. Pitman, Boston.
- Lee, J.H. & Salgado, R. 1999. Determination of pile base resistance in sand. *Jnl. Geotech. and Geoenv. Eng., ASCE*, 125(8): 673-683.
- Lehane, B.M. & Fahey, M. 2000. A simplified non-linear settlement prediction model for foundations on sand. To be published.
- Lehane, B.M. & Jardine, R.J. 1994. Displacement pile behaviour in a soft marine behaviour. *Can. Geot. Jnl.*, 31(2): 181-191.
- Leroueil, S. 1996. Compressibility of Clays: Fundamental and Practical Aspects. *Jnl. Geot. Eng., ASCE*, 122(7): 534-543. Lopes, F.R. and Gusmao, A.D. 1991. On the Influence of Soil-Structure Interaction in the Distribution of Foundation Loads and Settlements. *Proc. 10<sup>th</sup> Eur. Conf. SMFE, Florence*, 2: 475-478.
- Leussink, H. & Wenz, K.P. 1969. Storage yard foundations on soft cohesive soils. *Proc. 7<sup>th</sup> Int. Conf. S.M. & Found. Eng.*, Mexico City, 2: 149-155.
- Lin, D.G., Bergado, D.T. & Balasubramaniam, A.S. 1999. Soil structure interaction of piled raft foundation in Bangkok subsoil. Hong *et al.* (eds. *Proc. Eleventh Asian Regional Conference on Soil Mechanics and Geotechnical Engineering*, 183-187.
- Loganathan, N., Poulos, H.G. & Stewart, D.P. 2000. Centrifuge model testing of tunnelling-induced ground and pile deformations. *Géotechnique*, 50(3): 283-294.
- Lopes, F.R. & Gusmao, A.D. 1991. On the influence of soil-structure interaction in the distribution of foundation loads and settlements. *10<sup>th</sup> Europ. Conf. SMFE, Florence*. 2: 475-478.
- Love, J.P., Burd, H.J., Milligan, G.W.E., & Hously, G. T. 1987. Analytical and model studies of reinforcement of a layer of granular fill on a soft clay subgrade. *Can. Geotech. Jnl*, 24: 611-622.
- Mana, A.I. & Clough, G.W. 1981. Prediction of movement of braced cuts. *Jnl Geotechnical Division, ASCE*, 107: 759-778.
- Mandolini, A. & Viggiani, C. 1997. Settlement of piled foundations. *Géotechnique*, 47(4): 791-816.
- Martin, C.M. 1994. *Physical and Numerical Modelling of Offshore Foundations Under Combined Loads*, Ph.D. Thesis, The University of Oxford.
- Matlock, H. & Foo, S.C. 1980. Axial analysis of piles using a hysteretic and degrading soil model. *Proc. Conf. Num. Methods in Offshore Eng.*, 165-185, London, ICE.
- Matsui, T. 1993. Case studies on cast-in-place bored piles and some considerations for design. *Proc. BAP II*, Ghent, Balkema, Rotterdam, 77-102.
- Maugeri, M. & Motta, E. 1991. Stresses on piles used to stabilize landslides. *Landslides*, Ed. D. Bell, Rotterdam, 785-790. Balkema.
- Mayne, P.W. 1995. Application of  $G/G_{max}$  modulus degradation to foundation settlement analysis. *Proc. US-Taiwan Workshop on Geotech. Collaboration*, Nat. Science Foundn., Washington, and Nat. Science Council, Taipei, 136-148.
- Mayne, P.W. & Poulos, H.G. 1999. Approximate displacement influence factors for elastic shallow foundations. *Jl. Geotech. & Geoenvir. Eng. ASCE*. 125(6): 453-460.
- Meissner, H. 1991. Empfehlungen des Arbeitskreises 1.6 "Numerik in der Geotechnik", Abschnitt 1, "Allgemeine Empfehlungen". *Geotechnik*. 14: 1-10. (in German).
- Meissner, H. 1996. Tunnelbau unter Tage - Empfehlungen des Arbeitskreises 1.6 "Numerik in der Geotechnik", Abschnitt 2. *Geotechnik*, 19: 99-108. (in German).
- MELT 1993. Regles techniques de conception et de calcul des fondations des ouvrages de genie civil. CCTG, Fascicule No. 62, Titre V, Min. de L'Equipement du Lodgement et des Transport, Paris.
- Merifield, R.S., Sloan, S.W. & Yu, H.S. 1999. Rigorous solutions for the bearing capacity of two layered clay soils, *Géotechnique*, 49: 471-490.
- Mesri, G. & Godlewski, P.M. 1977. Time-and Stress-Compressibility Interrelationship. *Jnl. Geot. Eng., ASCE*, 103(GT5): 417-430.
- Mesri, G., Lo, D.O.K. & Feng, T-W. 1994. Settlement of Embankments on Soft Clays. *Geot. Spec. Pub. 40, ASCE*, 1: 8-56.
- Meyerhof, G.G. 1947. The settlement analysis of building frames. *Structural Engr. XXV*: 147.
- Meyerhof, G.G. 1951. The ultimate bearing capacity of foundations, *Géotechnique*, 2: 301-332.
- Meyerhof, G.G. 1953. The bearing capacity of foundations under eccentric and inclined loads, *Proc. 3<sup>rd</sup> Int. Conf. Soil Mechanics and Foundation Engineering*, Zurich, 1: 440-445.
- Meyerhof, G.G. 1956. Penetration tests and bearing capacity of cohesionless soils. *Jnl. S.M. and Found. Div., ASCE*, 82(SM1): 1-19.
- Meyerhof, G.G. 1974. Ultimate bearing capacity of footings on sand layer overlying clay. *Can. Geotech. Jnl*, 11: 223-229.
- Meyerhof, G.G. 1976. Bearing capacity and settlement of pile foundations. *Jnl. Geot. Eng. Div., ASCE*, 102(GT3): 195-228.
- Meyerhof, G.G. 1995a. Development of geotechnical limit state design. *Can Geotech. Jnl*. 32: 128-136.
- Meyerhof, G.G. 1995b. Behaviour of pile foundations under special loading conditions. 1994 R.M. Hardy keynote address, *Can. Geot. Jnl.*, 32(2): 204-222.
- Meyerhof, G.G. & Hanna, A.M. 1978. Ultimate bearing capacity of foundations on layered soils under inclined load. *Can. Geotech. Jnl*, 15: 565-572.
- Meyerhof, G.G. & Sastry, V.V.R.N. 1978. Bearing capacity of piles in layered soils: Part I & Part II. *Can. Geot. Jnl.*, 15(2): 171-189.
- Michaelidis, G, Gazetas, G, Bouckovalas, G. & Chryssikou, E. 1997. Approximate no-linear dynamic axial response of piles. *Géotechnique*, 48(1): 33-53.
- Michalowski, R.L. & Lei Shi 1995. Bearing capacity of footings over two-layer foundation soils. *Jnl Geotechnical Engg, ASCE*, 121: 421-427.
- Miller, G.A. & Lutegger, A.J. 1997. Predicting pile skin friction in overconsolidated clay. *Proc. 14<sup>th</sup> Int. Conf. Soil Mechs. Found. Eng., Hamburg*, 2: 853-856.
- Moore, P.J. & Spencer, G.K. 1969. Settlement of building on deep compressible soil. *JSMFD, ASCE*, 95(SM3): 769-790.
- Murchison, J.M. & O'Neill, M.W. 1984. Evaluation of p-y relationships in cohesionless soils. *Anal. and Des. of Pile Foundns.*, Ed. J.R. Meyer, ASCE, 174-191.
- Murff, J.D. 1994. Limit analysis of multi-footing foundation systems, *Proc. Int. Conf. Computer Methods and Advanced Geomechanics*, Morgantown, Eds Siriwardane & Zaman. Balkema, Rotterdam, 233-244.
- Mylonakis, G. & Gazetas, G. 1998. Settlement and additional internal forces of grouped piles in layered soil. *Géotechnique* 48(1): 55-72.
- Nauroy, J-F., Brucy, P., Le Tirant, P. & Kervadec, J-P. 1986. Design and installation of piles in calcareous foundations. *Proc. 3<sup>rd</sup> Int. Conf. Num. Methods in Offshore Piling*, Nantes, 461-480.
- NAVFAC 1982. *Soil Mechanics-Design Manual 7.1*. US Dept. Navy, US Govt. Printing Office, Washington.
- Nelson, J.D. & Miller, D.J. 1992. *Expansive soils. Problems and practice in foundation and pavement engineering.*, Wiley Interscience, New York.
- O'Neill, M.W. 2001. Side resistance in piles and drilled shafts. *Int. Geot. and Geoenv. Eng., ASCE*, 127(1): 3-16.
- O'Neill, M.W., Ghazzaly, O.I. & Ha, H.B. 1977. Analysis of three-dimensional pile groups with nonlinear soil response and pile-soil-pile interaction. *Proc. 9<sup>th</sup> OTC*, Houston, Paper OTC 2838, 245-256.
- Ohde, J. 1951. *Grundbaumechanik, Huette*, BD. III: 27, Auflage, (in German).
- Okamura, M., Takemura, J. & Kimura, T. 1998. Bearing capacity predictions of sand overlying clay based on limit equilibrium methods. *Soils and Foundations*, 38: 181-194.
- Ooi, L.H. & Carter, J.P. 1987. A constant normal stiffness direct shear device for static and cyclic loading. *Geot. Testing Jnl.*, ASTM, 10: 3-12.
- Ooi, P.S.K. & Duncan, J.M. 1994. Lateral load analysis of groups of piles and drilled shafts. *Jnl. Geotech. Eng., ASCE*, 120(6): 1034-1050.
- Osborne, J.J., Trickey, J.C., Hously, G.T. & James, R.G. 1991. 'Findings from a joint industry study on foundation fixity of jackup units', *Proc. 7<sup>th</sup> Offshore Technology Conference*, Houston, 3: 517-533.
- Padfield, C.J. & Mair, R.J. 1984. *Design of retaining walls embedded in stiff clays*. CIRIA Report No. 104, Construction Industry Research and Information Association, London.
- Parry, R.H.G. 1971. A Direct Method of Estimating Settlements in Sands

- for SPT Values. *Proc. Symp. Interaction of Struct. and Found.*, Birmingham, 29-32.
- Peaker, K.R. 1984 Lakeview tower: a case history of foundation failure. *Proc. Int. Conf. on Case histories in Geot. Eng.*, Ed. S. Prakash, Univ. of Missouri Rolla, 7-13.
- Peck, R.B. 1969. Deep excavations and tunneling in soft ground. State-of-the-Art-Report, *Proc. 7<sup>th</sup> Int. Conf. On Soil Mechanics and Foundation Engineering*, Mexico City, State-of-the-Art- Volume, 225-290.
- Peck, R.B. & Bazaraa, A.R.S. 1969. Discussion to Settlement of spread footings on sand. *JSMFD, ASCE*, 95(SM3): 905-909.
- Peck, R.B., Hansen, W.E. & Thornburn, T.H. 1974. *Foundation Engineering. 2<sup>nd</sup> Edition*. John Wiley, New York.
- Perau, E.W. 1997. Bearing capacity of shallow foundations. *Soils and Foundations*, 37: 77-83.
- Polshin, D.E. & Tokar, R.A. 1957. Maximum allowable non-uniform settlement of structures. *Proc. 4<sup>th</sup> Int. Conf. Soil Mechs. Found. Eng., London*, 1: 402.
- Potts, D.M. & Fourie, A.B. 1984. The behaviour of a propped retaining wall: results of a numerical experiment. *Géotechnique*, 34(3): 383-404.
- Potts, D.M. & Fourie, A.B. 1985. The effect of wall stiffness on the behaviour of a propped retaining wall: results of numerical experiments. *Géotechnique*, 35(3): 347-352.
- Poulos, H.G. 1971a. Behaviour of laterally loaded piles: I- single piles. *Jnl. S.M. & Found. Div., ASCE*, 97(SM5): 711-731.
- Poulos, H.G. 1971b. Behaviour of laterally loaded piles: II-pile groups. *Jnl. S.M. & Found. Div., ASCE*, 97(SM5): 733-751.
- Poulos, H.G. 1975a. Lateral load-deflection prediction for pile groups. *Jnl. Geot. Eng. Divn., ASCE*, 101(GT1): 19-34.
- Poulos, H.G. 1975b. Settlement Analysis of Structural Foundation Systems. *Proc. 4<sup>th</sup> SE Asian Conf. SMFE, Kuala Lumpur*, pp. 4-54 - 4-62.
- Poulos, H.G. 1982a. Single pile response to cyclic lateral load. *J. Geot. Eng., ASCE*, 108(GT3): 355-375.
- Poulos, H.G. 1982b. Developments in the analysis of static and cyclic lateral response of piles. *Proc. 4<sup>th</sup> Int. Conf. Num. Meth. Geomechs., Edmonton*, 3: 1117-1135.
- Poulos, H.G. 1987. Piles and piling. *Ch. 52 of Ground Engineer's Reference Book*, Ed. F.G. Bell, Butterworths, London.
- Poulos, H.G. 1988a. Cyclic stability diagram for axially loaded piles. *J. Geot. Eng., ASCE*, 114(8): 877-895.
- Poulos, H.G. 1988b. *Marine Geotechnics*. London, Unwin Hyman.
- Poulos, H.G. 1989. Pile behaviour - Theory and application. 29<sup>th</sup> Rankine Lecture. *Géotechnique*, 39(3): 65-415.
- Poulos, H.G. 1989. Pile behaviour-theory and application. *Géotechnique*, 39(3): 365-415.
- Poulos, H.G. 1991. Analysis of Piled Strip Foundations. *Comp. Methods and Adv. In Geomechs., Ed. G. Beer et al., Balkema*, 1: 182-191.
- Poulos, H.G. 1993. Settlement of bored pile groups. *Proc. BAP II, Ghent, Balkema, Rotterdam*, 103-117.
- Poulos, H.G. 1994a. An approximate numerical analysis of pile-raft interaction. *JNAMG*, 18: 73-92.
- Poulos, H.G. 1994b. Settlement prediction for driven piles and pile groups. *Spec. Tech. Pub. 40, ASCE*, 2: 1629-1649.
- Poulos, H.G. 1994c. Analysis and design of piles through embankments. *Proc. Int. Conf. on Des. and Constrn. of Deep Foundns.*, Orlando, 3: 1403-1421.
- Poulos, H.G. 1995. Design of reinforcing piles to increase slope stability. *Can. Geot. Jnl.*, 32(5): 808-818.
- Poulos, H.G. 1996a. Measured and Predicted Settlement of Shallow Foundations on Sand. *Proc. 7<sup>th</sup> ANZ Conf. Geomechs., Adelaide*, 686-692.
- Poulos, H.G. 1996b. A comparison of methods for the design of piles through embankments. *Proc. 12<sup>th</sup> S.E. Asian Geot. Conf., Kuala Lumpur*, 2: 157-167.
- Poulos, H.G. 1997a. Failure of a building supported on piles. *Proc. Int. Conf. On Found. Failures*, Singapore, Inst. Engrs. Singapore. 53-66.
- Poulos, H.G. 1997b. Piles subjected to negative friction: a procedure for design. *Geot. Eng.*, 28(1): 23-44.
- Poulos, H.G. 2000a. Design of slope stabilizing piles. *Slope Stability Engineering*, Ed. N. Yagi, T. Yamagami & J-C. Jiang, Balkema, Rotterdam, 1: 83-100.
- Poulos, H.G. 2001. Pile foundations. *Ch. 10 of Geotechnical and Geoenvironmental Handbook*, Ed. R.K. Rowe, Kluwer Academic Publishers, Boston, 261-304.
- Poulos, H.G. & Chen L. 1996. Pile response due to unsupported excavation-induced lateral soil movements. *Can. Geot. Jnl.*, 33: 670-677.
- Poulos, H.G. & Chen L. 1997. Pile response due to excavation-induced lateral soil movement. *J. Geot. & Geoenv. Eng., ASCE*, 123(2): 94-99.
- Poulos, H.G. & Chua, E.W. 1985. Bearing capacity of foundations on calcareous sand. *Proc. 11<sup>th</sup> Int. Conf. Soil Mech. Found. Eng.*, San Francisco, 3: 1619-1622.
- Poulos, H.G. & Davis, E.H. 1980. *Pile foundation analysis and design*. New York, John Wiley.
- Poulos, H.G. & Hull, T.S. 1989. The role of analytical geomechanics in foundation engineering. *Found. Eng.: Current Principles and Practices*, ASCE, New York, 2: 1578-1606.
- Poulos, H.G., Hull, T.S. & Chua, E.W. 1984. Foundation behaviour in calcareous sands. *Proc. 9<sup>th</sup> Aust. Conf. Mechs. of Structures and Materials*, Sydney, 28-32.
- Prakash, S. 1962. Behaviour of pile groups subjected to lateral loads. *PhD thesis, Univ. of Illinois*, Urbana, Ill.
- Prakash, S. & Kumar, S. 1996. Nonlinear lateral pile deflection prediction in sands. *Jnl. Geotech. Eng., ASCE*, 122(2): 130-138.
- Prandtl, L. 1921. Über die Eindringungsfestigkeit plastische Baustoffe und die Festigkeit von Schneiden. *Zeitsch. Angew. Mathematik und Mechanik*, 1: 15-20.
- Pullar, M. 1996. *Deep excavations - a practical manual*. Thomas Telford, London.
- Randolph, M.F. 1981. Response of flexible piles to lateral loading. *Géotechnique*, 31(2): 247-259.
- Randolph, M.F. 1983. Design considerations for offshore piles. *ASCE Spec. Conf. Geot. Practice in Offshore Eng.*, Austin, 422-439.
- Randolph, M.F. 1992. Settlement of pile groups. *Lecture No. 4, Modern Methods of Pile Design, Univ. of Sydney*, School of Civ. and Min. Eng.
- Randolph, M.F. 1994. Design methods for pile groups and piled rafts. *Proc. 13<sup>th</sup> Int. Conf. S.M. & Found. Eng.*, 5: 61-82.
- Randolph, M.F. & Clancy, P. 1993. Efficient design of piled rafts. *Deep founds. on bored and auger piles*, Ed. W.F. van Impe, Balkema, Rotterdam, 119-130.
- Randolph, M.F. & Simons, H. 1986. An improved soil model for one-dimensional pile driving analysis. *Proc. 3<sup>rd</sup> Int. Conf. Num. Meth. in Offshore Piling*, Nantes, 3-17.
- Randolph, M.F. & Wroth, C.P. 1978. Analysis of deformation of vertically loaded piles. *Jnl. Geot. Eng. Div., ASCE*, 104(GT12): 1465-1488.
- Randolph, M.F. & Wroth, C.P. 1979. An analysis of the vertical deformation of pile groups. *Géotechnique*, 29(4): 423,439.
- Randolph, M.F., Carter, J.P. & Wroth, C.P. 1979. Driven piles in clay - the effects of installation and subsequent consolidation. *Géotechnique* 29 (4): 361-393.
- Rankine, W.J.M. (1857). On the stability of loose earth. *Phil. Trans. Roy. Soc. London*, 147: 9-27.
- Rausche, F., Goble, G.G. & Likins, G. 1985. Dynamic determination of pile capacity. *J. Geot. Eng., ASCE*, 111(3): 367-387.
- Reddy, A.S. & Srinivasan, R. J. 1967. Bearing capacity of footings on layered clays. *Jnl Soil Mech. Found. Div., ASCE*, 93: 83-99.
- Reese, L.C., Cox, W.R. & Koop, F.D. 1974. Analysis of laterally loaded piles in sand. *Proc. 6<sup>th</sup> Offshore Tech. Conf.*, Houston, paper OTC 2080: 473-483.
- Reissner, H. 1924. Zum erddruckproblem, *Proc. 1<sup>st</sup> Int. Congress on Applied Mechanics*, Delft. C.B. Biezeno & J.M. Burgers, eds. Technische Boekhandel en Drukkerij J Waltman Jr., Delft, The Netherlands, 295-311.
- Robert, Y. 1997. A few comments on pile design. *Can. Geot. Jnl.*, 34: 560-567.
- Rollins, K.M., Clayton, R.J. & Mikesell, R.C. 1997. Ultimate side friction of drilled shafts in gravels. *Proc. 14<sup>th</sup> Int. Conf. Soil Mechs. Foundn. Eng.*, Hamburg, 2: 1021- 1024.
- Rowe, P.W. 1952. Anchored sheet pile walls. *Proc. Institution of Civil Engineers, London*, 1: 27-70.
- Rowe, P.W. & Peaker, K. 1965. Passive earth pressure measurements. *Géotechnique*, 15: 57-78.

- Sandhu, R.S. & Wilson, E.L. 1969. Finite element analysis of seepage in elastic media. *J. Eng. Mech. Div. ASCE*, 95(3): 641-652.
- Schmertmann, J. 1978. Guidelines for cone penetration test – in performance and design. *US Dept. Transport., Fed. Highways Admin., Washington D.C.*
- Schultze, E. & Sherif, G. 1973. Prediction of Settlements from Evaluated Settlement Observations for Sand. *Proc. 8<sup>th</sup> ICSMFE, Moscow*, 1.3: 225-230.
- Schweiger, H.F. 1991. Benchmark Problem No. 1: Results, *Computers and Geotechnics*, 11: 331-341.
- Schweiger, H.F. 1997. Berechnungsbeispiele des AK 1.6 der DGGT - Vergleich der Ergebnisse für Beispiel 1 (Tunnel und 2 (Baugrube. *Tagungsband Workshop "Numerik in der Geotechnik", DGGT/AK 1.6: 1-29*, (in German).
- Schweiger, H.F. 1998. Results from two geotechnical benchmark problems. *Proc. 4<sup>th</sup> European Conf. Numerical Methods in Geotechnical Engineering*. Cividini, A. (ed.), 645-654.
- Schweiger, H.F. 2000. Ergebnisse des Berechnungsbeispiels Nr. 3 "3-fach verankerte Baugrube". *Tagungsband Workshop "Verformungsprognose für tiefe Baugruben", DGGT/AK 1.6: 7-67*, (in German).
- Selvaduri, A.P.S. 1979. *Elastic Analysis of Soil-Foundation Interaction*. Elsevier Publishing Co., New York.
- Semple, R.M. & Rigden, W.J. 1984. Shaft capacity of driven piles in clay. *Anal. and Design of Pile founds.*, ASCE, 59-79.
- Shield, R.T. 1955. On the plastic flow of metals under conditions of axial symmetry, *Proc. Royal Soc.*, 233(A): 267-287.
- Simpson, B., Pappin, J.W. & Croft, D.D. 1981. An approach to limit state calculations in geotechnics. *Ground Eng.*, 14 (6): 21-28.
- Sinha, J. 1997. Piled raft foundations subjected to swelling and shrinking soils. *PhD thesis*, University of Sydney, Australia.
- Sinha, J & Poulos, H.G. 1997. Piled raft foundation systems in swelling and shrinking soils. *Proc. 14<sup>th</sup> Int. Conf Soil Mechs. Found. Eng., Hamburg*. 2: 1141-1144.
- Skempton, A.W. & Bjerrum, L. 1957. A contribution to the settlement analysis of foundations on clay. *Géotechnique*, 7(3): 168-178.
- Skempton, A.W. & MacDonald, 1956. The allowable settlements of buildings. *Proc. Instn. Civ. Engrs.*, III(5): 727-768.
- Skempton, A.W., Peck, R.B. & MacDonald, 1955. Settlement analyses of six structures in Chicago and London. *Proc. ICE, London*, 4(1): pp. 525-544.
- Small, J.C. 1998. CONTAL Users Guide. *Centre for Geot. Research, Univ. of Sydney*.
- Small, J.C. 1998. FEAR Users Guide. *Centre for Geot. Research, Univ. of Sydney*.
- Small, J.C., Booker, J.R. & Davis, E.H. 1976. Elasto-plastic consolidation of soil. *Int. J. Solids & Structs.*, 12: 431-448.
- Sokolovsky, V.V. 1960. *Statics of soil media*. Butterworth, London.
- Standards Australia, 1995. Australian standard – piling – design and installation. *AS2159-1995, Standards Australia*, Homebush.
- Stas, C.V. & Kulhawy, F.H. 1984. Critical evaluation of design methods for foundations under axial uplift and compression loading. *Report for EPRI, No. EL-3771*, Cornell University.
- Stewart, D.P., Jewell, R.J. & Randolph, M.F. 1994. Design of piled bridge abutments on soft clay for loading from lateral soil movements. *Géotechnique*, 44(2): 277-296.
- Sullivan, W.R., Reece, L.C. & Fenske, C.W. 1980. Unified method for analysis of laterally loaded piles in clay. *Num. Methods in Offshore Piling*, I.C.E. London, 135-146.
- Ta, L.D. & Small, J.C. 1996. Analysis of piled raft systems in layered soils. *Int. J. for Numerical and Analytical Methods in Geomechs.* 20: 57-72.
- Taiebat H. & Carter J.P. 2000a. Numerical studies of the bearing capacity of shallow footings on cohesive soil subjected to combined loading. *Géotechnique*, 50(4): 409-18.
- Taiebat H. & Carter J.P. 2000b. Bearing capacity of strip and circular foundations on cohesive soil subjected to vertical load and moment. Submitted to *Int. J. Geomechanics*.
- Tan, C.K. & Duncan, J.M. 1991. Settlement of Footings on Sands- Accuracy and Reliability. *Proc. Geot. Eng. Congress, ASCE, Geot. Spec. Pub. 27. 2: 446-455*.
- Tani, K. & Craig, W.H. 1995. Bearing capacity of circular foundations on soft clay of strength increasing with depth, *Soils and Foundations*, 35: 21-35.
- Tatsuoka, F. & Shibuya, S. 1991. Deformation characteristics of soils and rocks from field and laboratory tests. *Proc. 9<sup>th</sup> Asian Reg. Conf. on Soil Mechs. Foundn. Eng.*, Bangkok, 2: 101-170.
- Terzaghi, K. 1936. A fundamental fallacy in earth pressure computations. *J. Boston Soc. Civil Engrs*, 23: 71-88.
- Terzaghi, K. 1943. *Theoretical soil mechanics*. John Wiley, New York.
- Terzaghi, K. 1951. The influence of modern soil studies on the design and construction of foundations. *Building Research Congress*, London, 68-74.
- Terzaghi, K. & Peck, R.B. 1948. *Soil mechanics in engineering practice*. John Wiley, New York.
- Terzaghi, K. & Peck, R.B. 1967. *Soil mechanics in engineering practice. 2<sup>nd</sup> Ed.*, John Wiley, New York.
- Thaier, M. & Jessburger, H.L. 1991. Investigation of the behaviour of pile-raft foundations by centrifuge modelling. *Proceedings of the 10<sup>th</sup> European conf on Soil Mechs. and Foundation Engineering, Florence, May 1991*. 2: 597-603.
- Tomlinson, M.J. 1986. *Foundation design and construction. 5<sup>th</sup> Ed.*, Harlow. Longman.
- Turner, M.J. 1997. Integrity testing in piling practice. *Rep. 144, CIRIA*, London.
- US Army Corps of Engineers 1994. *Retaining and flood walls*. ASCE Press, New York.
- Van Impe, W.F. 1991. Deformations of deep foundations. *Proc. 10<sup>th</sup> Eur. Conf SM & Found. Eng.*, Florence, 3: 1031-1062.
- Van Weele, A.F. 1957. A method of separating the bearing capacity of a test pile into skin friction and point resistance. *Proc. 4<sup>th</sup> Int. Conf S.M. & Found. Eng.*, London, 2: 76.
- Van Weele, A.F. 1979. Pile bearing capacity under cyclic loading compared with that under static loading. *Proc. 2<sup>nd</sup> BOSS Conf*, London, 485-488.
- Vesic, A.S. 1967. A study of bearing capacity of deep foundations. *Final Rept., Proj. B-189, School of Civil Eng., Georgia Inst. Tech.*, Atlanta, Georgia.
- Vesic, A.S. 1969. Experiments with instrumented pile groups in sand. *ASTM, STP 444: 177-222*.
- Vesic, A.S. 1970. Research on bearing capacity of soils (unpublished).
- Vesic, A.S. 1972. Expansion of cavities in infinite soil mass. *Jnl. Soil Mechs. Foundn. Divn., ASCE*, 98 (SM3): 265-290.
- Vesic, A.S. 1973. Analysis of ultimate loads of shallow foundations, *Jnl Soil Mechanics and Foundation Division, ASCE*, 99: 45-73.
- Vesic, A.S. 1975. Bearing capacity of shallow foundations, *Foundation Engineering Handbook*, Eds Winterkorn & Fang, Van Nostrand Reinhold, New York, 121-147.
- Viggiani, C. 1981. Ultimate lateral load on piles used to stabilize landslides. *Proc. 10<sup>th</sup> Int. Conf SM & Found. Eng.*, Stockholm, 3: 555-560.
- Vinod, P. 1995. *Analysis of two-layer soil systems beneath rigid footings*. PhD Thesis, Indian Institute of Science, Bangalore.
- Wahls, H.E. 1994. Tolerable deformations. Vertical and Horizontal Deformation of Foundations and Embankments. *Geot. Spec. Pub. 40, ASCE*, 2: 1611-1628.
- Wang, C.X. 2000. Large deformation analysis of strip footings on layered purely cohesive soils", *Proc. 4<sup>th</sup> Australia New Zealand Young Geotechnical Professionals Conf*, Astralian Geomechanics Society, 229-234.
- Wang, C.X. 2001. *Large deformation and no-tension analysis of selected problems in soil mechanics*, PhD Thesis, The University of Sydney.
- Wang C.X. & Carter J.P. 2000. Penetration of strip and circular footings into layered clays. *Advances in Theoretical Geomechanics - Proceedings of the John Booker Memorial Symposium*; 2000 Nov 16-2000 Nov 17; Sydney. Rotterdam: Balkema. 193-210.
- Whitman, R.V. 1984. Evaluating calculated risk in geotechnical engineering. *Jnl. Geotech. Eng., ASCE*, 110(2): 145-188.
- Whitman, R.V. 2000. Organizing and evaluating uncertainty in geotechnical engineering. *Jnl. Geot. and Geoenv. Eng., ASCE*, 126 (7): 583-593.
- Winterkorn, H.F. & Fang, H-Y. (eds) 1975. *Foundation Engineering Handbook. 2<sup>nd</sup> Edition*, Van Nostrand Reinhold, New York.
- Xu, X. 2000. *General analysis of pile foundations and application to defective piles*. PhD Thesis, The University of Sydney.
- Yamaguchi, H. 1963. Practical formula of bearing value for two layered ground. *Proc. 2<sup>nd</sup> Asian Regional Conference on Soil Mechanics and Foundation Engineering*, 1: 99-105.
- Yamashita, K., Yamada, T. & Kakurai, M. 1998. Simplified method for

- analyzing piled rafts. *Deep Foundations on Bored and Auger Piles*, van Impe and Haegeman (eds), 457-464, Rotterdam, Balkema.
- Yang, Q.J. 1997. Numerical analysis and design of strutted deep excavation. *Computer Methods and Advances in Geomechanics*, Proc. 9th IACMAG Conference, Wuhan. 3: 1909-1914.
- Yao, Z.E. & Zhang, J.R. 1985. An assessment of the effects of structure/raft/soil interaction. *Proceedings of the 5<sup>th</sup> international conference on Numerical Methods in Geomechanics, 1-5 April, Nagoya, Japan*. 2: 813-819.
- Yasufuku, N., Ochiai, H. & Maeda, Y. 1997. Geotechnical analysis of skin friction of cast-in-place piles. *Proc. 14<sup>th</sup> Int. Conf. Soil Mechs. Found. Eng.*, Hamburg, 2: 921- 924.
- Zhang, B.Q. & Small, J.C. 1994. Finite Layer Analysis of Soil-Raft-Structure Interaction. *Proceedings of the XIII International Conference on Soil Mechanics and Foundation Engineering*, New Delhi, India, January 5-10. 2:587-590.
- Zhang H.H. & Small J.C. 2000. Analysis of capped pile groups subjected to horizontal and vertical loads. *Computers and Geotechnics*. 26(1): 1-21.